AN OPTICAL MEASUREMENT SYSTEM TO MEASURE FREE FORM SURFACES

LIFONG ZOU

l.zou@qmul.ac.uk

Submitted to the University of London
for the Degree of Doctor of Philosophy

2002

Department of Adult Oral Health
Bart's and The London
Queen Mary's School of Medicine and Dentistry
Queen Mary
University of London
Turner Street
London E1 2AD
United Kingdom

When you can measure what you are speaking about and express it in numbers you know something about it; but when you cannot measure it, and cannot express it in numbers, your knowledge is of a meagre and unsatisfactory kind.

Lord Kelvin

1824 – 1907

Abstract

Free form surface measurement and its subsequent analysis is becoming a subject of considerable interest, not only within the engineering field, but also in bioengineering, medical and dental research. In particular, within the field of dental research, the oral structures comprise a variety of complex free form surfaces, which are often recorded by elastomeric impression materials. In this study, an optical triangulation-based, non-contact probe fitted onto a Co-ordinate Measuring Machine was used to acquire three-dimensional co-ordinate data from such complex free form surfaces.

When using an optical probe to digitise a complex free form surface represented by impressions, an optimal digitisation strategy is critical to limit the uncertainty of the data acquisition procedure, because the raw data are the basis for later surface measurement and analysis.

This study attempted to optimise a method for three dimensional free form surface data acquisition, measurement and analysis. A theoretical and systematic analysis of error distribution was carried out using standard objects and optimal digitisation strategies were proposed in relation to specified models. Two simulation models of two typical human tooth surfaces were extensively analysed and evaluated. Three reference

systems were developed for comparative measurements of those surfaces that have fewer geometrical features. An integrated automatic data acquisition procedure was also developed to scan a large number of impressions. Several successful research applications have been carried out using the methodology developed in this study.

To My Wonderful Son

Haibo LI

Table of Contents

List of Figures

List of tables

1 INTRODUCTION AND LITERATURE REVIEW

1.1 Measurement

Measurement is about quantifying characteristics, such as, shapes, dimensions, colours and weights of objects, as well as the physical, chemical and optical properties of the materials from which objects are made.

Measurement has been important ever since man settled from his nomadic lifestyle and started using building materials, occupying land and trading with his neighbours. As society has become more technologically orientated, much higher accuracies of measurement have been required in an increasingly diverse set of fields, ranging from micro-electronics to astronomy.

One of the oldest units of length measurement used in the ancient world was the 'cubit' which was the length of the arm, from the tip of the finger to the elbow. This was then subdivided into shorter units like the foot, hand (which at 4 inches is still used today for expressing the height of horses) or finger, or added together to make longer units like the stride. The cubit could vary considerably due to the variation in sizes of people.

As early as the middle of the tenth Century, it is believed that the Saxon King Edgar kept a "yardstick" at Winchester as the official standard of measurement. A traditional tale tells the story of Henry I (1100-1135) who decreed that the yard should be "the distance from the tip of the King's nose to the end of his outstretched thumb".

But variations caused problems in trading goods, and a standard of measurement became a serious requirement. It was in 1960 that the first laser was constructed and by the mid 1970s lasers were being used to set length standards. In 1983 the krypton-86 definition was replaced and the metre was defined as "the length of the path travelled by light in a vacuum during a time interval of 1/299 792 458 of a second" and it is realised at NPL by iodine-stabilised helium-neon lasers which have a reproducibility of better than ± 3 parts in 100,000,000,000.

Historically the industrial and trading needs of man have led not only to greater accuracies of measurement but also changes in definitions, culminating in the world-wide acceptance of the metre and the metric system.

Today length measurement is used in every sphere of life to enable fair trading conditions and to develop new and improved products and

processes that enhance our standard of living. These range from the production of microscopic electronic devices with circuit dimensions made to accuracies of some ten thousand millionths of a metre, to millimetre accuracy in distance measurement in construction over many kilometres, for example, to enable the Channel Tunnel works between France and England to meet in the middle. But this also extends to everyday life where we rely on accurate length measurement to ensure, for example, that our clothes fit or that our self assembly furniture goes together properly. In the medical field, measurements are used to provide precise dimensional information on the structure of human bodies; and the measurement of tooth morphology can provide three dimensional geometrical information to assist automation processes in restorative dentistry, such as for milling crowns or bridges controlled by a CAD/CAM system.

1.2 Surface measurement

Surface measurement is one branch of length or dimensional measurement. It is a scientific discipline that originated from the need for surface specification in production engineering. Now it has been expanded from the automotive, aeronautical and astronautical industries into electronics, optics, and more recently into medicine and dentistry.

Surface measurement, in particular, is concerned with the texture and geometry of a surface.

Surface geometry includes its geometric form (shape), dimension and deviation (tolerance). These are large subfields of dimensional metrology which parallel or exceed surface finish in scope and complexity. However, there is an increasing overlap between geometric measurements and surface texture measurements, so it is helpful to be aware of some basic concepts in surface measurement.

Surface measurement can be applied to any surface, with an irregularity or non perfection whether it is manufactured or naturally formed. Irregularities of surfaces or profiles can be decomposed into form, waviness and texture (roughness) according to the ratio of the distance between irregularities to their depth (Humienny, *et al.*, 2001).

Form

Form refers to the intentional shape of a surface which differs from a flat line or plane.

Waviness

Waviness is one of the three basic forms of surface geometry which is caused by the way a component is manufactured.

Texture/Roughness

Surface texture is the combination of short wavelength deviations of a surface from a nominal surface. It includes all those with deviations shorter in wavelength than form deviations.

Form

$$\frac{\text{distance of deviations}}{\text{depth}} > \frac{1000}{1}$$

Waviness

$$\frac{\text{distance of wave}}{\text{depth}} \text{ within } \frac{1000}{1} \text{ and } \frac{100}{1}$$

Texture/Roughness

$$\frac{\text{distance of grooves}}{\text{depth}} \text{ within } \frac{150}{1} \text{ and } \frac{5}{1}$$

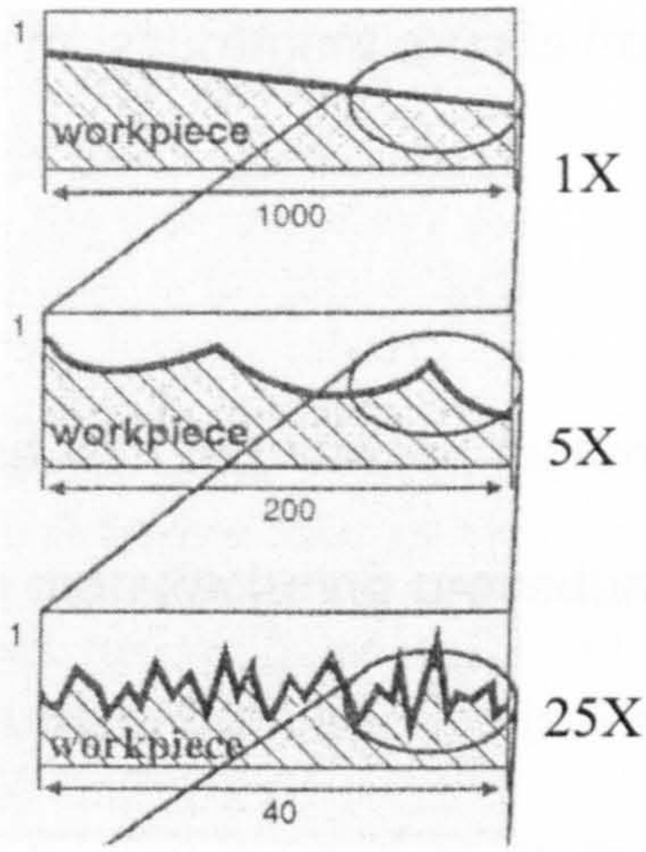

Figure 1-1: Surface form, waviness and roughness (adapted from Humienny, *et al.*, 2001).

Fig.1.1 illustrates the scales and relationships between form, waviness and texture or roughness. Within production engineering, the *form* of a part is the shape that it has been designed to be; *Waviness* is related to the function that the surface is created for, and it also can be a residual from a manufacturing process; surface *texture/roughness* is a micro-structure of the surface which reflects the characteristics of a material and the vestiges of the manufacturing procedure which produced it.

Surface form measurement is concerned with the global characterisation of three dimensional (3-D) surfaces. For example, to examine a spherical object, form measurement is concerned with its sphericity and dimensions, normally such dimensional measurements are coupled with an error band. The resolution of an instrument used for surface form measurement is required to be in a range of 1-10μm, and a measurement area is from 10 – 100mm^2.

Surface texture measurement is concerned with the surface features of a material. Such features are shaped by the manufacturing procedure or by nature. Short wavelength deviations of a surface from the nominal surface are measured. If a metal ball machined by a lathe is used as an example, the surface texture of the ball is related to those marks left by the cutting tool during its manufacture. For such measurement, the resolution of the measuring equipment is required to be in the sub-nm to sub-tenth of nm level, and the measurement area is usually in the 1mm^2 to 100μm^2 range.

The boundary between surface form and texture is not uniquely defined (Raja *et al.*, 2002). In fact, the boundary can vary based upon the size or the resolution of the assessment requested, or the function which the surface is required to perform. For example, tribology analysis is primarily related to surface texture measurement, and in limited circumstances, to

surface form too, as it is concerned with surface details which affect lubrication, friction and wear. Nevertheless in the practice of surface measurement, surface form and texture are often considered as two sub-fields.

1.3 Free form surfaces and their measurement

1.3.1 Free form surfaces

A free form surface can be defined as a surface that cannot be described by a single mathematical equation. This is not an official definition. However, there is no other one to be found in current metrology standards.

Parts produced by manufacturing engineering processes differ quite considerably from those found in human development. Usually such parts are developed from geometric concepts specified over centuries, use materials known to sustain the function of components and products, and a 'whittling-down' process is used to create the shape required for the desired engineering product. The main object of the parts and assemblies produced is that they are 'fit-for-function' and yield the appropriate design life for which the product was intended.

In contrast, human ‘components’ have been created by a 'bottom-up' approach and are refined through centuries of human evolution to become 'optimally efficient' for their functional purposes. The fact that human ‘components’ have evolved, rather than been developed, implies that they have not been constrained by limitations of engineering design and geometric considerations, but have evolved as 'free-form' parts and systems which are, therefore, dissimilar to most engineered products. Their evolution follows no obvious rules of mathematics or geometry, although the kinematics of movement is often similar to those developed (in reality copied) by inventors for engineering. In addition to the physical evolution of the part of the human form, motor systems, the muscles and ligaments, are more efficient in terms of power conversion than their mechanically equivalent counterparts.

When attempts are made to analyse human 'free-form' surfaces using engineering metrology products, it is important to recognise that often their character does not easily fit the constraints of the current generation of machines. As a consequence, it is necessary to adapt such machines, usually through software modifications and careful attention to probe selection, and to employ appropriate measurement strategies to meet the needs and constraints of the human 'free-form' surfaces that are required to be assessed.

Entering the twenty first Century, and driven by the computing industry, it is possible to achieve both higher resolution and accuracy measurement results using contemporary measurement equipment. The new challenge of surface form measurement is to attempt the measurement of arbitrary free form surfaces from a wide range of applications in bio-engineering, medical and dental research. The author's research described in this thesis falls into this category. Meanwhile, developments in surface texture measurement move towards a nanometre level of investigations.

Free form surface measurement and analysis are newly developing areas in the discipline of modern metrology. This progression has been driven by product design for application to automobile, aerospace, telecommunication, and surgical products (Chow, 1997; Osanna *et al.*, 1995, Cheng *et al.*, 1995; Rioux *et al.*, 1987). Furthermore, the demands of bio-engineers and medical researchers, have encouraged the development of optical equipment, and the availability of fast calculation and large capacity data storage using computers. Free form surface measurement and analysis is becoming a subject of considerable interest, not only within the engineering field, but also in bioengineering and medical research (Saito and Miyoshi, 1991; Bhat and Smith, 1994).

1.3.2 Free form surface measurements

Free form surface measurement concentrates on the measurement of geometrical features and dimensions. In the practice of modern metrology such measurement involves two key procedures, data acquisition and development of the correct fitting algorithm (Summerhays *et al.*, 2002). Each of these problems has numerous solutions which largely depend upon the specified application. For example, the application of non-contact measurement methods has expanded into many new areas from traditional industrial applications; to the medical field, such as measurements of the human face and other parts of the human body (Aung *et al.*, 1995; Shahrom *et al.*, 1996; Fan, 1997). Gradually, researchers have required the process to be used on more complicated surfaces such as in the quantification of tooth morphology (Seymour *et al.*, 1995, 1996a, 1996b, 1998, 1999a, 1999b).

Traditional form and dimensional measurement often deals with a designed geometrical shape or a superimposed combination of designed geometrical shapes. When measurement of such a shape is intended, an appropriate standard measurement method can be followed. In contrast, complex biological free form surfaces require more complex measurement strategies because of irregularities (see Fig.1-2) in their shape and consequent uncertainty, such that these strategies are enormously

different to the standards required in conventional engineering. In addition, there is no existing standard for 3-D free form surface measurement either nationally or internationally.

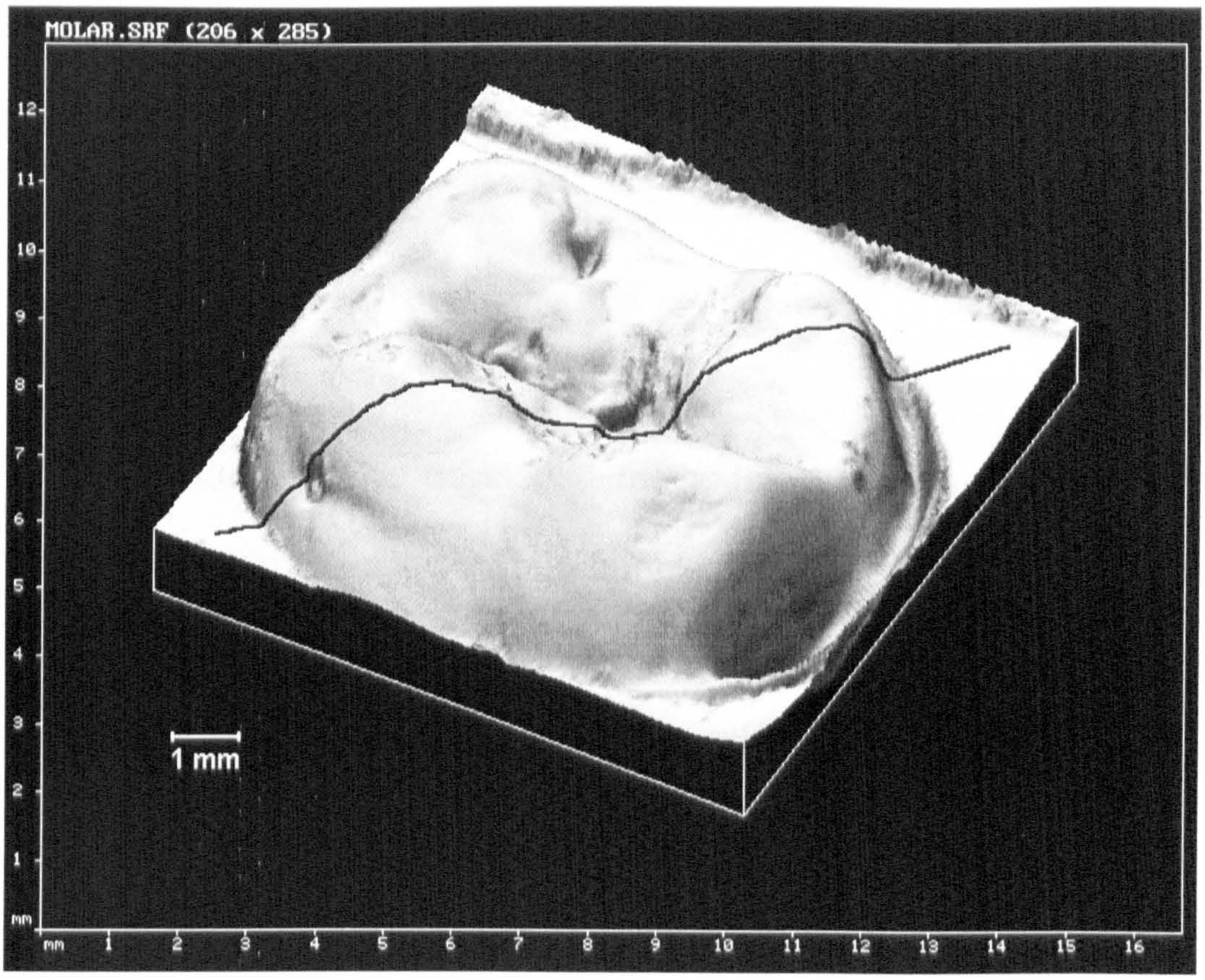

(a)

(b)

Figure 1-2: (a) The occlusal surface of a human molar tooth (b) A Profile across the surface of the molar tooth.

Fig.1.2 (a) shows the typical nature of the occlusal surface of a molar tooth. This surface is revealed to be irregular in shape. There are cusps, pits and fissures. The variation is also great from one tooth to another, and from one person to another. So it is not difficult to understand that the geometrical assessment of such surfaces is a challenging task, even with the aid of sophisticated instruments.

This study attempted to develop a methodology for free form surface measurement of such complex free form surfaces. The applications using the methodology developed are strongly linked to bio-engineering, medical and dental research.

1.4 A review of contemporary 3-D measurement techniques

There are number of techniques currently used to obtain accurate surface measurements, each has its own strengths, weaknesses and areas of applicability. These include Scanning Probe Microscopes (SPM), Scanning Tunnelling Microscopes (STM), and Atomic Force Microscopes (AFM). These can produce very high accuracy in surface measurements up to nano or sub-nanometre ranges, but are incapable of performing large surface contour measurements, as a consequence of instrument

design and also due to the large amount of data required for comprehensive assessment (Stout, 1994).

For surface form (shape) measurements, Co-ordinate Measuring Machines (CMMs) have been employed for the inspection of automotive parts in industry since the 1950's (Bosch, 1995). CMM produces 3-D co-ordinates at points on an object surface utilising a probe fitted on the CMM column. Geometrical features of a part can be inspected by manipulating these co-ordinate data. CMMs are widely used in industry for a large range of measurement tasks.

The interface between the CMM and the measurement object or surface is a probe. The probe plays a very important role in obtaining the co-ordinates of a surface, and there are several kinds of probes commercially available at the present time.

Touch trigger probes are by far the most commonly used with CMMs due to their simplicity and low cost. One of the problems with touch probes is that even under well-controlled conditions and at a generally accepted measuring speed and force, damage to the surface being scanned can occur because of the inertia effects of some probe parts (Win *et al.*, 1998). Win also indicated that initial plastic yielding of a surface can easily occur when probing with a sphere, and at higher probing speeds, multiple

bouncing of the probe may occur, which reduces the resolution for all mechanical probe systems. This was also one of the reasons why it was decided in this study to investigate the use of an optical probe in a measurement system intended for dental research.

The optical probe has the great advantage of non-contact with the surface being measured. By the late 1980's, non-contact laser probes were widely accepted for surface measurement, especially in surface digitisation techniques.

1.5 Surface digitisation technology

Surface digitisation is a procedure by which digital data is acquired from a surface of interest in order to obtain more knowledge of the shape and dimensions of the object. This is achieved through a series of interactions between the measurement equipment and the surface being assessed. Digitisation usually provides a string of 3-D co-ordinates in ASCII format.

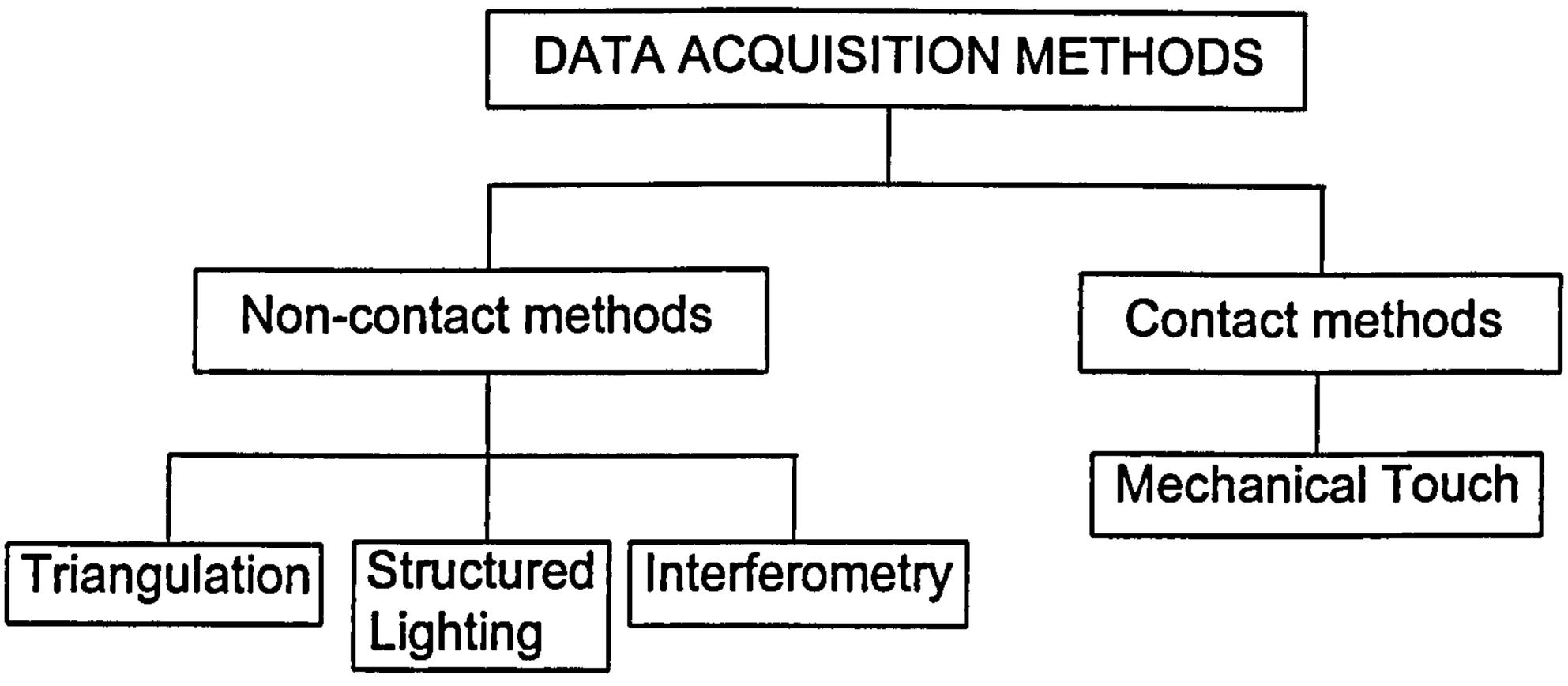

Figure 1-3: A classification of data acquisition methods.

There are many different methods for acquiring co-ordinate data, as shown in Fig.1-3. Essentially, each method uses some mechanism or phenomenon for interacting with the surface of the object of interest.

Contact methods use mechanical contact through a contact probe at the end of an arm or the column of a CMM (Jarvis, 1983) to obtain surface geometrical information. Development of this method was driven by reverse engineering (Milroy *et al.*, 1996; Dalton, 1998) and re-manufacturing (Chow, 1997). In each case, an appropriate sensor determines a precise position on the object's surface.

Contact types of measurement use trigger-type CMMs to acquire point data by touching the probe on the measurement object, and are appropriate for measuring simple geometrical features that need only a small number of point data.

Non-contact methods use scanning–type CMMs to capture larger numbers of sampling points, and have been used successfully for measuring surface form (Bradley and Vickers, 1992; Lee *et al.*, 2001; Chang and Lin, 1999). A recent study comprising questionnaire respondents from research institutions and companies engaged in surface topography in the European Community, revealed that non-contact optical techniques are more popular and widely used than previously thought (Dong *et al.*, 1994). Three dimensional non-contact measurement methods started to be used in the 1980's (Bosch, 1995; Stout, 1994).

There are three distinct optical methods: triangulation, structured light, and interferometry.

1.5.1 Triangulation

Triangulation is a method which uses fixed distances and angles between light sources combined with photoelectrical sensing devices to deduce position. A high energy light source is focused and projected at a specified angle to the surface of interest. A photosensitive device, usually a position sensitive device or a video camera, senses the reflection of the surface and then by using geometric triangulation from the known angle and distances, the position of a surface point relative to a reference plane can be calculated. The light source and the sensor can be mounted on a

travelling platform which produces multiple scans of the surface. These scans are therefore relative measurements of the surface of interest. Different high energy light sources can be used, but lasers are the most common. Triangulation can acquire data at very fast rates (Clarke *et al.*, 1990; Goh *et al.*, 1985; Silvaggi *et al.*, 1986; Clarke, 1995). The accuracy is largely determined by the resolution of the photosensitive device. Motavalli and Bidanda (1991) presented a reverse engineering strategy using laser triangulation. Moss *et al.* (1989) presented a detailed discussion of a classic laser triangulation system which was used to capture surface form data from faces. The use of laser triangulation with a CMM was presented by Modjarrad (1988). These references give a broad survey of the methods, approaches and limitations of the triangulation method. However, the accuracies quoted were not quantified in relation to the geometry of the surfaces measured, and this can have a major influence on measurement accuracy, especially for a free form surface.

1.5.2 Structured lighting

Structured lighting involves projecting patterns of light upon a surface of interest and capturing an image of the resulting pattern reflected by the surface. The image is then analysed to determine co-ordinates of data points on the surface. A popular method employing structured lighting is the shadow Moiré, where an interference pattern is projected onto a surface producing illuminated contour lines. These contour lines are

captured and analysed to determine the distance between the lines. This distance is proportional to the height of the surface at the point of interest and hence the co-ordinates of individual surface points can be deduced. Structured lighting can acquire large amounts of data with a single image frame, but analysis to determine positions from the data can be rather complex. Will and Pennington (1972) used grids projected onto the surface of objects to determine point locations. Wang and Aggarval (1987) used a similar approach but used stripes of light and multiple images. This method is relatively simple and mobile in terms of hardware, but is much more complicated in data analysis, and is especially limited where complex surfaces are to be analysed.

1.5.3 Interferometry

Interferometry measures distances by using interference patterns, and can be a very accurate method of measurement. Visible light has a wavelength in the order of hundreds of nanometres, whereas the dimensions of the most engineering parts and biological structures are in the cm to m range. A high energy light source is used to provide both a beam of monochromatic light to probe the object, and a reference beam for comparison with the reflected light (Stout, 1994). However, this method is very sensitive to the stability of the environment and requires an anti-vibration table, so that an interferometry measurement laboratory can be very expensive to set up.

1.5.4 Contact measurement

The contact method represents another commonly used means of shape capture. It began to be used in the 1950's, and was developed to meet industrial demands (Bosch, 1995). This method involves touching a surface using a mechanical trigger probe, and is particularly appropriate for measuring regular geometrical features which requires a small number of data points (Chang and Lin, 1999). Sensing devices in the joints of a support arm determine the relative co-ordinate locations. The method is not very effective for concave surfaces and is also slower in data acquisition. The contact method is often used in conjunction with a CMM. The CMM can be programmed to follow paths along a surface and to accumulate data points. Many papers have reported this method being used in industrial applications (Xiong, 1990; Sahoo and Meng, 1991; Butler, 1991).

The result of data acquisition is a 'point cloud', and the clouds can be formed in various formats depending on the digitisation strategy being employed. Intervals between digitisation points can be different, which are based on irregularity of the surface. In a digitisation procedure, a probe digitises data by tracing a group of parallel scan lines or radial scan lines, which again depend upon the contour of a surface to be measured. The

author has developed digitisation strategies that can obtain six differential digitisation results based on the need of a specified area.

1.5.5 Practical problems of data acquisition

Despite the advantages of the optical probe for digitisation, there are also a number of problems in practice, such as,

- accessibility,
- occlusion,
- noise,
- incomplete data,
- surface finish.

Accessibility relates to scanning data that is not easily acquired due to the configuration or topology of the object that is being measured. This usually requires multiple scans, but can also make some data impossible to acquire. For instance, scanning a surface through a hole is a typical example of an inaccessible surface.

Occlusion is the blocking of the scanning medium due to shadowing or obstruction. This is primarily a problem with optical scanners. However, the use of multiple scanning devices is one approach to obviate this problem. Rioux (1984) and Koivunen and Bajcsy (1992) mentioned the

problem, and suggested using structured light to overcome the problem in principle, but offered no further practical details.

Noise elimination in data samples is a difficult issue. Noise can be introduced in several ways, such as from extraneous vibrations and specular reflections. Many different filtering approaches can be used. If the noise is repeatable or has certain patterns associated with it, then a correction program can be applied to correct the raw data (Koivunen, 1992).

Incomplete data, one of the problems often experienced in optical digitisation, is the restoration of missing data or eliminating unwanted raw data. This is partly necessary in the case of inaccessibility and occlusion problems. Moreover, because of the nature of optical and even contact scanning, the data close to sharp edges are usually fairly unreliable.

The final issue is the surface finish of the part being measured. Smoothness and material coatings can dramatically affect the data acquisition process. Both contact and optical methods produce more noise when scanning a rough surface than a smooth one (Beckmann and Spizzichino, 1963).

The same problems inevitably also occur in dental applications. This study has successfully solved some of them by using multiple probe orientation digitisation methods (see Chapter 4). Throughout the assessment of each object, the accuracy or reproducibility are estimated; the occlusion, multiple probe orientations, and segmentation are described in Chapters 3, 4, 5 and 6, in their different aspects and applications. Although there are problems and sometimes serious problems occurring with practical data acquisition, this study has rigorously established a standard as data points are never allowed to be altered in any way, such as to take out 'bad' points or by smoothing and adding missing data points. A complete surface must be digitised using an appropriate digitisation strategy, which can be guaranteed to provide the entire data cloud and thereby truly represent the surface being measured.

1.6 Measurements in dentistry

Measurements in dentistry are often subjective (Dunne, 1989, Allred 1997). There appears to be no consensus on measurements in dentistry in the iterature (Allred *et al.*, 1987; Reisbick and Matyas, 1975; Lacy *et al.*, 1981; Eames *et al.*, 1979; Johnson and Craig, 1985, 1986; Linke *et al.*, 1985; Mendez , 1985; Gordon, 1990; Davis and Prebie, 1986; Woodward *et al.*, 1985). The instruments used in these studies varied from microscopes to callipers. Measurements were reported in various terms of

'precision', 'accuracy', 'inaccuracy' and 'accurate percentage', which make their conclusions hard to compare. Length measurement in 2-D is between two points, but tooth surfaces have a three dimensional form, and this requires many more points to be described and measured. Even with linear measurements of an outline of a tooth, calculated lengths need to relate to its curvature. Many measurements described neglect to account for the dimensional changes that exist along a 3-D surface (Linke *et al.*, 1985; Mendez, 1985; Davis and Prebie, 1986; Woodward *et al.*, 1985; Kaiser and Nicholls, 1976).

It has also been reported by Chadwick (1989) that there was a lack of repositional accuracy when microscopy, stereophotogrammetry and laser interferometry were used to trace a profile of sectioned replicas, to make the computer graphic assessment of occlusal mapping, and to assess the volumetric changes associated with tooth wear.

In order to digitise a complex free form surface like a tooth surface, both contact and non-contact measurement methods have been used with some successes (Seymour *et al.*, 1996a, 1999a; Johnson *et al.*, 1996; Yeganeh *et al.*, 1999; Yeganeh *et al.*, 1995, Delong *et al.*, 1985, 1989, 1991, 1993, 1999).

1.7 Representation of oral structures

Clinical dentistry almost inevitably involves the use of a replica technique to represent oral structures. The replica technique is non-destructive, and provides a permanent 3-D record of areas of interest, especially, it allows digital inspection of oral structures to be carried out in the laboratory, rather than at the chair-side.

Polyvinyl siloxane impression materials have applications in a variety of indirect procedures in Prosthodontics and Restorative Dentistry. These materials have numerous advantages, such as favourable handling properties, good patient acceptance and excellent physical properties, which have resulted in their current clinical popularity (Gohnson and Craig, 1985, 1986; Mandilos, 1998). Several investigations (Williams *et al.*, 1984; Tjan *et al.*, 1986; Chee *et al.*, 1992; Fano, *et al.,* 1992; Corso *et al.*, 1998; Barghi and Ontiveros, 1999; O'Mahony *et al.*, 2000) have reported the physical properties of silicone-based impression materials and found the dimensional accuracy to be in the region of 0.1%. It has also been suggested that using a surfactant (Hydrosystem) could improve the quality of impressions both in the laboratory and clinic (Millar, Dunne *et al.*, 1997, 1996; Robinson, Dunne *et al.*, 1994)

A review (Christensen, 1997) of available dental impression materials considered seven main aspects: rigidity; recovery from deformation; shrinkage; elongation; tear strength; wettability; and cost per ml. In relation to the representational accuracy, three aspects have particular importance in dentistry. They are high rigidity, low shrinkage, and good wettability. As a result of this report, the polyvinyl siloxane material, Extrude (Kerr, USA), was selected for use at the Barts and The London Dental School. It has been shown to be effective and reliable over several years of application.

1.8 Measurements of oral structures

Traditionally, the analysis of tooth morphology relies on the production of dental casts. The cast is a representation of the oral structures, and is a solid model made of plaster or stone. When making a dental cast, it is first necessary to take an impression of the patient's teeth, this dental impression is elastic, and non-rigid, which is contained in a semi-rigid tray. It is sent to a dental laboratory, and a dental cast is produced by pouring stone or plaster into it. Each stage of the procedure is capable of contributing a degree of variation to the resulting product, and these variations in turn act on one another to compound the overall distortion in the cast model.

Contact measurement methods can only measure rigid objects, such as in this case, a dental cast. Using a non-contact measurement method, both rigid and non-rigid objects can be measured. The surface information that obtained can be digitised directly from impressions using a non-contact probe, and an analysis software package can be used to interpret and reconstruct these digitised surfaces as positive 3-D images. Such a direct non-contact measurement of a dental impressions is both more accurate and efficient. More importantly, if the dental impression is digitised directly, it shortens the chain of the tooth representation procedure, and reduces reproduction errors in the procedure.

Contact measurement techniques were in use long before non-contact measurement methods, and have been recognised as being at least one order of magnitude more accurate (Bradley *et al.*, 1994). However, contact measurement has problems when measuring soft objects such as dental impressions.

Dental impressions are moulds of oral structures, and their physical characteristics are related to the Young's modulus of the impression material. They may be deformed or damaged if digitised using a touch probe. With such a complicated free form surface, the diamond tip of a contact probe may touch several points at the same time, or miss small

areas, if the curvature of the tip is larger than the curvature of the surface in the area where it has touched. In such cases, the use of touch trigger probes is inappropriate for measuring dental impressions. The non-contact optical measurement method with its high resolution sensitivity provides outstanding advantages in assessing soft surfaces, such as dental impressions.

A non-contact data acquisition and measurement system has been used for a number of years at Barts and The London School of Medicine and Dentistry, and it is evident that such an optical measurement system (CMM, IMS, UK; OP2, Renishaw, UK) has provided a powerful tool in support of dental research (Zou, *et al.*, 1993). The operating software has been developed within the School to allow both 2-D and 3-D measurements (Bedford, *et al.*, 1993) as well as a superposition function (Jovanovski, *et al.*, 1993).

1.9 An existing industrial based measurement system

During the late 1980's a CMM originally designed for industrial purposes was acquired by the Dental Metrology Research Unit (DMRU) at Barts and The London School of Medicine and Dentistry, Queen Mary, University of London. This measurement system consists of a CMM (Merlin II, IMS, UK), fitted with a non-contact laser probe (OP2, Renishaw, UK) based on

the optical triangulation working principle, and a probe head (PH9, Renishaw, UK). The probe head provides rotational flexibility in two orientations, around the Z axis within a range of -180° to +180° and around the X axis in a range of 0° to 105° with a step change of 7.5°. The construction and working principle of the CMM and OP2 are reviewed in Appendices I and II.

A report on the DMRU (Tan, 1990) stated the following:

- It is observed that with a scanning speed greater that 10 points per second, or at stepping distance smaller than 60μm, the chances of scan termination become more frequent.
- The scanning procedure is only capable of scanning a surface with no 'severe irregularity' and if the slope height in the probing direction is less than 1mm.
- The maximum data array can contain only 150×150 data points.
- The accuracy of the measurements is highly dependent on the ambient temperature.

These statements reveal:

- A considerable lack of quantification of the problems observed, such as the reasons for measurement termination. No solutions are suggested;

- Although the scanning of an edge was not recommended, since steep slopes often occur on tooth surfaces, it was necessary to find a way to deal with this situation;
- A molar or premolar tooth has an approximate cross section of 15mm×15mm, but because of the curvature of its surfaces, the actual surface length in each direction is much longer than this. Hence if a data acquisition interval of 0.1mm is selected, the number of points in one direction will be far more than 150 points. Hence there was a need to cope with larger data arrays, up to 250 × 250 points;
- No record was given of the probe orientations in relation to contour changes, and this is an important factor influencing the quality of digitisation over irregular free form surfaces.
- Quantification analysis of the system uncertainty was not performed, and no suggestions were provided to develop an optimal digitisation strategy.

1.10 Existing problems

Although the non-contact measurement system used in this Dental School is superior for non-destructive assessment, it also lends itself to applications in complex surface measurement. In the late 1980's, there was no mature non-contact measurement system available for dental research, although the CMM was well developed and widely used for

manufacturing industrial measurement purposes. The non-contact probe had not been used for long enough to explore the problems associated with complicated free form surface measurement. Considerable research was necessary to develop suitable optimal working conditions for a non-contact measurement system. Whilst the pre-existing calibration, specification and equipment guidelines might have been useful in industrial measurements, they were not appropriate for use with complicated surface measurements, since the standards were adapted from the touch probe to optical probes, and the explanation of the parameter settings was not clearly defined for applications to free form surface measurement.

A number of the research publications concerned with optical geometry measurements in dentistry have not contained an equipment performance evaluation. This is inappropriate since system uncertainty is strongly affected by the specific measurement methods applied to a particular surface, in other words, how the instrument was operated.

1.11 Objectives

The objectives in performing this research were as follows:

- Systematic assessment of performance accuracy of the existing non-contact measurement system;

- Systematic investigations of free form surface measurement using an optical triangulation based non-contact probe;
- To provide an optimal digitisation strategy and accurate digitisation method for complex free form surface measurement;
- To apply this newly developed method to dental and bio-engineering research.

The investigations are listed as follows:

- Determination of optimal digitisation parameter settings for scanning direction, scanning speed, sampling interval, and optical threshold setting.
- Investigations of error distributions in relation to optical axis and surface geometry.
- Investigation of the effect on surface digitisation using multiple probe orientations.
- Investigation of a stepped cylindrical model similar to a crown preparation on a tooth.
- Investigation of a model of four attached balls similar to the occlusal surface of a molar tooth surface.
- Development of two datum systems to provide a reference frame for comparative measurements of sequential specimens.

- Development of an automatic digitisation procedure to meet the requirement for rapid digitisation of a large number of samples in dental research.

1.12 Layout of thesis

The layout of the material within this thesis reflects that the work undertaken encompasses several stages, each of which is distinct but dependent on those preceding it. Therefore a modular structure was adopted with each topic presented within its own separate Chapter, for this reason an introduction, materials and methods, results and discussions relevant to each module are presented in each Chapter.

This Chapter has given a general introduction to the subject. It will then be developed into systematic analysis of measurement strategy in relation to surface geometry in Chapters 2, 3, and 4.

Chapter 2 is concerned with the optimisation of the digitisation parameters; Chapter 3 studies the error distribution when using an optical triangulation based laser probe over a standard sphere. It is aimed at discovering the digitisation error in relation to the geometry of a measured surface; and Chapter 4 deals with digitisation using multiple probe orientations. Considering applications in dental research, two geometrical

simulation models of two types of typical tooth surfaces were studied to obtain an optimal digitisation strategy, and these are presented in Chapters 5 and 6.

Two datum systems were also developed to obtain comparative measurements of these surfaces, which have a lack of geometrical features which are used to 'land mark' the surface superposition. These investigations are presented in Chapter 7.

An automatic digitisation procedure was developed to meet the requirements of a large number of specimen scans for dental research, and this is described in Chapter 8.

Finally the clinical significance of using the techniques developed from this research, the Conclusion and Future Work relevant to the thesis are presented in Chapters 9, 10 and 11.

2 AN INVESTIGATION OF OPTIMAL DIGITISATION PARAMETERS

2.1 Introduction

Three-dimensional (3-D) metrology has lead to significant changes in dimensional measurement. It generates co-ordinates from a surface, and measures geometrical features, instead of only measuring dimensions and positions. Thus, the measurement output is a collection of digitised co-ordinates of surface points. From these surface points, the topography of a surface can be reconstructed, and geometrical features at various sections over the surface can be measured and analysed. Hence, the surface co-ordinates, as the raw data, are the fundamental information subsequently used for lateral analysis.

Digitisation is the procedure whereby co-ordinate information of a surface is extracted from the measurement object. The procedure is directed by sequence of commands from a software program. This software program controls and directs an optical and a mechanical system; to co-ordinate the focusing of the laser beam, the movement of a probe in three directions (X,Y,Z) and two rotations, and also the optical and electrical signals. To control such procedures, five digitisation parameters provide the interface between the operator and the measurement system.

2.2 Digitisation procedures and operator- variable parameters

The digitisation procedure is set by five operator-variable parameters:

1) scanning direction,
2) scanning pitch,
3) scanning speed,
4) optical threshold level,
5) probe orientation.

As probe orientation is the most complicated issue, it is investigated separately in Chapter 3.

2.2.1 Scanning direction

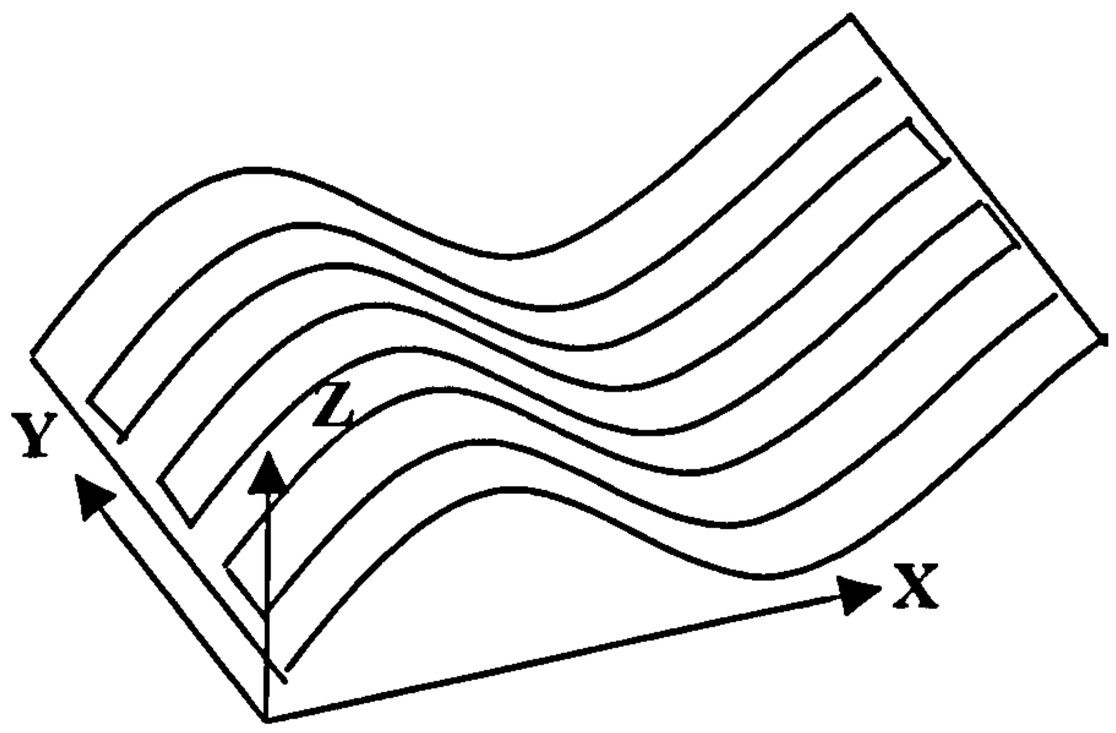

Figure 2-1: The definition of directions in a digitisation procedure.
'+X' is the scanning direction,
'+Y' is the lock direction and '–Z' is the probing direction.

In order to digitise a surface, two directions of probe movements need to be defined. The first direction is that in which the probe moves as it captures co-ordinate data, and this is called the 'scanning direction', '+X'

in Fig.2-1; the other is the direction in which the probe deviates from one scan line to the next, so as to continue the data capturing procedure, and this is called the 'lock direction', '+Y' in Fig.2-1. The lock direction is always perpendicular to the scanning direction, so as to form a rectangular area. The probing direction is the direction in which the probe approaches to focus on the surface being measured, '-Z' in Fig.2-1. In the scan direction, the probe captures the surface data, moving at a given speed. This process involves an acceleration and deceleration in the moving direction and also movement in the probing direction towards the surface normal; it also varies in its orientation depending on the curvature of the surface.

2.2.2 Scanning pitch (sampling interval)

The scanning pitch is the distance between each captured point, also called the sampling interval. Theoretically, the more measurement points that are digitised, the closer the fidelity of the representation of a measured surface. In practice, there is also an internal regulation between the data density and surface representation (Than *et al.*, 1996; Choi *et al.*, 1998). For example, for a hemisphere, reconstructing a surface using 5 digitised points gives a different result when compared to 50 points, but there is much less improvement gained when 50 points are increased to 500 points, as 50 points are sufficient to represent the main features of a hemisphere, whilst 500 points are excessive. In this case, a high density

of capturing data comes at the expense of time needed for data processing, which needs to be optimised in practical situations.

2.2.3 Scanning speed

A high scanning speed is possible by using a triangulation probe and is one of its main advantages over mechanically contacting probes. Investigations (Report EUR 15314 EN, 1994) have indicated that delays are produced by processing the measuring signals, especially with low light levels of the beam spot which require relatively long integration or averaging time. This introduces an uncertainty in the effective reading time of the spot position.

Increasing the scanning speed can save time, but the probe has less time for processing. When the scanning speed exceeds the ability of synchronic focus, error reading and missing data are likely to occur. An investigation of optimal speed was carried out, which is discussed in section 2.5.2 in this Chapter.

2.2.4 Optical threshold setting

Investigations (Report EUR 15314 EN, 1994) have shown that errors when using an optical triangulation probe can be due to variations in macroscopic and microscopic reflectivity of the measured object. Dark objects have higher thermal losses and require a higher output power and

a lower sensitivity of the detector which can be adjusted by changing the optical threshold level within the Direct Computer Control (DCC, IMS, UK) software.

To determine a suitable threshold level, a pre-scan with several different optical threshold levels needs to be carried out, especially in areas where the light level is low. The threshold level is set up prior to the scanning procedure, and cannot be changed during the entire surface scan. Over a free form surface, there may be several high intensity reflection areas, for example peak areas, and low intensity of reflection areas such as valleys. Ideally the threshold level would be changed accordingly. Unfortunately this is not achievable within this measurement system. Therefore, the threshold level has to be set at the lowest level, to prevent termination during a digitisation procedure.

The threshold level also reflects the Signal to Noise (S/N) level. When it is set at a low value, the background noise has a larger influence.

2.3 Digitisation strategy

When using an optical triangulation-based non-contact method, various constraints require to be considered. Although laser scanners have been widely used in recent years, few studies on laser scanning are reported. Xi (1999) developed a CAD-based path planning system for a 3-D linear

laser scanner. They tried to maximise the coverage of the object by finding the best set-up for the field of view of the laser scanner, and its orientation. However, the system was developed for industrial parts which only have primitive features. Bernard and Veron (1999) developed a method that automatically scanned an object using off-line CMM programming. To facilitate the data acquisition process, a software module called 'the Paint' was used to find the region illuminated by the laser beam. The system, however, needed development when complex objects were to be scanned. Zussman *et al.* (1994) and Funtowicz *et al.* (1998) developed an algorithm that determined the location of a laser sensor, but that algorithm was only applicable to a 2-D profile of a surface and could not be used to scan the entire surface of an object. Numerous publications have reported (Elber and Zussman, 1998; Yau and Menq, 1995; Lim and Menq, 1994; Spitz *et al.*, 1999) their researches in optimisation of scanning strategies. However, they are all limited to simple smooth shaped surfaces, although some of them could deal with free form surfaces.

Scanning parameters are interrelated to each other. For example, increasing the scanning pitch (sampling interval) results in a decrease of the scanning speed. The scanning direction and probe orientation are both affected by the geometry of the surface. However, investigations are

required to obtain an optimal balance between parameters for free form surfaces.

An obvious example of a measurement in dentistry shows the need of optimisation of digitisation strategy. Fig.2-2 (a) presents two images that were digitised at two different parameter settings from a dental impression, in both cases derived from the user manual provided by the manufacturer. However, the results show a maximum difference as much as 0.618mm at an identical cross section (Fig.2-2(b)).

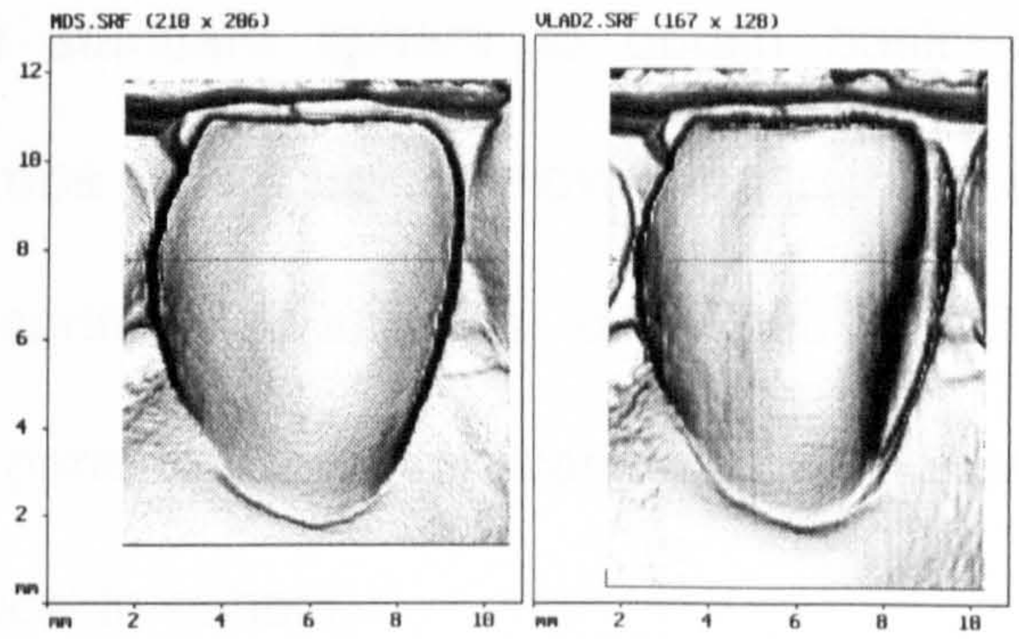

Figure 2-2(a): Two images obtained with different system settings from a dental impression of a lower incisor tooth.

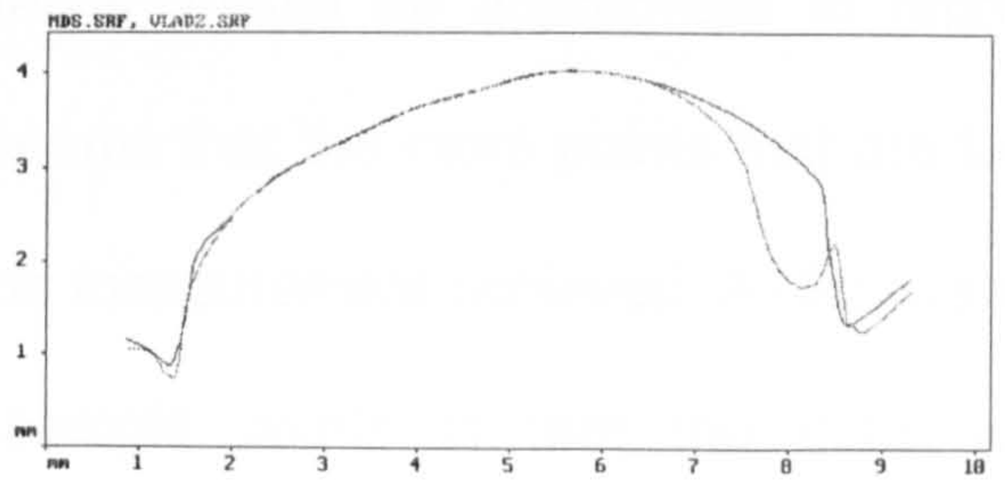

Figure 2-2(b): Profiles obtained at a cross section indicated by the lines in Fig.2-2(a). The differences are revealed and the maximum value is 0.618mm.

To overcome the problems described above, it was necessary to undertake several investigations during this study, to provide guidelines for digitising free form surfaces.

This Chapter is focused on a study to determine four optimal digitisation parameters for two standard objects to reflect the complexity of applications in dental research: (1) the scanning direction based on a corrugated surface with shape contour changes to simulate the situation of an inlay preparation in dentistry, and (2) three other parameters were studied using a standard sphere to obtain basic knowledge of the specified laser probe (OP2), before moving on to the complex model using four arbitrarily connected spheres described in Chapter 6. These additional three parameters were scanning pitch, scanning speed, and setting of the optical threshold.

2.3.1 Sampling interval and speed

The sampling interval should be appropriate to represent the surface being studied. It seems that the more points that are taken the better will be the fidelity of the measurement achieved. A disadvantage of increasing the number of sample points is that the data acquisition time is significantly increased, as is the processing time. A CMM requires significant capital investment, both for the equipment itself and also for the infrastructure required for maintaining suitable environmental conditions

for its proper operation. Skilled operators are generally required to oversee the measurements and to interpret their results. It is desirable to maximise the output of these machines by developing an optimal sampling interval to minimise the digitisation time, because the total measurement time is proportional to the number of sample points collected. The desirability of optimal sampling interval and speed needs to be balanced with the fidelity of the digitisation required from a surface and the time taken for its subsequent computation and analysis.

Increasing scanning speed can result in a kinetic error of the optical probe, as simultaneous changes in slope and distance vary the contributions of the optical aberrations. A low light level of the reflection often requires longer integration or averaging time from the photoelectric sensor. These factors make the time of the effective reading and the probe's position over the object surface uncertain.

Although the sampling rate or size and scanning speed have been studied in the industrial field (Kim and Raman, 2000; Edgeworth and wilhelm, 1999; Cho and Kim, 1995; Chan *et al.*, 1996; Weckenmann *et al.*, 1995; John and Galip, 1995), they are largely related to the use of touch probes on industrial parts, or to a specific optical device like a CCD camera. In

this Chapter, optimal digitisation parameters are related to the optical triangulation-based laser probe employed in this Dental School.

2.3.2 Probe scanning direction

It has been observed that the probe scanning direction has an impact on the quality of data acquisition during digitisation. An impression of a corrugated object (IMS, UK) was used for an investigation to quantify the influence of digitisation directions. A standard sphere (IMS, UK) was used to quantify the influence of sampling rate, scanning speed and optical threshold settings.

2.3.3 Optical threshold setting

Along with the advantage of an optical probe being free of surface contact, it also has its own character, that is, an optimal measurement condition is dependent upon the material, the surface texture, and surface topography of the surface being assessed. Certain materials and surface texture are not compatible with the OP2. For example, transparent or semi-transparent materials proportionally reflect the incident laser beam from the surface and subsurface layers, which are therefore unsuitable to be inspected using the OP2 probe. Other types of materials have a honeycomb surface texture, which results in very low intensity beam reflections, and are also incompatible with the OP2 laser probe. When the surface topography changes, even within the capable detection range, the

format and intensity of the beam reflections also vary. Therefore, an attempt was also made to determine the optimal optical threshold setting.

2.4 Materials and methods

2.4.1 Bi-directional and uni-directional scanning

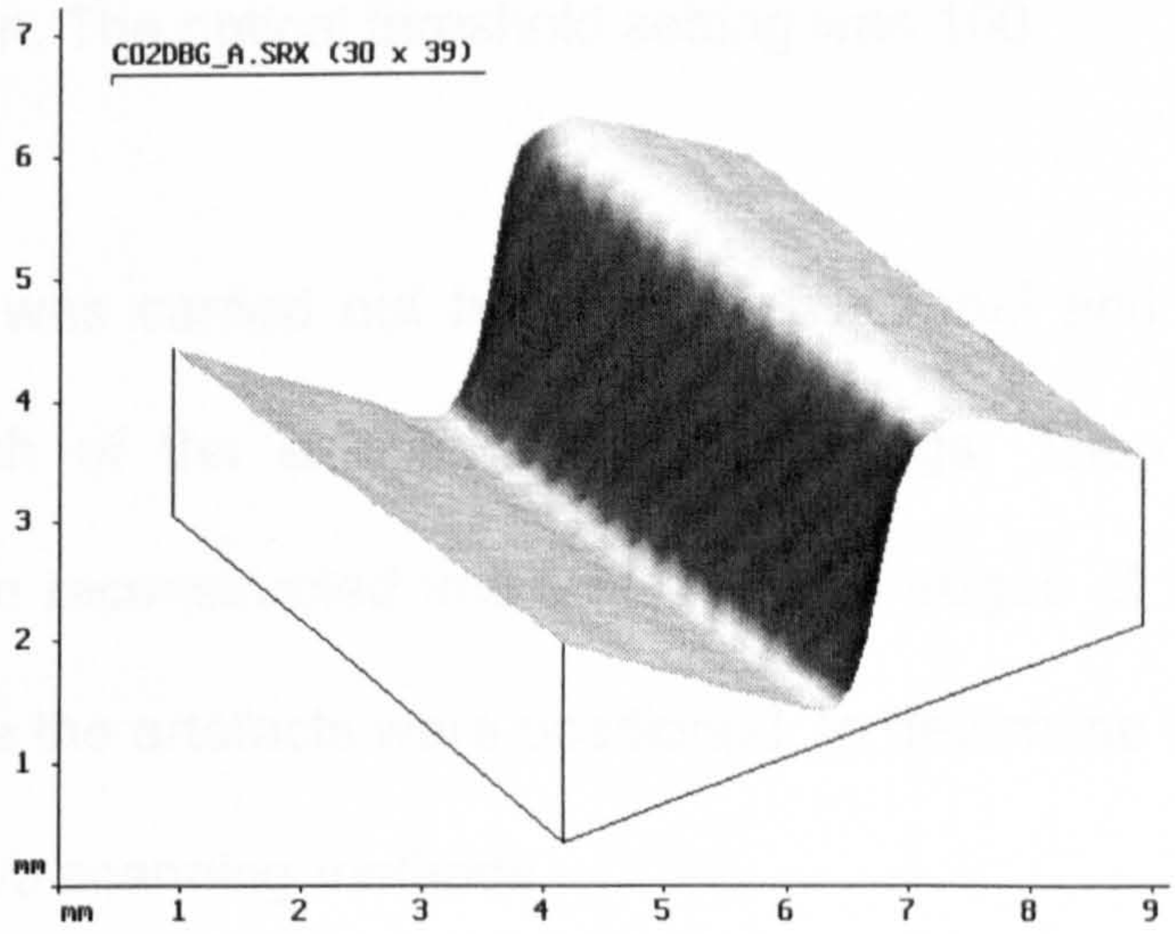

Figure 2-3: A "zigzag" phenomenon is revealed in a bi-directional scanned image.

A "zigzag" phenomenon has been observed at the edge of deep slopes when bi-directional scans was carried out (Fig.2-3). Bi-directional scanning was the only scanning mode provided by the manufacturer of the system. An impression (Extrude, medium viscosity, blue; Kerr, USA) was taken of a 2mm corrugated surface. Sampling intervals of 0.040mm, 0.100mm and 0.200mm were selected to scan the impression. The scanning speed used was 10 points per second; scan area was 8mm×8mm; probe orientation was set to maintain the optical plane perpendicular to the scanning

direction. The scanning direction was set in two modes, one was bi-directional where the probe moved up and down the corrugated steps during the scanning procedure, and other was uni-directional where the probe moved in 'up-steps' only during digitisation, and movement in the opposite direction was used only to return the probe to its next scan starting position. The optical threshold setting was 100.

Superposition was carried out between bi-directional and uni-directional scans for each of the sampling interval settings. Then profiles were calculated from reconstructed images along the edges of the corrugated surfaces where the artefacts were positioned, to determine the differences between the two scanning methods.

2.4.2 Scanning pitch, scanning speed and optical threshold setting

A standard sphere 25mm in diameter was provided by the manufacturer of the CMM. It was selected to investigate optimal digitisation parameters, because it was a standard object with known diameter and form, and also provided a curved geometry. As this sphere was quadrant symmetrical, a digitisation length of radius 12.5mm was defined, then five sampling intervals of 0.1mm, 0.125mm, 0.165mm, 0.25mm and 0.5mm were selected to scan a quadrant sphere. These intervals relate to 125, 100, 76, 50 and 25 data points in a length of 12.5mm. The differences between these scans were then examined against the standard quadrant sphere.

Six scanning speeds were selected as 5, 10, 20, 30, 40, and 50 (maximum possible speed, IMS user manual) points per second, and four optical threshold settings 100, 400, 800 and 1200 were investigated.

2.5 Results

2.5.1 Bi-directional and uni-directional scanning

Following the digitisation procedure, a set of X, Y and Z co-ordinates were obtained as shown in Fig.2-4(a). At every (X, Y) position a value of Z was measured. From this set of data a 3-D surface was interpolated (Fig.2-4, b), and was orientated (Fig.2-4, c) and analysed.

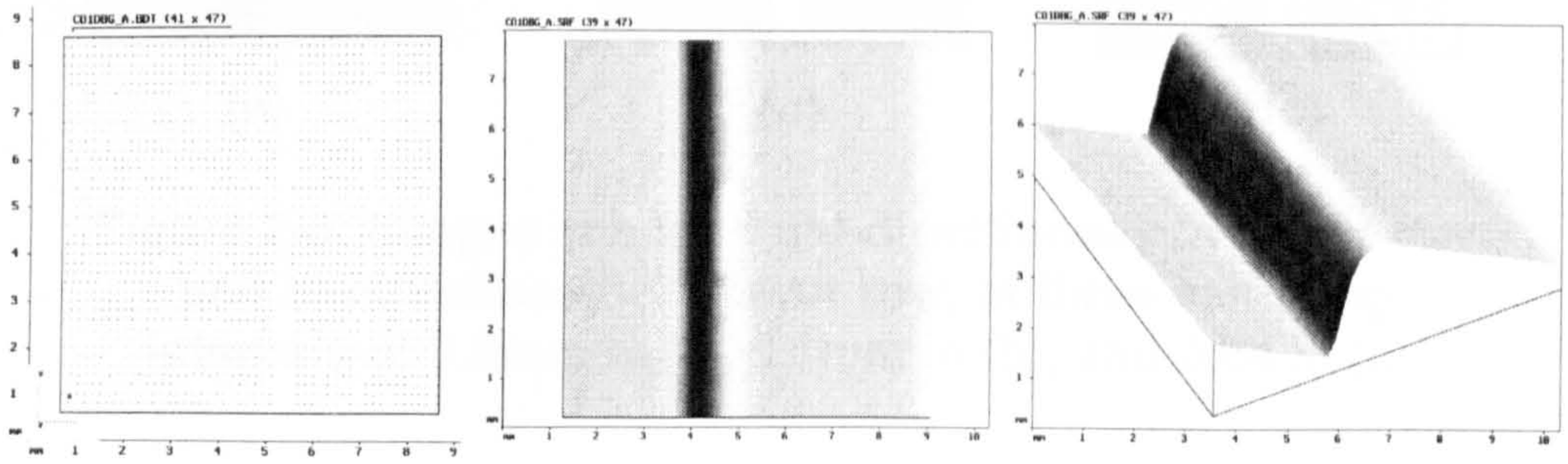

Figure 2-4: A set of co-ordinates obtained from digitisation (a), it was then interpolated into a surface (b), and this image was orientated at an angle (c) for a better visualisation.

Fig.2-5 shows three pairs of images, scanned at three sampling intervals of 0.2mm (a), 0.1mm (b) and 0.04mm (c). They were scanned uni-directionally in the top row and bi-directionally in the bottom row. Although

these images have been digitised from the same impression, the smaller sample interval provided greater surface detail; and more importantly, a 'zig-zag' artefact was clearly seen on the bi-directional scans (lower row) at the edge of the step.

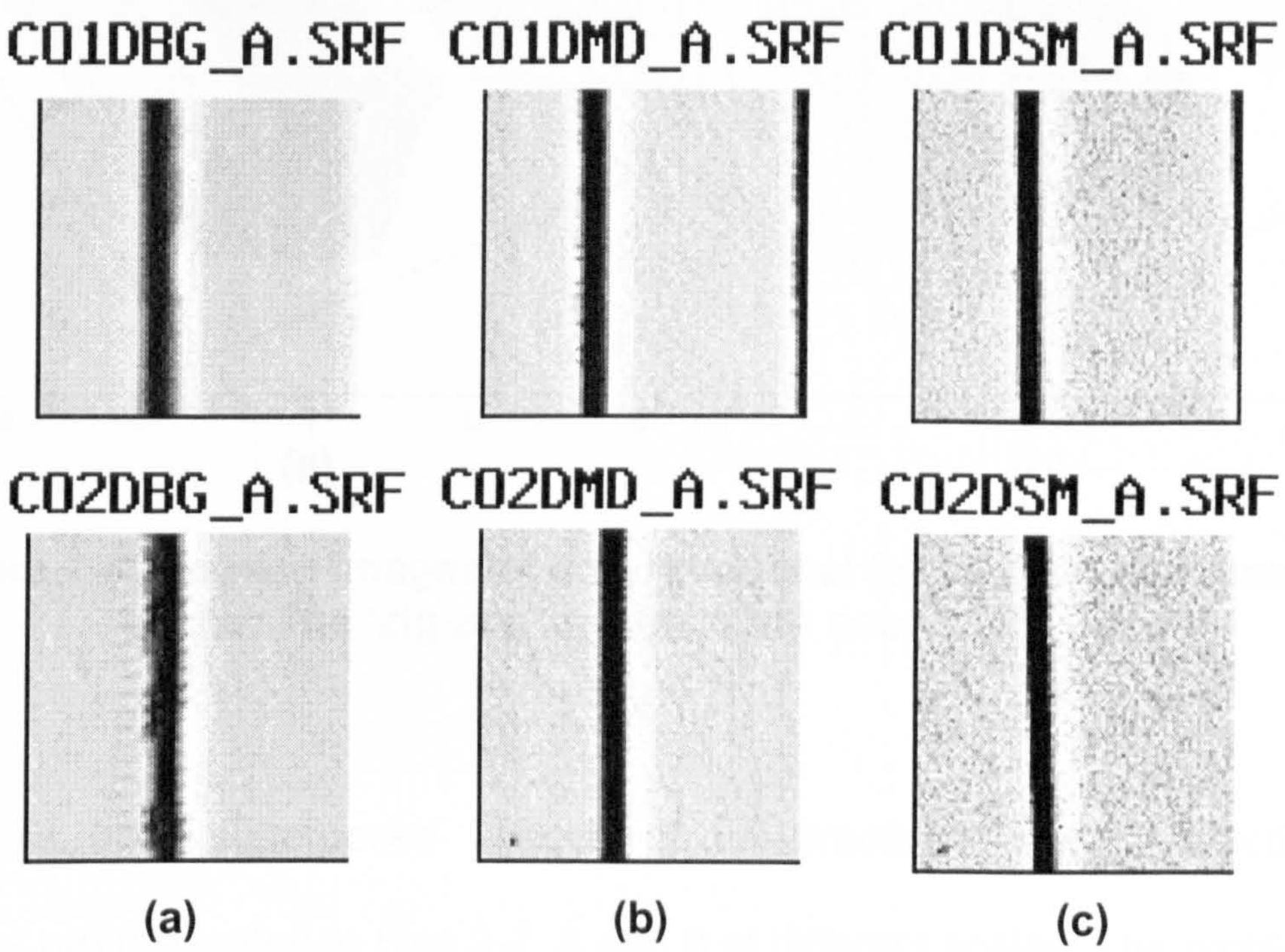

Figure 2-5: Images scanned uni-directionally in upper row and bi-directionally in lower row, at three sampling intervals of 0.2mm in (a), 0.1mm in (b), and 0.04 in (c).

To make these 'zig-zag' artefact more obvious, the images have been rotated, and are shown in pairs of uni-directional and bi-directional scan images in Fig.2-6.

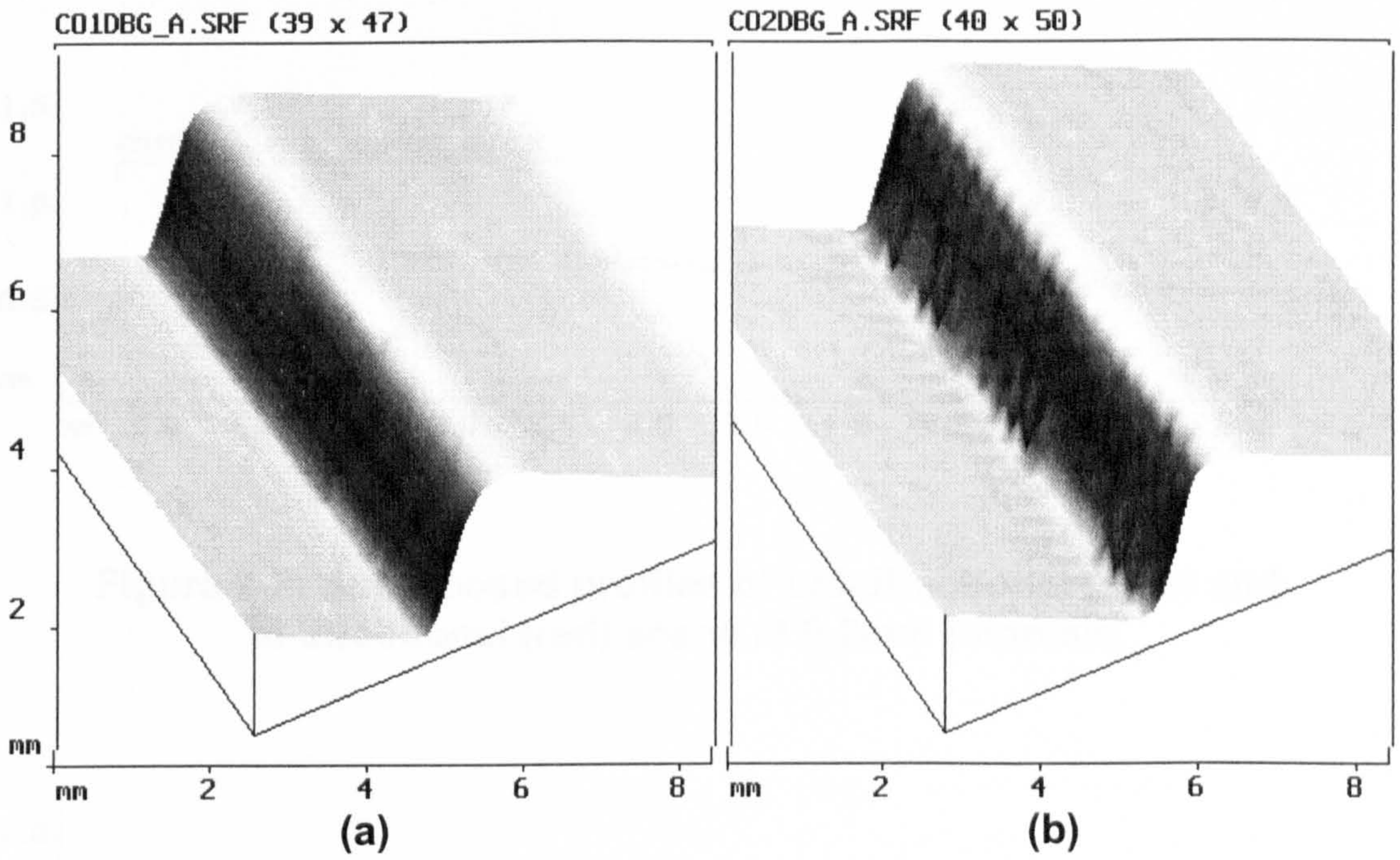

Figure 2-6: Rotated images of uni-directional (a) and bi-directional (b) scans; The 'zig-zag' artefacts are seen in (b) only.

Profiles from superposed images of uni-directional and bi-directional scans are presented in Figs.2-7, 8 and 9 at different scales. The profiles in red represent the cross sections from bi-directional scans, whilst the blue ones represent the cross section from uni-directional scans. These clearly show that the variation bands of the "zig-zag" artefacts are related to the sampling interval. Larger sampling intervals resulted in a larger variation band of 'zig-zag' artefacts. The wavelength of the artefacts indicated that one wavelength related to one cycle of "up and down the step" in the bi-direction scans, which explained how these peaks and valleys of Z measurement were obtained. The uni-directional scans showed no such phenomena at the edges.

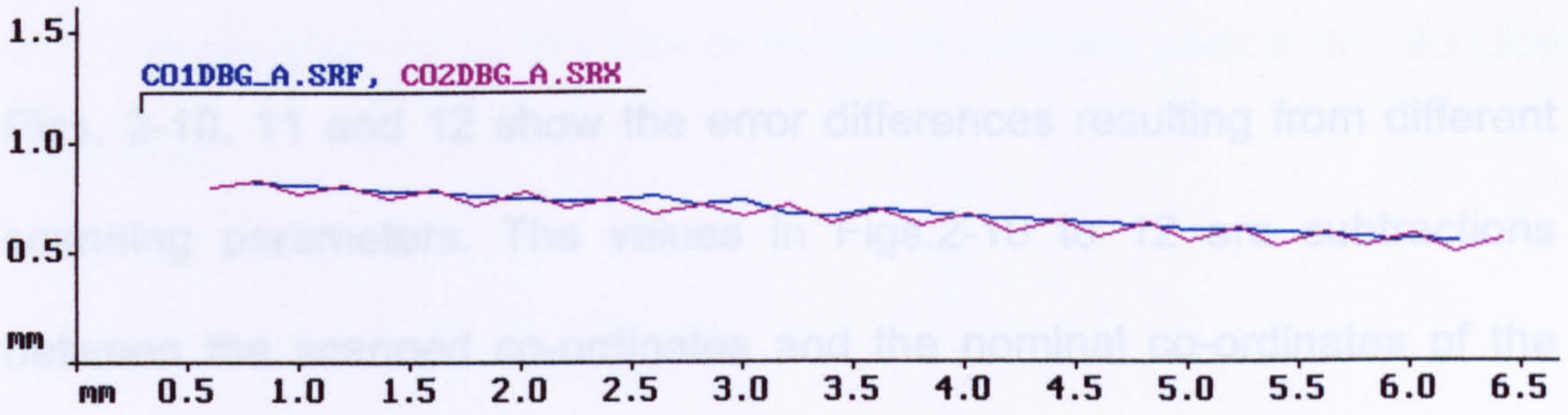

Figure 2-7: Superposed profiles of uni-directional (blue) and bi-directional (red) scans at 0.2mm intervals.

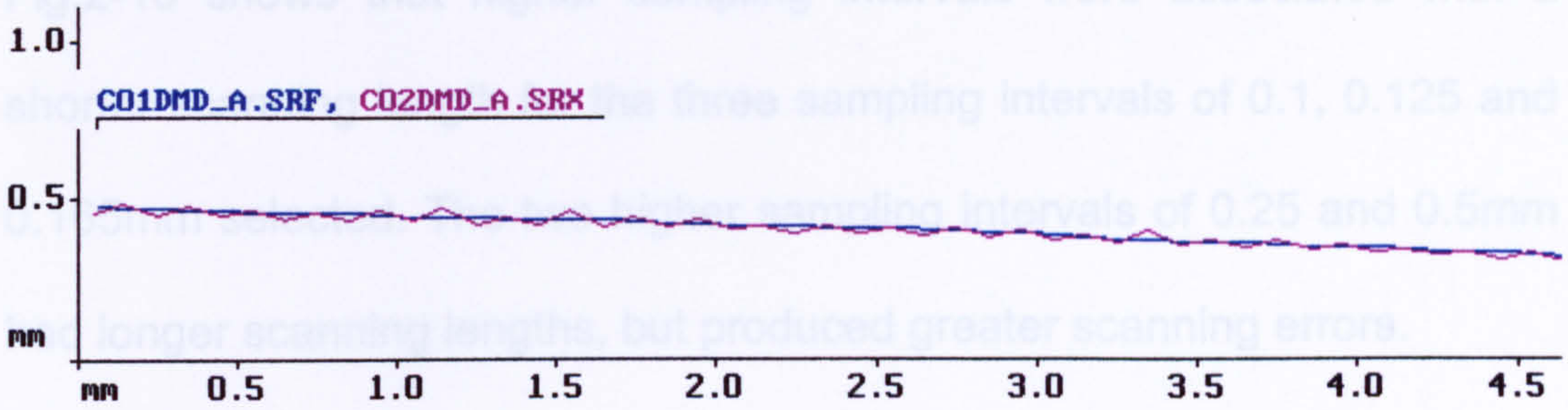

Figure 2-8: Superposed profiles of uni-directional (blue) and bi-directional (red) scans at 0.1mm intervals.

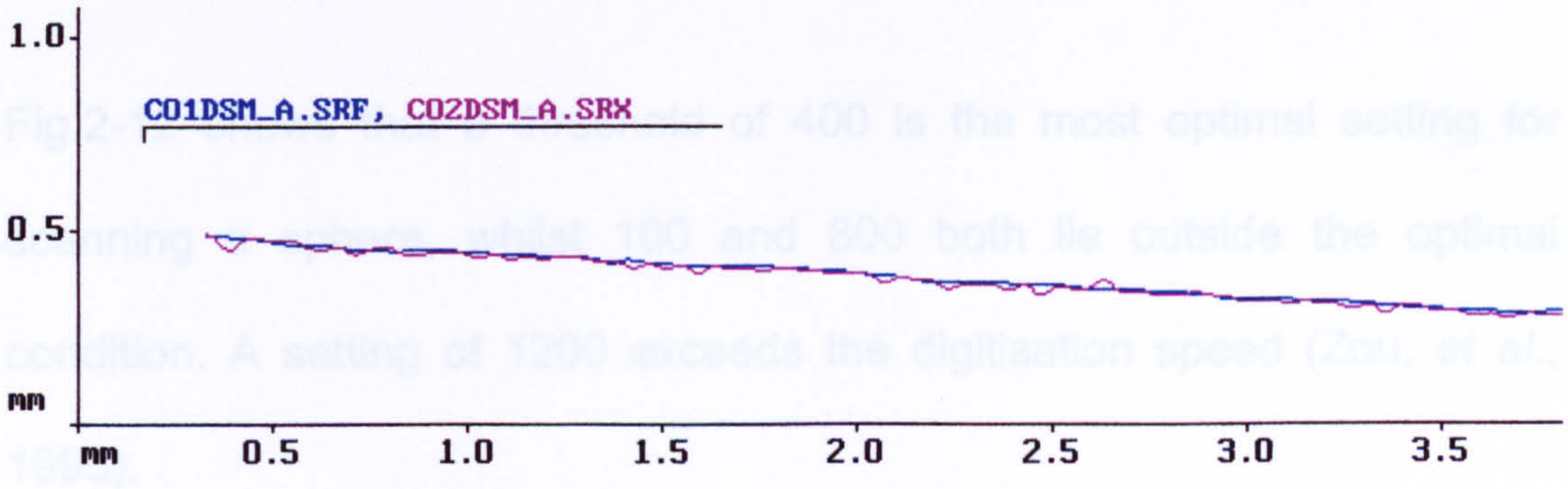

Figure 2-9: Superposed profiles of uni-directional (blue) and bi-directional (red) scans at 0.04mm intervals.

2.5.2 Sampling interval, scanning speed and threshold setting

Figs. 2-10, 11 and 12 show the error differences resulting from different scanning parameters. The values in Figs.2-10 to 12 are subtractions between the scanned co-ordinates and the nominal co-ordinates of the standard sphere. It was concluded from Figs.2-10 to 12, that the scanning parameters employed should be those that produced the smallest error.

Fig.2-10 shows that higher sampling intervals were associated with a shorter scanning length for the three sampling intervals of 0.1, 0.125 and 0.165mm selected. The two higher sampling intervals of 0.25 and 0.5mm had longer scanning lengths, but produced greater scanning errors.

Fig.2-11 shows that a slower speed has a longer scanning length within the same error band, and faster speed has a shorter scanning length.

Fig.2-12 shows that a threshold of 400 is the most optimal setting for scanning a sphere, whilst 100 and 800 both lie outside the optimal condition. A setting of 1200 exceeds the digitisation speed (Zou, *et al.*, 1995).

The wavy effect on all of the scanning results represents the surface roughness, as this standard diffused sphere had been sand blasted to

improve the diffusion of light. The wavelength of the surface roughness was directly affected by the size of the sand particles used in the surface treatment.

Figure 2-10: Digitisation errors related to sampling intervals (PCH).

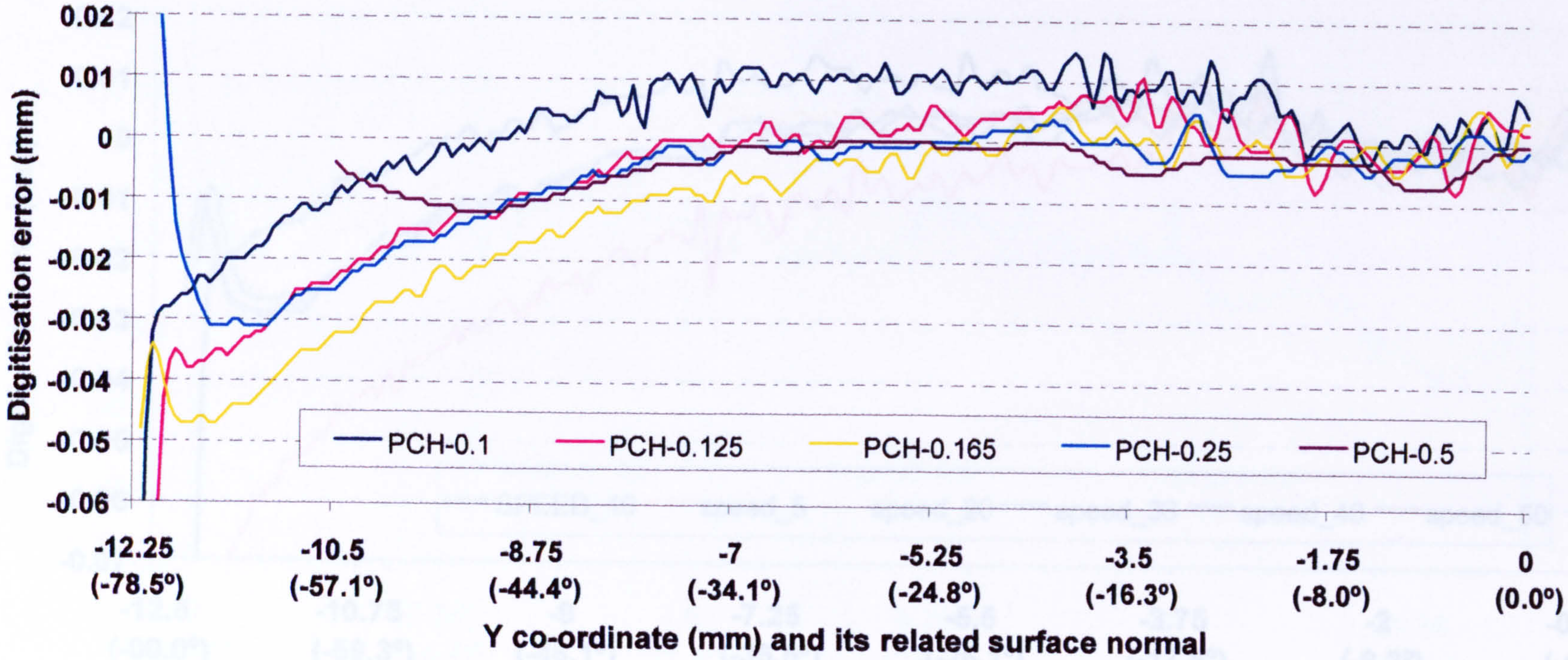

Figure 2-11: Digitisation errors related to scanning speeds.

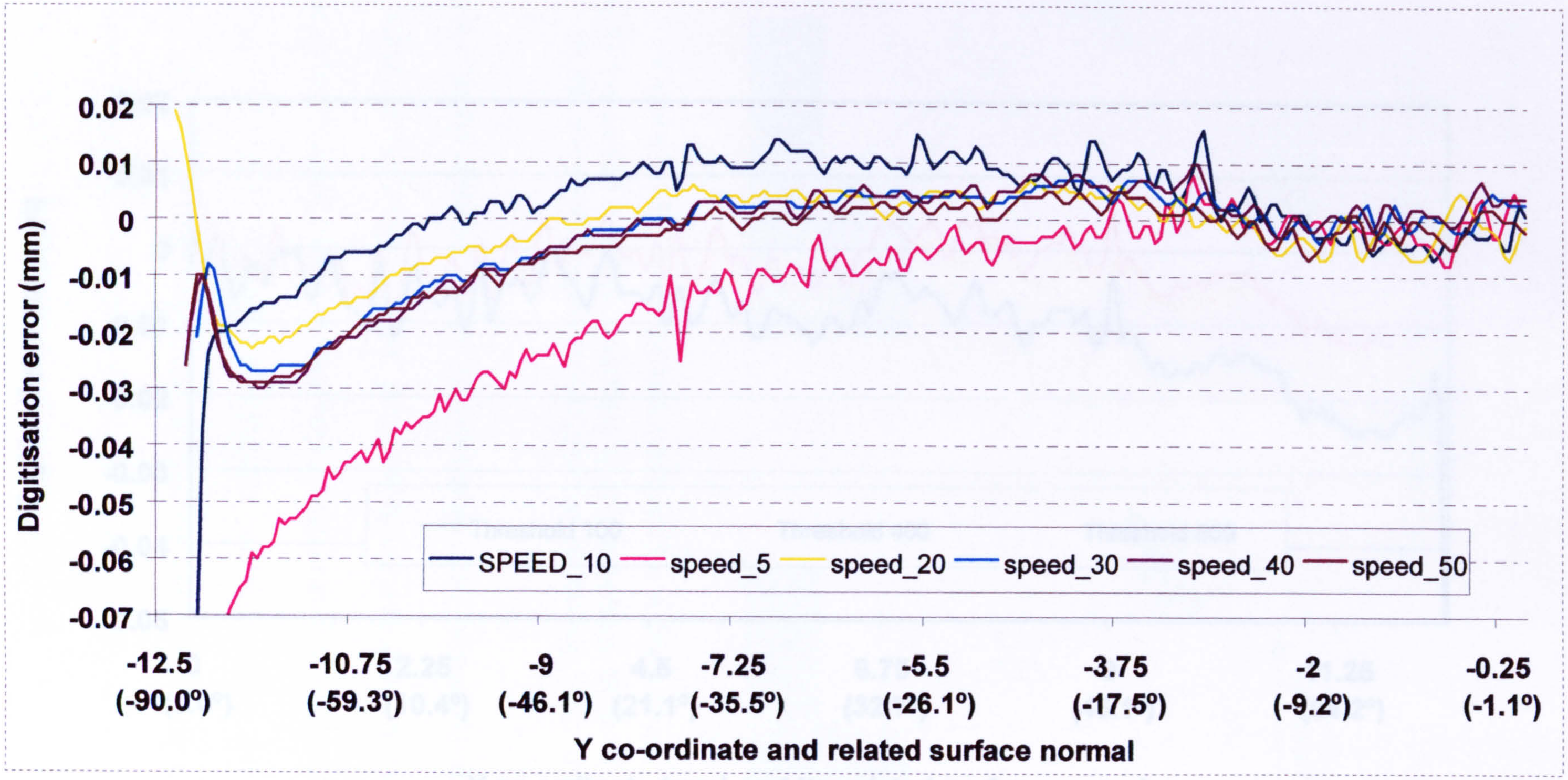

Figure 2-12: Digitisation errors related to threshold settings.

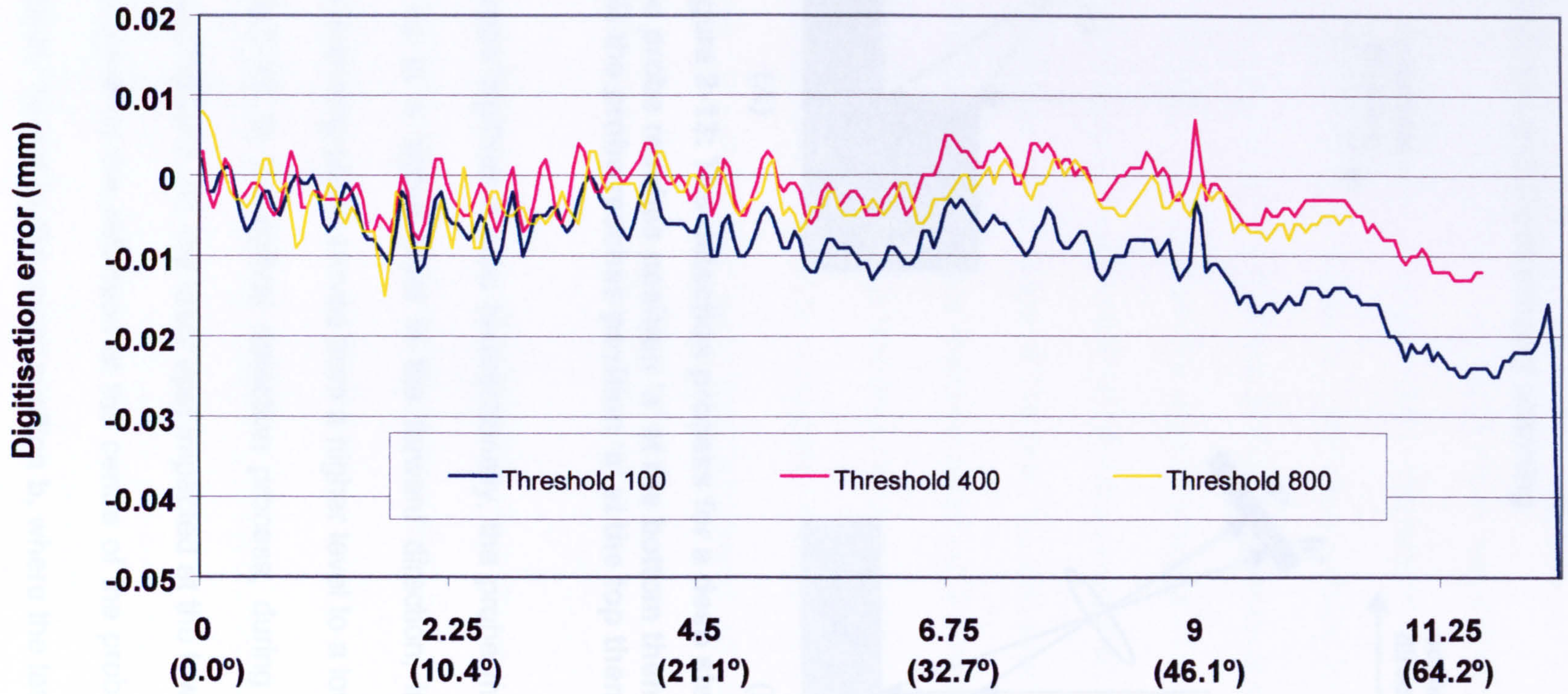

2.6 Discussion

2.6.1 Bi-directional and uni-directional scanning

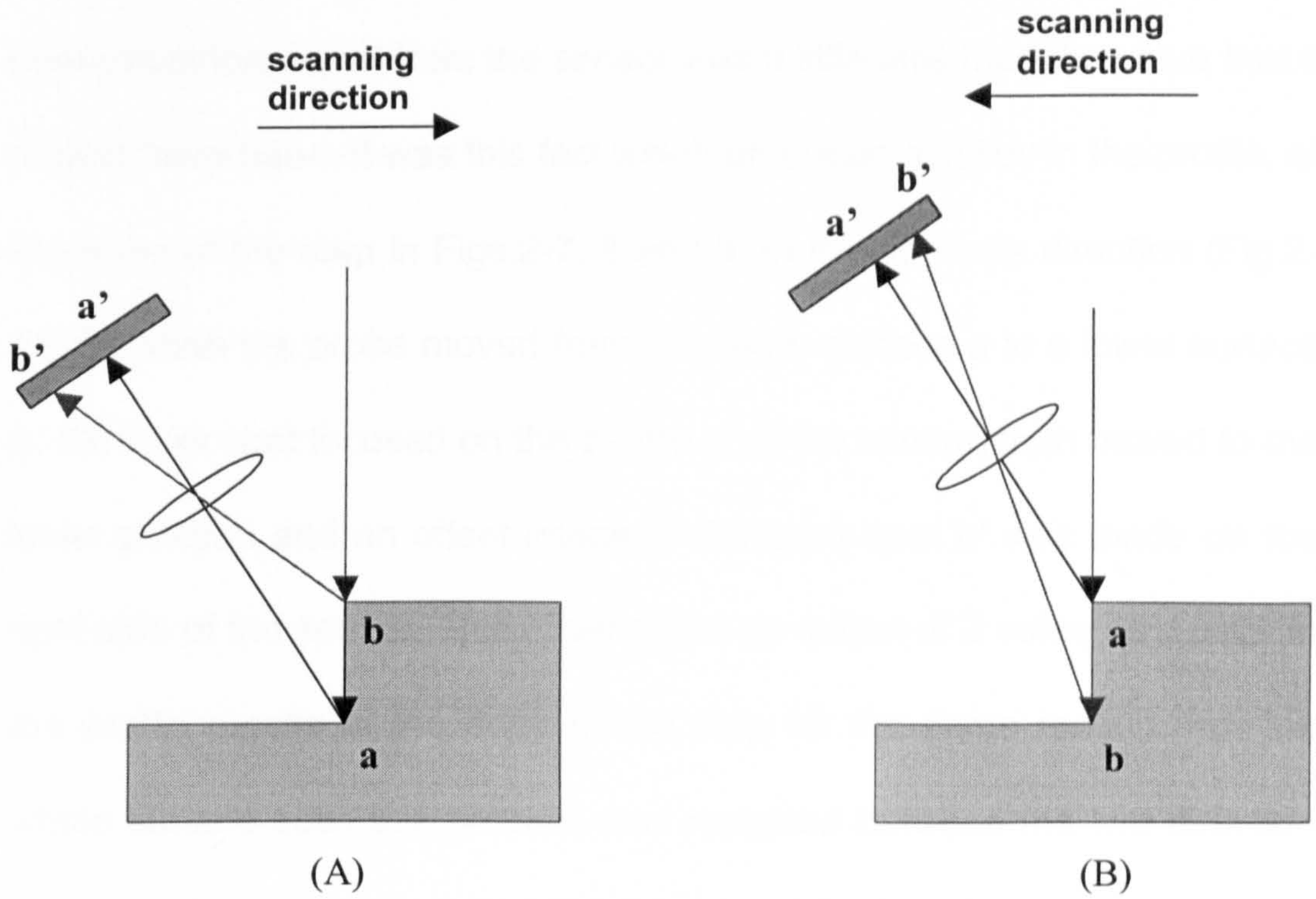

Figure 2-13: The detection process for a deep step.
In (A) the probe reaches position 'a' at the bottom then 'b', and in (B) the probe reaches position 'a' at the top then 'b'.

When the probe digitises a step bi-directionally, the probe moves from a lower level up to a higher level in the forward direction, in the return direction the scanning probe moves from a higher level to a lower level, as shown in Fig.2-13. In the optical detection process, during the forward direction scan (Fig.2-13, A), the laser spot impacted at the lower surface **a** and it was imaged by the reflection at the centre of the probe sensor **a'**, then immediately moved to the upper position **b,** where the laser spot was

imaged on left side **b'** of the photoelectrical sensor. Because of the large movement at the step, there was insufficient time allowed for the probe to adjust its focus, and to make an output of the Z value. The Z value of a photoelectrical signal from the sensor was a little less than the value that it should have been. It was this fact which produced a valley in the profile, at the edge of the step in Figs.2-7, 8 and 9. In the opposite direction (Fig.2-13, B) when the probe moved from the upper surface **a** to a lower surface **b**, the laser spot focused on the centre **a'** of the sensor, then moved to the lower position and an offset image of the laser spot **b'** was made on the right side of the sensor. This offset made an output of Z value as a peak in the profile results at the edge of the step for the same reason. For the whole surface scan this process was repeated between the two direction scanning lines, and a "zigzag" error was introduced into the scanning results.

During uni-directional scanning, the deviation from these up and down movements was reduced to at least half, as seen in Figs.2- 7, 8 and 9.

2.6.2 Sampling interval, scanning speed and threshold settings

The procedure of an optical digitisation process involves complex interactions between the mechanical transportation of the CMM, the optical and electrical signal transactions and the computer controls.

Collaborations in microprocessors are precise in a dynamic mode. The settings of operator-variable parameters directly influence the microprocessors. For example, when an instruction for the digitisation of a point is executed, the probe accelerates to a travelling speed as a system default, moving in a direction which is parallel to the surface, then decelerates to approach the target position, and stops at the digitising point; probe motion then changes towards the surface normal in a probing direction and at a probing speed, which is often slower than the probe travelling speed. Normally when measuring the height of the surface, the probing direction is in the '-Z' direction, and the travelling direction is in the X or Y direction to form a surface area. The probing speed is much slower than the travelling speed, as it executes a focussing process of 'up' and 'down' movements of the probe to estimate the surface height until it is automatically focused within the working range of the instrument. The probe then waits for the next instruction, and meanwhile the optical probe impacts the incident on the surface, and collects the diffused reflections, then adjusts the focus position following an instruction from the sensor until the probe is focussed on the surface and passes a signal to the computer to record the X, Y and Z co-ordinates into the memory.

A smaller sampling interval and quicker scanning speed requires more frequent interactions, and these may be compatible or incompatible with

the parameter settings. For example, in the sampling interval investigation, when large intervals of 0.5mm were used, the probe spent too long in movement and less time on the important focus procedure, and this resulted in the digitisation being terminated at the side of the sphere in a shorter scan distance. The sampling interval of 0.1mm had the longest scan length and smallest digitisation error, which can be recognised as an optimal setting.

Following the same theory, the optimal speed should be 10 points per second and the threshold setting may be within the range of 100 to 400 units. A higher value of optical threshold setting reflects a higher signal/noise ratio. Thus, within the allowable range, the higher value of optical threshold value provides a better condition of quality control in digitisation.

2.6.3 Applications in Dentistry

2.6.3.1 Digitisation of buccal tooth surfaces

The buccal surfaces of teeth are often measured, for example, to examine the progression of the accumulation of bacteria or plaque over a specified time, also to investigate wear and erosion under controlled circumstances, and in the assessment of root caries and its treatment.

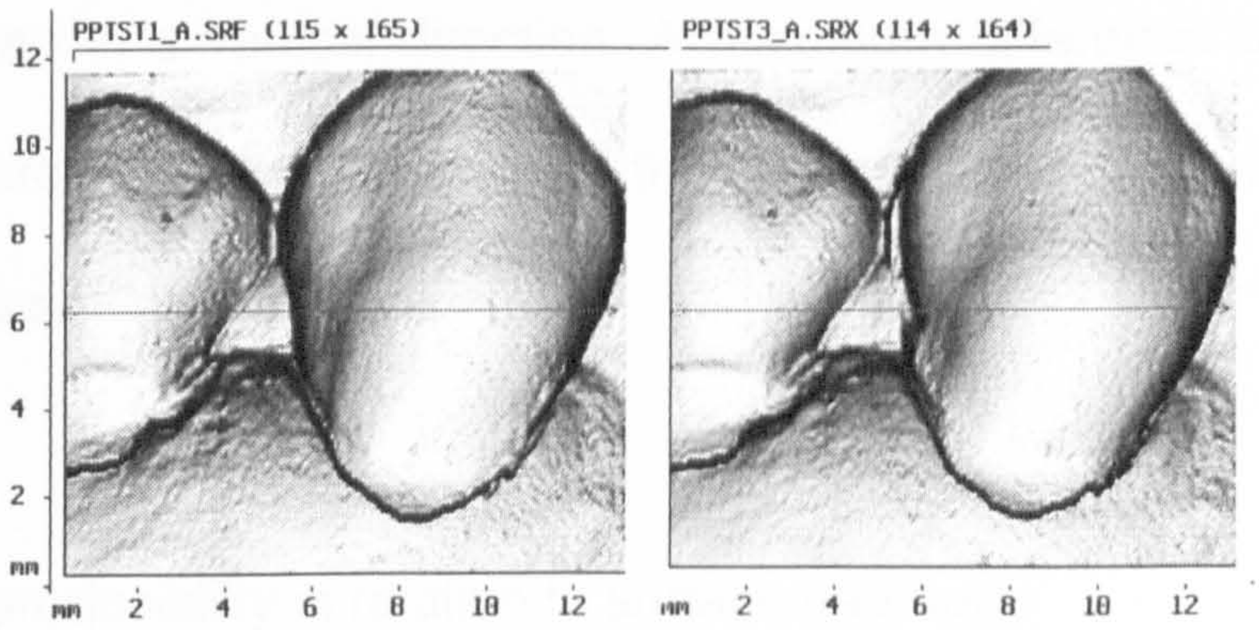

(a) (b)

Figure 2-14: Two images scanned from one impression using different scanning directions.

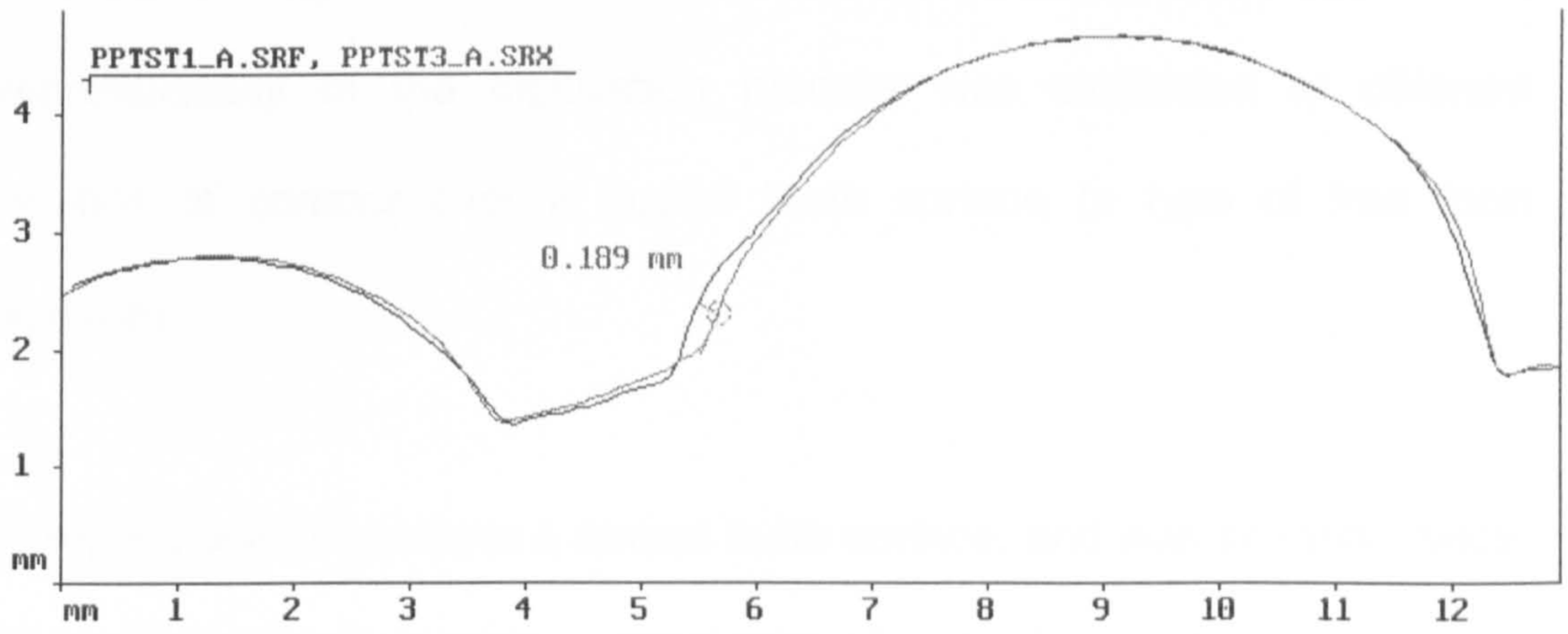

Figure 2-15: Two cross section profiles obtained from superposed images in Fig.2-14. A max. difference of 0.189mm was revealed.

When a buccal tooth surface is scanned, the incident light spot is likely to be distorted at both sides of the tooth. If such a situation occurs in the scanning direction, the quality of the digitising procedure is reduced. It can be improved if such conditions can be avoided by defining the scanning direction in a rather smooth change of direction. For example in Fig.2-14, the contour along a single line changes more rapidly in a horizontal

direction than in a vertical direction. A maximum difference of 0.189mm was measured (Fig.2-15) between the scan images from vertical and horizontal scanning directions.

2.6.3.2 Reproducibility in relation to surface geometry

The complexity of the surface contour is one of the factors influencing digitisation reproducibility. Especially in concave regions, multiple reflections may be formed randomly by ambient illumination. The reproducibility of the digitisation process was examined at different regions of contour over a buccal tooth surface (a type of free form surface).

A replica was taken from a buccal tooth surface, and was scanned twice, under the optimal scanning parameters of vertical scan direction, 0.1mm scan pitch, 10 points per second scanning speed, and 200 units of optical threshold.

Comparative measurements at different regions over the surface were analysed as shown in Figs.2-16 to 21.

These comparative assessments indicated that a better reproducibility was obtained in the smoother regions of the surface as Fig.2-18 reveals

where the reproducibility is 4.0μm. In contrast, at regions with an irregular surface contour, the system produced a poor reproducibility as shown in Fig.2-19, where the reproducibility is 6.7μm. The other areas also measured are shown in Figs. 16 to 21. The reproducibility measurement values given in the captions to each Figure to show the visual relationship between the images and measurement values.

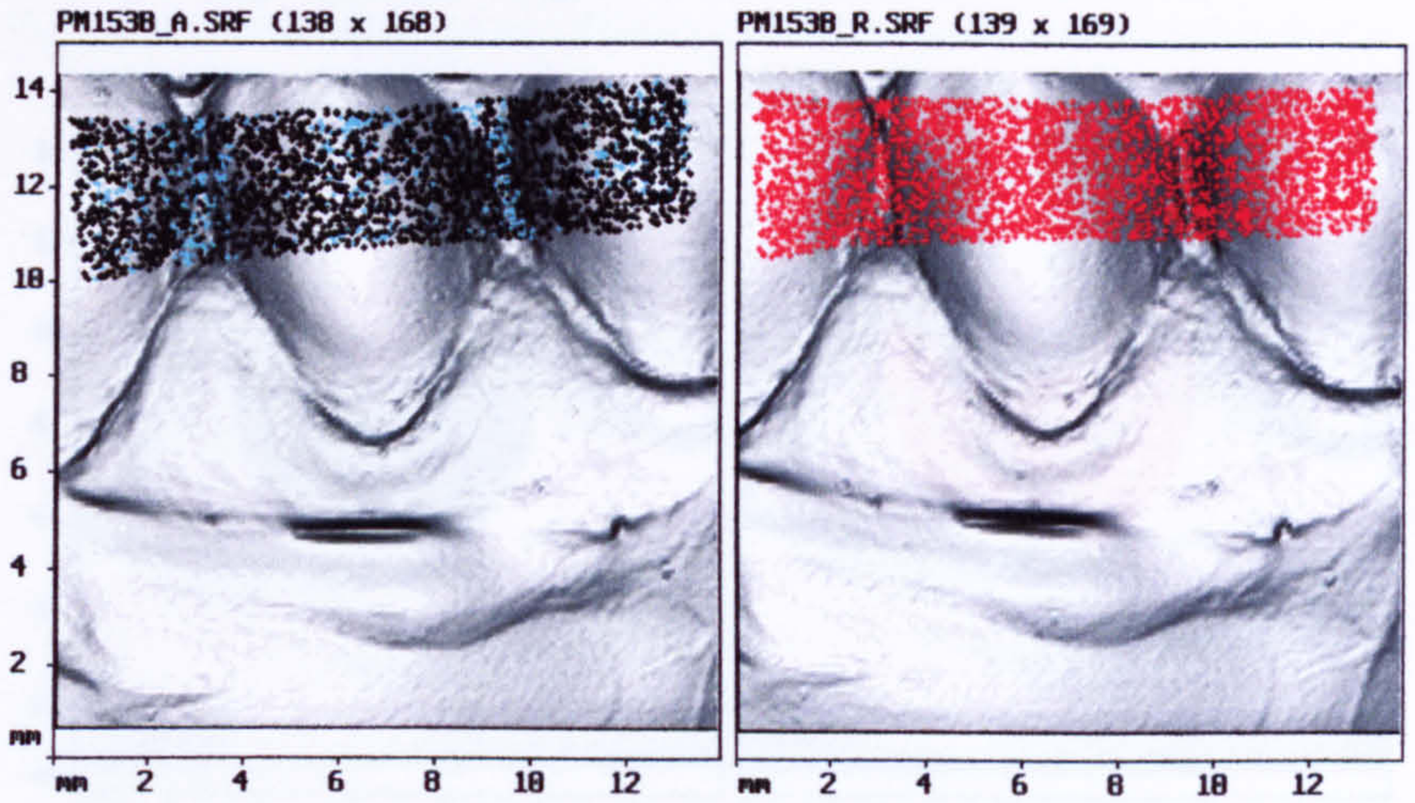

Figure 2-16: Reproducibility at the incisal area of the teeth: 4.9μm.

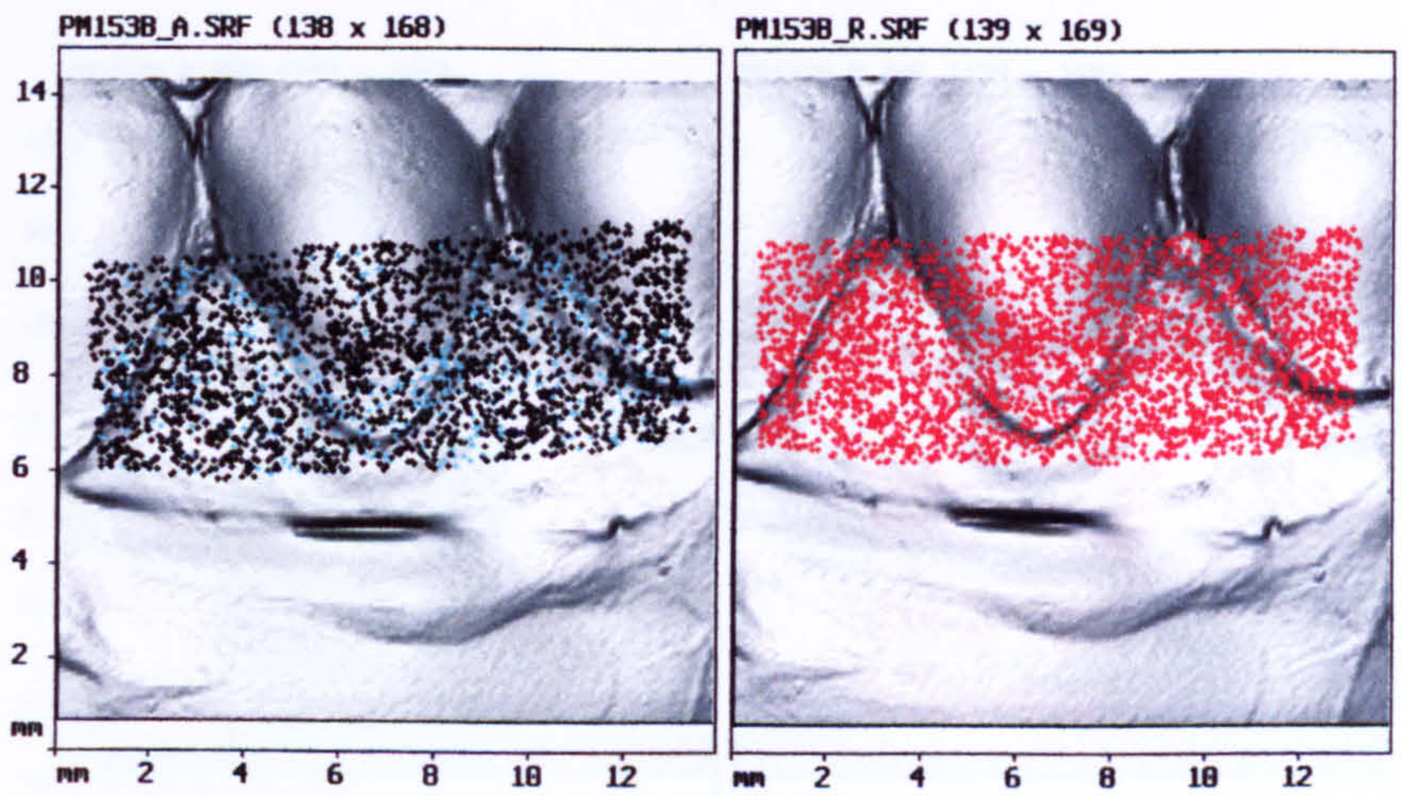

Figure 2-17: Reproducibility at the gingival area of the teeth: 6.0μm.

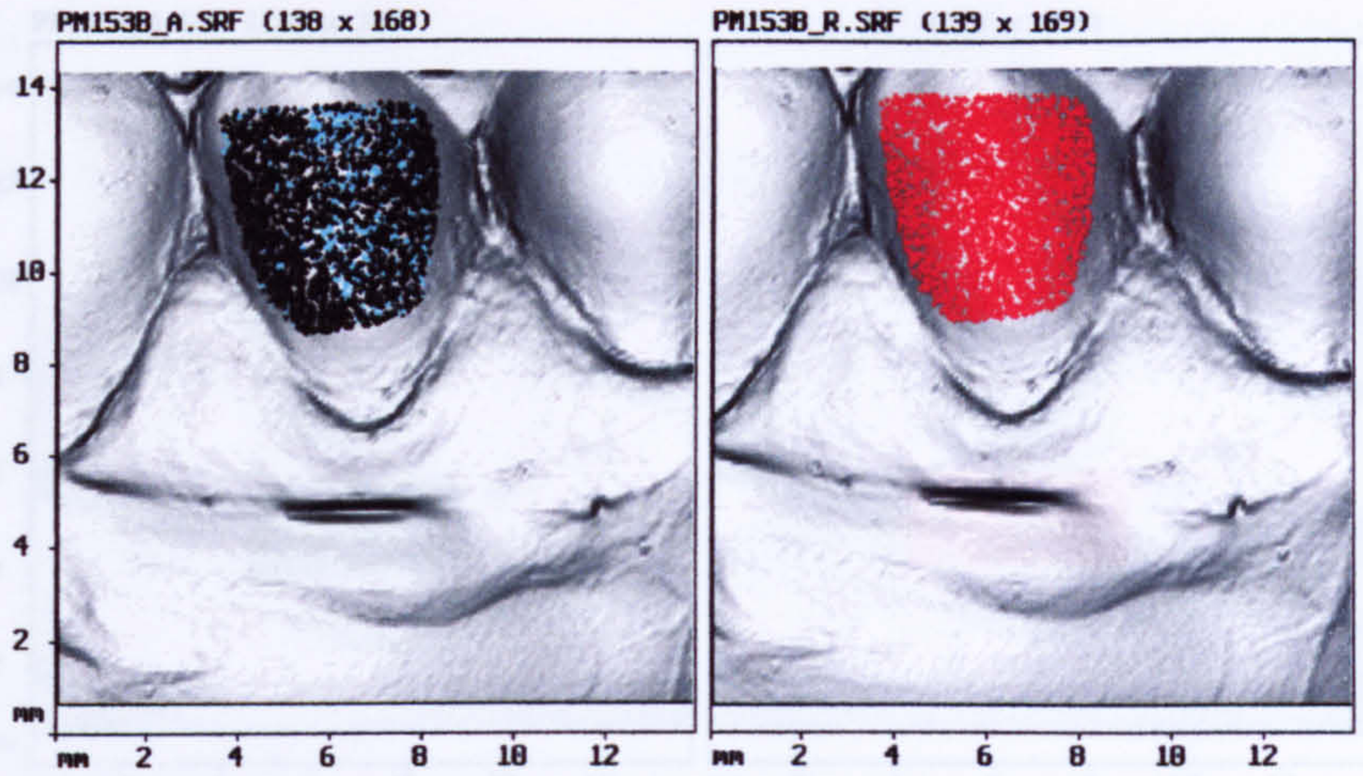

Figure 2-18: Reproducibility at mid-labial area of the teeth: 4.0µm.

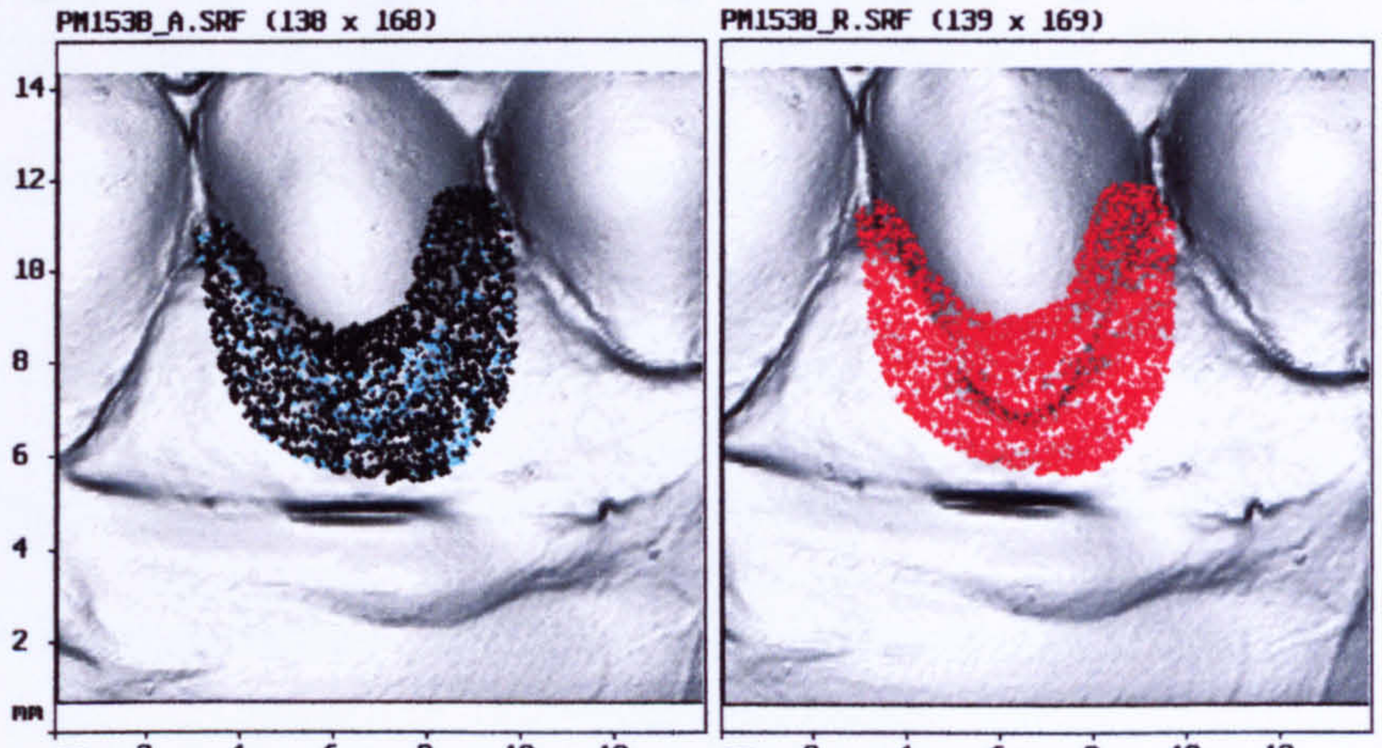

Figure 2-19:Reproducibility at the gingival margin of the teeth: 6.7µm.

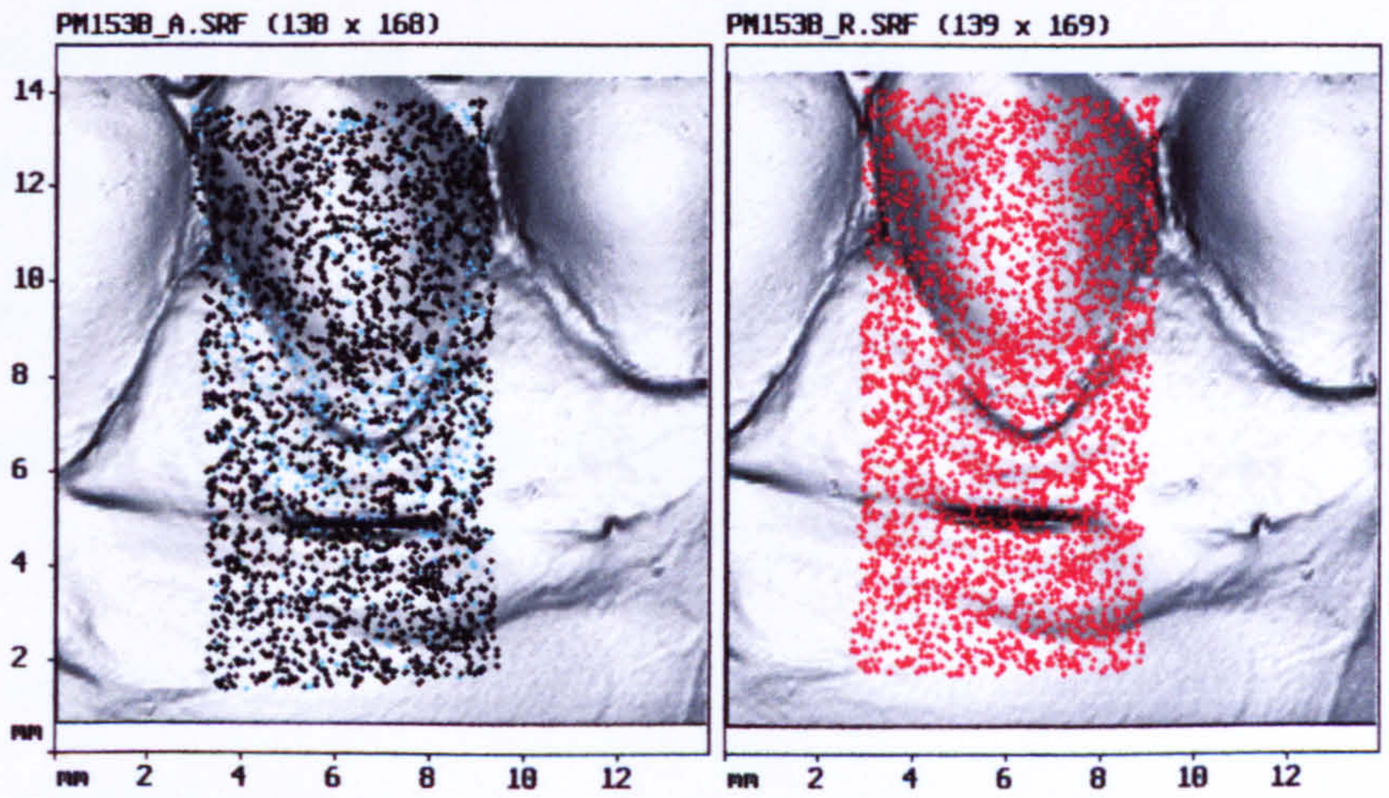

Figure 2-20: Reproducibility at the region of tooth and gum: 5.5µm.

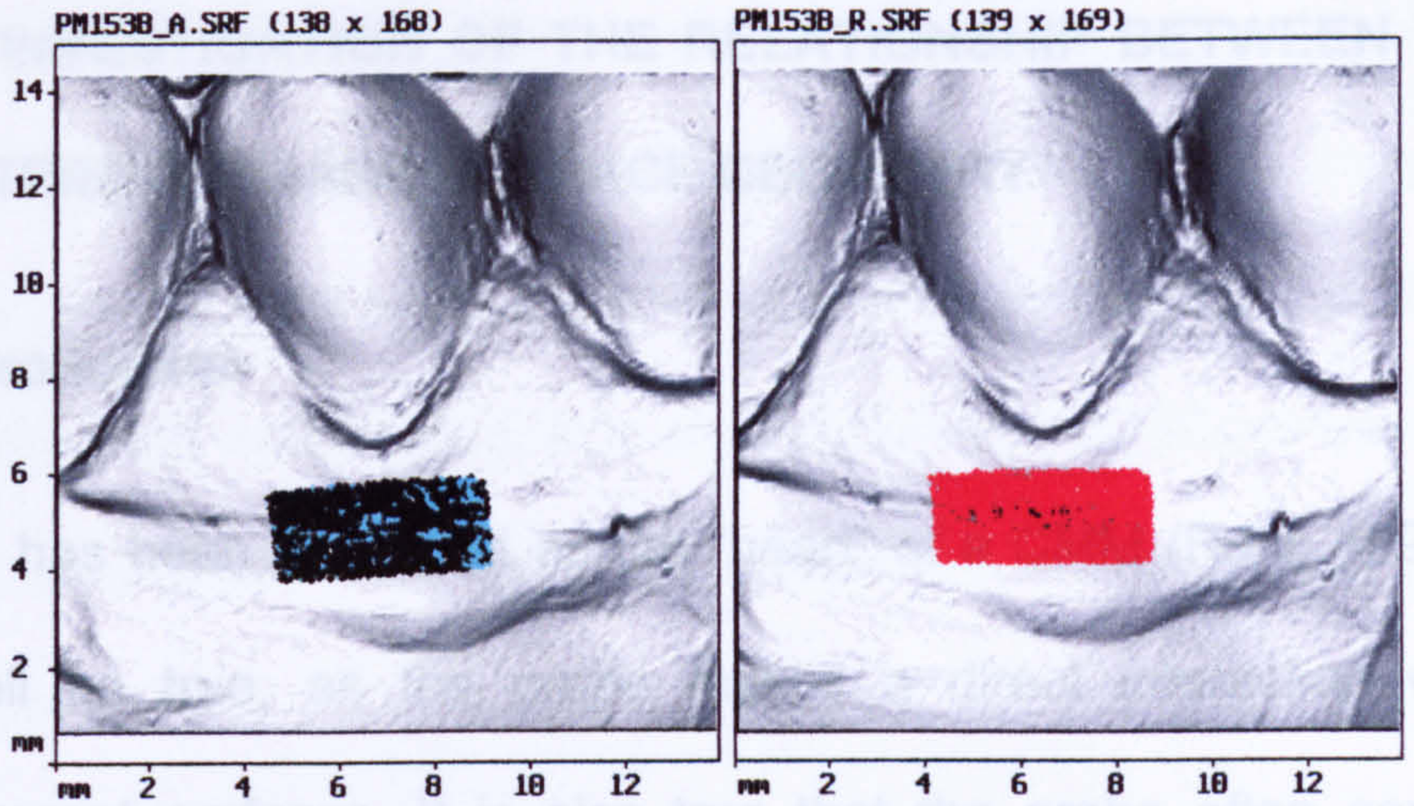

Figure 2-21: Reproducibility at the gum region: 4.9µm.

3 AN INVESTIGATION OF THE RELATIONSHIP BETWEEN ERROR DISTRIBUTION AND SURFACE GEOMETRY

3.1 Introduction

A probe has been described as the "heart" of a CMM (Reid, 1995). This may well be true, as the probe makes a direct interaction with the measurement surfaces. It is also true that the probe often contributes larger errors than the combined errors of the rest of the system (Butler, 1991; Yang and Butler, 1996; Mainsah *et al.*, 1995, 1996).

Although optical probes have been in use for almost two decades, and despite the popularity of optical probe-based techniques, they are still very much under-represented in National and International Standards (BS6808 1987, ISO1032-2 1994). Information, for example, on calibration is not readily available and many have used the stylus model for calibration of an optical probe. Hence, a 'non-standardised' situation is revealed for optical probe specifications stated by manufacturers. It is essential, as part of future research, that optical probe calibration becomes the subject of well defined International Standards.

Several researchers have attempted to evaluate the uncertainty of optical measurements (Lartigue *et al.*, 2002; Feng *et al.*, 2001, Dorsch *et al.*, 1994; Hoppe *et al.*, 1992; Baribear and Rioux, 1991; Bes, 1998).

However, their researches were related to a specified optical probe over a particular region on industrial work parts, which had been designed as geometrical or smooth surfaces. In fact, no general evaluation method has been published, and indeed, it is difficult to suggest a general method which is appropriate to cover all the optical circumstances that might be encountered.

The optical triangulation-based probe is largely influenced by the topography of the surfaces being measured, as it relies on the reflection of incident light from the surface. Both lack of reflection or multiple reflections can confuse the photoelectrical sensor and result in a faulty reading. To quantify such influences as digitisation error in respect of the relationship between optical axis and surface geometry, error distribution over a standard sphere has been investigated in this Chapter.

A method of assessment and calibration of an optical probe using a sphere (D=22mm) for surface texture measurement was recommended by Mainsah *et al.* (1996). It was at almost exactly at the same time that the author carried out a similar test on a standard sphere (D=25mm), but was concerned with free form surface measurement (Zou *et al.*, 1996(a)). Using a standard sphere as an analytical object has advantages over other traditional gauges, such as a length bar, step gauge or ring gauge. It

is superior in assessing the maximum measuring height and length, as it provides a continuing geometrical change across its surface. It also offers all possible slopes and can be probed from all directions. A standard sphere possesses an absolute measure (the diameter) and no alignment is needed because of its shape.

3.2 Materials and methods

A standard diffused sphere supplied with the CMM was selected for this investigation. This sphere has a precisely known diameter of 25mm±0.003mm (IMS, UK, at 20°C±2°C).

The following scanning parameters were used in the investigation: scan pitch = 100μm; measuring speed = 1mm/s; threshold level = 100; with the probe orientations shown in Fig.3-1. The probe triangulation plane is in the XOZ plane of the CMM machine space, and the incident laser beam forms an angle of 35° with the reflected beam to the photoelectrical detector.

3.2.1 The design of the investigation

Scanning the sphere in four directions of –X, +X, -Y and +Y using the same probe orientation was employed, as it provides four different optical phenomena, in terms of the geometrical relationship between reflections from the sphere and position of the sensing device.

(1) In the -X scanning direction, the diffused reflection was towards the probe sensor, and the optical plane (defined by the incident beam and the reflection beam) was in line with the probe motion plane. That was the direction recommended by the manufacturer; an accurate scan length is the arc of 60° between the probe orientation and the surface normal, which is equivalent to the scan length in the X direction of 12.5×sin(60°)=10.825mm.

(2) In the +X scanning direction, the diffused reflection was away from the probe sensor and there was no advice in the user manual to guide the use of the probe in this situation.

(3) In +Y and (4) –Y directions, the optical plane (XOZ) was perpendicular to the probe motion plane (YOZ), and the diffused reflections were neither towards nor away from the probe sensor, but proportional reflections were detected by the sensor. Again, no explanation of scanning under these conditions was given in the user manual.

3.2.2 The stages of the scanning procedure

(1) A square area of 2mm×2mm at the top of the standard sphere was scanned. A program was written to compare the Z value of all these scanned points, and to specify the upper most point “T” on the sphere,

which has the highest Z value. This point "T" was defined as the origin of the sub co-ordinate system in CMM space.

(2) Starting from the upper point "T" (0,0,0), one probe orientation of zero in each orientation axis was used to scan four profiles in the directions of +X, -X, +Y, and -Y. These four directions tested four different optical situations of the optical axis and surface geometry (Fig.3-1).

The scanning program allowed the scans to run for as long as necessary, until the probe sensor could sense no more signals, then the digitisation procedure stopped. The scan lengths in each direction represented the farthest distance that the probe could function at the specified probe orientation.

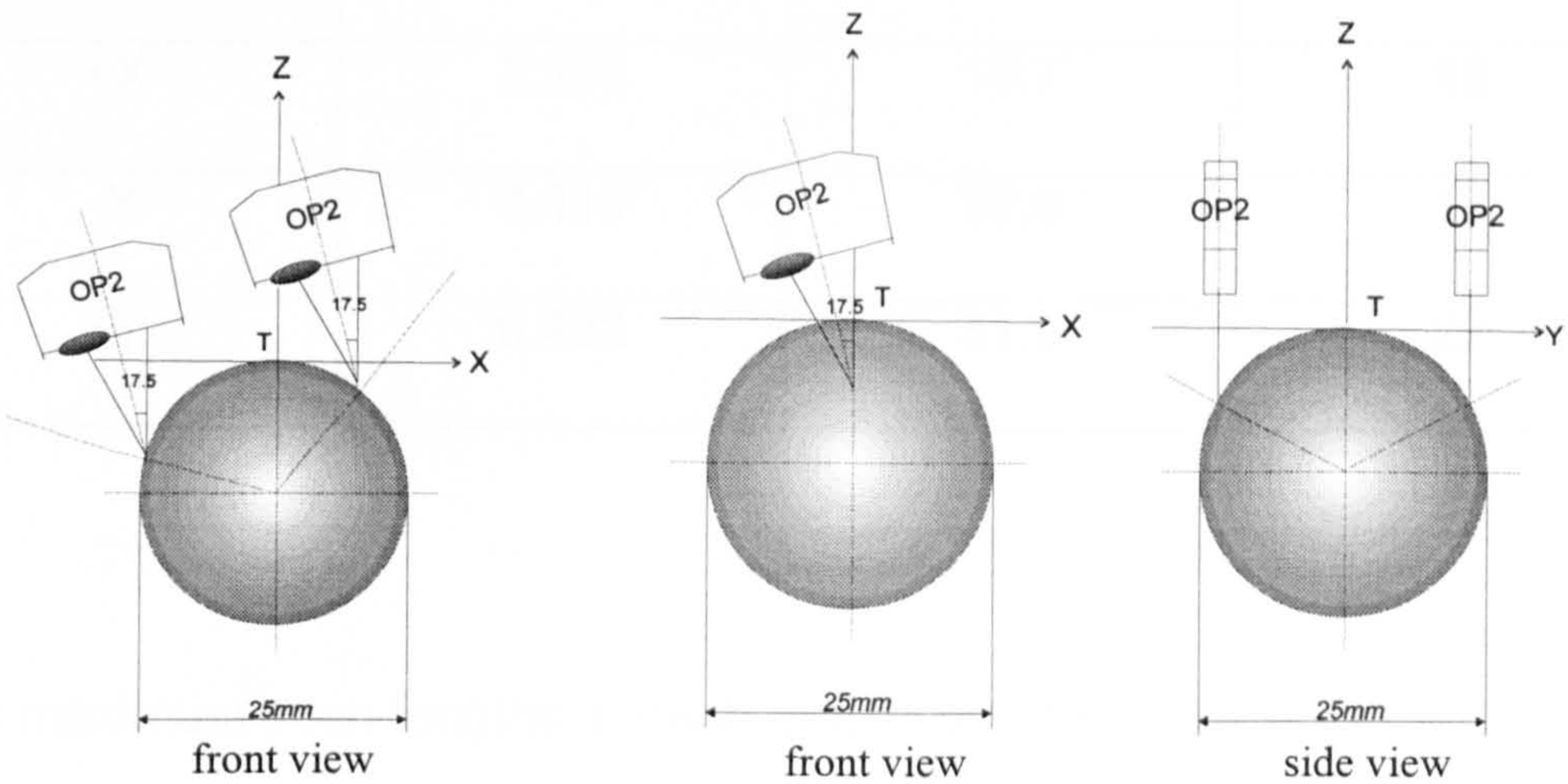

Figure 3-1: The probe orientations along the X directions (a) and Y directions (b and c).

3.2.3 Error distribution analysis

The digitisation error was analysed by superposing reconstructed profiles against the theoretical profile with known dimensions and calculating the difference between the two. Line charts were then employed to present the error distributions in each direction.

3.3 Results

Table 3-1: Max. scan length (mm) and the relevant angle(°) between surface normal and probe axis at the position of max. scan length, with the relevant digitisation error:

Direction	Max. Scan Length (mm)	Max. angle between normal & probe in relation to Max. scan length (°)	Max. error (μm)
-X	**10.153**	**54.3**	**130**
+X	**3.392**	**15.7**	**18**
-Y	**6.412**	**30.9**	**16**
+Y	**6.492**	**31.3**	**22**

The maximum scan lengths in each of four directions were: (1) 10.153mm in -X, (2) 3.392mm in +X, (3) 6.412mm in -Y and (4) 6.492mm in +Y, and are shown in Fig.3-2.

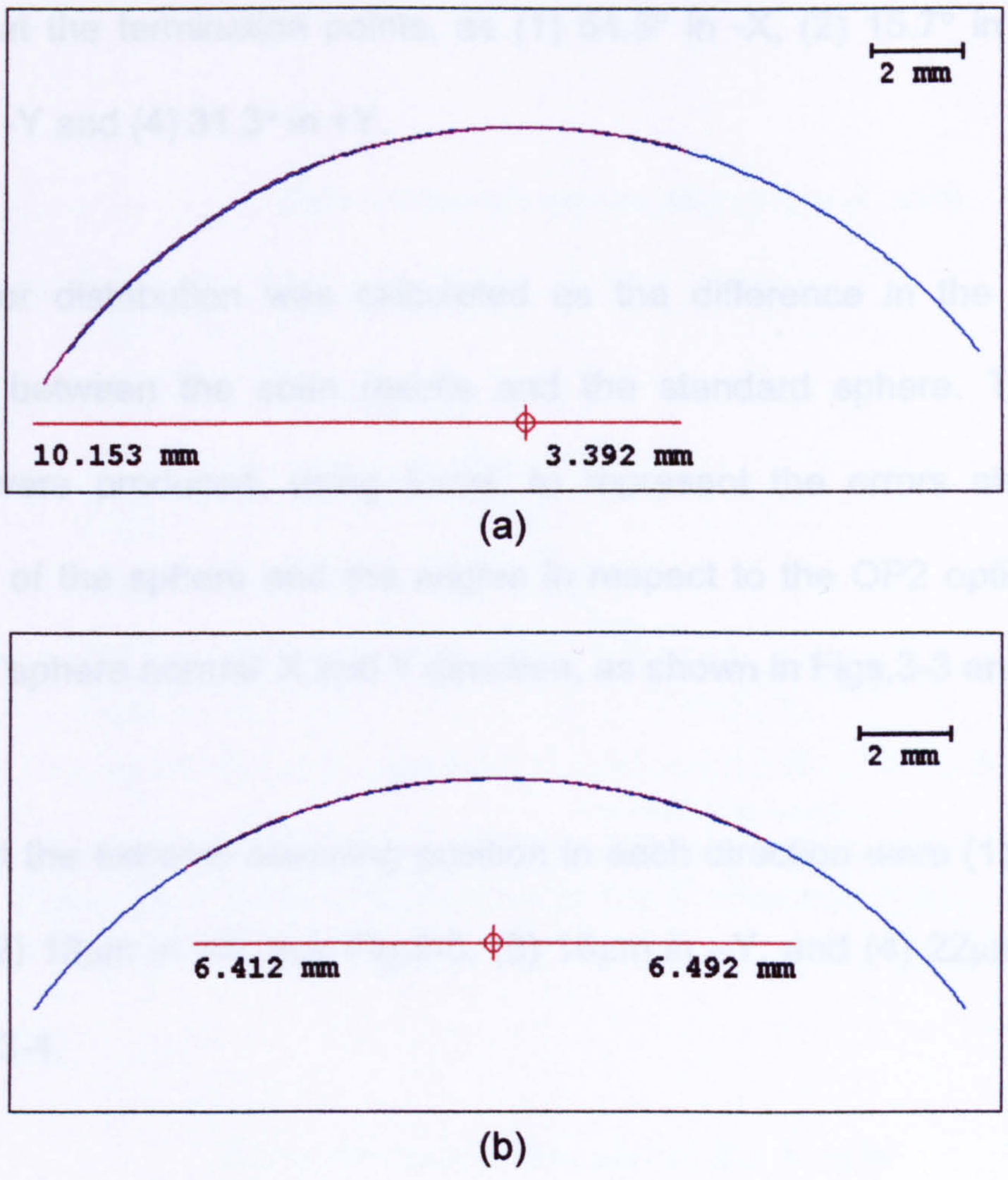

Figure 3-2: Superposed scanning profiles (red) and standard sphere profiles (blue).
(a) in X direction and (b) in Y direction.

Fig.3-2 shows the scanning results in X and Y directions superposed onto a standard sphere. Although direct results were obtained for these maximum scan lengths, they in fact reflected the optical relationship between the reflections and the surface topography at the farthest scanning positions in the four directions. They were determined in respect of the angles between the optical axis of the OP2 probe and sphere

normal at the termination points, as (1) 54.3° in -X, (2) 15.7° in +X, (3) 30.9° in -Y and (4) 31.3° in +Y.

The error distribution was calculated as the difference in the 'sphere normal' between the scan results and the standard sphere. Two line charts were produced, using Excel, to represent the errors along the position of the sphere and the angles in respect to the OP2 optical axis and the 'sphere normal' X and Y direction, as shown in Figs.3-3 and 3-4.

Errors at the extreme scanning position in each direction were (1) 130μm in –X, (2) 18μm in +X, see Fig.3-3, (3) 16μm in –Y, and (4) 22μm in +Y, see Fig.3-4.

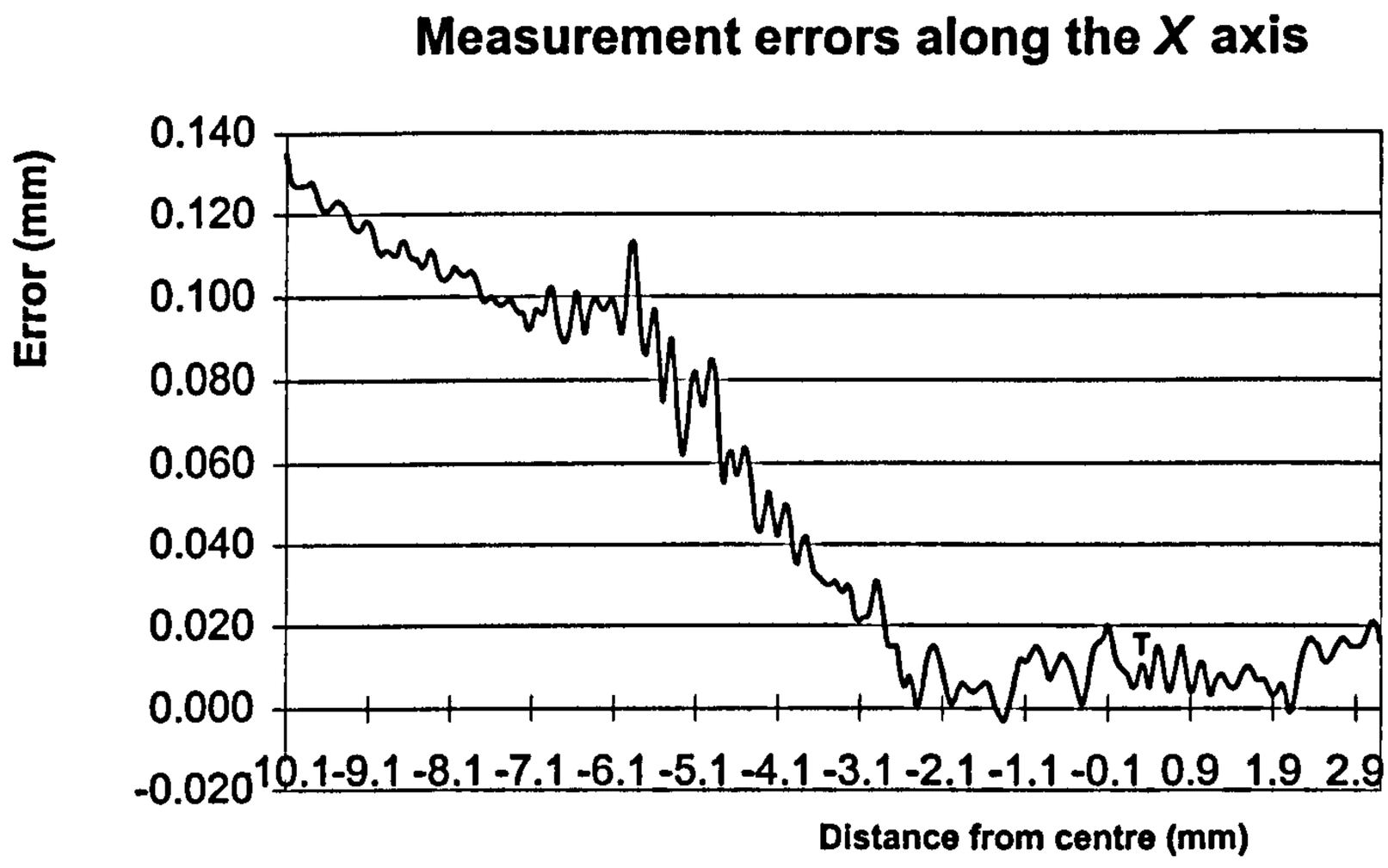

Figure 3-3: Error distribution in the X direction (mm).

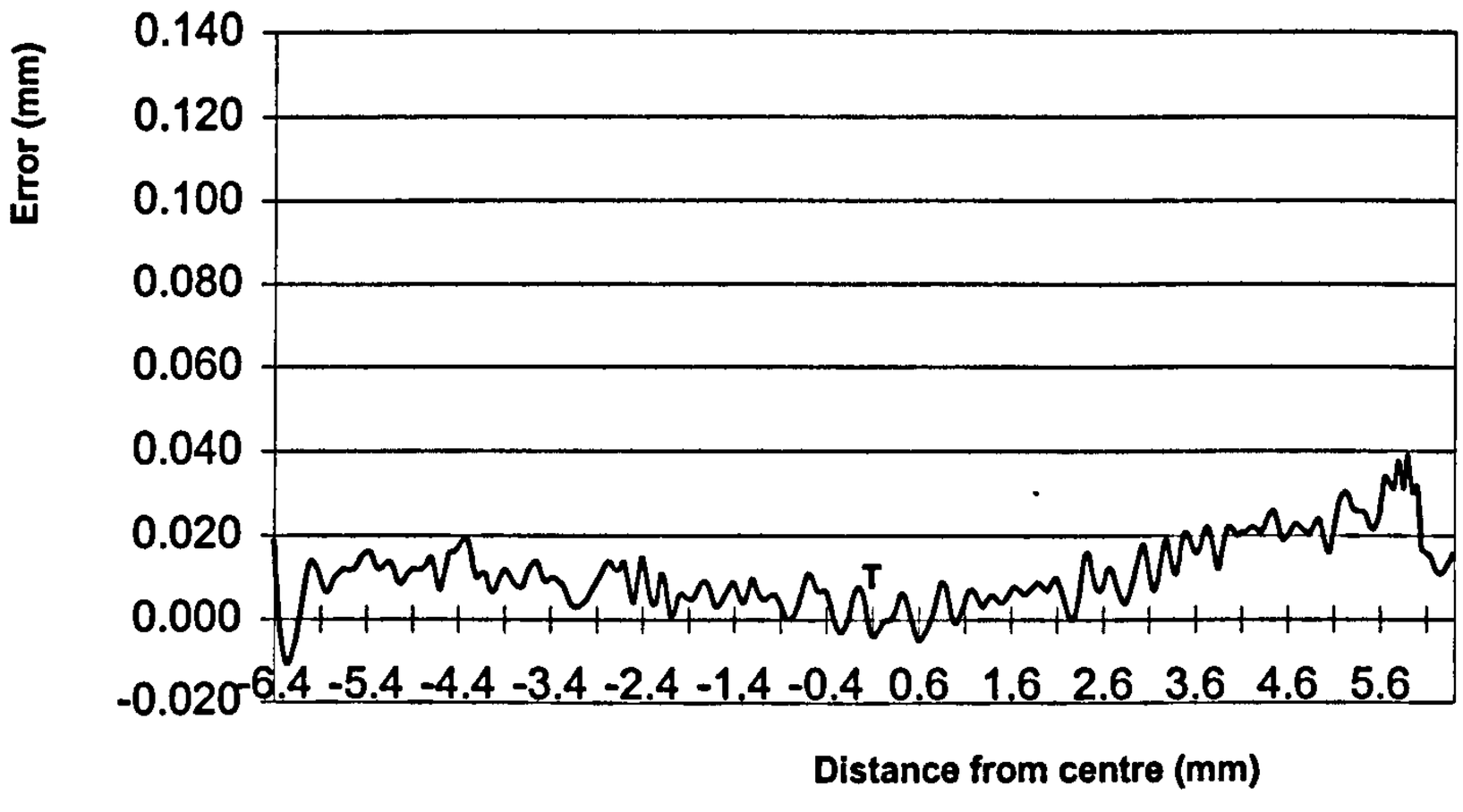

Figure 3-4 Error distribution in Y direction (mm).

3.4 Discussion

The scanning length in -X of 10.153mm was almost equal to the expected value of 10.825mm, but the digitisation error of 130μm was considerably higher than the value of ±10μm given in the user manual. In +X, despite this not being a recommended arrangement, from the result shown in Fig.3-3, there is still a short scanning distance of 3.392mm with small errors of ±10μm; the reason for such errors is that the reflecting beam moves away from the probe detector, and causes a termination at the extreme position. In the X scanning direction the error started to increase after a scan length of 2.6mm, which was caused by the degradation of the laser spot image at the probe sensor.

The situation was different in the Y direction, because the probe sensor had been set to a mutual state, which made the probe to move neither towards nor away from the surface normal, and the optical plane of the probe was perpendicular to the probe scanning direction. This presented a better reflection situation and the intensity of the reflection beam to the sensor, consequently the errors in this direction were much smaller than in the X direction. As can be seen in Fig.3-4, the result also showed that the appropriate scanning lengths in –Y and +Y were almost the same, and that the error distribution was symmetrical to be within ±10μm, so that this probe orientation should be used in the later scans.

3.4.1 The effects of surface slope

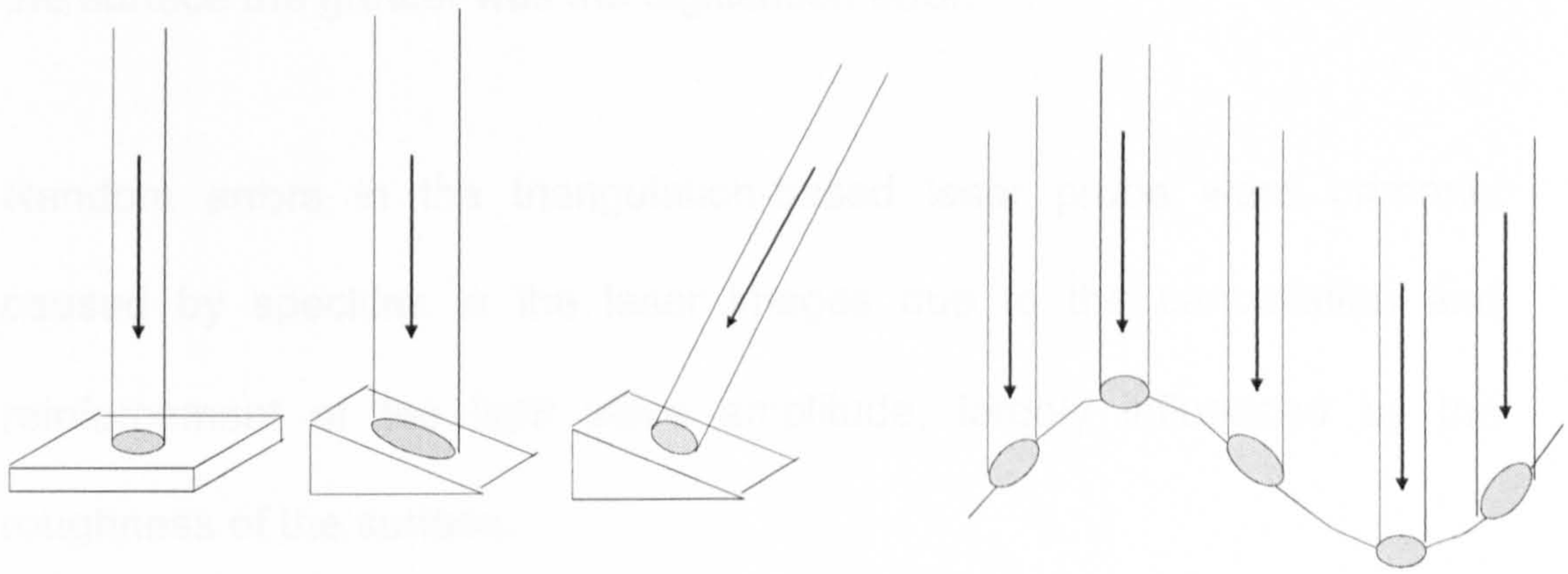

Figure 3-5: The effects of a deformation of the laser spot by slopes on a free form surface.

Slopes on the surface of an object produce changes in the size and shape of the light spot (see Fig.3-5), from a circular spot to an asymmetrical spot. This phenomenon leads to intensity changes at the photoelectrical sensor. However, when the changes are within a limited range, the error was tolerable. For example, when the angle between the optical axis and surface normal was smaller than 30.3°, the error was within ±10μm. This finding was compatible with earlier work by Rioux *et al.* (1987) who found that the intensity of the diffuse laser light focused on the photodetector array was the main factor affecting laser digitising accuracy.

Fig.3-5 also shows that the reflected laser ray imaged on the photodetector changed when the surface normal changed which caused a change in the intensity of the laser spot on the detection array; consequently, the reading of the data changed and a digitisation error

occurred in respect of the change of the light spot. The more angled was the surface the greater was the digitisation error.

Random errors in the triangulation-based laser probe were primarily caused by speckles in the laser images due to the cancellation and reinforcement of the light wave amplitude, largely influenced by the roughness of the surface.

Apparently the projected angle is not considered in the standard calibration procedure, this results in the optical triangulation probe presenting a combination both of random error and systematic error. Feng *et al.* (2001) reported a similar finding where a larger incident angle resulted in a greater error; the worst error observed being 160μm. Their study used a CCD photodetector.

3.5 Conclusions

This study gave a guidance on determining the probe orientations when a curved surface was to be scanned. The digitisation quality is strongly influenced by the orientation of the probe in relation to the surface normal. It is suggested that the optical plane is set perpendicular to the probe scanning direction, and that the angle between the surface normal and optical axis should be within 30.3°. From this investigation it is also

revealed that such a setting reduces digitisation error to no more than ±10μm.

4 USING MULTIPLE PROBE ORIENTATIONS TO DIGITISE A HEMISPHERE

4.1 Introduction

In Chapter 3, digitisation error in relation to the curvature of a surface was quantified, and indicated that multiple probe orientations are required to scan a surface if its curvature exceeds 60°. In the following study a multiple probe orientation method will be employed when a surface with a curvature greater than 60° is to be measured. Such a surface needs to be divided into sections, and then each section is digitised at a specific probe orientation. Other researchers have tried a different approach and used structured illumination from more than two light sources (Che and Ni, 2000). Ni's method requires multiple orientations of laser projectors to obtain an optimal projecting angle for the laser beam; this method has been used mainly for larger objects, such as aeroplane and car body inspections.

A hemisphere impression of an acetabular hip cup was scanned by a Talysurf – a surface measurement equipment (Taylor Hobson, Leicester Ltd, UK). The Talysurf uses a touch probe to scan an impression of the acetabular cup directly. Its accuracy is very precise, and in the hundreds of nm range, but the scan was only capable of producing a profile, even

though the maximum measurement range over a profile was an arc of approximately 120° (Fig.4-1). Additionally, a single profile can only represent very localised information, and the aim here is to measure and analyse an entire 3-D hemi-sphere.

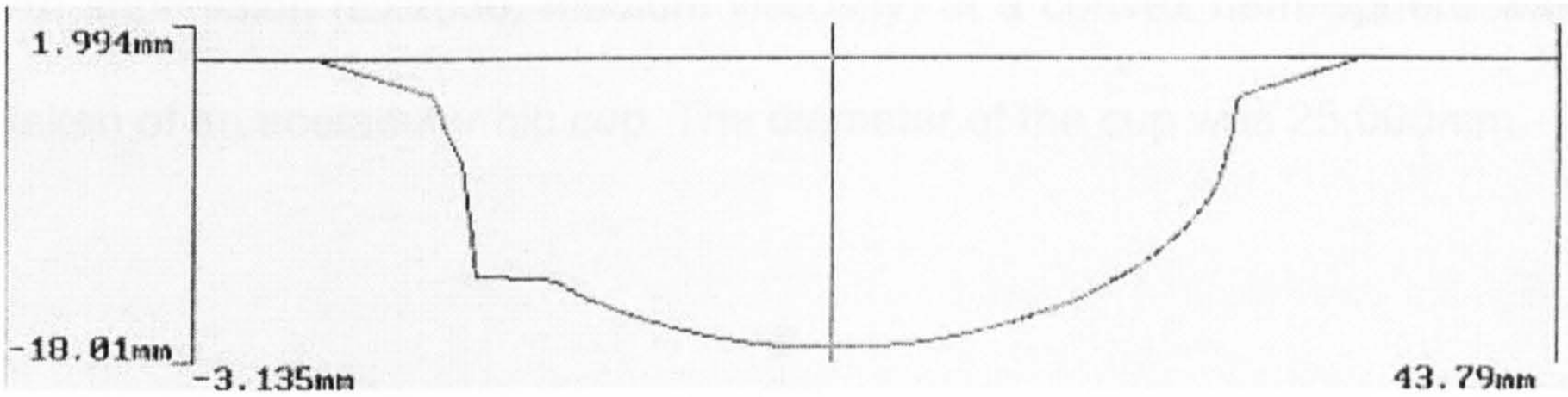

Figure 4-1: A scan of the impression of an acetabular hip cup using the Talysurf (Taylor Hobson, UK).

From the investigation of single probe orientation over a standard sphere in a previous study, a scientific basis for the selection of multiple probe orientations was obtained. The following study focused on achieving the digitisation of a convex hemisphere by using multiple probe orientations.

For the present study, common Materials and Methods (Section 4.2) are introduced such as the calibration of probe orientations and selection of scanning parameters. The digitisation arrangements for executing the multiple-probe orientation scan will be described separately later in this Chapter, as the different numbers of probe orientations used present different problems and solutions to the scanning arrangement. For example, a four probe orientation scan is very different to a six probe

orientation scan. To aid clarity, the individual scanning methods, Results and Discussions are presented in Sections 4.3 and 4.4.

4.2 Materials and Methods

An impression (Extrude, medium viscosity) of a convex hemi-sphere was taken of an acetabular hip cup. The diameter of the cup was 25.000mm.

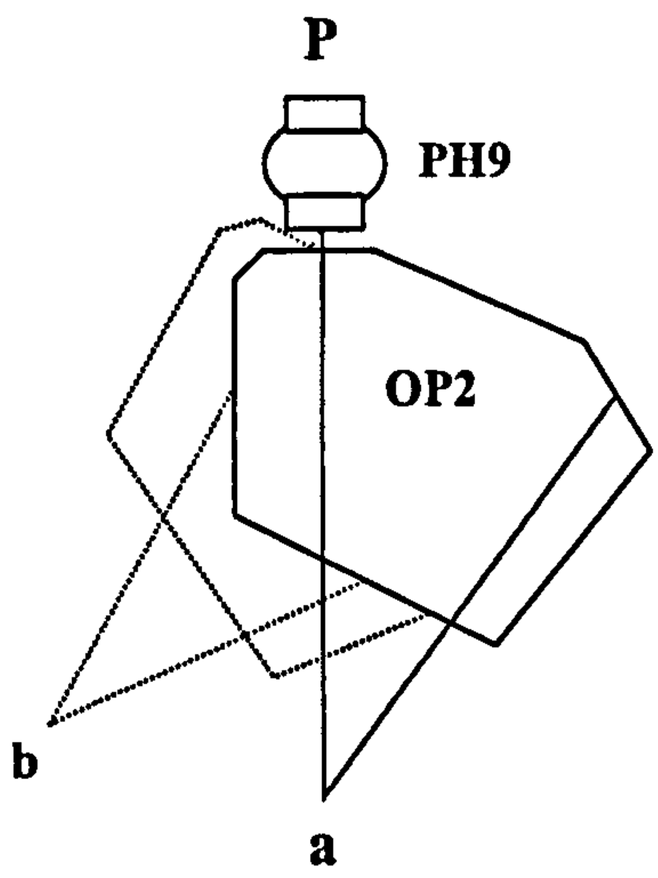

Figure 4-2: With the same position of a probe, the tip position 'a' and 'b' can vary at different probe orientations, so probe orientations need to be calibrated before a scan.

Although the probe head had the same position 'P', the probe tip position 'a' and 'b' moves according to the probe orientations in the CMM space as shown in Fig.4-2. Therefore, probe orientations require to be calibrated prior to digitisation, to allow the control system to recognise the position of the probe tip in respect of its specified probe orientations. The tip positions

'a' and **'b'** were defined in respect to the probe orientations of **1** and **2,** which are referred in the control programme.

The surface to be measured was divided into segments, each segment was digitised at a specified probe orientation, and these segments were scanned in a specifically defined order. During this process, digitised data was stored within temporary 'layers', so that, when the segment digitisation was finished, re-arranging and 'stitching' of data was required to produce the complete surface. A user derived program was written to establish the link between probe orientation and the segment, to control the scanning process of each segment at a defined size and position, then to reorganise the order of the digitised points in each segment, and finally to 'stitch' these segments into one reconstructed surface. Such stitching is a common process for assembling data from discrete scans.

Apart from the calibration of probe orientation, for every digitisation procedure three operational parameters needed to be defined and inputted into the digitisation control programme. For this experiment, the parameters were set as follows:

(1) scan pitch: 1mm,

(2) scan speed: 10 points per second,

(3) optical threshold setting: 100.

The scanning directions and probe orientations vary in each segment of the surface, and these variables were programmed into the executing programme.

4.3 Four Probe Orientations

4.3.1 Method

A digitisation error of ±10μm was regarded as an acceptable tolerance in this study. In Chapter 3 it was shown that a quarter of a hemisphere can be scanned without reorienting the probe, so that four probe orientations of I: (45°, 45°), II: (45°, 135°), III: (-45°, 45°) and IV: (-45°, -135°) were sufficient to scan four surface segments of I, II, III and IV respectively as shown in Fig.4-3. A subspace co-ordinate system was defined, with axes parallel to the CMM machine axes, and their origin at the top of the hemisphere. The starting points of the scanning path for each of the four segments (Fig.4-3) were near the origin of the subspace. To avoid overlapping of the scans, a gap of 20μm was left between each segment. An uni-directional scan was used in all cases. Using this approach, all of the scans started along two sides of the Y axis and moved away from the top, to the side of the hemisphere (see Fig.4-3).

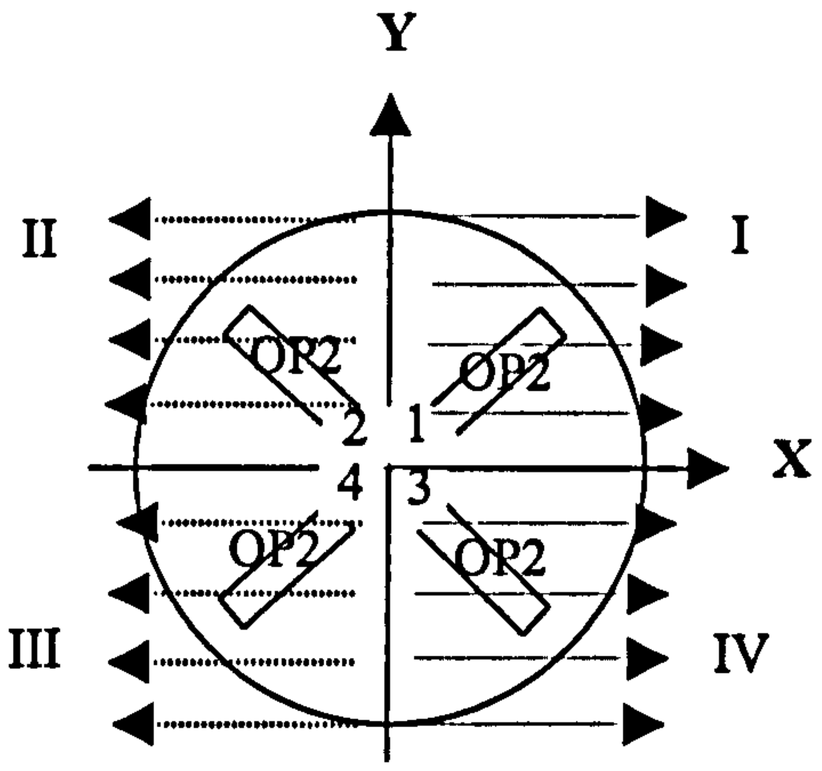

Figure 4-3: Four probe orientations used to scan a hemisphere.

4.3.2 Results

A complete convex hemisphere was digitised and reconstructed to produce an image of the entire surface in 3-D as shown in Fig.4-4. The reconstructed surface is shown in Fig.4-4(a) and the distribution of digitised points is shown in Fig.4-4(b).

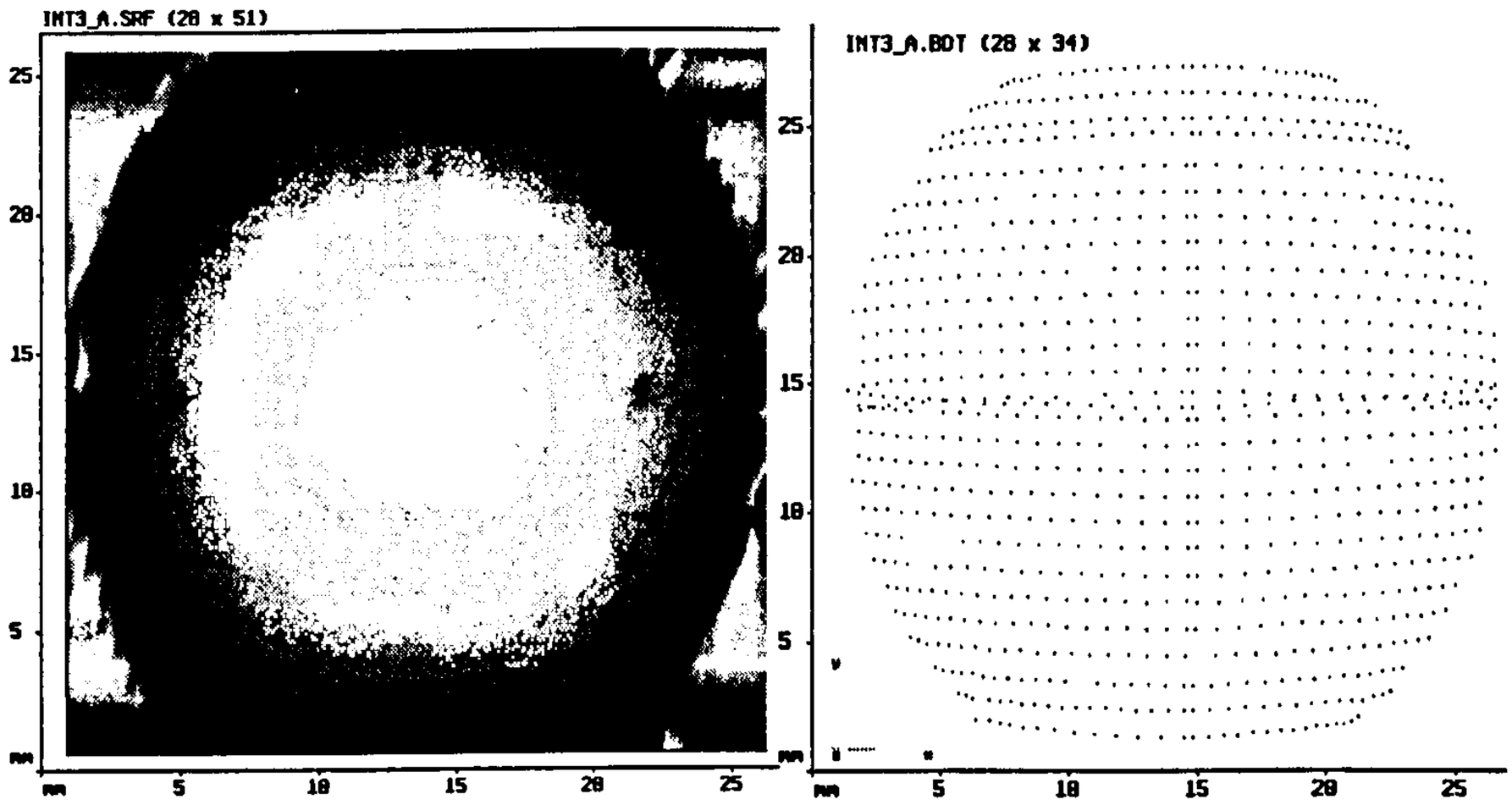

(a) A reconstructed image (b) A cloud of digitised data

Figure 4-4: A convex hemisphere digitised using four probe orientations.

The artefacts visible in Fig.4-4(a) are a consequence of the x-y distribution of data points shown in Fig.4-4(b). The characteristics of this distribution are:

1) The data point spacing is variable in x.
2) The scan lines are not straight and some of them intersect.
3) The deviations of the x-y locations of the data points from a nominal rectangular grid are not irregular but are related to the sphere's geometrical properties, being more apparent at the sides than at the top of the hemisphere.

The intersecting scan lines arise from the process of merging the four partial scans and arose at the Segment I / III and Segment II / IV boundaries. Thus, in the affected regions the distribution of the data points

was such that it adversely affected the accuracy of the particular interpolation method used in these studies.

4.3.3 Discussion

The artefacts revealed in Fig.4-4 have been comprehensively discussed and analysed in this section. Two solutions are described. Section 4.3.3.1 is a simple approach that regards the hemisphere as a flat surface as the scanning interval is much smaller than the diameter of the hemisphere. Section 4.3.3.2 is a more complex solution, which takes account of the sphere and its contribution to the artefacts.

4.3.3.1 Cause of the deviation in sampling space – simple explanation

In Fig.4-4 two features of the artefacts were clearly revealed: (1) the uneven spacing between digitised points, and (2) the non-straight and intersecting scanning lines.

Generally, the distribution of x-y locations of data points is optimal when those points lie on a rectangular grid. When this is not the case, the surface interpolation becomes more difficult and less accurate. It is therefore important to determine which factors are the cause of a non-rectangular data point distribution and to quantify their effect.

The nominal interval D between the digitised points in the direction of probe movement is one of the digitisation input parameters. The direction of each scan line is defined by the digitisation direction, and it should be straight and parallel to one of the axes in the co-ordinate system. This is indeed the case if the laser beam is oriented vertically. However, if the laser beam is inclined away from the vertical, then the x and y co-ordinates of the locations of digitised points will be subject to deviations depending on where the laser beam intersects the surface of the hemisphere. The deviations in x and y are discussed in turn.

Deviations in x (variable point spacing)

Let D denote the nominal sampling interval and let α denote the angle between the laser beam and the x-y plane. A vertical probe orientation, for example, would correspond to $\alpha = 90°$.

In Fig.4-5 we examine a region of the sphere's surface which lies between two adjacent data points. As the sampling interval D is usually much smaller than the radius of the sphere, it is reasonable to approximate the surface of the sphere with its tangent plane at the digitising location. Let β be the angle between the x-y plane and the normal to the tangent plane

(e.g. a horizontal plane would have $\beta = 90°$). The interaction of the probe orientation and surface gradient results in a variable spacing of D'.

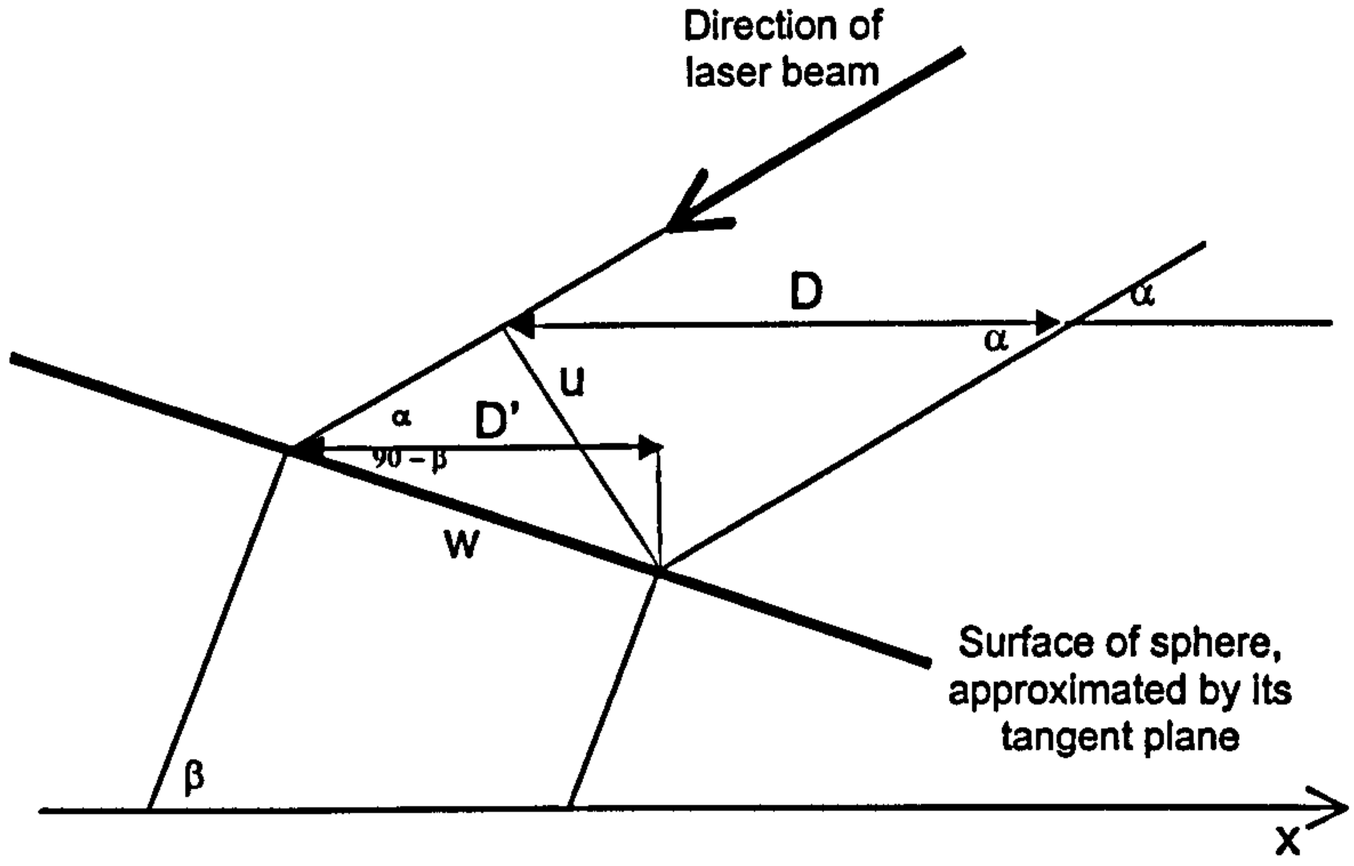

Figure 4-5: Nominal vs actual spacing in x.

From Fig.4-5 it is easily verified that $D' = w\sin\beta$, $w = \frac{u}{\cos(\alpha - \beta)}$ and $u = D\sin\alpha$.

Therefore

$$D' = D\frac{\sin\alpha\sin\beta}{\cos(\alpha - \beta)} \qquad (1)$$

It can be seen that near the top of the hemisphere, $\beta \approx 90°$, $\cos(\alpha - \beta) \approx \sin\alpha$ and consequently $D' \approx D$.

Near the periphery of the hemisphere, $\beta \to 0°$, $\sin\beta \to 0$ and consequently $D' \to 0$.

Deviations in y (non-straight scan lines)

Again, let α denote the angle between the laser beam and the x-y plane. In Fig.4-6 the probe is moving parallel to the x axis (away from the page and towards the viewer), maintaining a constant value of y, denoted by y_{probe} and a constant height denoted by z_{probe}. The laser beam intersects the surface at some point P whose z co-ordinate is denoted by z_{data} and whose y co-ordinate is y_{data}.

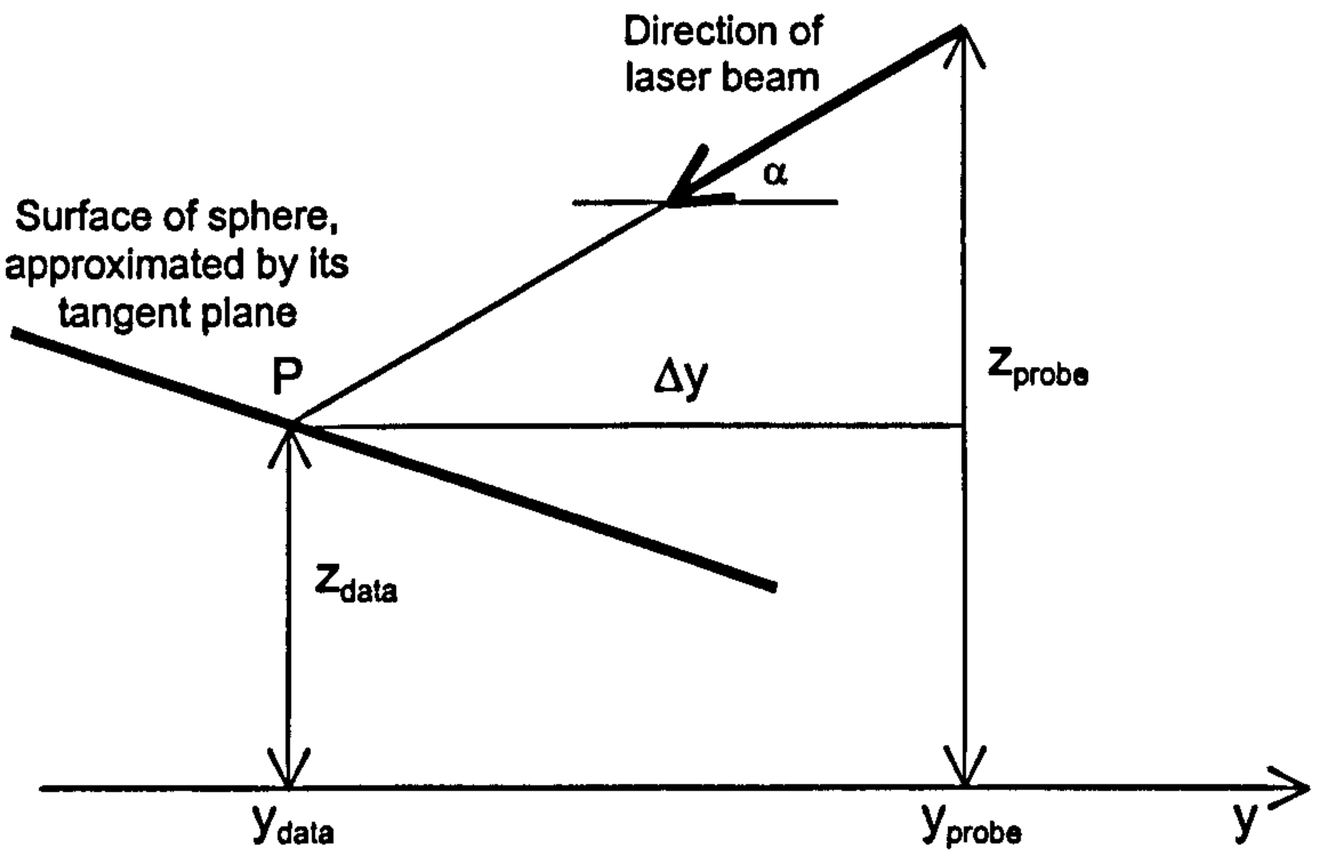

Figure 4-6: Deviation from a straight scan line.

If the laser beam is not vertical, then y_{data} is different from y_{probe} and the magnitude of the deviation in y is

$$\Delta y = \left| y_{data} - y_{probe} \right| = \frac{\left| z_{probe} - z_{data} \right|}{\tan \alpha} \qquad (2)$$

When the probe is vertical, then $\alpha \to 90°$, $\tan \alpha \to \infty$ and consequently $\Delta y \to 0$.

From formulae (1) and (2) it follows that for any given fixed probe orientation, the irregularity of the x-y data grid depends on the variability of the surface gradient angle β and the variability of its height in z.

In the 4-segment scan in Fig.4-3, the variability of β is 45° and the variability in z is equal to the hemisphere's radius R.

It is evident that if a surface region A is contained within another region B, then the variability of region A cannot be greater than that of B. Therefore, one way of reducing the total variability for a fixed probe orientation is to scan a smaller region. For this purpose a six-probe orientation scanning pattern was designed and implemented.

4.3.3.2 Cause of the deviation in sampling space – complex explanation

In Fig.4-4 two defects were clearly revealed. One appeared as uneven spacing between digitised points, and the other was caused by the presence of non-straight scanning lines. Both problems were more severe at the sides than at the top of the hemisphere.

The interval between the digitised points should remain the same since this is one of the digitisation parameters, and is controlled by the executive program. The scan line is defined by the digitisation direction, and it should be straight and parallel to one axis of the co-ordinate

system. This is indeed the case if the laser beam is oriented vertically. However, if the laser beam is inclined away from the vertical, then the X and Y co-ordinates of the locations of digitised points will be subject to variations depending on where the laser beam intersects the surface of the hemisphere. These variations manifest themselves in two ways.

The unfavourable spatial distribution of the locations of digitised points is thus a consequence of the curvature of the sphere and of the inclined probe orientation. Fig.4-7 illustrates the geometrical relationships between the probe orientation and the curvature of a hemisphere.

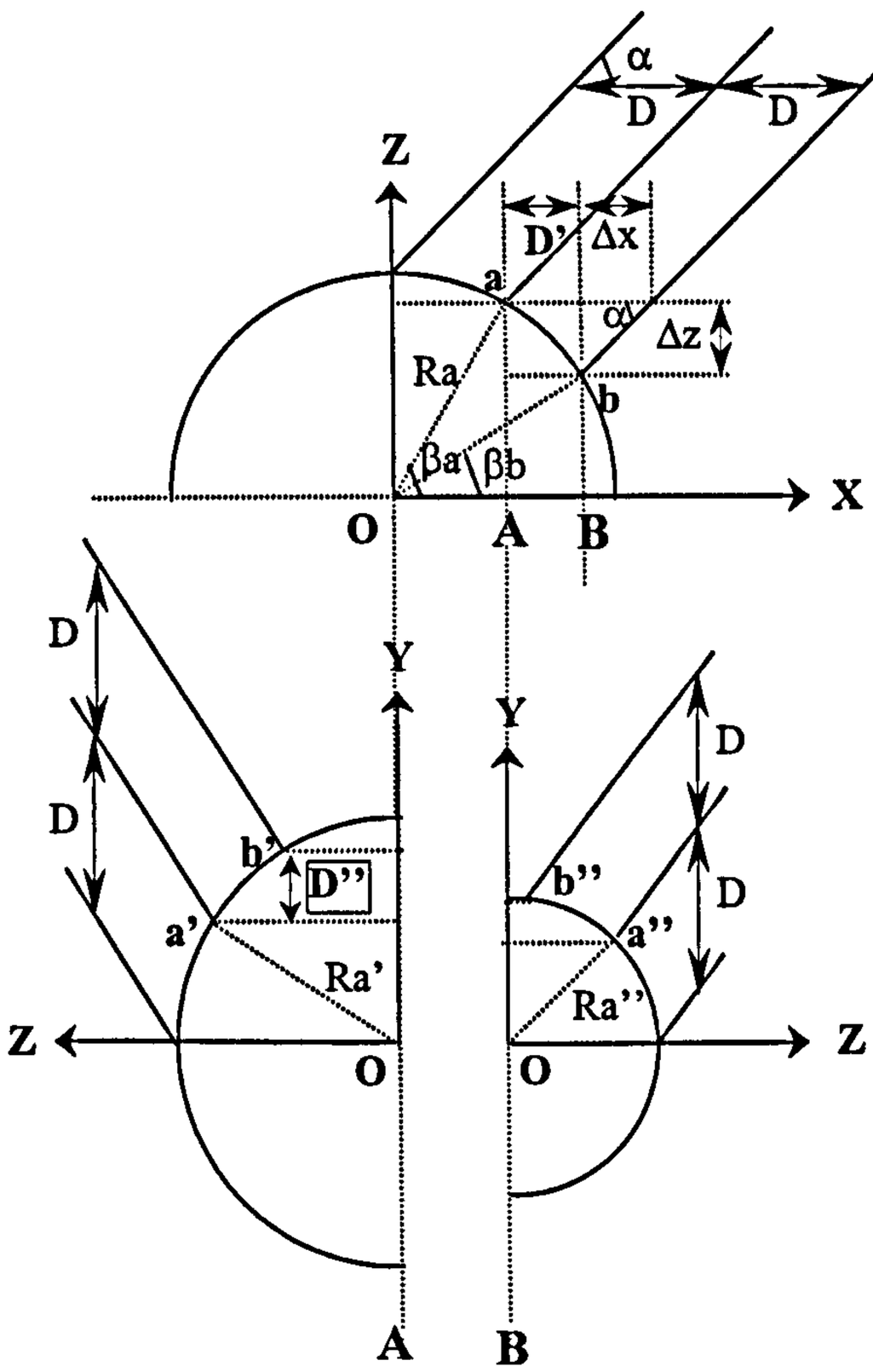

Figure 4-7: Spacing shift

In Fig.4-7 (above), the probe orientation is represented as α, and the defined sampling interval is D, a constant value controlled by the CMM and OP2 measurement system. The interaction of the probe orientation and surface curvature results in a variable spacing of D' and D'' in the X and Y directions respectively. These variations in X and Y directions are similar, since a hemisphere is quadrant symmetrical, so an analysis of defects in X direction only will be made.

If we use Δx to represent the deviation of the actual interval of D' from the defined position, the interval D in X direction ($\Delta x = |D - D'|$) is as shown in Fig.4-7, and a formula can be derived as follows to quantify the value of the change which is caused by the probe orientation (α) and the curvature of the hemisphere (R, βa and βb):

$$\Delta x = D - Ra \times \text{cotan}(\alpha) \times (\sin(\beta a) - \sin(\beta b)) \quad \ldots\ldots\ldots (1)$$

The equation (1) explains two problems. D is the nominal constant value of the scanning pitch. In a section of the hemisphere, Ra is the radius of the circle and Ra is constant in this section through the position of **a** in the plane which is parallel to the XOZ, Ra varies from the position, for example, when **a** is at the top position of the sphere, Ra is equal to the radius of the hemisphere, and when **a** is at the equator of the sphere, Ra

will be zero. The probe orientation was also regarded as a constant value in this situation, which means α is a fixed value when probe orientation is determined, and it can be changed at the decision making period. βa and βb are related to the position of **a** and **b** for the analysis, they are changeable within a range of 0° to 90° (in a hemisphere), the difference of $\sin(\beta a)$ and $\sin(\beta b)$ becoming greater when βa and βb change from 90° (at top position of the circle) to 0° (at the equator). Δz is more obvious as a change in height between the positions **a** and **b**. At the positions where the height value has a larger Δz, for example, at the equator of the hemisphere, it results in a bigger spacing change, consequently a smaller interval, for example the projection of **AB** is smaller than **OA** in the upper picture. The lower pictures follow the same rule at b' and b", but variations exist in the Y direction.

To improve the problem of spacing shifts, a six-probe orientation method was designed and implemented. This way α is reduced from 45° to 30°, the reduction of the shift will be reduced 1.7 times in both directions of X and Y (referring to the formula (1)).

The lack of straightness of the scanning lines can also be explained by equation (1). Imaging at the section of the circle in different positions of the hemisphere, where different Ra values occur, for example a bigger Ra

would be obtained at the top area than at the side area, and consequently a smaller Δx resulted at top area, and a bigger change appeared at the side. These defects are caused by the interaction of the probe orientation and the curved surfaces.

4.4 Six probe orientations

4.4.1 Method

Six probe orientations were calibrated as I: (0°, 180°), II: (30°, -45°), III: (30°, -135°), IV: (0°, 0°), V: (30°, 45°), and VI: (30°, 135°). Six segments were digitised separately using these six probe orientations. The arrangement is shown in Fig.4-8. Digitisation parameters were selected, based on the investigation carried out in Chapter 2 as: sampling interval: 1mm, scanning speed: 10 points per second, and optical threshold setting: 400.

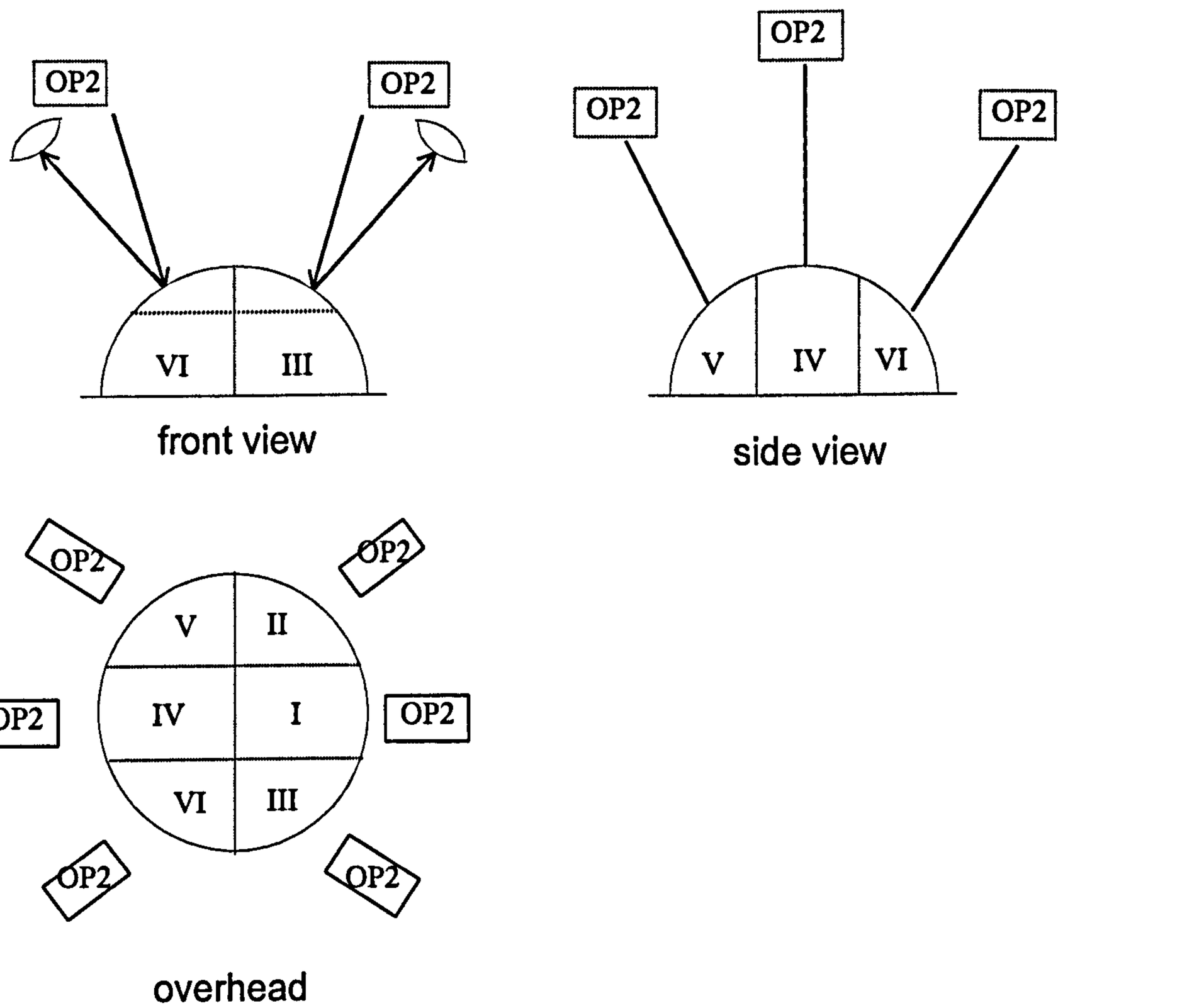

Figure 4-8: Scanning six surface segments using six probe orientations.

4.4.2 Results

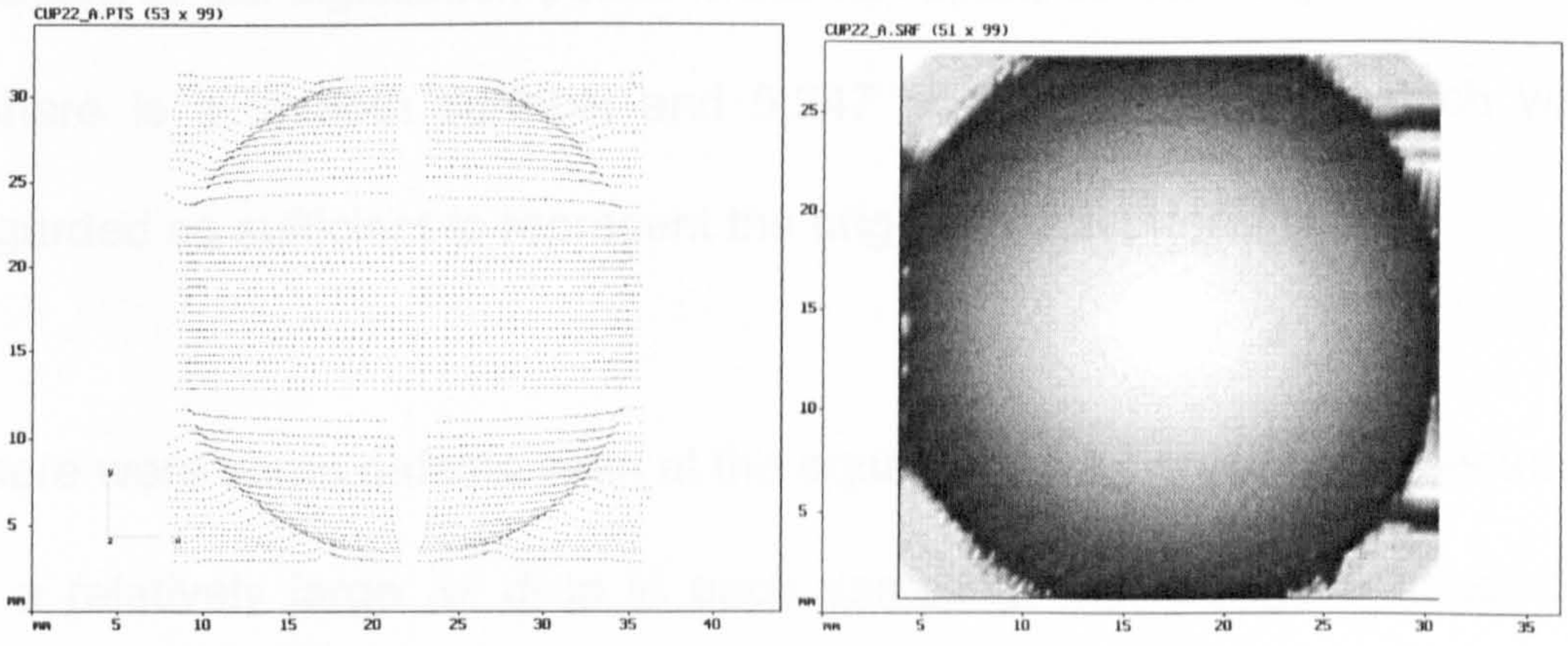

Figure 4-9: A convex hemi-sphere digitised using six probe orientations.

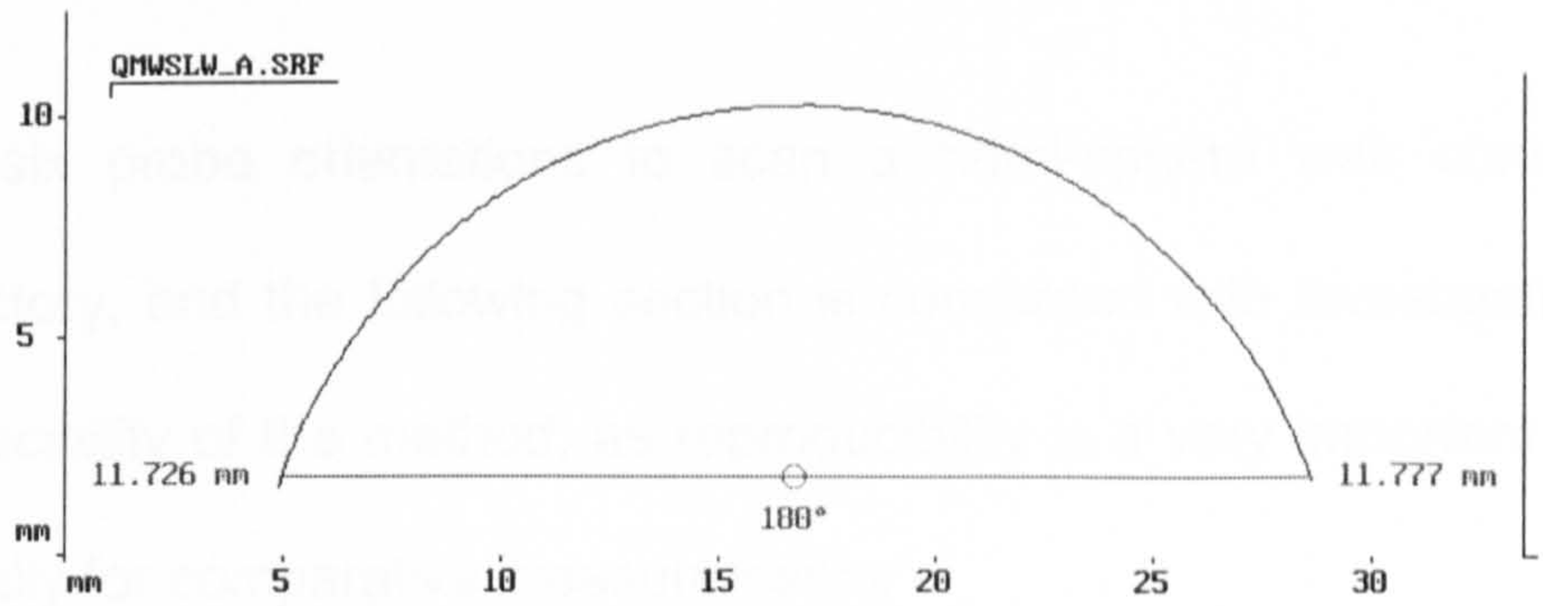

Figure 4-10: A reconstructed profile of the sphere

A significant improvement was seen using a six-probe orientation scan as shown in Fig.4-9. The digitised data points are shown in Fig.4-9 (a), and the reconstructed image in Fig.4-9 (b). A cross section of the digitised image is shown in Fig.4-10, which demonstrates a perfect half circle, and a controlled digitisation error was less than ±10μm.

Although the 'crossing-over' of the scan lines has been eliminated, the spacing of the digitisation points is still not even, considering that a hemi-sphere is a smooth surface, and 5,247 points were taken, which was regarded as sufficient to represent the original hemisphere.

There were some defects seen at the equator of the hemisphere, because of a relatively large Δz drop in each sampling interval; these caused a sudden acceleration of probe movement, and a resultant defect.

4.5 Reproducibility of the six probe orientation scan

Using six probe orientations to scan a hemi-sphere was considered satisfactory, and the following section is concerned with investigating the reproducibility of the method, as reproducibility is a very important factor, especially for comparative measurements.

4.5.1 Materials and methods

A reproducibility inspection was implemented by repeating the digitisation procedure five times over the impression of a hip cup whilst using six probe orientation scans. Each procedure was repeated under the same datum space, which was aligned prior to data acquisition. Using the software analysis package, reconstructed surface images were

superimposed and volume differences were calculated over a 400mm^2 central square area.

4.5.2 Results

The 'pairwise' volumetric differences (ΔV) of 1.756mm^3 were calculated over rectangular areas of 400mm^2, and are given in Table 4-1, in which V11, V12, V13, V14 and V15 represent five scanned images. The values listed in the table are the calculated differences in volume between the images indicated by column and rows in Table 1. The overall mean difference in volume is 0.465±0.107 mm^3.

Table 4-1: Volume differences between repeat scan images (mm^3):

Δ	V11	V12	V13	V14	V15
V11	-	**0.517**	**0.507**	**0.674**	**0.535**
V12	-	-	**0.301**	**0.352**	**0.374**
V13	-	-	-	**0.492**	**0.426**
V14	-	-	-	-	**0.468**
V15	-	-	-	-	-

Colour coded images (Fig.4-11) show the distribution of the differences over the calculation area (400mm^2). In the most of the area, the differences were less than ±5μm (grey), scattered small areas (yellow and blue) had differences in the range of ±5μm to ±10μm. A very small area exceeds ±10μm (orange and red).

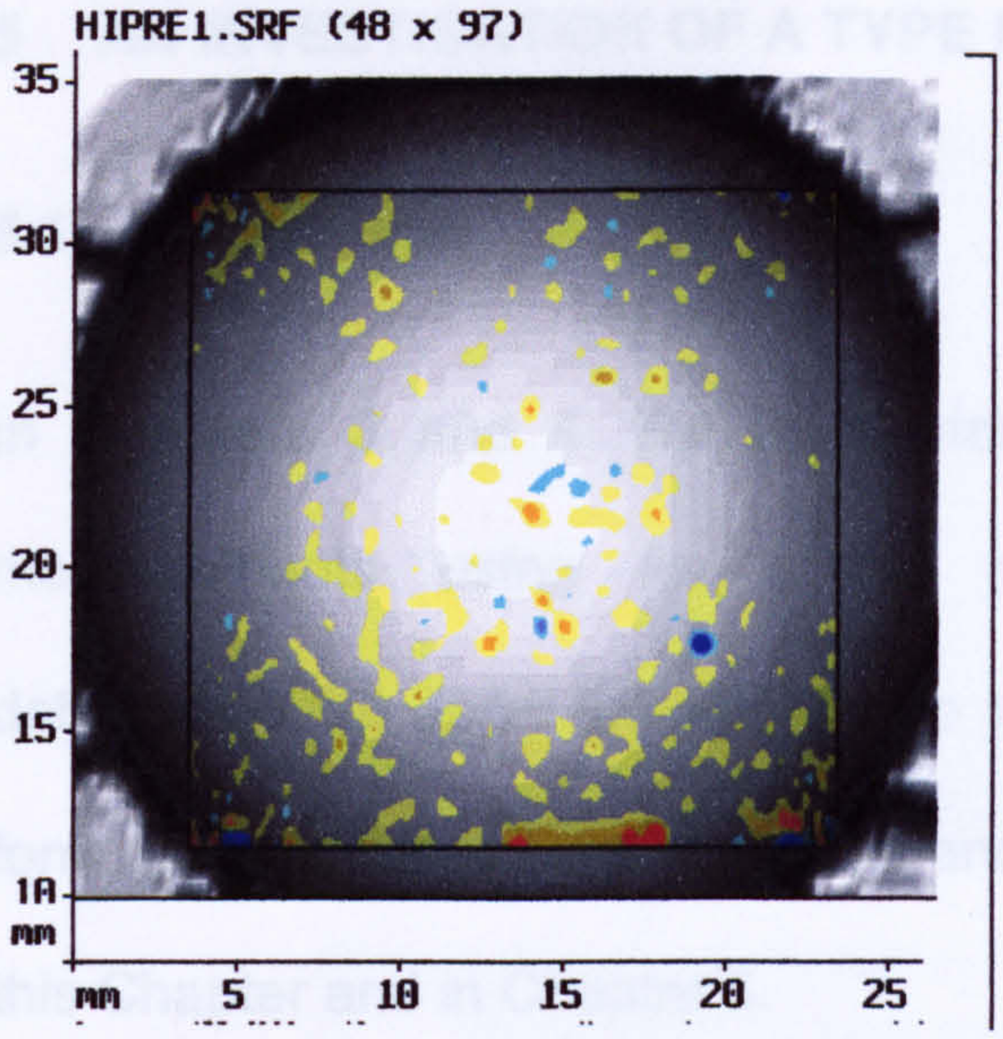

Figure 4-11: A colour coded image to show the differences between superposed two images of hemisphere.

4.5.3 Discussion

A laser scanner has constraints limited by the orientation of the normal of the scanned surface, a large deviation from the normal direction can hinder the ability to detect the reflected ray of the laser.

Digitisation of a complete hemisphere using six-probe orientations was regarded as satisfactory. There were very small areas on the surface where the reproducibility was greater than 10μm, and these were regarded as random errors due to contamination of the surface, maybe due to grease or dust, because the appearance was not regular or at any particular location.

5 AN INVESTIGATION OF A TYPE I SIMULATION MODEL

5.1 Introduction

In Chapters 3 and 4, the appropriate methods for free form surface measurements using an optical triangulation based probe were determined. To apply this knowledge to dental applications, complex free form tooth surfaces were simulated and analysed, and this is described in this Chapter and in Chapter 6.

Tooth morphology may be classified into two types based on its geometry. One is the molar occlusal surface, which has a very complex free form, related to its grinding function. This type of surface is referred to as Type II in this thesis, and will be investigated in Chapter 6. The other type of surface to be studied, in this Chapter, is designated to be as Type I, and it includes the buccal surfaces of incisors and the molar teeth, as these have the common feature of being curved in a horizontal direction but almost straight in a vertical direction, and has a similar geometrical features as a cylinder. If we extend our considerations from the teeth to the gingival area, then a shape similar to a stepped cylinder is revealed. This type of surface is one typically studied in dental research, such as in crown and veneer preparations (Fig.5-1). Geometrical shape and dimensions have been shown to be particularly important to the quality and longevity of such restorations (Seymour, 1995, 1996, 1999).

Figure 5-1: A stepped cylinder used as a die to simulate a dental crown preparation.

Whilst the surface of a tooth and crown preparation has a free form nature, at the prepared shoulder region the tooth is similar to a stepped cylinder. Accordingly, a die containing a stepped cylinder was produced to simulate a crown and veneer preparation, and an optimal scanning strategy was developed using this model (Fig.5-1).

It is a routine task to measure the dimensions of a cylinder in industry using touch trigger probes, but in this study we have used a different measuring method. A stepped cylinder is a geometrical shape, it has straight lines at the sides, and is circular in sections across its axis. The inspection and quantification of such a shape needs only a few points over both cylinders and at the sides of the step. In this study, although the stepped cylinder was no different from one encountered in industry, this particular model was to be used as a simulation of a tooth with a crown or

veneer preparation, and as such, should represent the free form surface that is the tooth. Hence, measurements had to be performed over the whole surface, rather than just at a few points. The study in this Chapter had the objective of devising an optimal digitisation strategy for a stepped cylinder, but treating it as a free form surface, so that later this strategy could be employed to digitised tooth crown preparations.

5.2 Material and methods

5.2.1 Model design

The shape and dimensions of the stepped cylinder are shown in Fig.5-2. It was manufactured by the Department of Medical Physics, St. Bartholomew's and The Royal London School of Medicine and Dentistry.

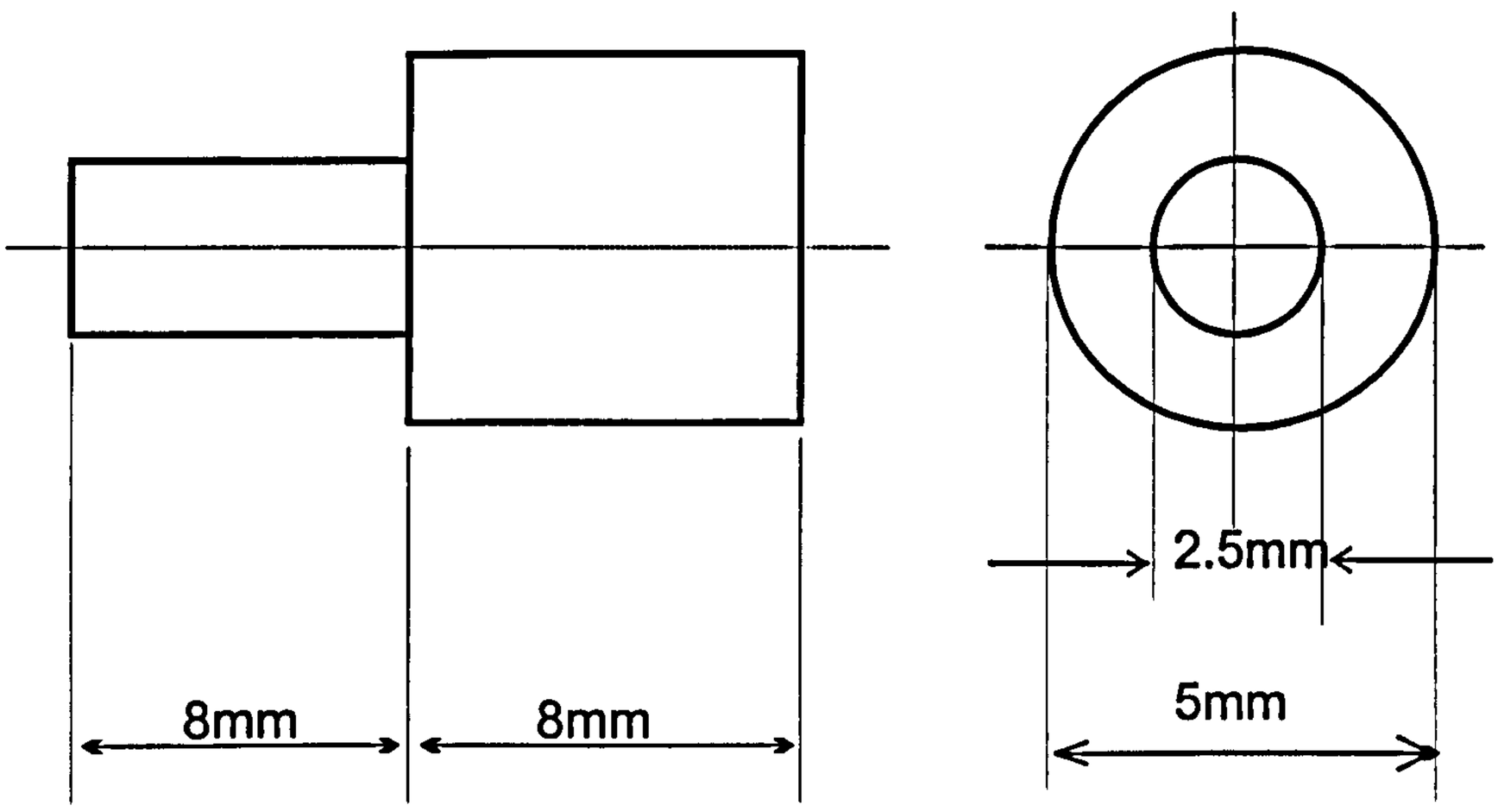

Figure 5-2: The simulation die of a stepped cylinder used in this study.

5.2.2 Impression

A replica technique was once again used in this study, and impressions were used for the evaluation.

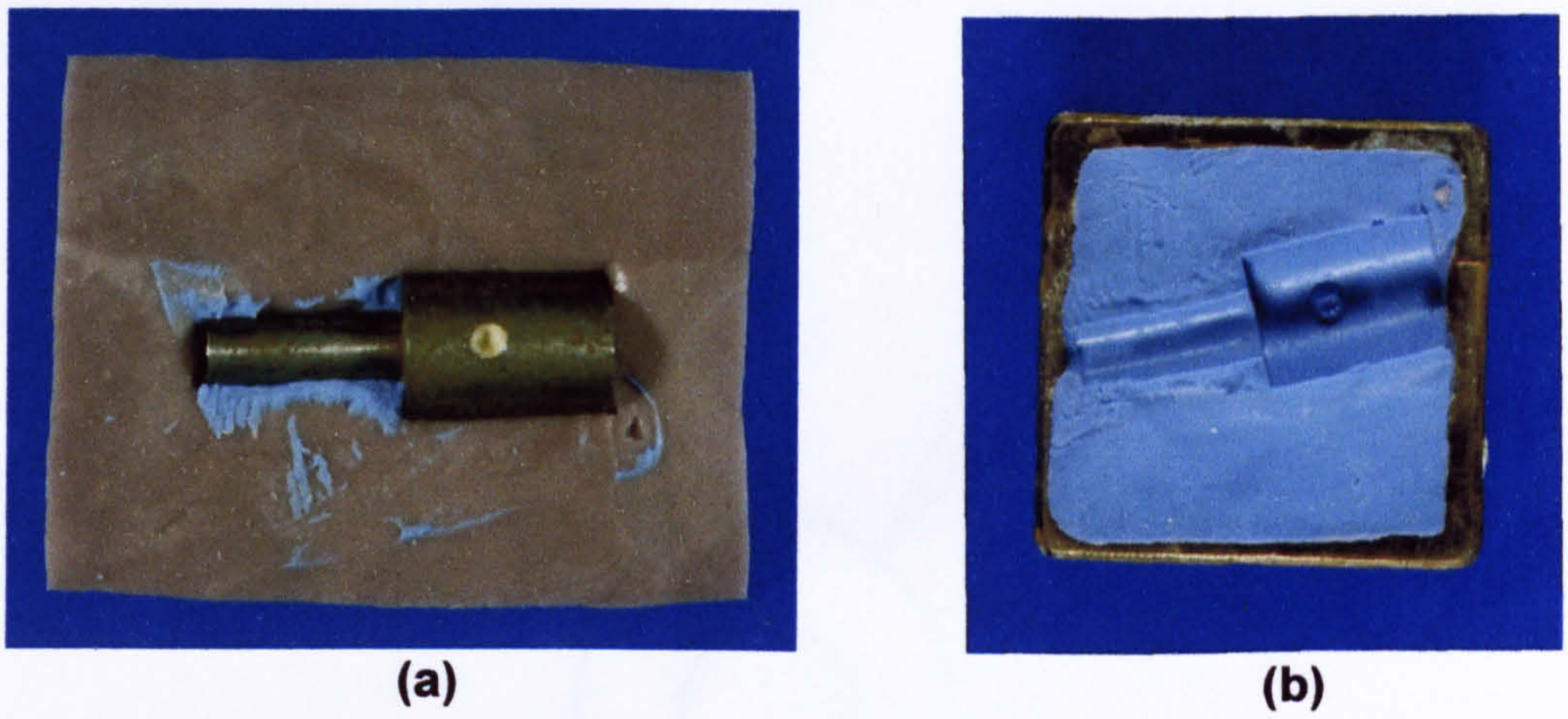

(a) (b)

Figure 5-3: An impression(b) is taken from stepped cylinder die(a).

The simulation die was embedded in a cubical stage made of putty (Extrude, Kerr, UK) as shown in Fig.5-3(a), and an impression (Extrude, Kerr, UK) was taken from this embedded die as shown in Fig.5-3(b).

5.2.3 Digitisation strategy

Following the earlier investigations in Chapters 2, 3 and 4, the digitisation strategy used to scan this stepped cylinder die was set as follows:

1. Probe Orientation: This was used for a semi-cylindrical surface, needing two probe orientations to cover the curvature of the entire semi-cylinder as shown in Fig.5-4.

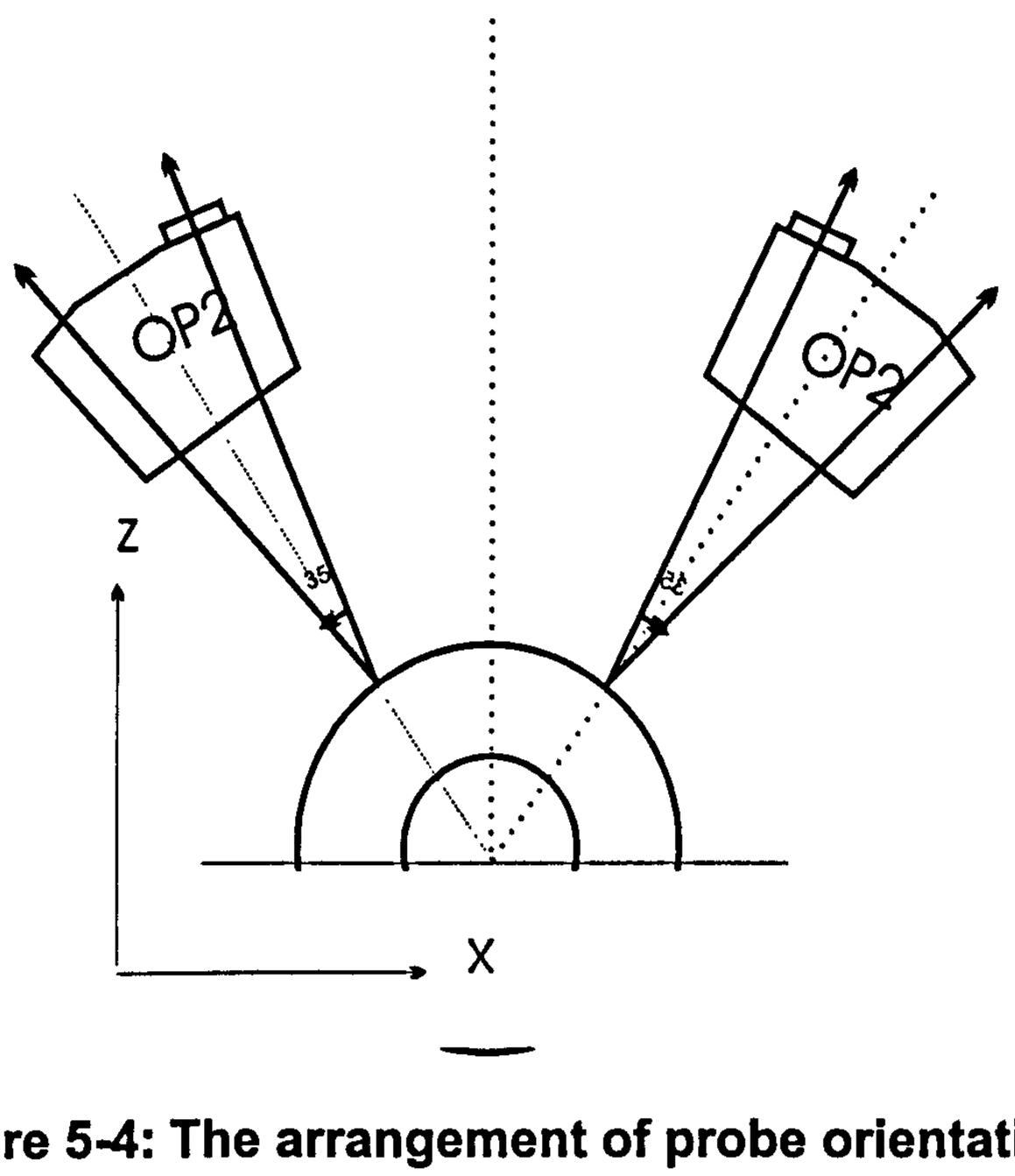

Figure 5-4: The arrangement of probe orientations used to scan the stepped cylinder die.

2. Scanning direction: Either the X or Y direction could have been selected as the scanning direction, but scanning along the X direction would have resulted in too many interruptions, as the probe would have had to change the orientation at every scan line. This would have taken a much longer time and repositioning of probe orientation would certainly have introduced a kinetic error into every scan line. In addition, contour changes would certainly have varied more in X than in Y. Hence, a scanning direction in the Y direction was considered more appropriate in this case. This selection of scanning direction was also consistent with the

conclusion of Chapter 3, in that the probe motion direction is perpendicular to the probe optical plane. Chapter 2 concluded that uni-directional scanning should be the method of choice. To avoid a deep slope at the step region, the impression was tilted at a 30° angle when placed on the working table of the CMM.

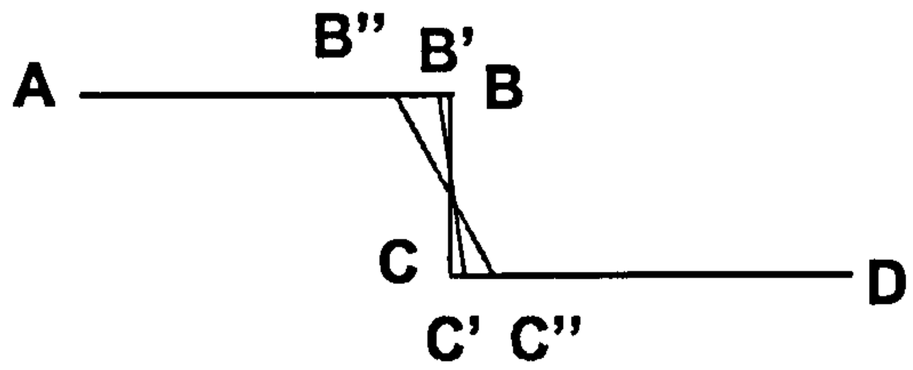

Figure 5-5: The effect of scanning pitch on accuracy at the step region.

3. Scanning pitch: This was determined after consideration of random digitisation at the shoulder of the die. Fig.5-5 shows that increased scanning pitch results in a larger random digitisation error (B"C"). In this study, since one of the aims was to obtain an accurate measurement at the region of the step, a smaller scan pitch of 20μm was selected.

4. Scanning speed: 10 points per second.

5. Optical threshold setting: 100.

5.2.4 Reproducibility

The impression of the stepped cylinder was measured 5 times continuously, using an identical digitisation strategy. These raw data were stored in binary format in data files, from which five reconstructed surfaces were interpolated. These were then supermposed, in order to examine the differences, using the 'best fit' method. The comparative measurement of 'before' and 'after' 'best fit' would give some indication of the behaviour of the measurement system.

Both 'before' and 'after' 'best fit' comparative results are shown as colour coded images. Measurements of height and volume were made 'pairwise' from these results, and each was compared with the first scan image.

5.3 Results

The five reconstructed images obtained are shown in Fig.5-6. Each image appeared completely without distortions, as was expected.

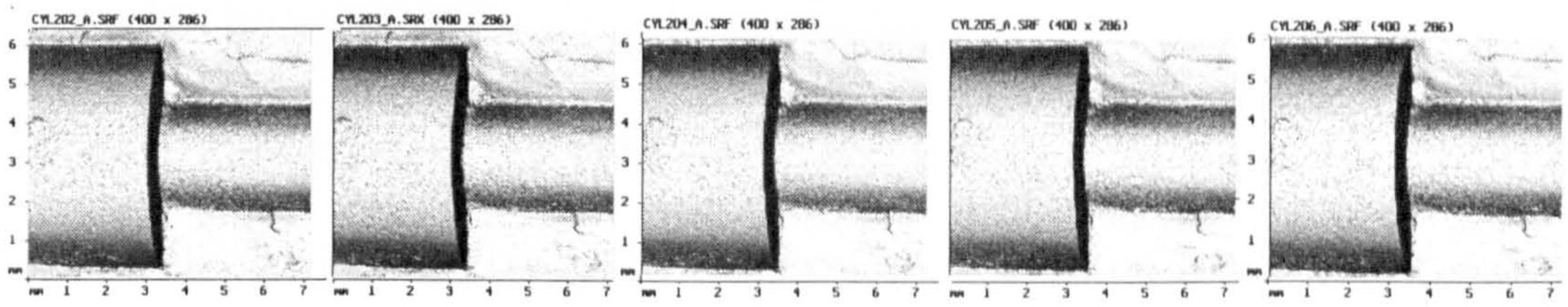

Figure 5-6: Five reconstructed images from the same impression of the die.

The stepped region showed a true 90° angle and no distortions were evident in Fig.5-7, which is a reconstructed 2D profile. The approach and strategy used in this study was unique.

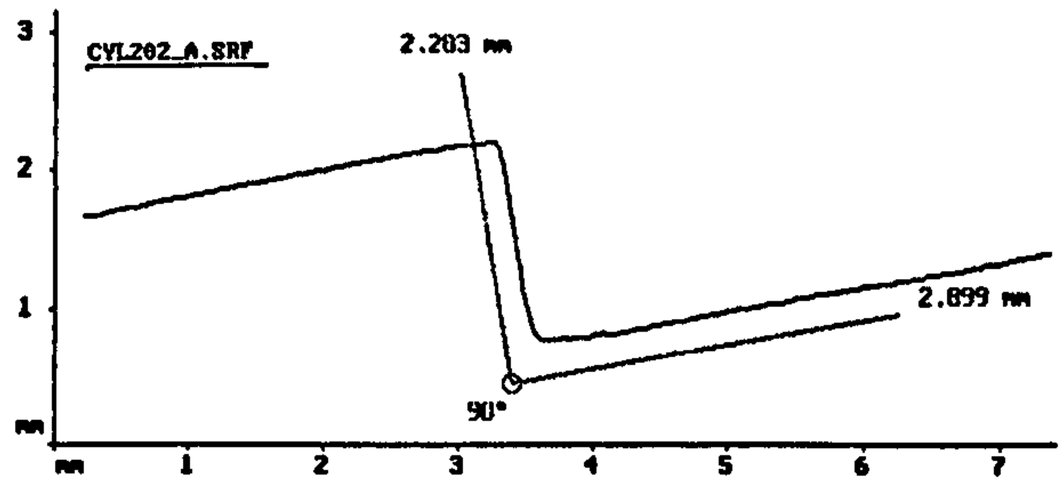

Figure 5-7: A reconstructed profile of the die.

5.3.1 Evaluation of the digitisation procedure

Fig.5-6 shows the appearance of the reconstructed images, which appear identical. However, unlike objects that have a regular shape, as a free form surface, the entire surface of this simulation die needed to be digitised, in addition a small pitch was used to reduce the random error at the step region. This meant that the time taken for the data acquisition was much longer. For example, the stepped cylinder was digitised at a sample interval of 0.02mm and speed of 10 points per second, which meant it took 3 hours to obtain 114,400 points for one surface scan. With such time constraints, the ambient conditions can change considerably during this long data acquisition period, in terms of illumination,

temperature, vibration and the instability of the electrical power supply. All these sources of error could lead to measurement uncertainty.

Therefore, the results of comparative measurements were carried out by superposing these five scanned images (Figs.5-9 to 12). The differences in volume are presented in Table 5-1.

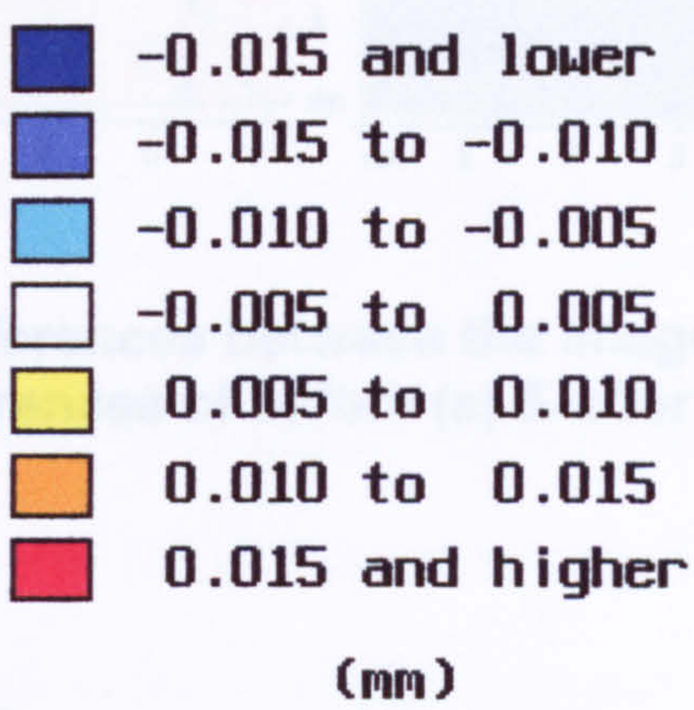

Figure 5-8: The height differences (mm) in relation to the colours used in Figs.5-9 to 12.

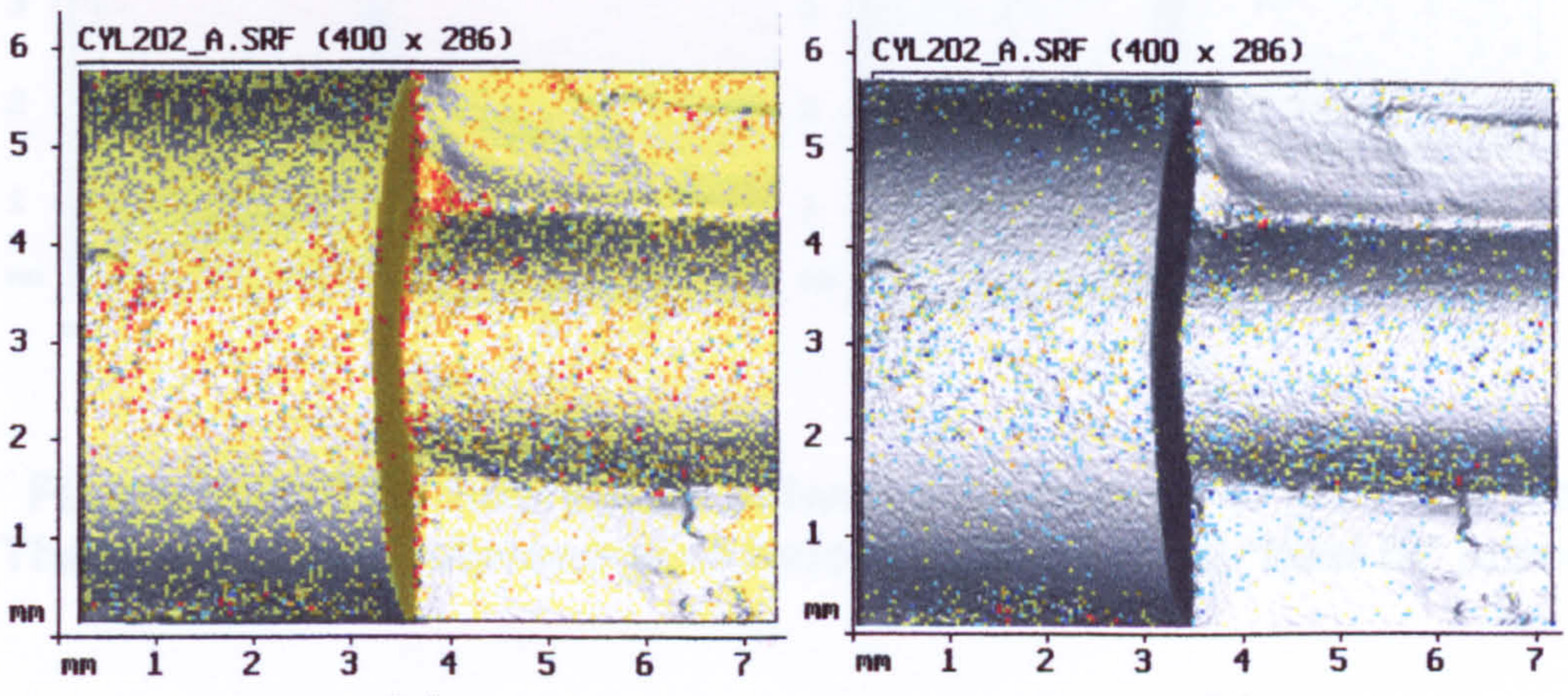

(a) (b)

Figure 5-9: The differences between the images of No.1 and No.2. These show the differences of before (a) & after (b) 'best fit' process.

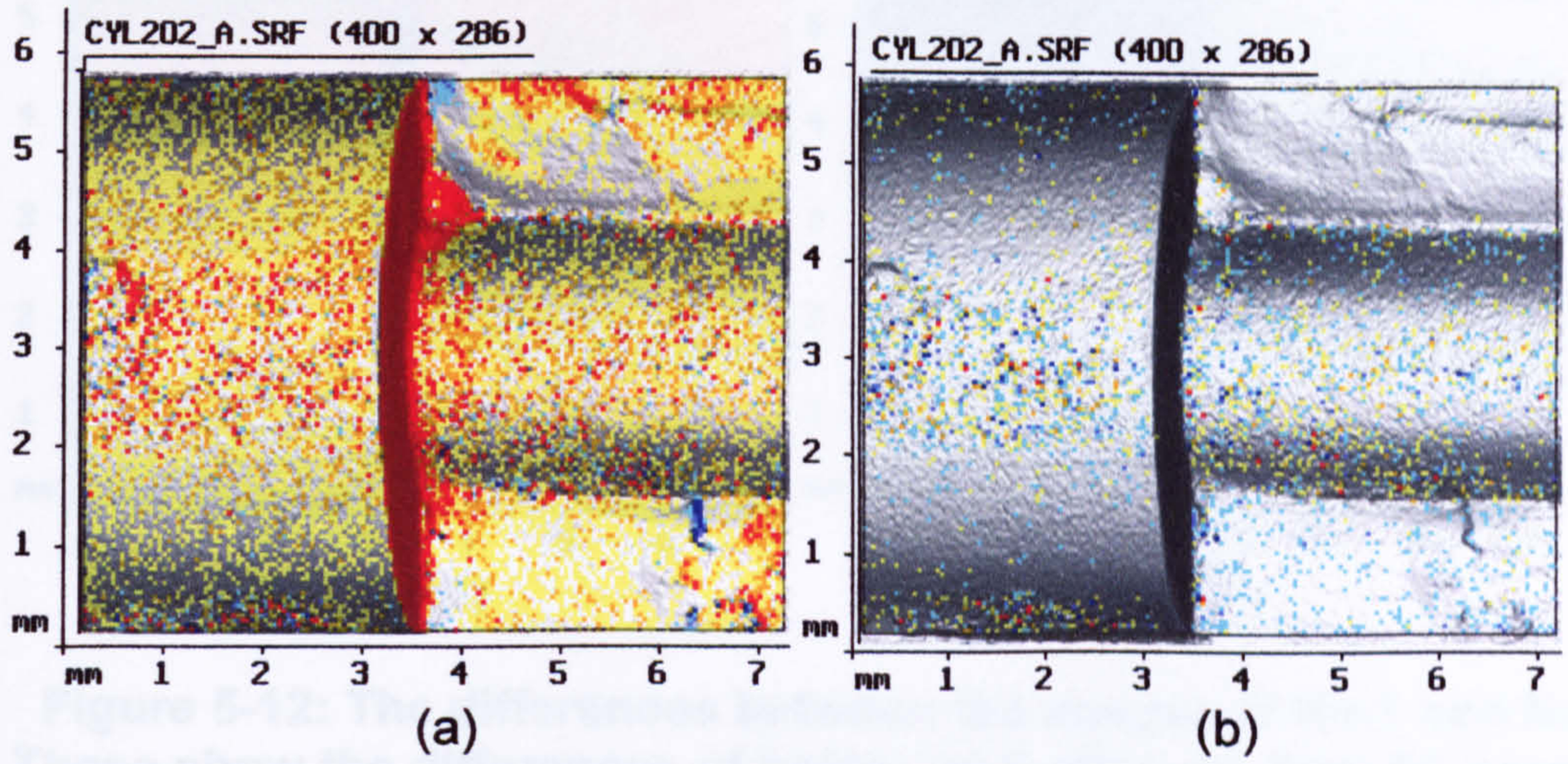

Figure 5-10: The differences between the images of No.1 and No.3. These show the differences of before (a) & after (b) 'best fit' process.

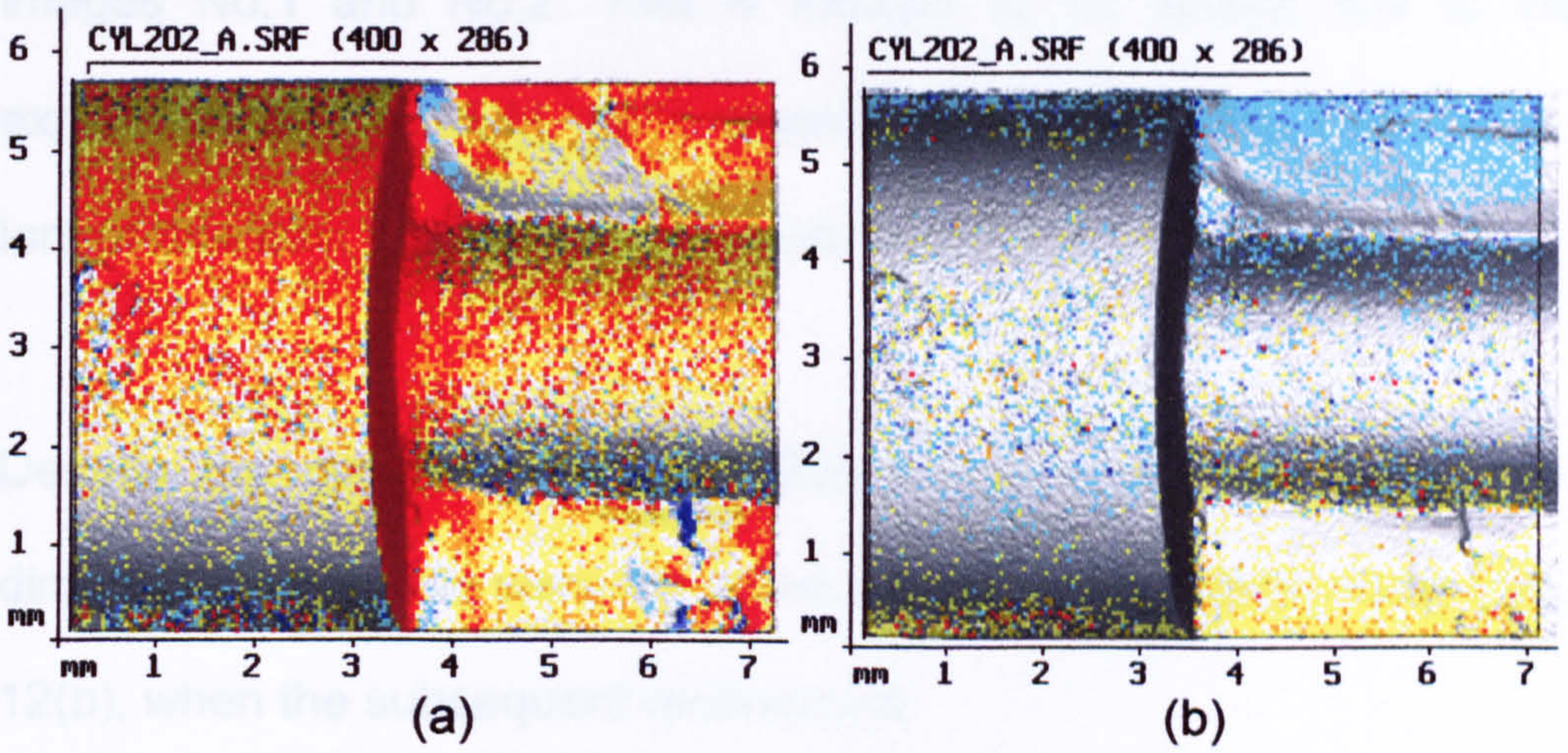

Figure 5-11: The differences between the images of No.1 and No.4. These show the differences of before (a) & after (b) 'best fit' process.

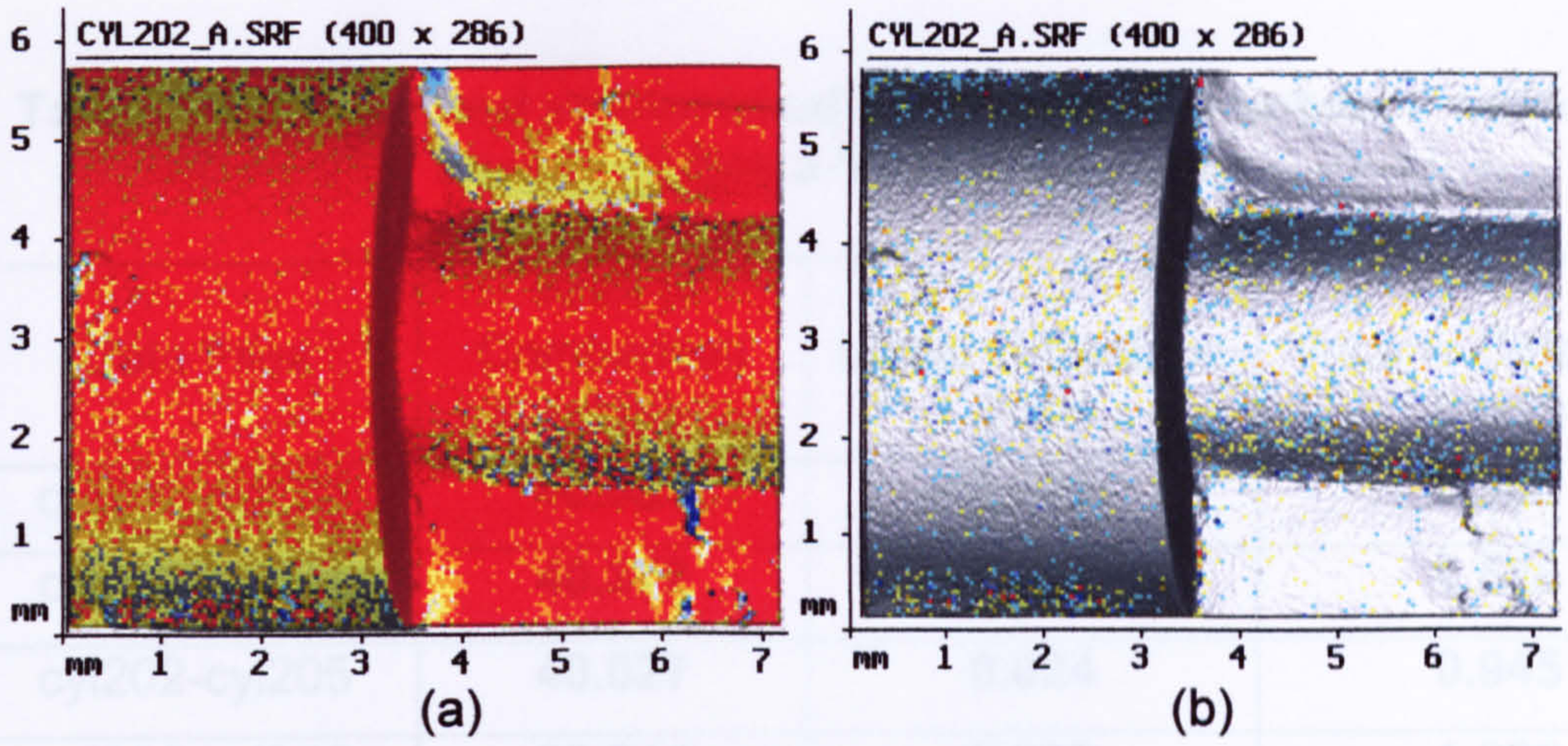

Figure 5-12: The differences between the images of No.1 and No.5. These show the differences of before (a) & after (b) 'best fit' process.

From these comparisons, the largest differences were seen between images of No.1 and No.5, whilst the smallest differences were between images No.1 and No.2. This is thought to be largely due to thermal expansion of the CMM, as it appeared related to the time taken. The longer this was, the greater the resulting drift.

Despite the occurrence of this displacement, the over all shape and dimensions of the die were the same, as show in Figs.9(b),10(b),11(b) and 12(b), when the subsequent reconstrucs

ions were superposed.

Quantification of the differences in depth and volume **before** and **after** the 'best fit' process were determined and listed in Table 5-1 and 5-2.

Table 5-1: Linear and volumetrical measurements between scanned images before a 'best fit' process

Data Files	Area of Comparison (mm^2)	Linear Difference (mm)	Volume Difference (mm^3)
cyl202-cyl203	**40.091**	**0.009**	**0.360**
cyl202-cyl204	**40.272**	**0.016**	**0.626**
cyl202-cyl205	**40.027**	**0.024**	**0.945**
cyl202-cyl206	**39.944**	**0.032**	**1.288**

Table 5-2: Linear and volumetrical measurements between scanned images after a 'best fit' process

Data Files	Area of Comparison (mm^2)	Linear Difference (mm)	Volume Difference (mm^3)
cyl202-cyl203	**40.091**	**0.003**	**0.127**
cyl202-cyl204	**40.272**	**0.004**	**0.137**
cyl202-cyl205	**40.027**	**0.005**	**0.187**
cyl202-cyl206	**39.944**	**0.003**	**0.126**

From Tables 5-1 and 5-2, it seems that the drifting occurred due to the time taken for measurement (time dependent expansion), and can increase up to a maximum of 0.032mm as a linear value, which is equivalent to 1.288 mm^3 in volume difference over 12 hours. However, in fact this linear drifting is not a problem in form measurement, since as it has been shown, it can be eliminated by superposition, hence,

maintaining reproducibility in linear form measurement by as little as 0.003mm, which is equivalent to 0.126 mm^3 as a volume difference.

5.4 Discussion

Measurement of stepped cylinders is widely encountered in component inspection in manufacturing industry, where quality control is more concerned with the roundness of the two cylinders and the concentricity of the geometrical relationship between them. The inspection is often carried out by taking a number of points on both cylinders and the step face using a touch probe. Then, a software package is used to 'best fit' the data into a cylinder, and report the 'best fit' results as a diameter and length of the cylinder. Measurement of a crown or veneer preparation requires overall surface form information, and more importantly, the change between the two, in other words comparative measurement.

Regarding the sampling interval, it would be more logical to use a small sampling interval in the regions close to the steps, and a relatively larger sampling interval in the smoother area of the cylindrical parts. Although this can be achieved in the digitisation procedure, the subsequent surface interpolation can not cope with the variations in the co-ordinate spacing. Therefore, a compromise of a fixed small scan pitch was used in this investigation, giving a high reproducibility at the step region.

It is important to recognise that although thermal expansion was seen in +Y direction in CMM space, using comparative measurements this error can be cancelled out during the superimposition procedure.

5.5 Applications in dental research

5.5.1 Assessment of crown preparations

The technique developed has been successfully applied to dental research in the assessment of crown preparations as shown in Figs. 5-13 and 5-14.

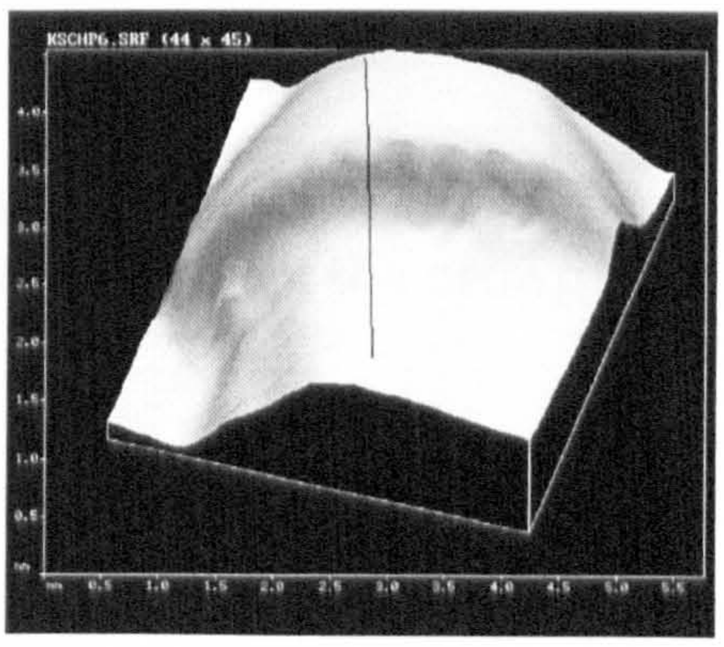

Figure 5-13: A labial scan with the mid-labial profile defined for measurement.

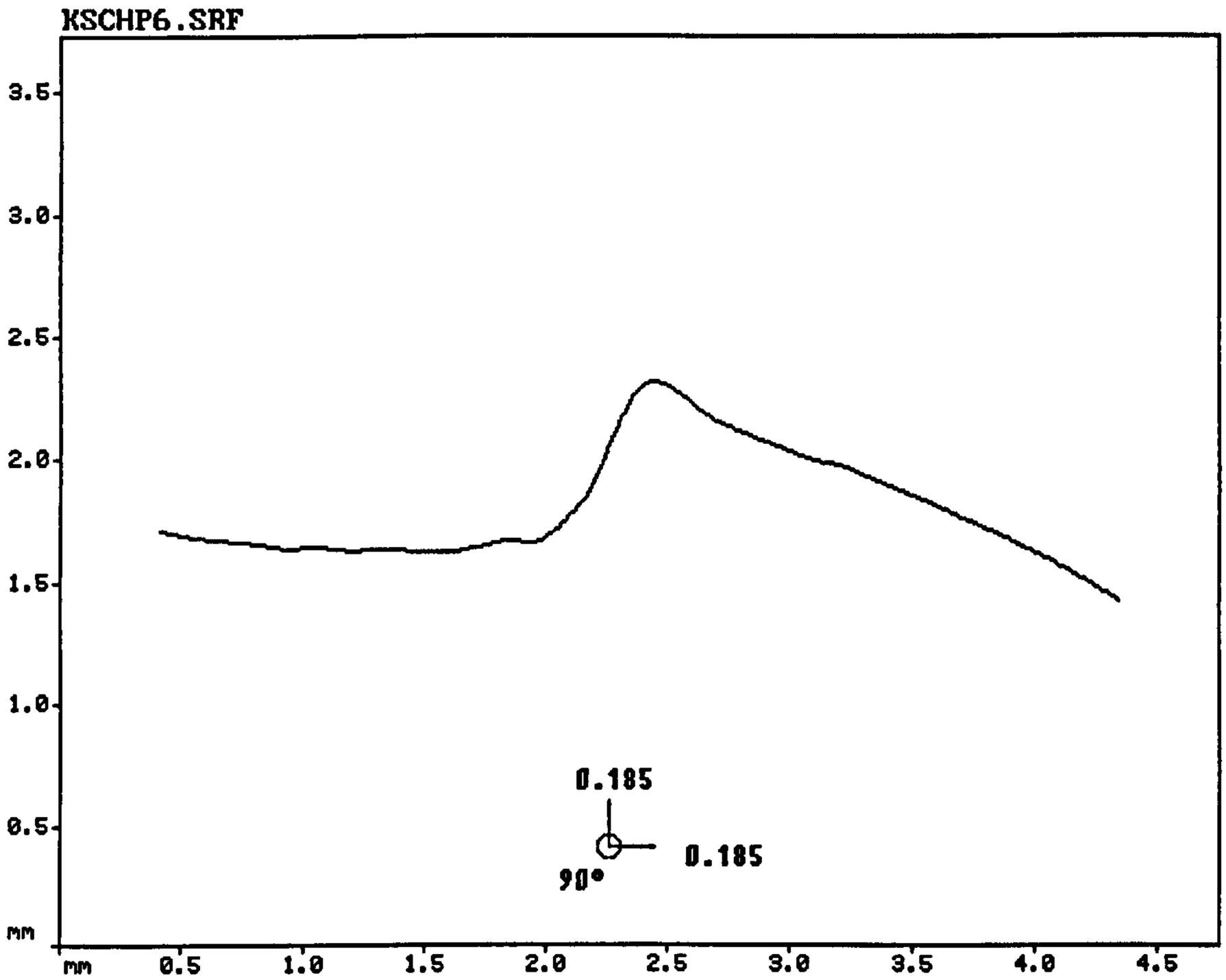

Figure 5-14: The mid-labial profile as defined in Fig.5-13 shows the shape of the crown preparation.

This research project indicated a tendency for clinicians to under-prepare and over-angle shoulder preparations for metal ceramic crowns, which has implications for the final restoration, in terms of contour, appearance and strength. This work has been published and presented widely (Seymour *et al.*, 1995, 1996, 1998, 1999).

5.5.2 Assessing the quality of porcelain veneer preparations

This project provided an objective measurement method to compare various techniques available in the preparation of a porcelain veneer. The findings have been published and presented (Cherukara *et al.*, 2002).

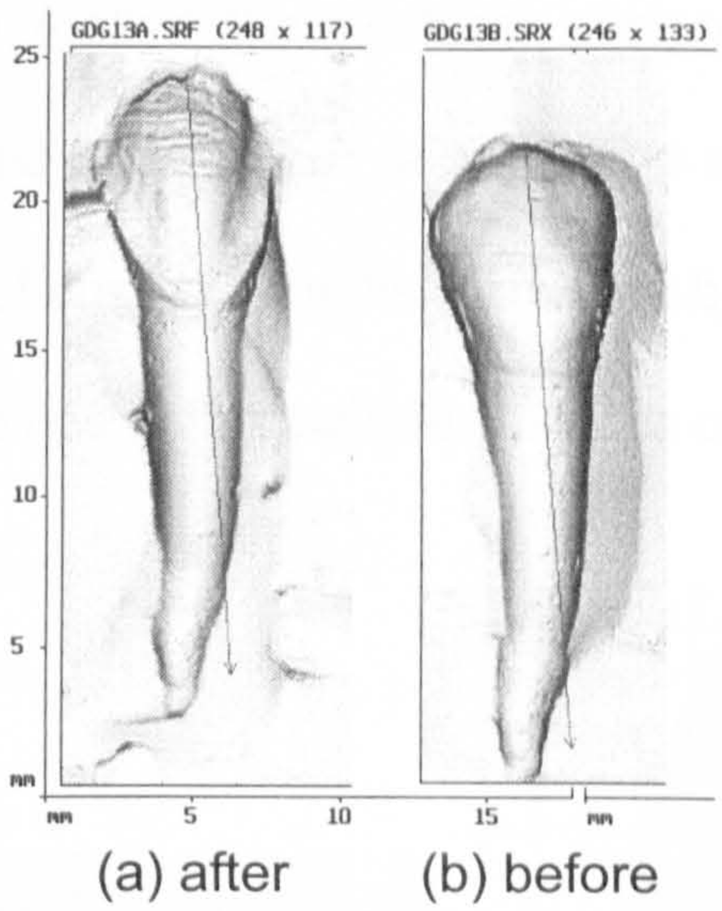

(a) after (b) before

Figure 5-15: Reconstructed images of before(b) and after(a) veneer preparation of an extracted incisor tooth.

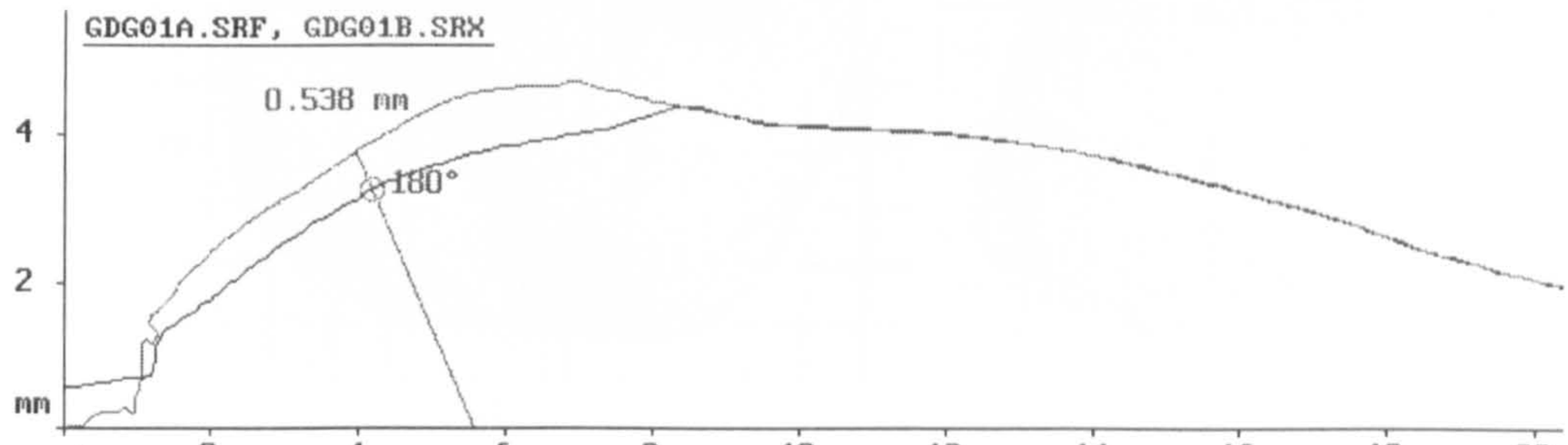

Figure 5-16: Indication of the depth of a veneer preparation (0.538mm) by two superposed profiles.

6 AN INVESTIGATION OF A TYPE II SIMULATION MODEL

6.1 Introduction

The form and dimensions of a molar tooth viewed from 2 different directions are shown in Fig.6-1. The approximate dimensions of the crown region can be seen as 12mm wide × 12mm deep × 6mm high. The top surface of the crown (called the occlusal surface), consists of cusps (peaks) and interspaced by fissures (valleys). The slopes form a modified pyramid from the tips of cusps to the fissures, and become more spherical in shape from the cusp tips to the outside surfaces of the tooth.

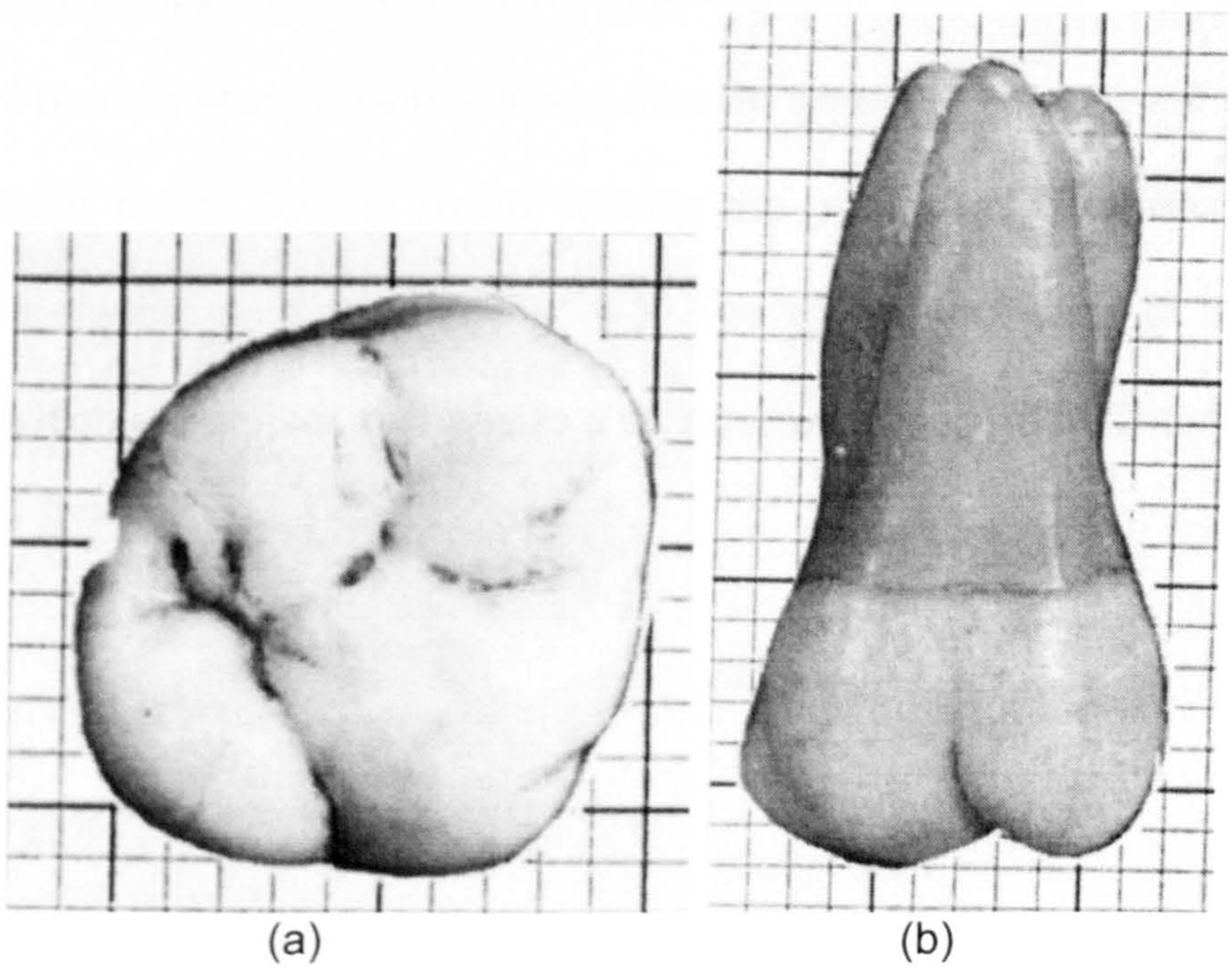

Figure 6-1: An upper right first molar viewed against graph paper (mm). (a) occlusal view, (b) palatal view.

On the upper surface, the contours change sharply at the fissures. The complex geometrical features of a molar give no obvious clues to the selection of suitable probe orientations for scanning this type of free form surface.

A digitisation strategy for such an irregular surface was developed and evaluated in this Chapter. A model of known geometry with shapes and dimensions similar to a molar tooth was initially designed as shown in Fig.6-2. Although this model provides an appropriate shape, the manufacture of the internal pyramidal areas was difficult. Hence, an easier and simpler approach was taken by using four balls attached to each other. The diameter of each ball was 6mm to simulate the occlusal surface of a molar tooth. Such a model reflects the geometrical features of the molar surfaces, as shown in Fig. 6-3. The outside surfaces of a molar tooth, which are similar in shape to a cylinder were studied in Chapter 5.

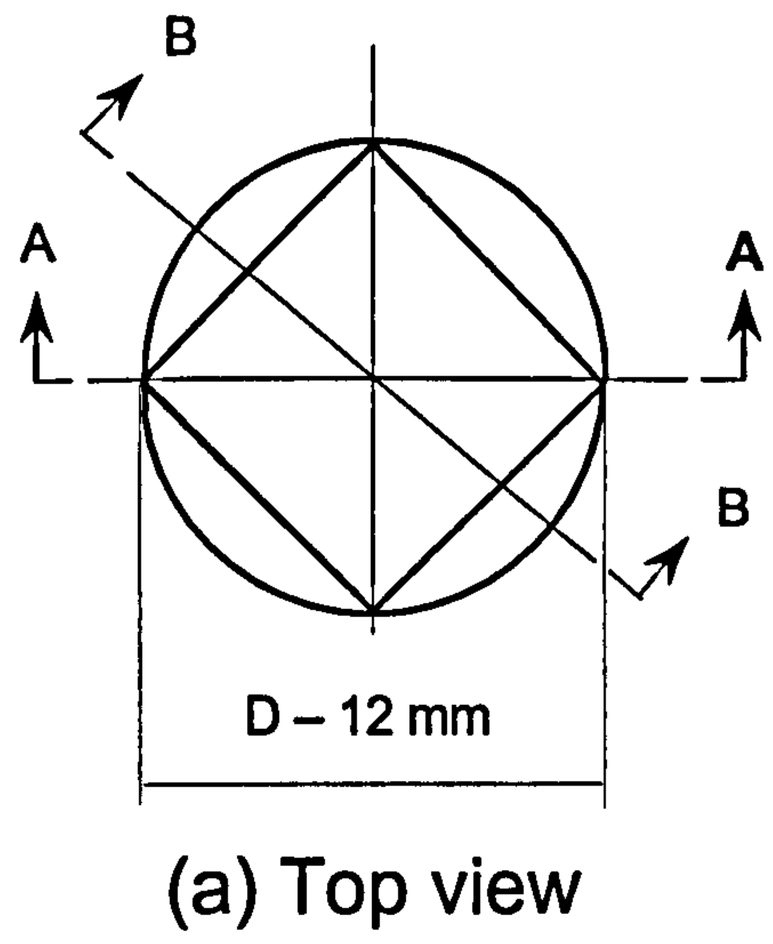

(a) Top view

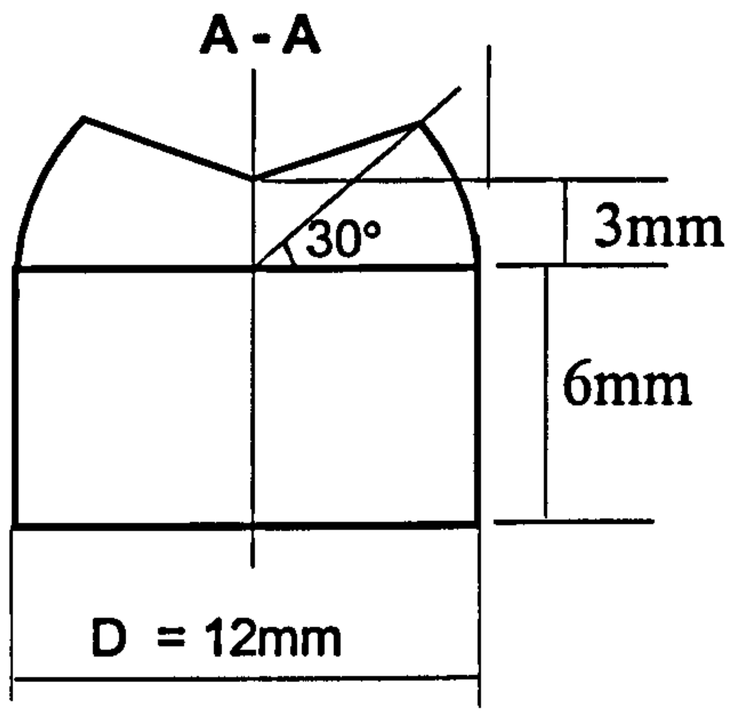

(b) view from A-A defined in (a)

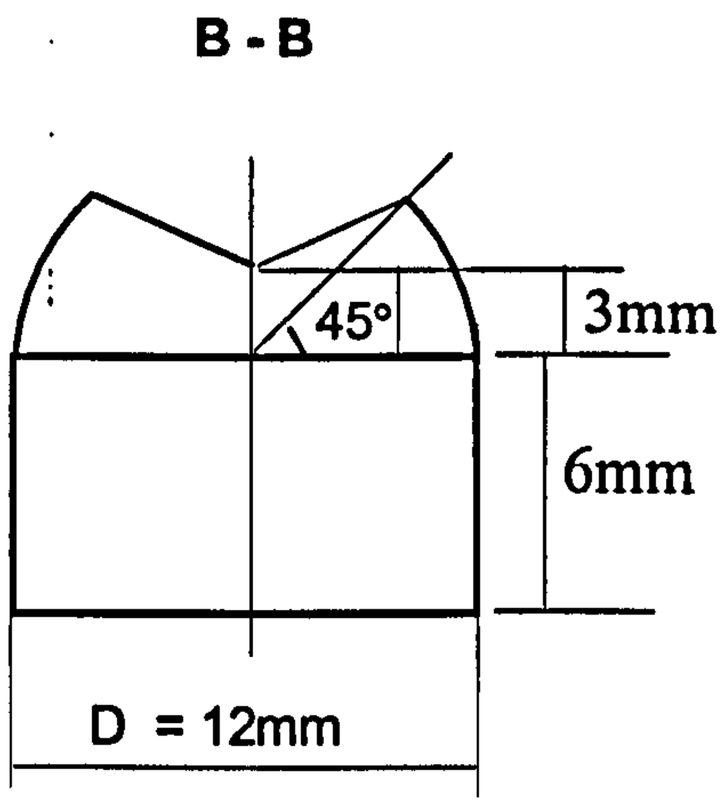

(c) view from B-B defined in (a)

Figure 6-2: A design for a crown simulation model.

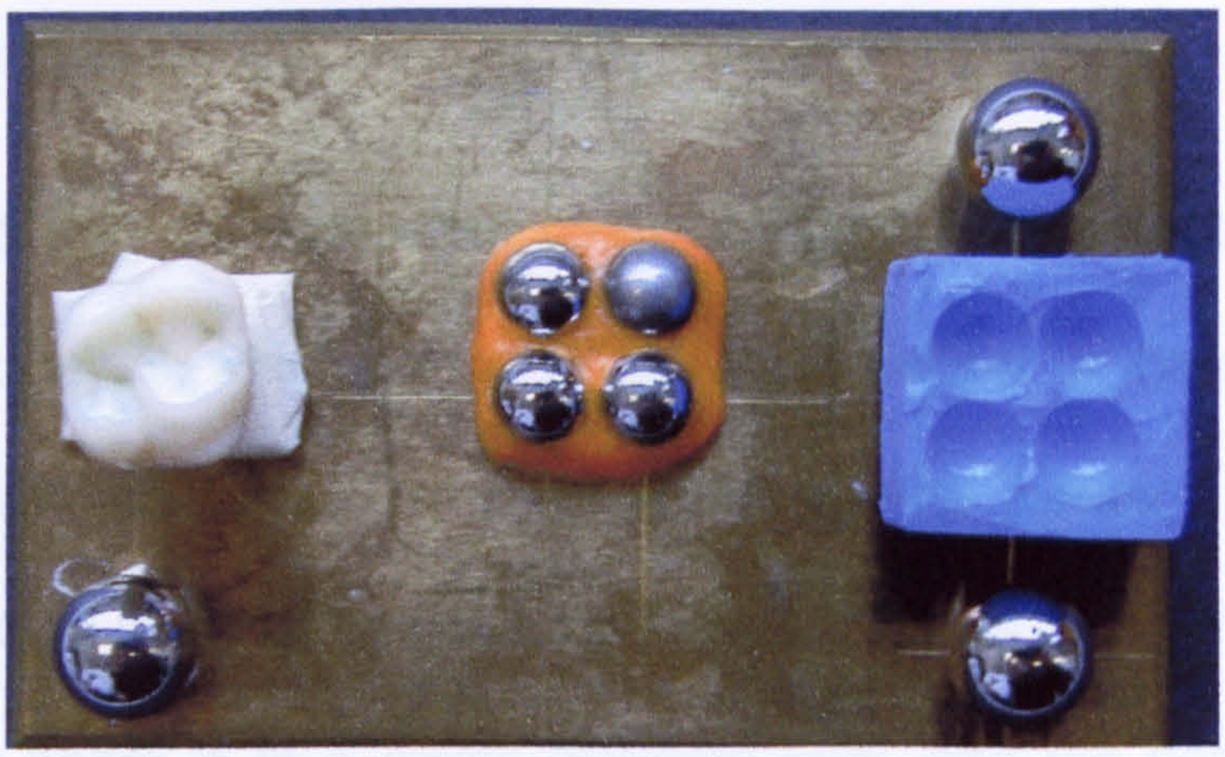

Figure 6-3: Four-ball-bearings arranged as a simulation model for the crown of a molar tooth. A molar tooth is seen on the left, and an impression of the model is on the right.

6.2 Materials and Methods

6.2.1 Assembly

Four steel balls 6mm in diameter were selected, rigidly assembled and secured on a steel plate as shown in Fig.6-3. The relative distances and heights between each ball were deliberately made unequal, to imitate the distances between the cusps on the occlusal surface of a molar tooth.

The four centres of the balls defined three planes, but the angles between the planes were not critical as long as they differed from each other, and they did not have to align with any of the axes in CMM machine space (frame), as it was the case with a real molar tooth surface.

6.2.2 Surface treatment

It was found that stainless steel ball bearings have too great reflectivity from their surfaces, which prevented the laser sensor of the probe (OP2) from operating properly. The OP2 probe on the sensor collects only diffuse reflected light. When the object surface is very shiny, the reflection of the laser beam is in a single direction only, and the detector of the probe receives either too little light when it is out of the reflected range, or too much light when it is directly receiving the reflection. To avoid this situation, various surface treatment methods were tried, such as sprays or paints. Unfortunately with these techniques, it was impossible to control the thickness of the materials applied.

This study aimed to simulate the scenario of an *in vivo* clinical trial, in which case the samples obtained would be impressions from patients' teeth, hence, impressions of the model rather than the model itself were digitised and evaluated.

6.2.3 Digitisation parameters

The target was scanned using a multiple probe orientation technique. The probe orientations were determined, and were based on the previous investigation of error distribution over a sphere as described in Chapter 6. The sampling rate was 0.05mm, and scanning speed was 10 points per

second, the optical threshold setting was 80. The probe orientations, definitions and arrangements were rather complicated, these are described in the following sections 6.2.4.

6.2.4 The digitisation arrangement for multiple probe orientations

This object surface consisted of four hemispheres. Each of the hemispheres was divided into four quadrant hemispheres, and allotted an identifying code. This resulted in a total of 16 segments, and each one was scanned using a specific probe orientation. To scan these 16 segments, it was not necessary to define 16 individual probe orientations, as the geometrical features of the balls were the same. Hence, only four probe orientations were required for each quadrant of the hemisphere. These were defined as I (30°, 135°), II (30°,-135°), III (30°,45°) and IV(30°, -45°). These same probe orientations were used for each of the four balls as shown in Fig.6-4.

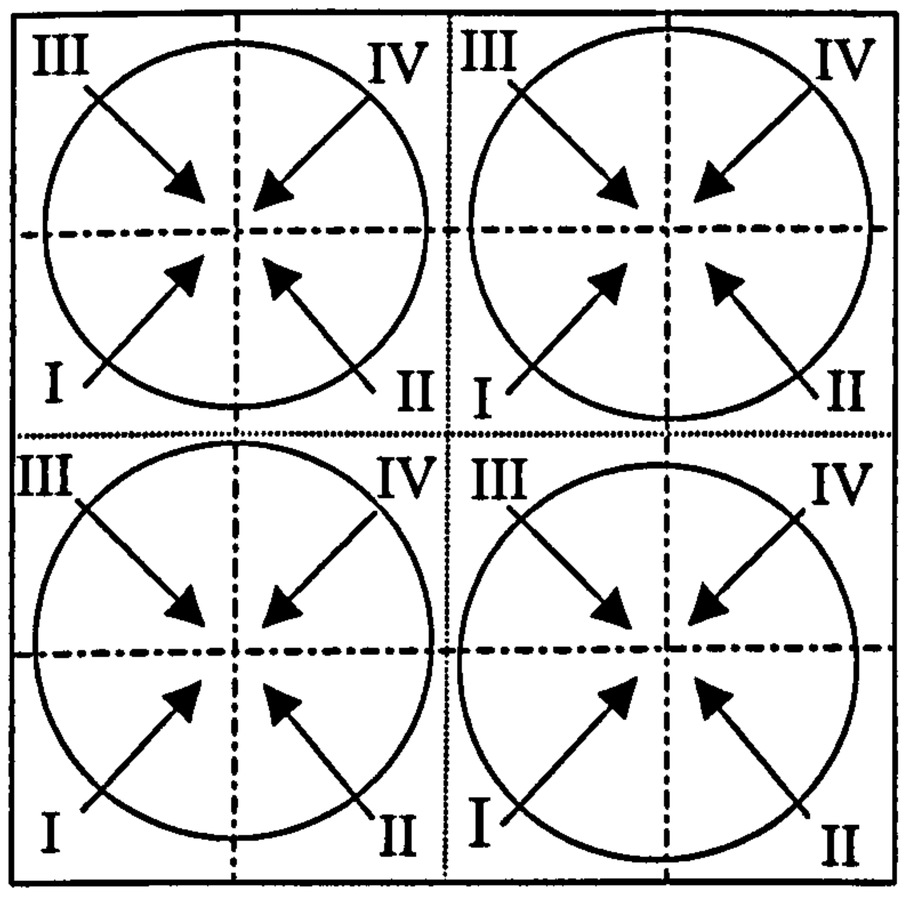

Figure 6-4: The arrangement of four probe orientations over four hemispheres.

Each segment scan was started at the highest point of the sphere. This was to avoid early termination occurring during the scan, as the largest surface contour changes are at the circumference of the sphere, and over the sphere the contour changes continuously. The method provided a uncomplicated digitisation procedure, but then required much more complex data re-arrangement, as the string of data co-ordinates was not in the right order between segments, in respect of the scanning direction. All scanned segment data was stored in a temporary storage layer, and produced a total of 16 layers in all. When the digitisation procedure was completed, the co-ordinate order was rearranged, and the each segment was merged to provide data to reconstruct the complete hemisphere.

The segment scanning directions for each ball were different as illustrated in Fig.6-5, and were identically applied to the other three balls. Although all four segment scans started at the top of the ball, they required a 20μm shift away from each other at the starting point, because the maximum positioning tolerance of the CMM was 20μm.

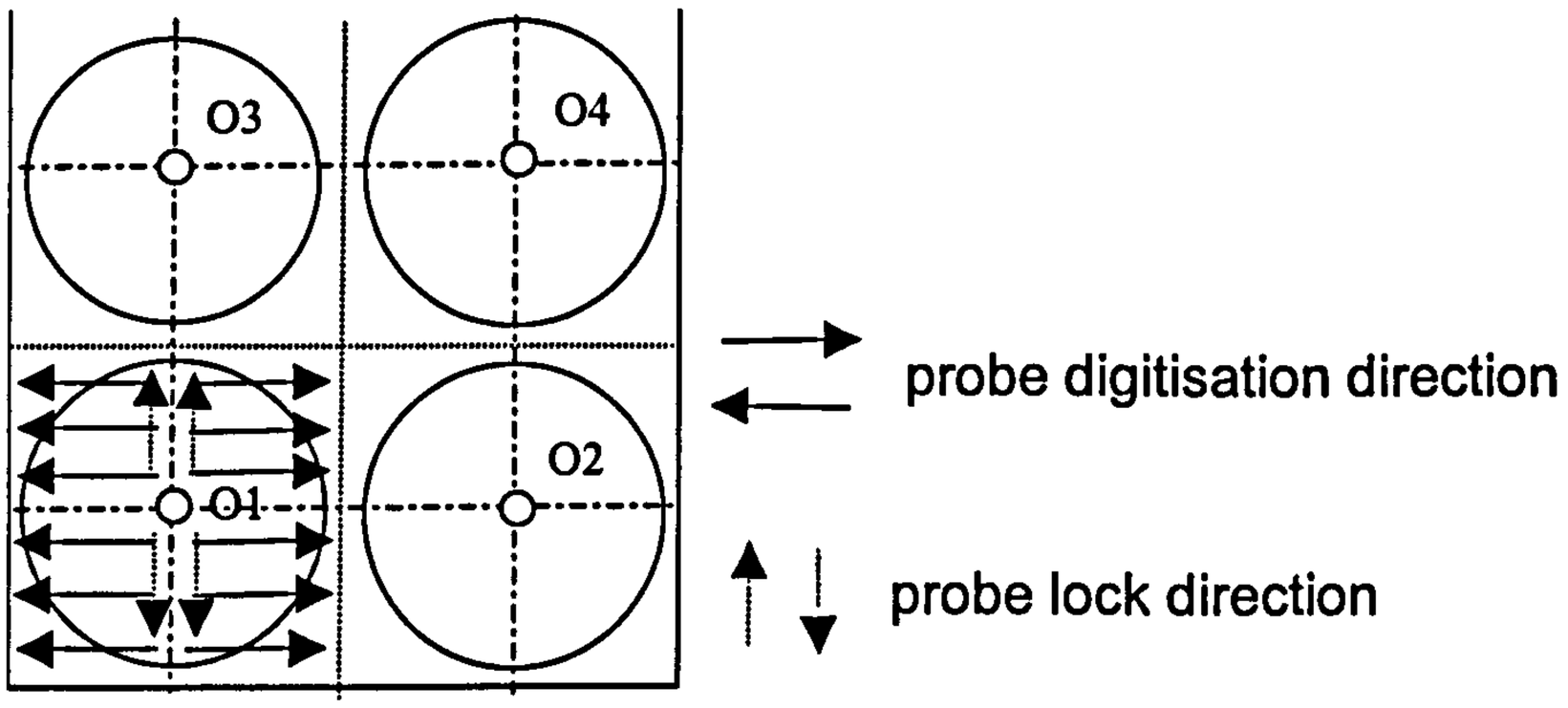

Figure 6-5: The arrangement of scanning and lock directions.

The scanning procedure so described was complicated and time consuming, especially in the merging procedure adoped for the 16 segments. However, it was possible to simplify the procedure, since four probe orientations could be used without re-addressing if the scanning process was arranged as Fig.6-6(a). After the first segment scans of the four balls, the data string order was re-arranged. In this manner the second segment scan data could be followed and saved in the same layer as the first segment as shown in Fig.6-6(b), which avoided the posterior data re-ordering previously required between the first and second

segments. This method was extended to the other three segments over the remaining three balls, so that the temporary storage layers reduced from 16 to 8, and posterior data arrangement was also reduced from 16 to 8 layers.

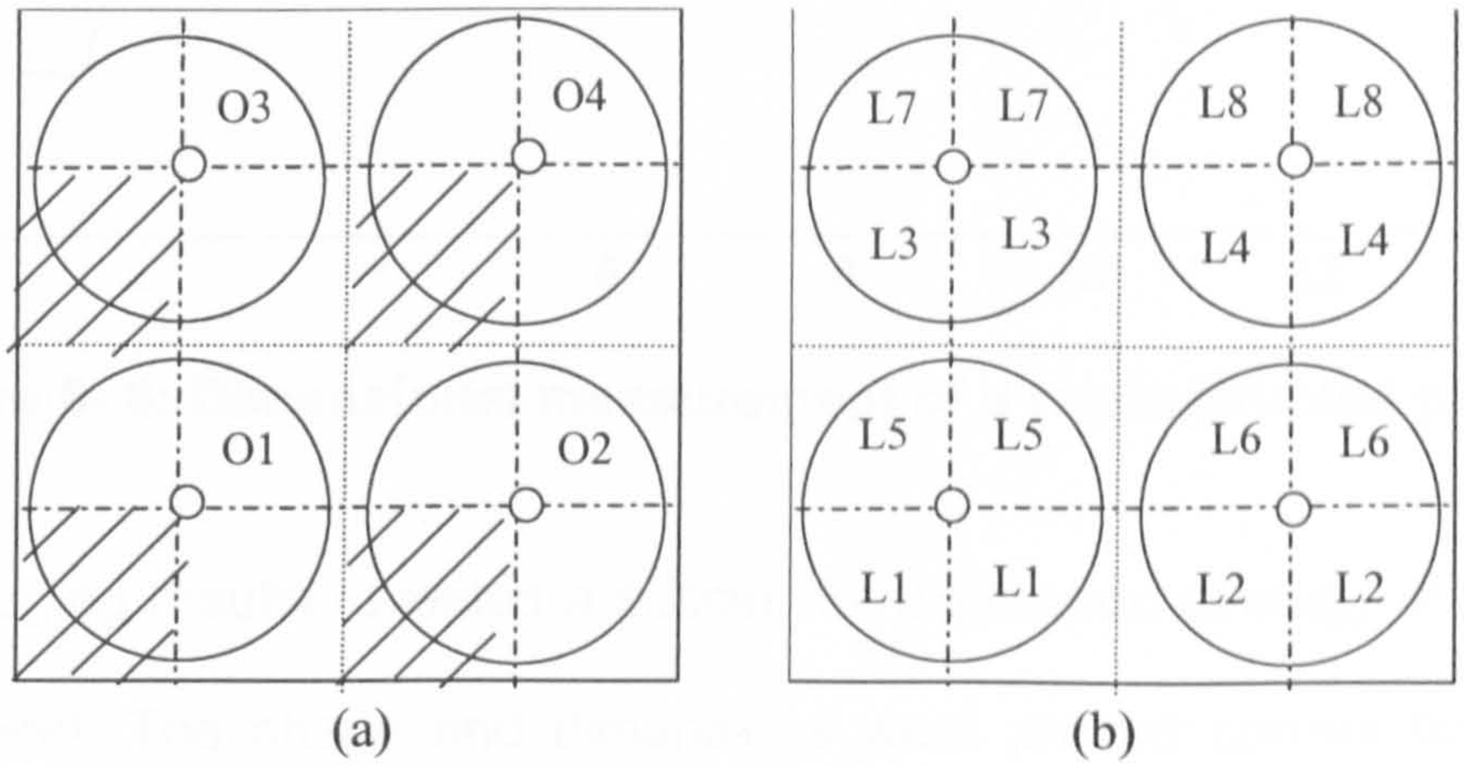

Figure 6-6: The scanning order used during surface digitisation as shown at (a) and the temporary data storage arrangement as shown at (b).

6.3 Results

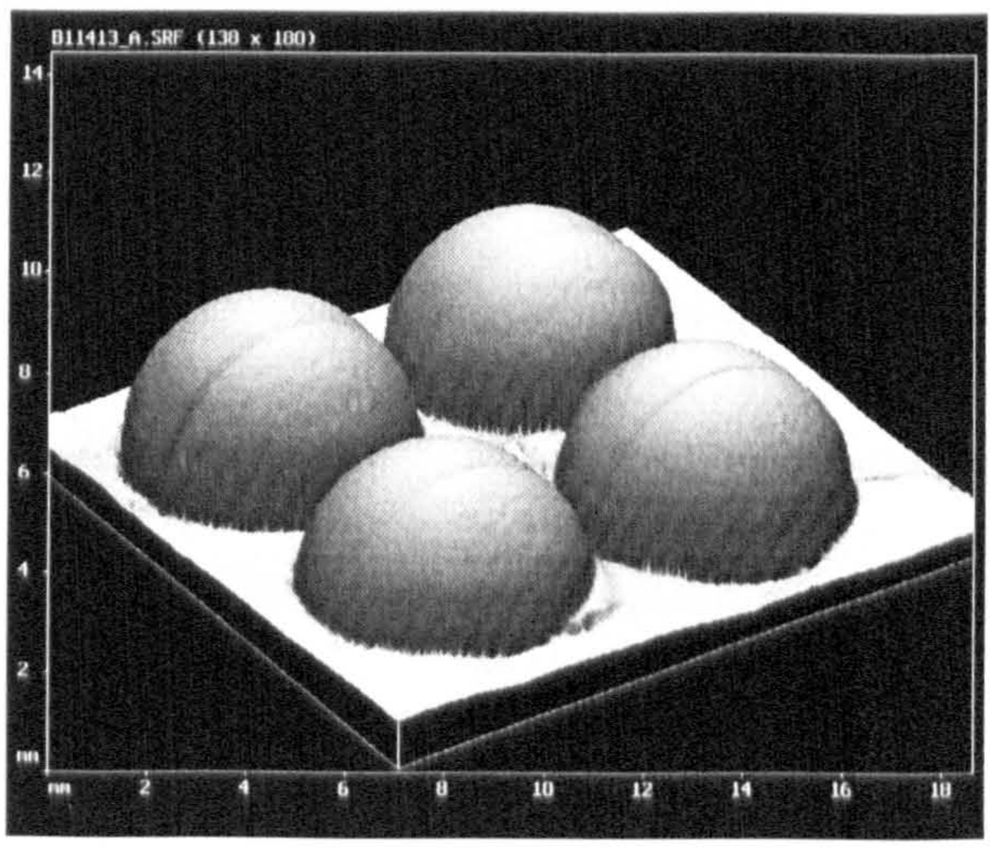

Figure 6-7: A reversed image of the impression of the four ball model.

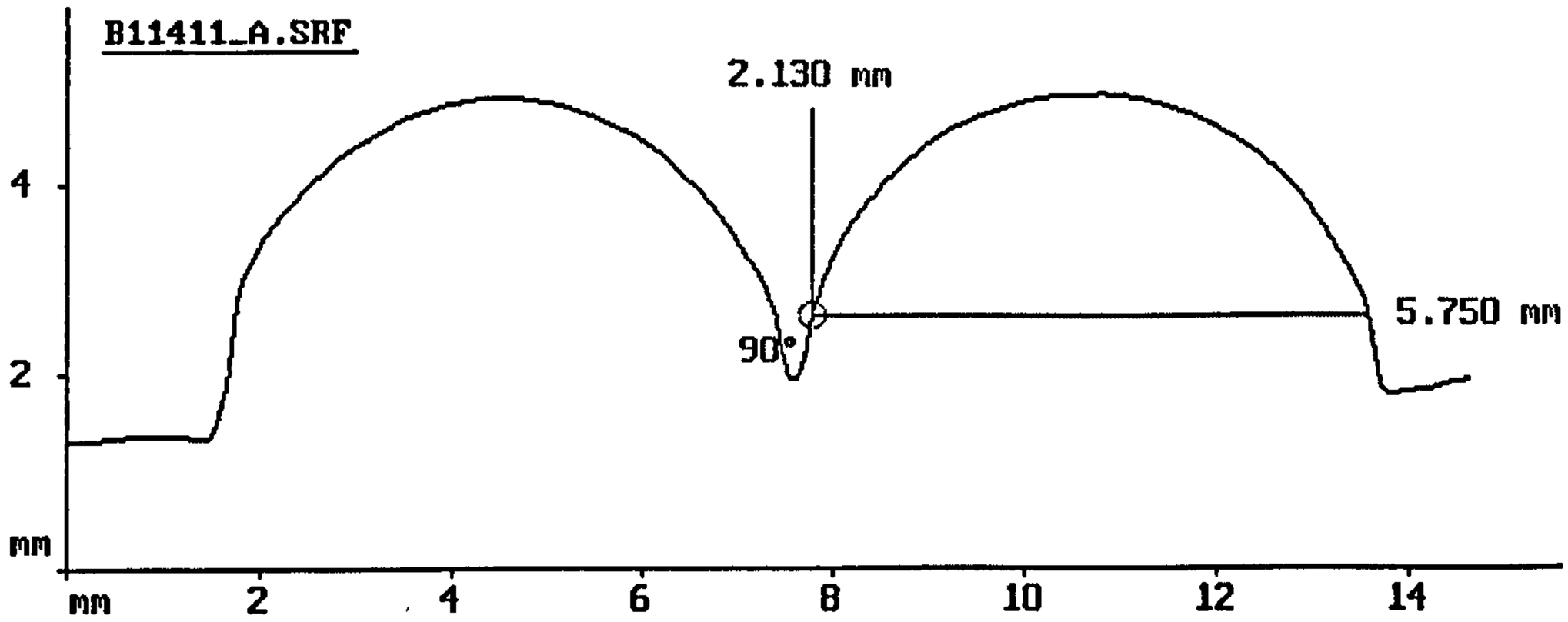

Figure 6- 8: Dimensional measurement of a reconstructed profile.

The imaging results revealed a successful digitisation strategy of the four ball model. The shape and dimensions were proved correct from data analysis of the reconstructed image, as shown in Figs.6-7 and Fig.6-8.

A defect was revealed along the middle of the sphere in Fig.6-7, where the probe orientation changed. This was expected as each hemisphere was scanned using four probe orientations, following the study concluded in Chapter 4. The difference here was that the diameter of the sphere was 6mm, compared with the 25mm sphere used in Chapter 4. From equation (1) in Chapter 4, with a smaller diameter sphere and by using a smaller scanning pitch of 0.05mm, the error caused by using four probe orientations was reduced significantly.

6.3.1 Reproducibility assessment

Reproducibility was assessed by scanning the same model five times continuously. The superposed images are shown in Figs.6-9 to 12. Volumetric measurements were made comparing the second, third, fourth and fifth images as related to the first image, and these values are given in Table 6.1.

Table 6-1: Volumetric differences between pairs of images over a 150mm² area.

	1 & 2	1 & 3	1 & 4	1 & 5
Volume differences (mm^3)	**0.715**	**0.777**	**0.799**	**0.950**

Paired colour-coded images are shown in Figs.6-9 to 12. A reproducibility of ±10μm was obtained in most cases as is shown in Figs.6-9 to 12; with a reproducibility of ±15μm (Fig.6-12). The errors seen at changes of the probe orientation were due to the relocation of the probe, which inevitably lead to mechanical deviation. One case with a slightly higher error was regarded as a random deviation.

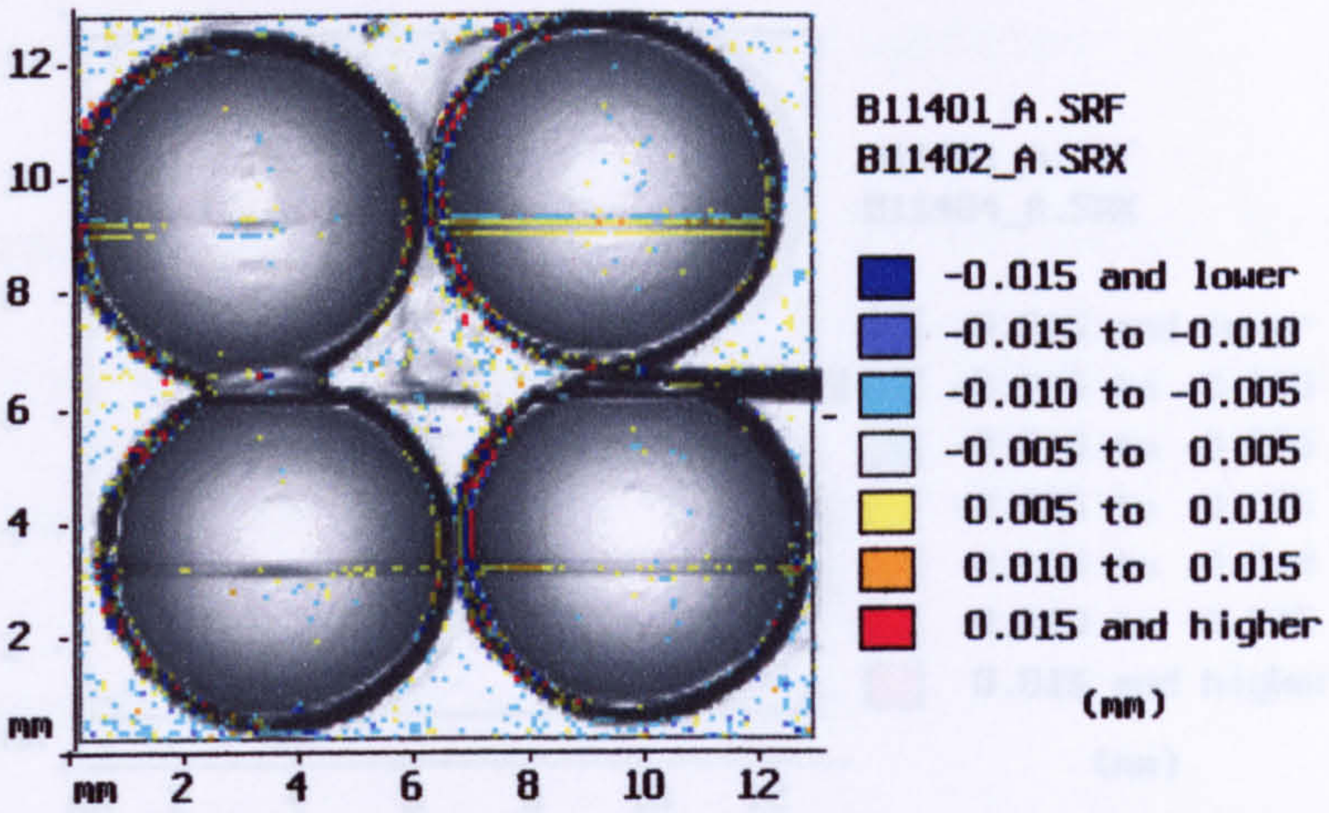

Figure 6-9: Colour coded image to show the difference between the No.2 and No.1 scans.

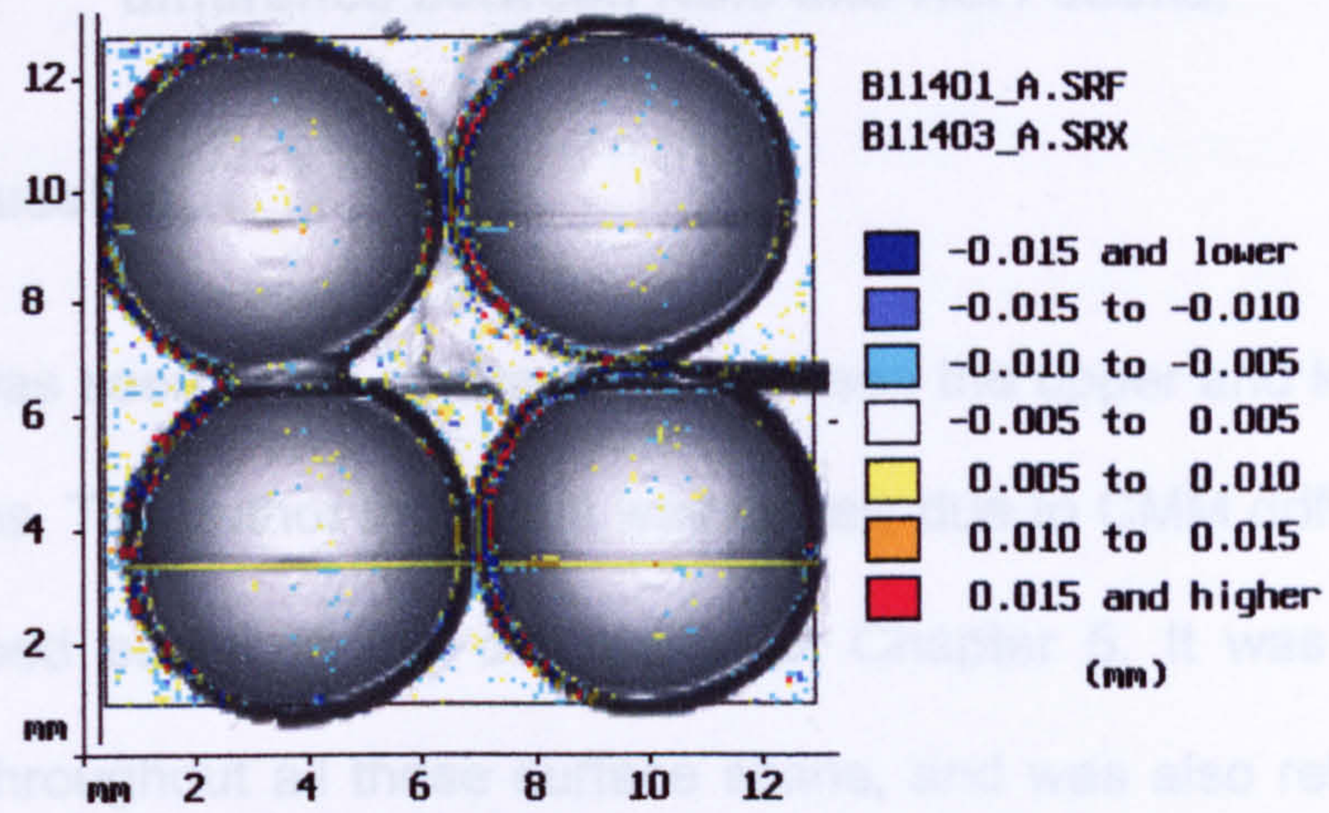

Figure 6-10: Colour coded image to show the difference between the No.3 and No.1 scans.

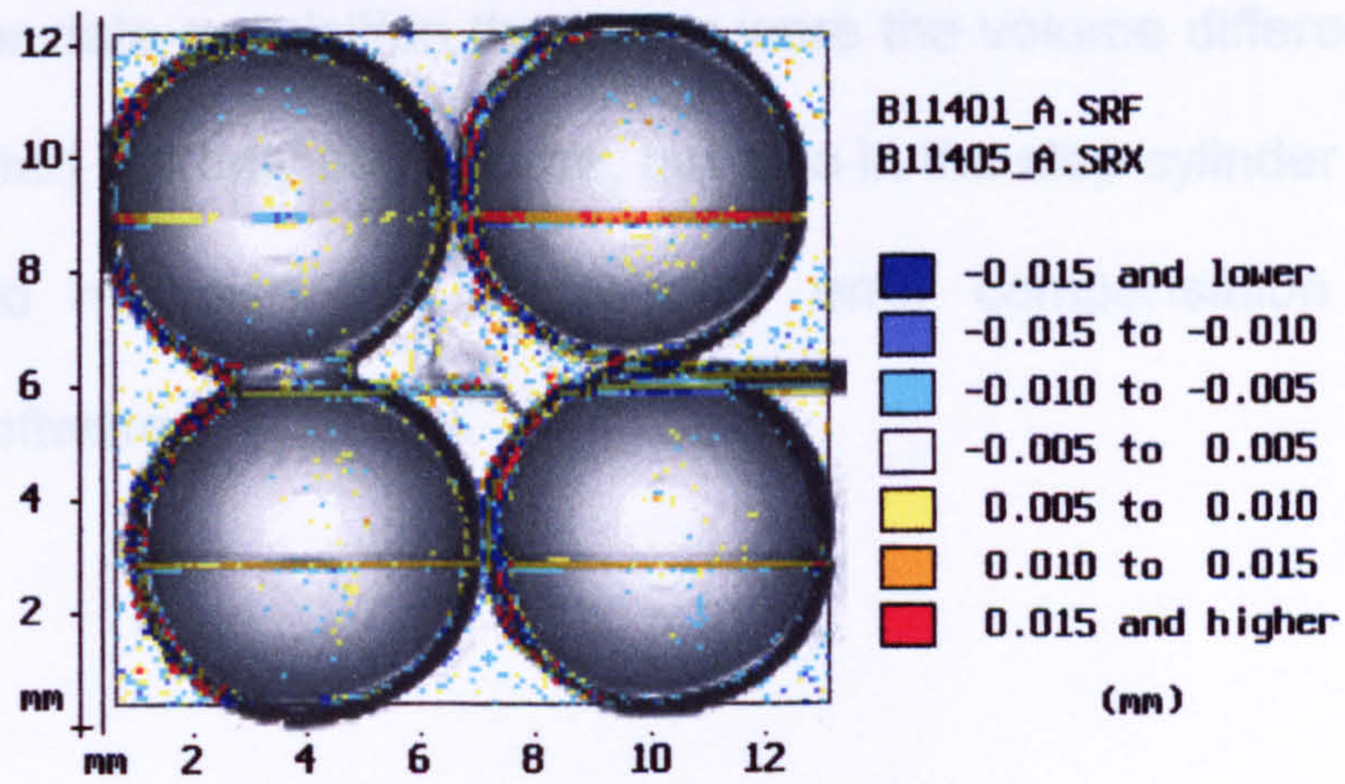

Figure 6-11: Colour coded image to show the difference between No.4 and No.1 scans.

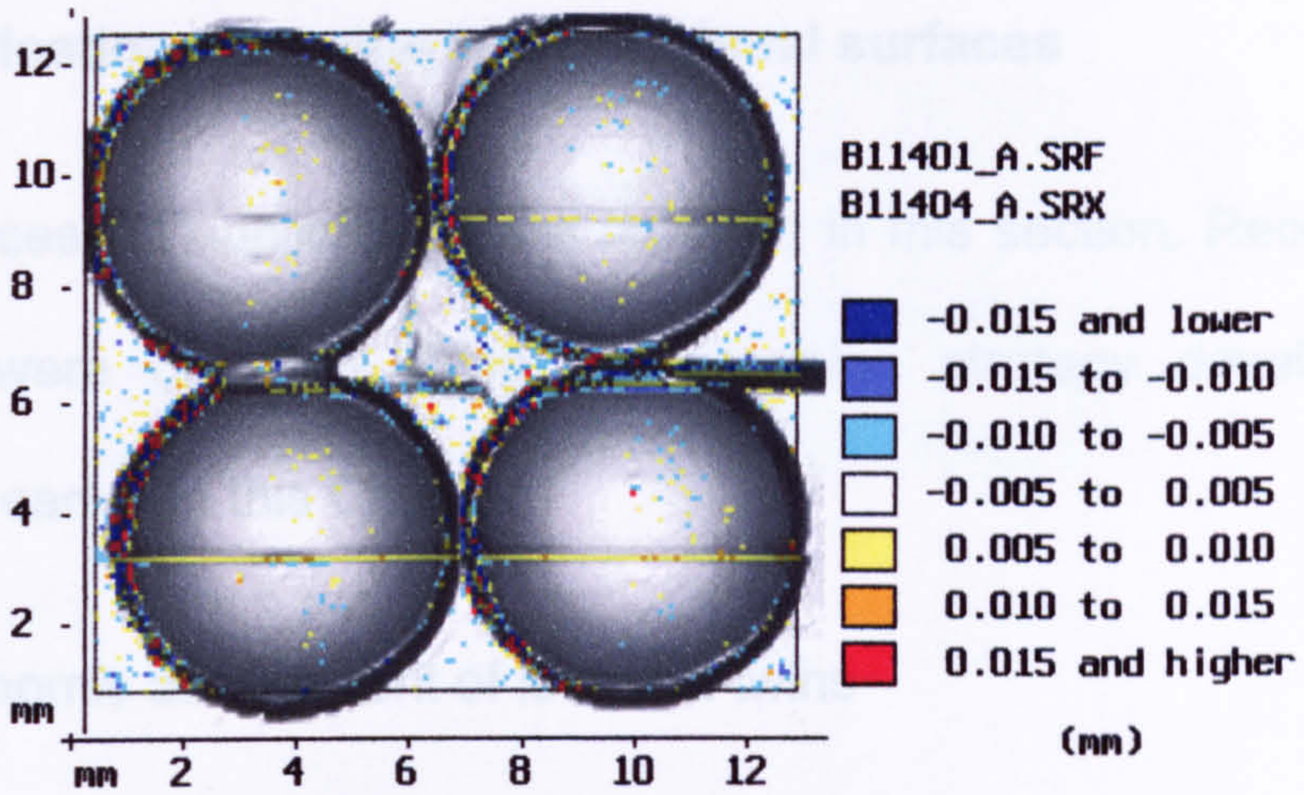

Figure 6-12: Colour coded image to show the difference between No.5 and No.1 scans.

6.4 Discussion

A defect was seen at the connections between the upper and lower half of the spheres. The author thought it was largely due to CMM drifting effects, as described earlier in the discussion in Chapter 5. It was repeatedly revealed throughout all these surface scans, and was also related to the time taken for the digitisation procedure. It has been shown that the longer the time for data acquisition the larger were the volume differences seen. This occurred not only in this case, but also in the step cylinder scans. It is possible to minimise this problem by error compensation using the analysis software.

6.5 Applications to molar teeth occlusal surfaces

Three successful applications are reported in this section. Reconstructed surfaces were obtained using the scanning strategy developed and described earlier in this Chapter.

6.5.1 Genomic assessment of identical twins

This project aimed to assess concordance of tooth size and occlusal morphology in monozygotic (identical) and dizygotic (non-identical) twins when compared with unrelated controls, in order to determine how much these dental traits were inheritance related. The results of this study have been published elsewhere (Kabban *et al.*, 2001).

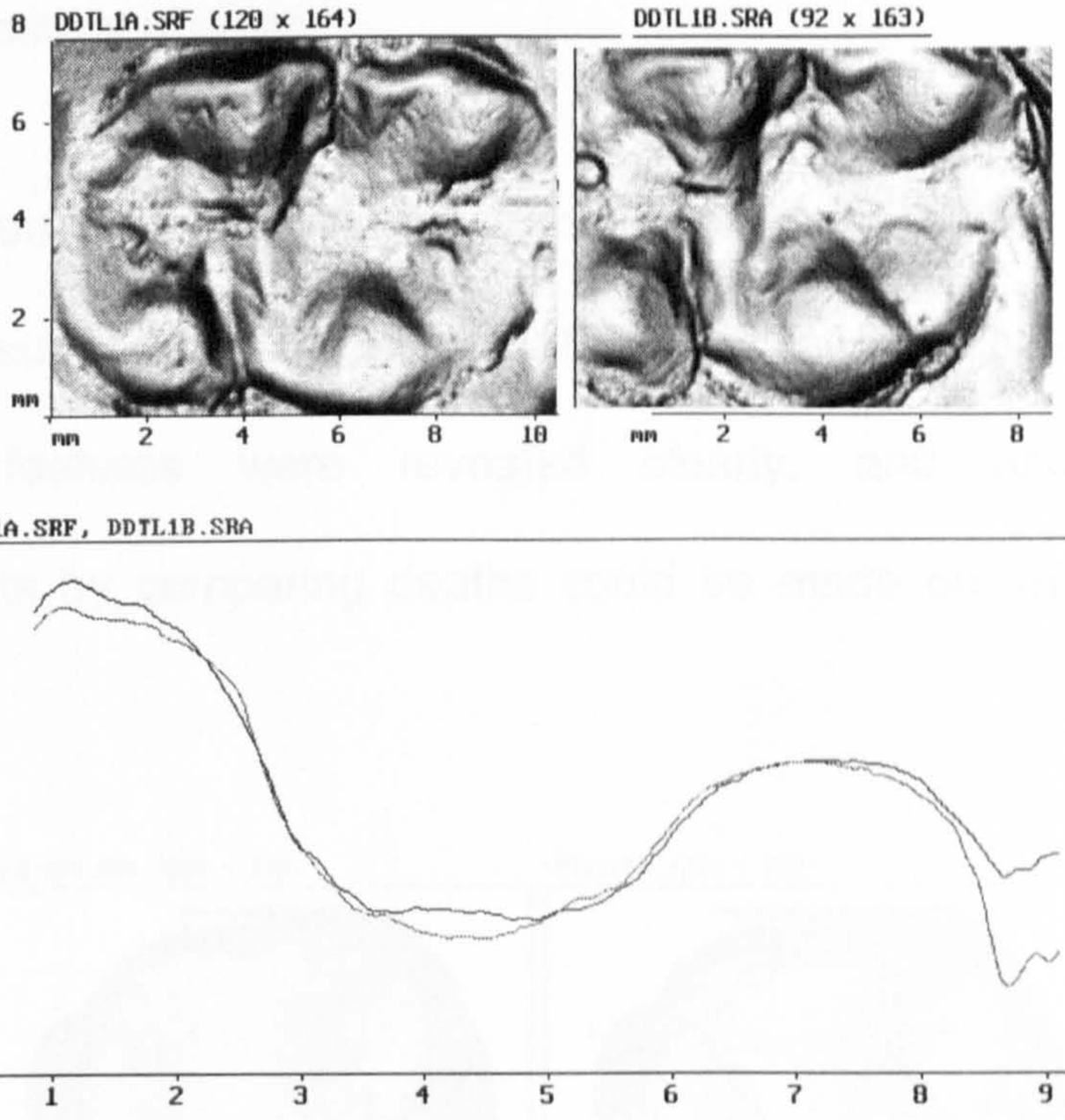

Figure 6-13: Similarity measurement of corresponding molar teeth of identical twins.

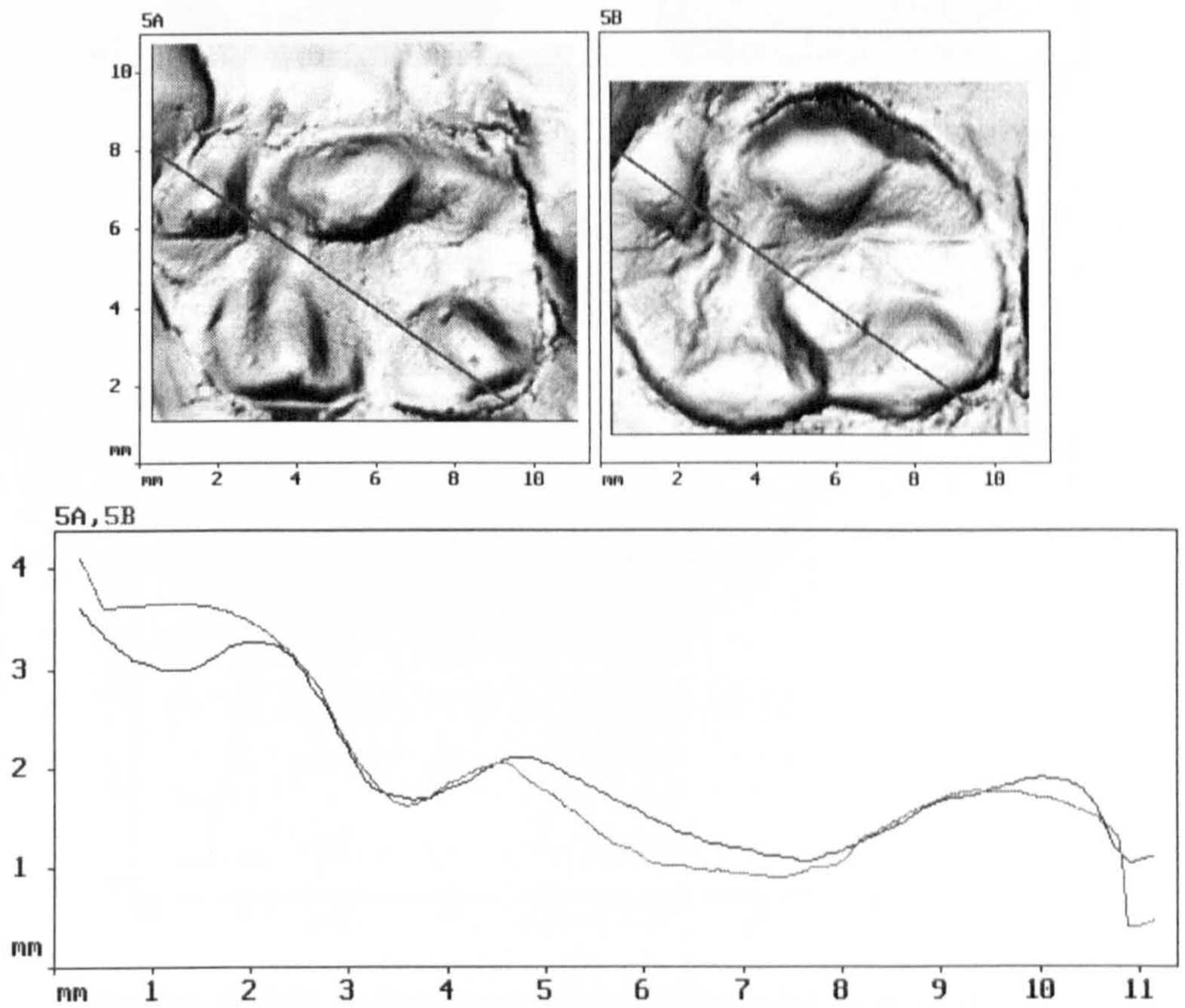

Figure 6-14: Dissimilarity measurement of corresponding molar teeth of non-twins.

6.5.2 Assessment of wear

Sequential wear measurement of a dental filling material was assessed on the occlusal surface of a molar tooth. From the reconstructed 3-D image, anatomical features were revealed clearly, and accurate wear measurements by comparing depths could be made on any part of the surface.

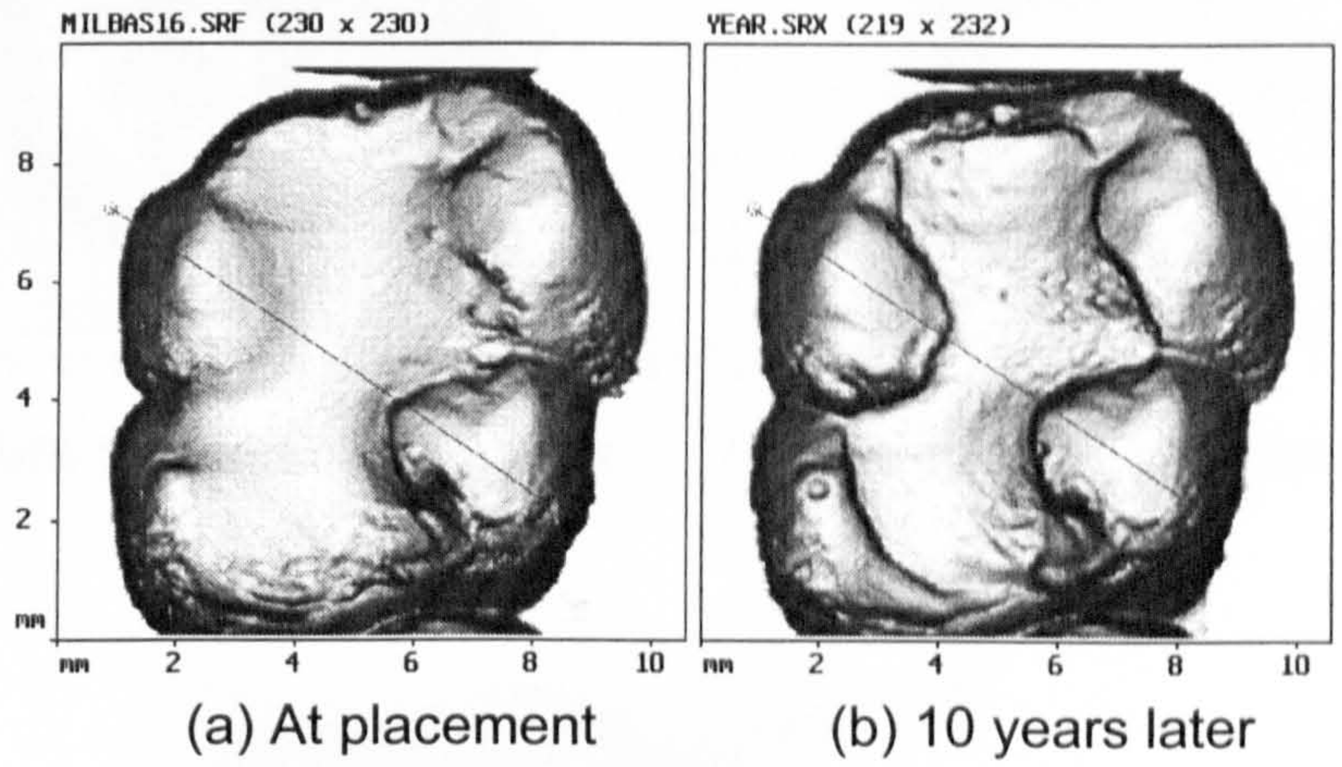

(a) At placement (b) 10 years later

Figure 6-15: Reconstructed images (a) at placement and (b) after 10 years.

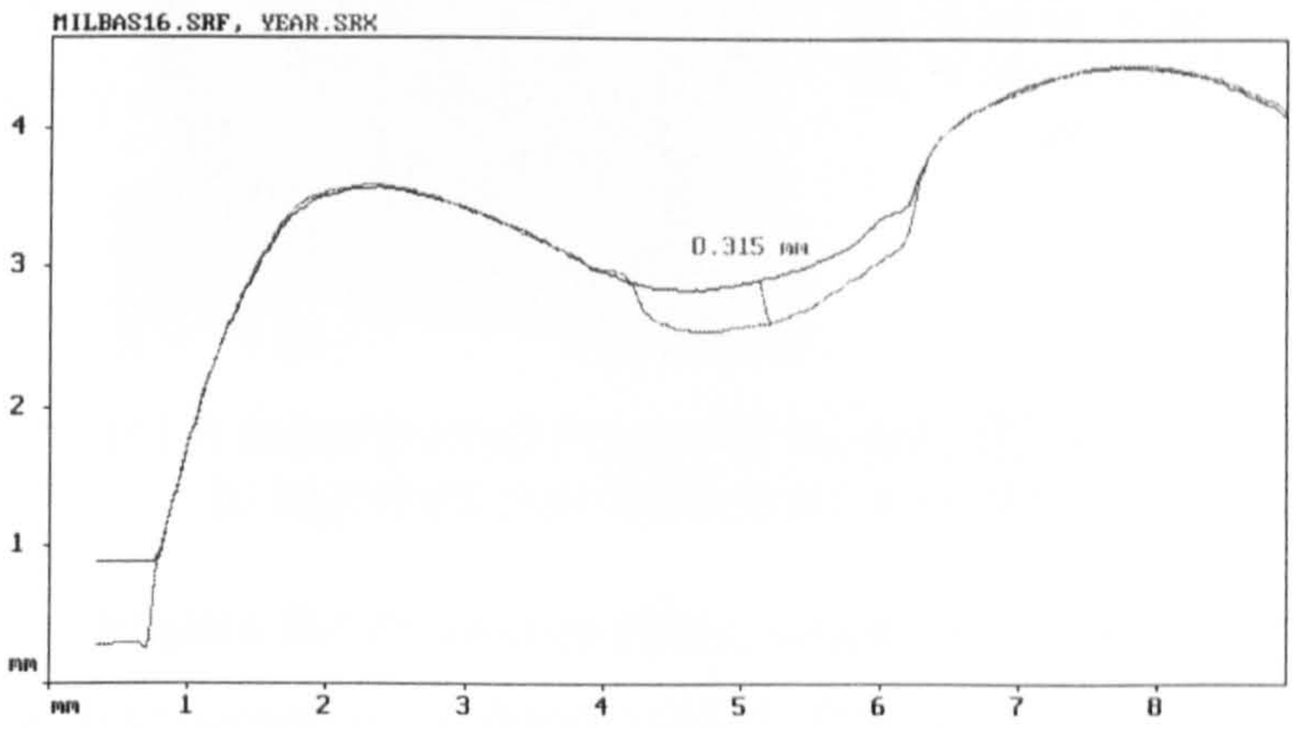

Figure 6-16: Superposed profiles show a reduction of 0.315mm in height of the filling over 10 years.

6.5.3 Assessment of sealants

Volumetric measurement of sealant application provides an accurate visualisation, and reveals where changes have occurred in depth, position and volume.

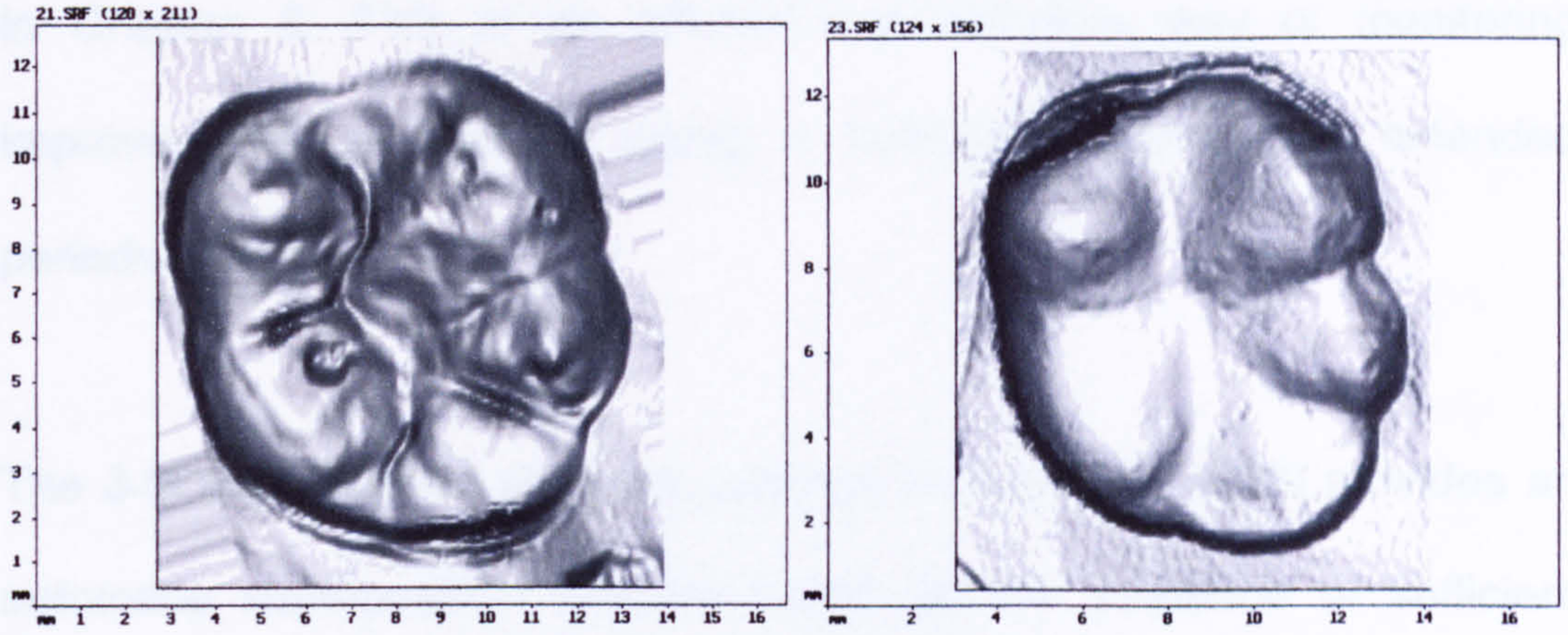

(a) Before placement of sealant (b) Immediately after placement

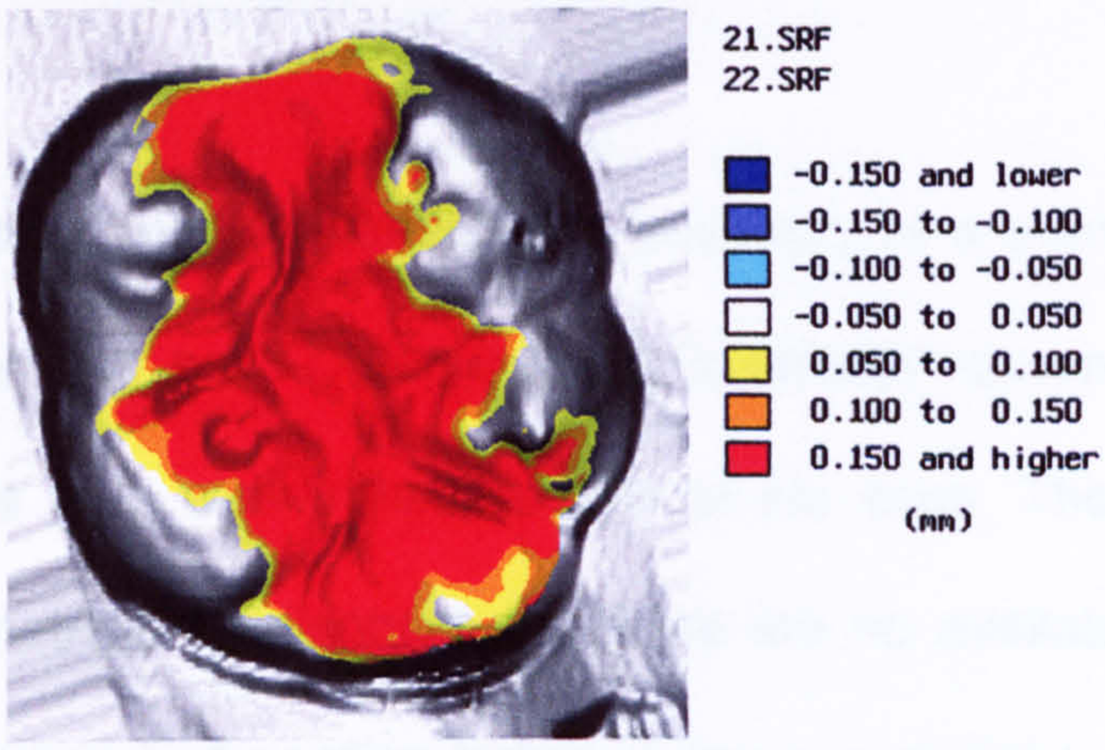

(c) A superposed image of (a) and (b) above to highlight the difference in contour

Figure 6-17: Linear (Max. depth = 1.53mm) and volumetric (volume=23.7 mm³) measurements were made of a sealant.

7 AN INVESTIGATION OF REFERENCE SYSTEMS

Compared with the type of measurements usually required in industry, one major difference in dentistry is the common need to obtain and compare measurements from sequential experiments, such as were seen in Chapter 6. This is an efficient and objective way of monitoring improvements or changes during a treatment regime over extended periods of time.

The 3-D data analysis software package (Jovanovski, 1999) provides an automatic superposition function based on the presence of sufficient unchanged surface features used as 'landmarks' where comparative measurements are required.

In bio-engineering, medical and dental research, in a number of cases, surface contour has no 3-D features to 'landmark' common areas. An example of this is in wear measurement of hip cups. The hip cup is a quadrant symmetrical hemisphere, so there are no available features to align the orientation and position between two sequential scan images. In such cases, extra information is required to act as a reference.

This Chapter considers experiments which required comparative measurements but lacked sufficient features to identify a 'landmark' for

their alignment. The development of reference systems are as a result of real research needs in bio-engineering and dentistry.

7.1 Using a cubic square as a reference device for deviation measurement of a tooth in a jaw model

The ability to measure the position of orthodontic brackets can be a valuable tool in orthodontic treatment. Aleaniz (1998) reported that the 3-D movement of teeth following orthodontic treatment could be measured by a computer-controlled optical data acquisition and processing system. Such a system achieved resolutions of 0.1mm and 0.2mm, but the paper did not mention the use of any reference system. Clearly, the measurement of orthodontic tooth movement involves a direct comparison of tooth position before and after the procedure, and inevitably any positional comparison must involve a reference frame for relative positional measurements to be achieved.

A reference system using a cubic square was developed specifically for 3-D positioning measurement during orthodontic treatment.

7.1.1 The othodontic jaw model

An upper jaw model (Typodont) made of acrylic was mounted on a perspex base by screws; fourteen teeth were embedded in the acrylic,

and to each tooth was bonded an alloy orthodontic bracket. The whole model consisted of two components, eleven teeth were fixed to the base, but three teeth were removable, and were attached to the fixed component by screws. Ten different removable sectors with differently designed bracket alignments, could be inserted into position in the fixed base (Fig.7-1).

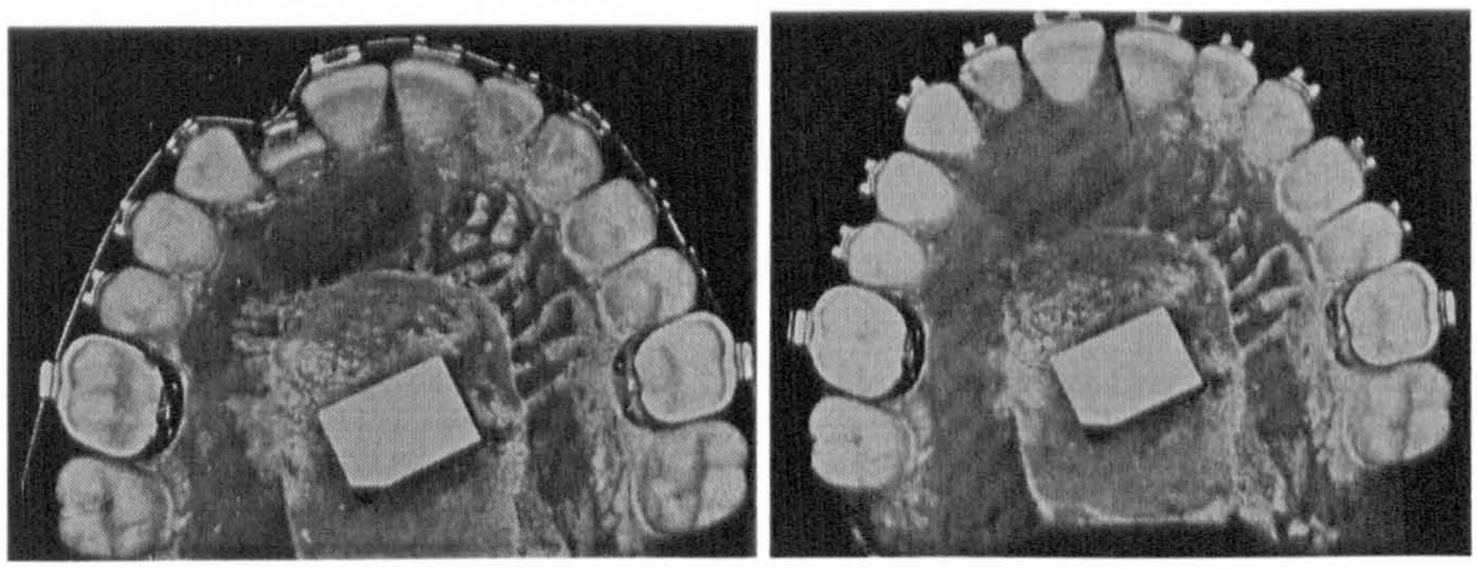

Figure 7-1: The upper jaw model used for analysis of position change in relation to the orthodontic force applied.

The aim of this study was to measure position changes of brackets on specified teeth, and to generate 3D co-ordinates of the brackets on each tooth, in order to develop a model for subsequent finite element method (FEM) analysis.

7.1.2 Measurement design

It was determinded that the co-ordinates of four points on each tooth at the centre of each bracket would be digitised. Further scans of the same points would be performed to measure the deviation of each tooth using

the same reference frame. This would produce data much more quickly than a complete scan of the whole facial surfaces of fourteen teeth. The deviation of each specified tooth was calculated after superposition, profiling and measurements. It would be intensive in terms of manpower, time and energy compare to these direct co-ordinate measurements under the same reference system.

7.1.3 The design of a reference device

An examination of the jaw model was made, and it was apparent that apart from the three movable teeth the positions of the other eleven teeth and the base of the model would remain unchanged. Hence, the model base was taken as a reference.

A cubic block was used as a reference device. A standard length bar of one and half inches in length with a geometrical accuracy of 0.1μm as certified by the National Physical Laboratory (NPL, UK), was embedded into the base of the model of the upper jaw using acrylic, whist ensuring that the upper part of the cube allowed sufficient space for the OP2 probe to access it from different angles.

The reference axis system was established as follows: (1) To level the XOY plane: three arbitrary points that did not lie in a straight line on the upper surface of the cubic block were digitised, and used for leveling the XOY plane; (2) To align the X axis: two points on one side of the cube were digitised and aligned as X axis; (3) To datum the origin of the

reference system: one point on the surface which connected the above two surfaces was digitised to datum the origin (O) of the reference axis system. This method allowed a reference frame to be established as shown in Fig.7-2.

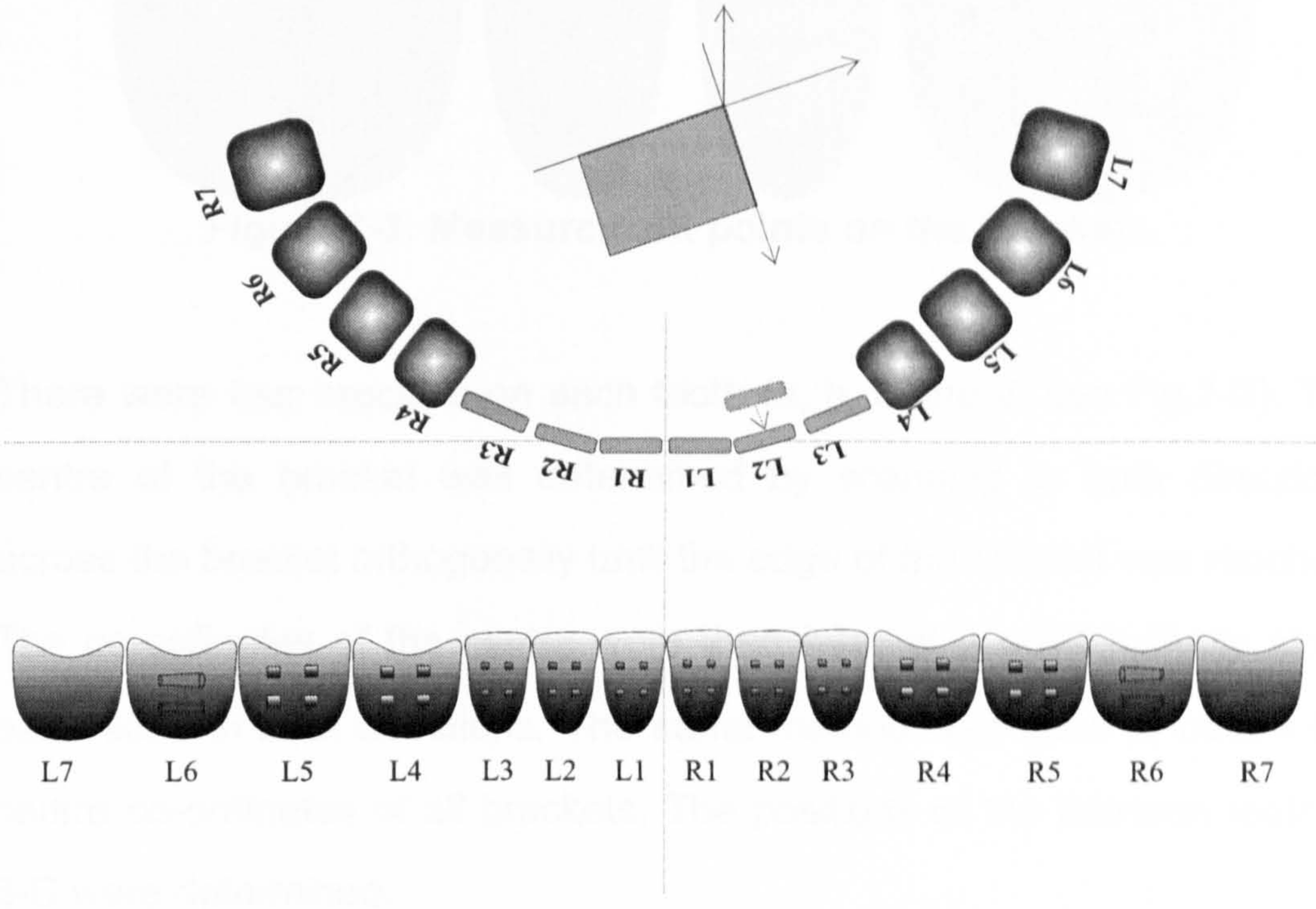

Figure 7-2: The reference system used to measure the displacement of tooth L2 in its pre and post orthodontic simulation test.

7.1.3.1 Co-ordinate measurements

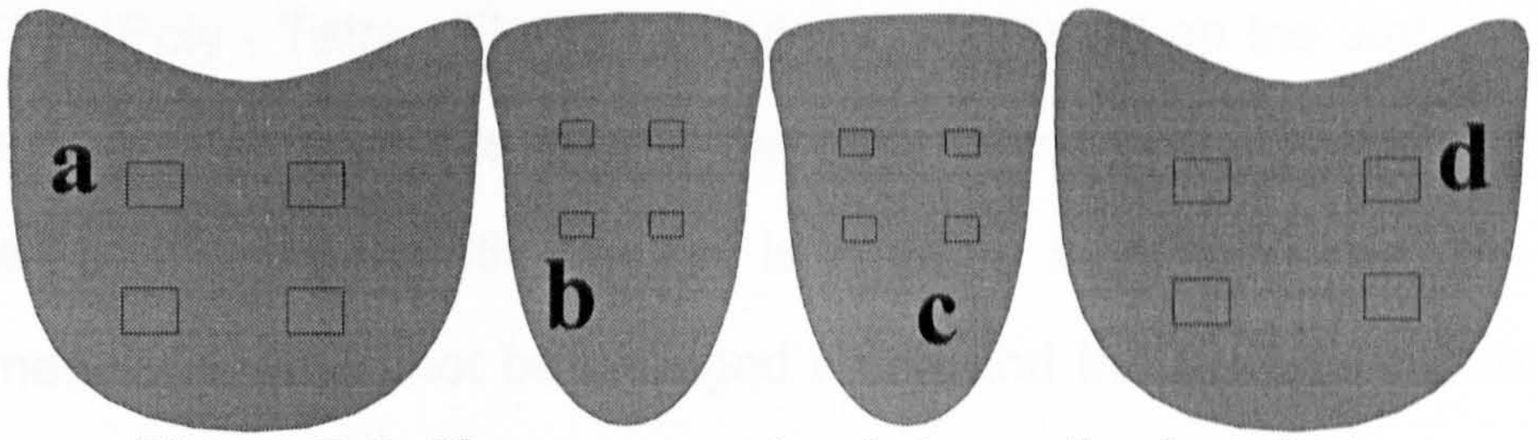

Figure 7-3: Measurement points on the brackets.

There were four brackets on each tooth (a, b, c and d, see Fig.7-3). The centre of the bracket was determined by scanning in both directions across the bracket orthogonally until the edge of the bracket was reached. The co-ordinates of the centre were then lying at a point halfway along each scan in both directions. The same method was used to obtain the centre co-ordinates of all brackets. The positions of the fourteen teeth in 3-D were determined.

7.1.3.2 Tooth deviation measurements

The deviation measurement of a tooth was easily determined within the reference frame by subtracting the co-ordinates | X1 – X2 |, | Y1 – Y2 |, | Z1 – Z2 |, obtained from position measurements before and after the orthodontic movements.

7.1.3.3 Scanning strategy

1. The brackets were metal and had a shiny surface. In order to produce a matt surface and a diffused laser beam reflection, a white spray - FTFE (Poly - Tetra - Fluoro - Ethylene) was used on the surface of the brackets. Although this altered the dimensions of the brackets, as the area of the orthodontic bracket is small in size, therefore, the 'new' dimensions would not be changed much and the measurements were constant during the procedure.

2. Scan parameters were as follows:
   - scan pitch = 0.1mm,
   - scan speed = 1mm/s,
   - threshold setting = 50.

7.1.3.4 Results

These were entered into Excel spreadsheets (see appendix III).

7.1.4 Uncertainty analysis of the cubic block as a reference device

Using a cubic block as the reference device, uncertainty is influenced by the working surface roughness; the flatness of the surface; and the squareness of the cubic block. If it is assumed that an error in length of the cubic block differs from the nominal by as much as δ_{xb} and δ_{xa}, then the error will be magnified in the measurements of the centres of the brackets.

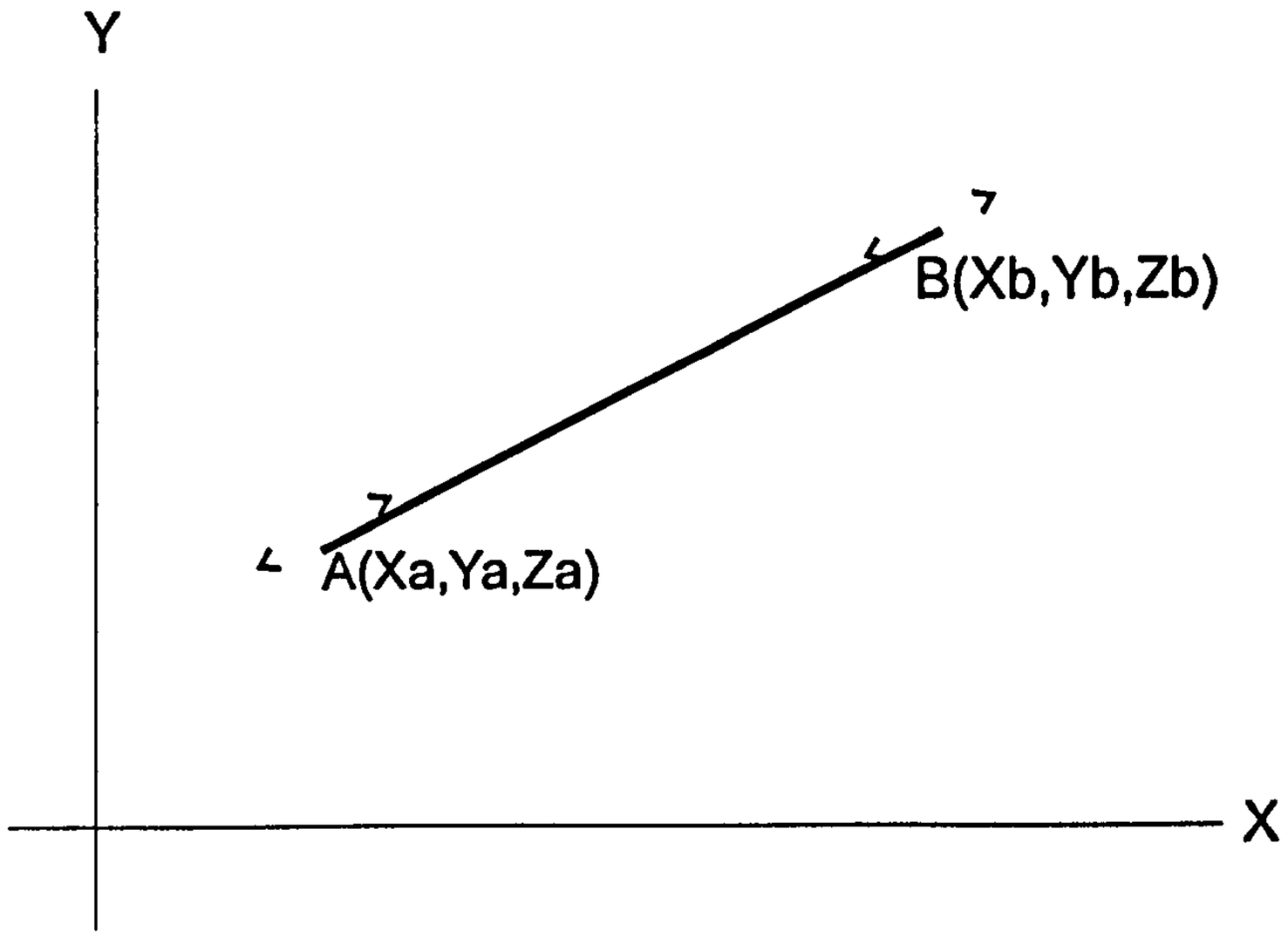

Figure 7-4: AB represents the distance from origin of the datum system to the measurement position.

$$L_{ab}= \sqrt{(X_b + \delta_{xb} - (X_a + \delta_{xa}))^2 +(Y_b + \delta_{yb} - (Y_a + \delta_{ya}))^2 +(Z_b + \delta_{zb} - (Z_a + \delta_{za}))^2}$$

$$= \sqrt{(X_b - X_a + \delta_{xb} - \delta_{xa})^2 + (Y_b - Y_a + \delta y_b - \delta y_a)^2 + (Z_b - Z_a + \delta_{zb} - \delta_{za})^2}$$

$$= \sqrt{(X_b - X_a)^2 + (\delta_{xb} - \delta_{xa})^2 + (Y_b - Y_a)^2 + (\delta y_b - \delta y_a)^2 + (Z_b - Z_a)^2 + (\delta_{zb} - \delta_{za})^2 + 2(X_b - X_a)(\delta_{xb} - \delta_{xa}) + 2(Y_b - Y_a)(\delta y_b - \delta y_a) + 2(Z_b - Z_a)(\delta_{zb} - \delta_{za})}$$

when $\delta_{xb} = \delta_{xa}$, $\delta y_b = \delta y_a$ and $\delta_{zb} = \delta_{za}$

then $L_{ab}= \sqrt{(X_b + \delta_{xb})^2 +(Y_b + \delta_{yb})^2 +(Z_b + \delta_{zb})^2}$

meaning the measurement errors have been counteracted;

but when $\delta_{xb} = - \delta_{xa}$; $\delta y_b = - \delta y_a$ and $\delta_{zb} = - \delta_{za}$

then Lab = $\sqrt{(X_b - X_a)^2 + (\delta_{xb} - \delta_{xa})^2 + (Y_b - Y_a)^2 + (\delta y_b - \delta y_a)^2 + (Z_b - Z_a)^2 + (\delta_{zb} - \delta_{za})^2 + \sqrt{2(X_b - X_a)(\delta_{xb} - \delta_{xa}) + 2(Y_b - Y_a)(\delta y_b - \delta y_a) + 2(Z_b - Z_a)(\delta_{zb} - \delta_{za})}$

meaning the measurement errors have been doubled.

7.2 Using two cones and a plate as a reference device

Hip joint replacement surgery is becoming a common operation. In the last fifteen years researchers have identified osteolysis, induced by wear debris from prosthetic polymeric acetabular cups, as a major cause of long-term failure (Revell *et al.*, 1997). Hip simulation studies have become an efficient tool for basic research (Barbour *et al.*,1999, Caddick and wimmer, 2001) in wear measurements (Bigsby *et al.*, 1997; Blunt *et al.*, 2000) as well as for pre-clinical testing to minimise risk to patients when receiving new implant types.

Wear measurements of ultra-high molecular weight polyethylene (UHMWPE) acetabular cups have been performed using three methods to examine different aspects of wear under the newly introduced standard ISO 14242 (Kaddick and Wimmer, 2001). In this paper, the three methods used to determine the wear were as follows:

1) the total polyethylene wear was determined by weight loss of the cups;

2) the wear depth and its distribution were measured by a CMM (Mitutoyo BHN 305, resolution 0.5μm); and
3) wear particle analysis was performed by using light and scanning electron microscopy (SEM).

A hip cup is a concave hemisphere in shape and is also quadrant symmetrical. To perform comparative measurements between two hemispherical hip cups, a reference device needed to be designed. Kaddick and Wimmer (2001) describe a reference technique in which the cup was clamped into a custom-made holder to ensure a firm location and to prevent linear deformation. It was not described how the reference frame was established in control of the rotation as it is the main problem with these spherical cups. A reference system will be described here using two cones placed at opposite sides of the cup to align the X axis; with a ring shape plane surrounding the cup to level the XY plane; and a point at 2mm above the plane and on the cone axis to datum the original point of the reference axis system. This method is described in detail in the following section.

This study was aimed at developing a methodology to measure wear depth and its distribution over an area approximately 30 mm×30 mm in size of an acetabular hip cup, following a walking simulation test.

7.2.1 Materials and methods

7.2.1.1 Replication

A replica technique was used to record the shape of the acetabular hip cup at specified stages during the walking simulation test, for example after half a million, or one million cycles. A dental polyvinyl siloxane impression material (see Chapter 1 section 1.7) was used again to record the details of the cup at each specified stage. A concave acetabular cup was replicated as a convexly shaped impression.

7.2.1.2 Design of a datum device for sequential impression measurements

When comparing sequential impressions, it is critical to have an accurate reference axis system for the measurements, which will ensure that data collected all lie within the same reference frame. With a solid object, a gauge is commonly used to fix the position of the specimen in relation to the machine space, however, with a soft body such as an acetabular cup impression, it is impossible to use such a location device. As a consequence a datum system was designed and referenced on the impression itself (Fig.7.5) as follows: (1) 10 points were recorded around the peripheral plane of the cup impression to level the *XY* plane; (2) The centres of two cones, placed diametrically opposite each other, were determined by slicing through the images of the cones at Z=2 mm, and the centres calculated from two circles obtained. These centres were used to

align the *X* axis; (3) The origin of the axis system was defined as the centre of one of these cones (Fig.7.6). An application program was written to allow the reference axis system to be set up automatically.

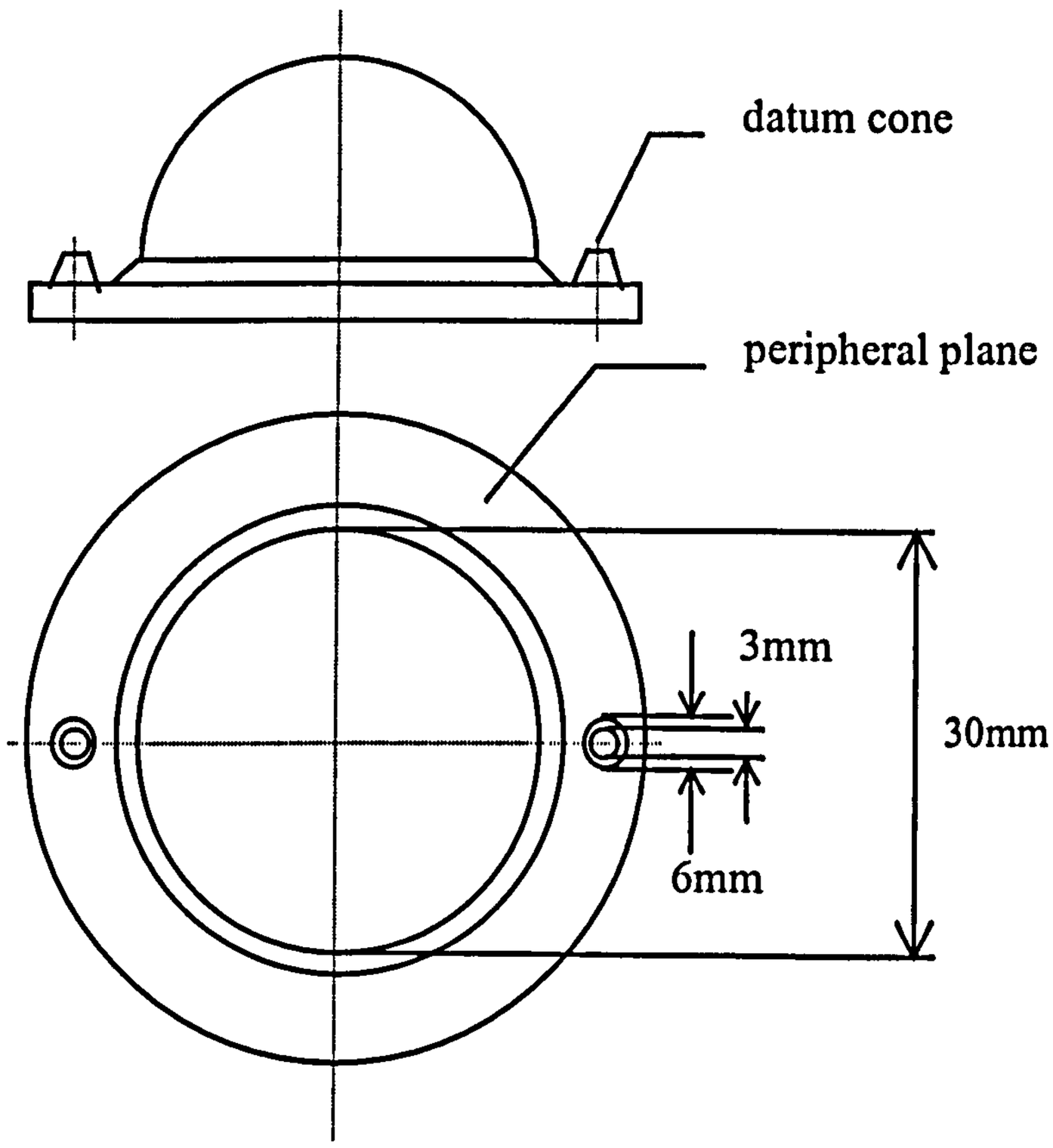

Figure 7-5: The hip cup with reference cones.

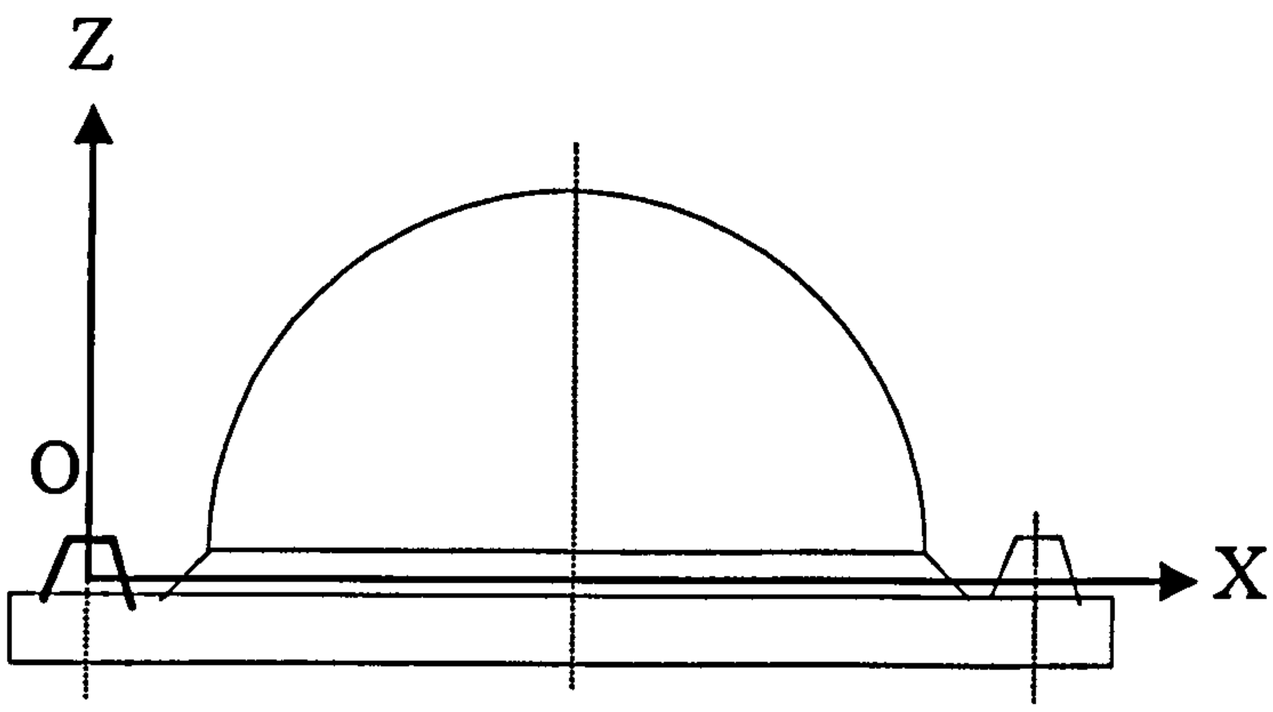

Figure 7-6: The reference axis system.

7.2.1.3 A digitisation strategy for a convex hemisphere

Scanning two half cones

Two half cone surfaces symmetrically opposite each other across the hemisphere were digitised at 0.1 mm intervals in both *X* and *Y* directions, with a scanning speed of 10 points per second, optical threshold setting of 80, and using two probe orientations.

Scanning the convex hemisphere

The methodology described in Chapter 4 was adapted to scan the convex hemispherical acetabular hip cup. The digitisation interval used was 0.1 mm in both *X* and *Y* directions; the scanning speed was set as 10 points per second; the optical threshold level was 200, and six probe orientations were used.

7.2.1.4 Reproducibility analysis

An investigation of the reproducibility of measurement and data acquisition was carried out to evaluate the stability of the measurement methods. The datum reproducibility was tested by repeating the digitising procedure eight times with the two cones and computing the centre co-ordinates of each.

7.2.2 Results

Reconstructed half cones are shown in Fig.7-7. Complete scanning of the cones was not possible due to the optical effects of multiple reflections between the cones and the hemisphere. Two profiles (Fig.7-8) generated at *Z*=2 mm enabled the centre co-ordinates to be determined by fitting a circle to 6 points evenly distributed around each semicircle.

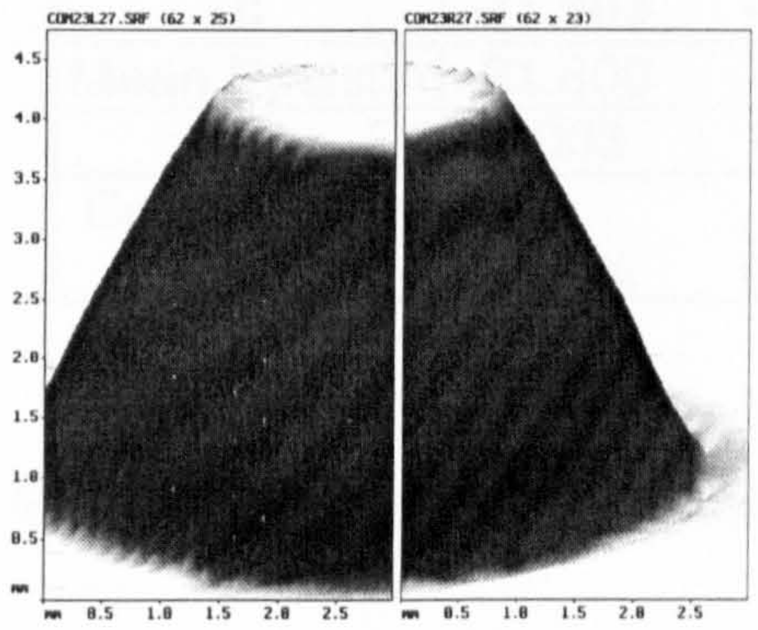

Fig.7-7: Reconstructed half cones

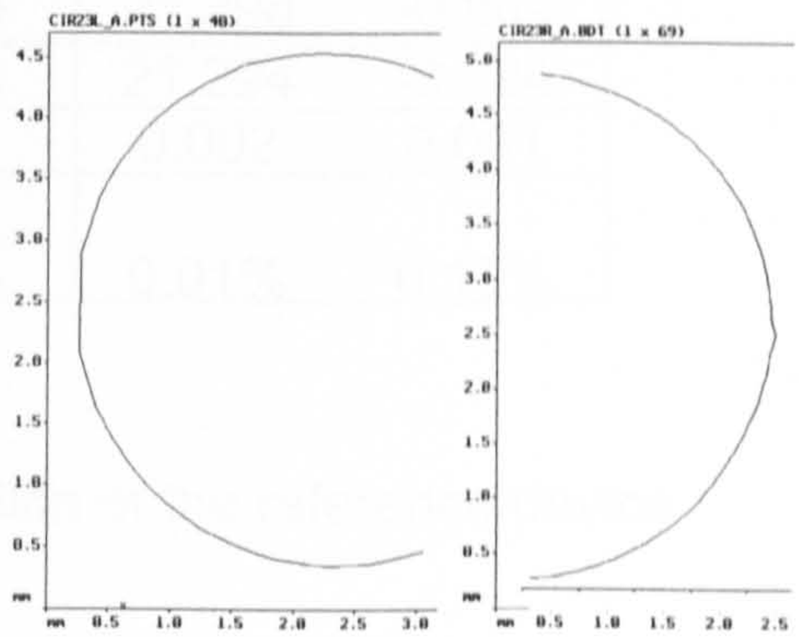

Fig.7-8: Two profiles of cones obtained at Z=2mm

Reproducibility of datum co-ordinates is critical to ensure the validity of measurements. The co-ordinates of the recorded centre points for the origin are shown in Table 7-1. They reveal that the variations in the co-ordinates are small, as demonstrated by the low values for the standard deviations. The *X* and *Y* co-ordinates were determined with a coefficient of variation of less than 0.42%.

Table 7-1: Reproducibility of the cone centre points:

	CONE1		CONE2	
	X/ mm	*Y*/ mm	*X*/ mm	*Y*/ mm
1	-21.793	-0.312	21.294	-0.886
2	-21.798	-0.311	21.293	-0.884
3	-21.799	-0.311	21.292	-0.883
4	-21.799	-0.311	21.293	-0.885
5	-21.803	-0.311	21.291	-0.883
6	-21.802	-0.308	21.294	-0.882
7	-21.804	-0.309	21.296	-0.883
8	-21.803	-0.309	21.298	-0.884
Mean Position	-21.800	-0.310	21.294	-0.884
SD	0.003	0.001	0.002	0.001
Coefficient of Variation	0.02%	0.42%	0.01%	0.13%

7.2.3 Wear measurements as an application of the reference device

7.2.3.1 A comparative measurement of two impressions from one cup

Fig.7.9 shows a superposed image, which is reconstructed from digitised data within the reference frame. Fig.7-10 shows an excellent profile around the whole of the cup impression. A volumetric difference of 1.411±0.225 mm^3 was calculated over 400mm^2. This difference included the sum of impression taking, the digitisation process and data reconstruction and analysis.

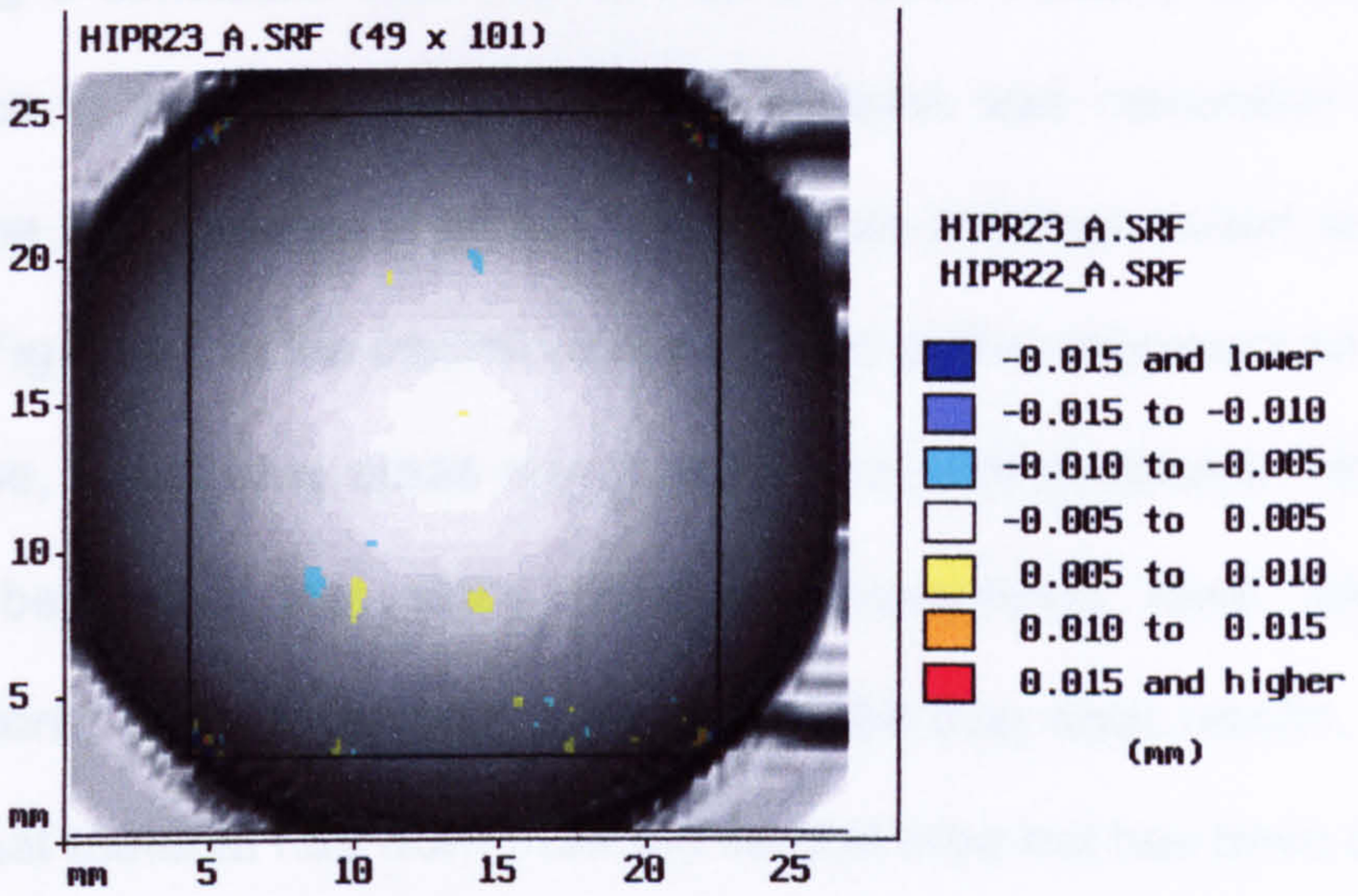

Figure 7-9: Two reconstructed images of two impressions of the same cup.

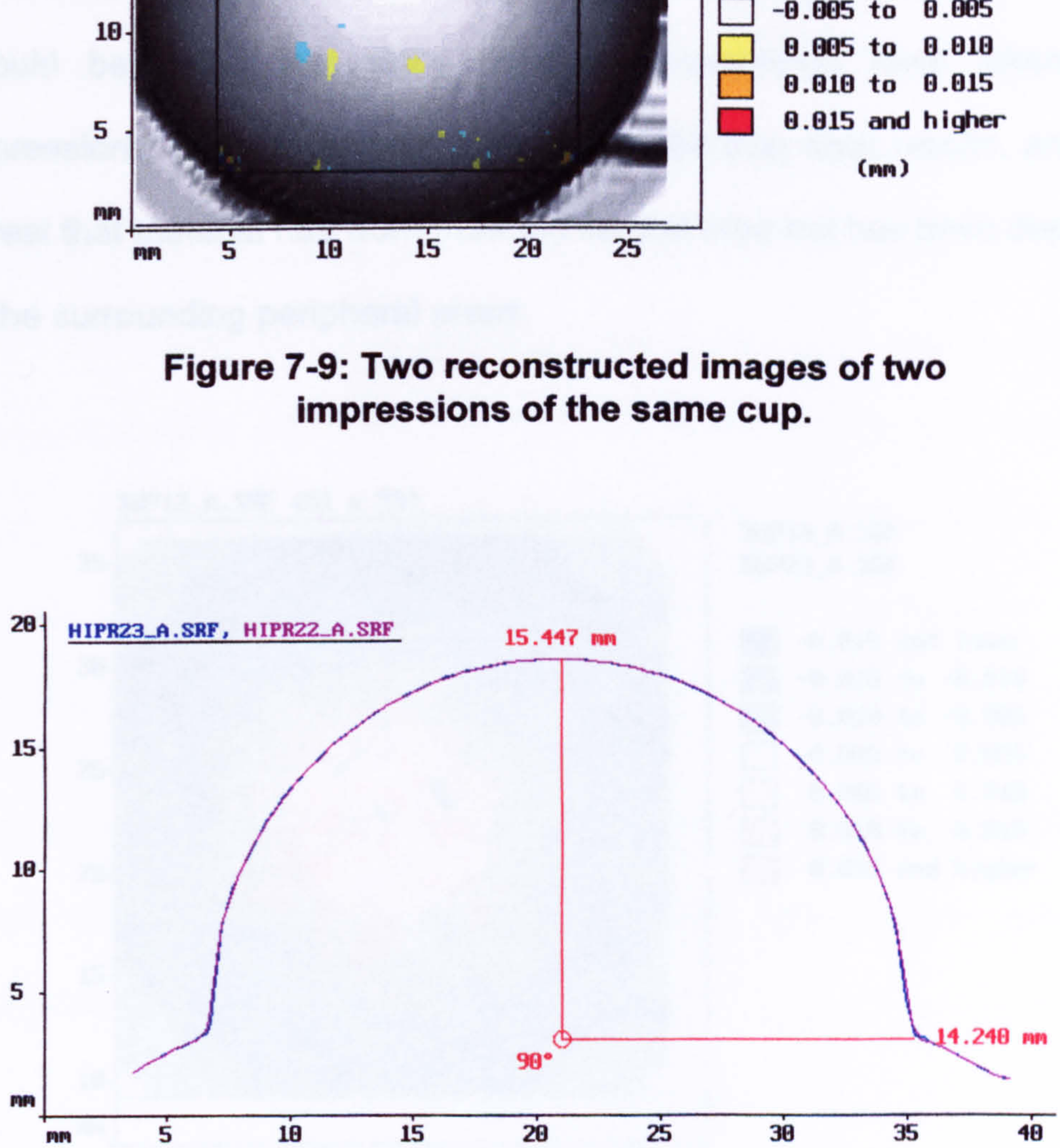

Figure 7-10: Two superposed profiles.

7.2.3.2 Superposition of two impressions from two hip cups

Following a simulated wear test of half a million walking cycles, the total difference in volume between two impressions was calculated as 5.341 mm^3. The wear pattern is again displayed as a colour coded subtraction image (Fig.7.11). In the central areas red and yellow represent an increase in volume, whilst blue areas represent a decrease in volume. However, it should be noted that since these measurements were taken from impressions, they represent the inverse of the true wear results, and they reveal that material has worn from the central area but has been deposited in the surrounding peripheral areas.

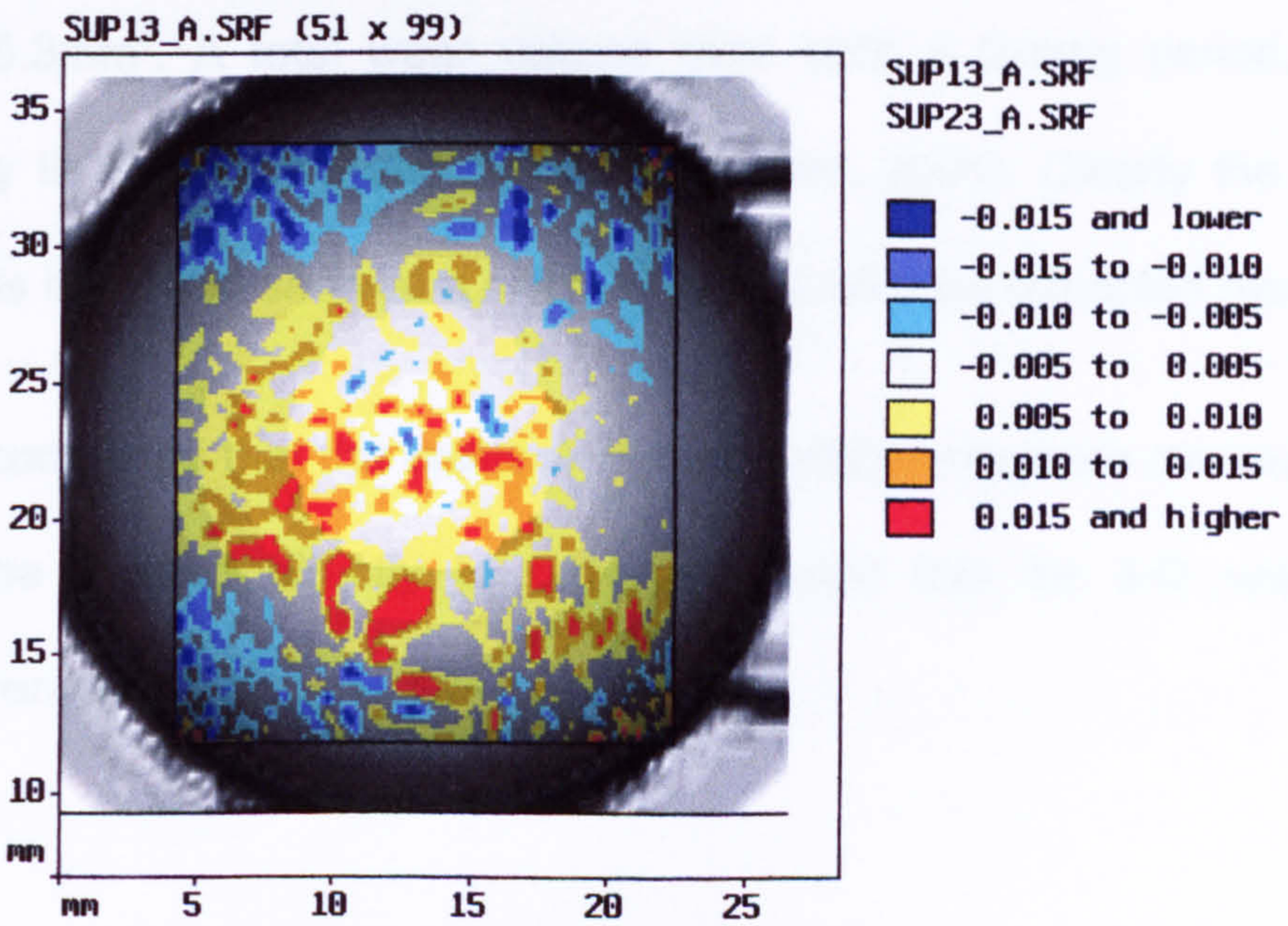

Figure 7-11: The wear pattern seen after half a million cycles. colours represent differences in height (μm).

7.2.4 Discussion

The good reproducibility of the datum system indicated that this was a suitable technique for sequential measurements. The strategy derived for scanning the whole surface of a hemisphere produced excellent results, with a only little distortion towards the periphery of the scans. Since the least accurate data was at the periphery of the scans, all calculations related to volume change were determined over the accurate central area. This central region of 400mm^2 showed good reproducibility when two surfaces were compared, with a mean volumetric difference of 1.4mm^3. When comparing the impressions of two cups taken before and after undergoing half a million wear cycles, the volumetric difference was found to be 5.3mm^3. A total wear volume over such a testing period, would typically lie between 8 and 12mm^3 (Bowsher, 2001). Clearly the results from this initial test showed a high correlation with the expected results.

It was concluded that this method of sequential hemisphere measurement could be applied directly to provide a valid tool for 3-D volumetric measurement.

8 THE DEVELOPMENT OF AN AUTOMATIC DIGITISATION PROCEDURE

8.1 The special requirements of dentistry

This measurement system so far described is a sophisticated integration of optics, electronics, mechanics and computer science. In a non-contact process an optical probe is the interface between the measurement system and the object to be measured; the electronics signal conditioning suite transfers data between the electrical components; the CMM provides the measurement co-ordinate system and the transportation to support the measurements; and a personal computer (PC586, Elonex, UK) controls the entire measurement system.

The host computer controls and co-ordinates the movements and activities of the laser probe (OP2), the CMM (Merlin II) and the signal conditioning unit. It runs software written in High Tech Basic (HTBasic). HTBasic is a technical programming language compatible with Hewlett Packard's "Rocky Mountain" BASIC for HP9000 Series 200/300. It has extensive graphics, instrument control capabilities, and interactive programming aids to speed up program development.

The software consists of three main parts: the Direct Computer Control (DCC337, IMS, UK) core system control software package, this part of the

program contains 27,435 commands. The automatic operation software package was developed by the Author to facilitate automatic batch scanning of replicas. Thirdly a data analysis software package, for 3D imaging and analysis of the morphology of oral structures from co-ordinate data was developed by Jovanovski (1999).

There are significant differences in the measurement requirements of dental research compared with the measurements required for manufacturing industries (Seokbae *et al.*, 2002). Clinical trials are fraught with many problems (Chadwick, 1989), and such trials are very time consuming. Large sample sizes involving, for example, 100 pairs of impressions, are often required, to allow for the drop-out of participants, and these need to be analysed quickly. Impressions are often taken from teeth of the same morphological type, meaning the surface forms of the impressions obtained are very similar, so they can utilise a similar digitisation strategy for each scan. Such projects often require sequential comparative measurements, so that an efficient and consistent measurement process is required. A batch scan procedure is ideal in this case.

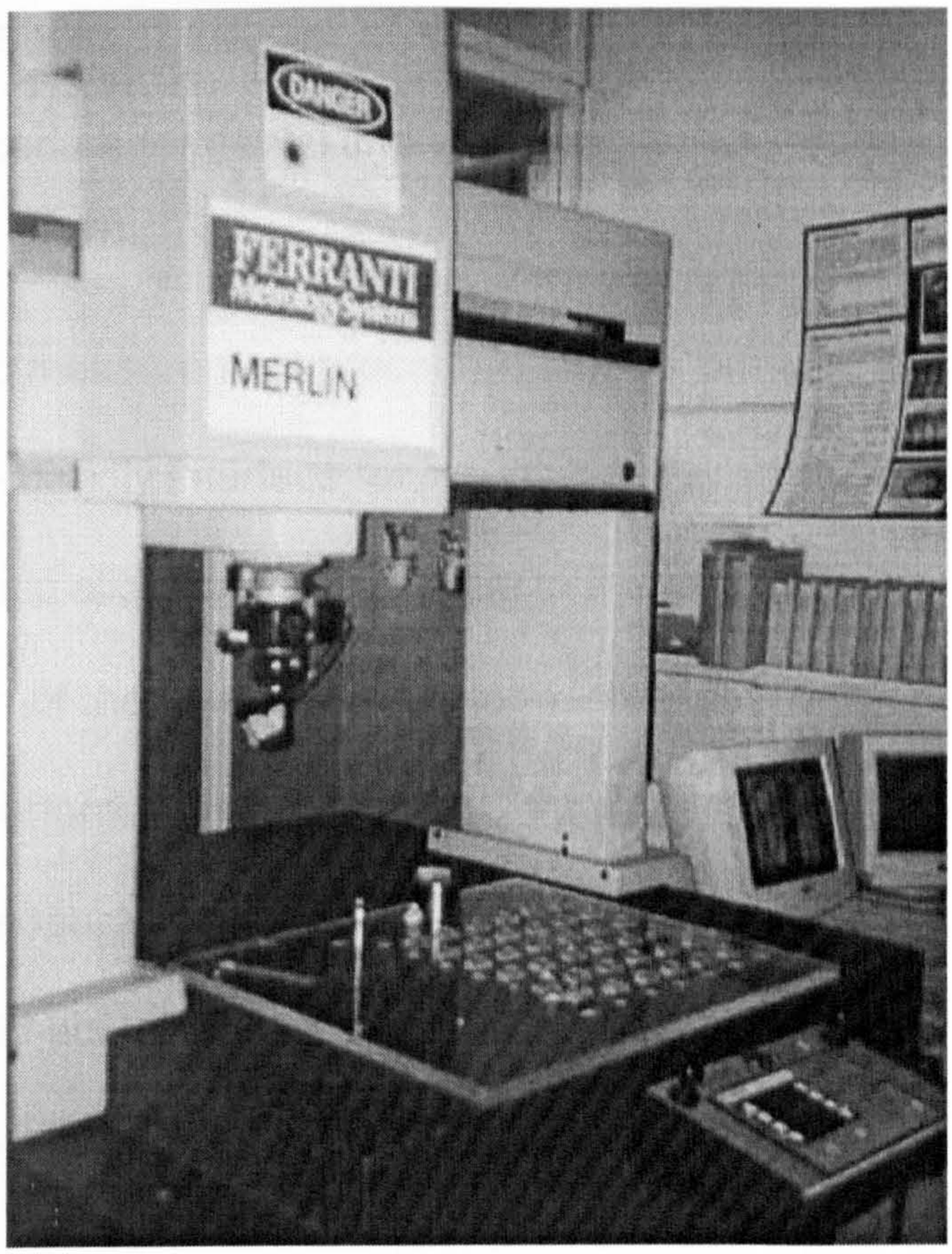

Figure 8-1: 36 impressions set up for overnight digitisation as a batch.

In dental research, the size of the impressions are small leaving a great deal of space available on the CMM working table. If multiple impressions have been set up for scanning continuously without human intervention, effective scanning hours could be extended from perhaps eight working hours, to 24 hours a day during the week, and 48 hours over weekends, which greatly increases the efficiency of the use of the CMM.

This objective was the focus of this Chapter, to develop an automatic scanning procedure for dental impressions.

The automatic measurement procedure aims to provide:

- A user-friendly interface for inputting the scanning parameters
- automatic allocation of the probe to the impressions
- location of the centre position for each experiment
- good performance in 2D and 3D measurement
- high measurement accuracy
- fast data acquisition times
- increased flexibility in scanning free form surfaces.

8.2 The auto-digitisation procedure

A flow chart has been produced to provide an overview of the software package, to include the scanning sequence, the output format, and the data analysis functions. These three functions are identified within three squares A, B and C in the flow chart. Area A is as provided by the CMM and OP2 manufacturer; Area B has been developed by the Author of this Thesis, and Area C was developed by another research colleague (Jovanovski, 1999).

A functionalised flow chart of the measurement system

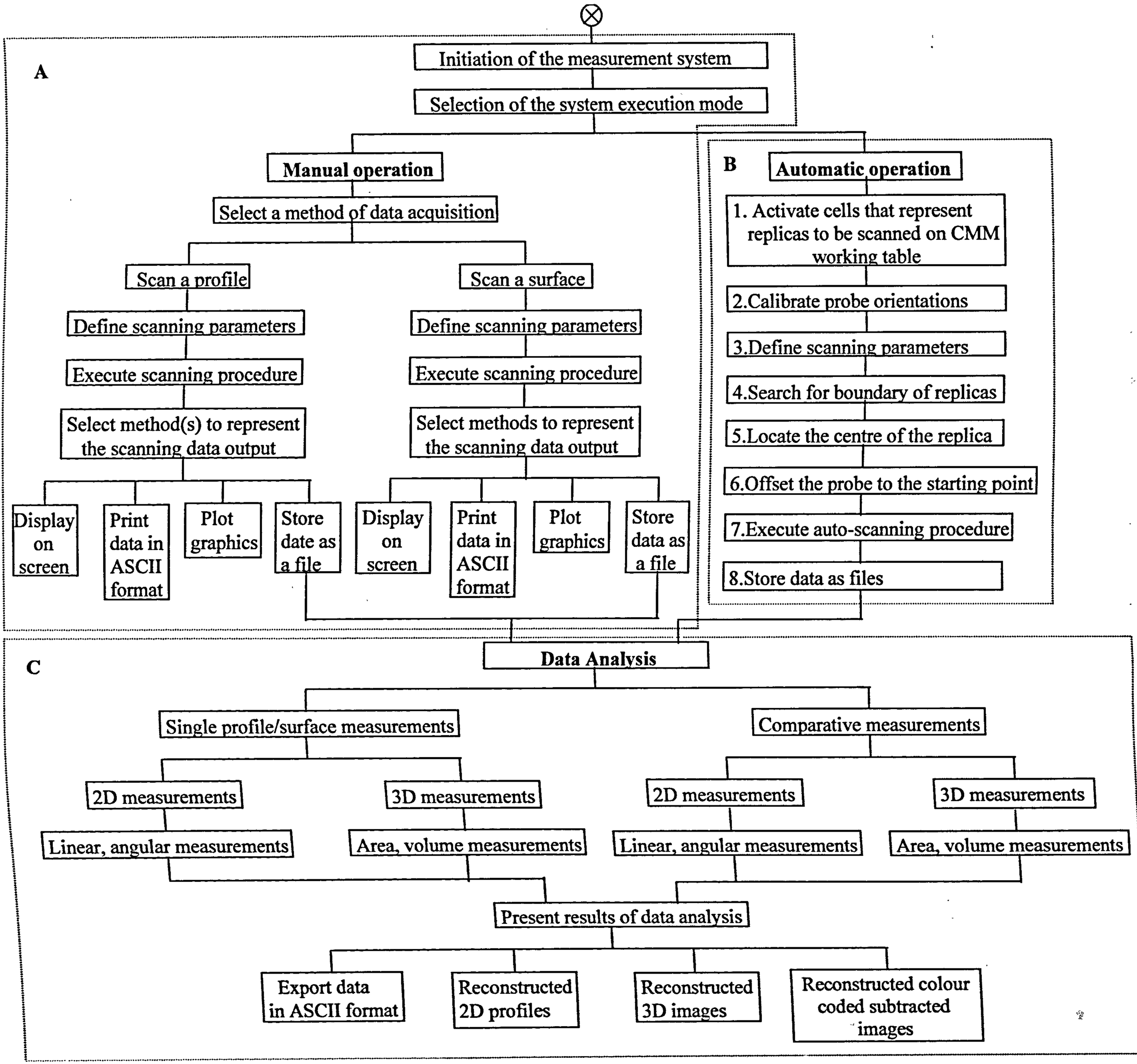

8.2.1 Automatic data acquisition

An unmanned batch data acquisition process was developed to meet the needs of dental research, as already described (8.1.1). A flow chart of this process follows:

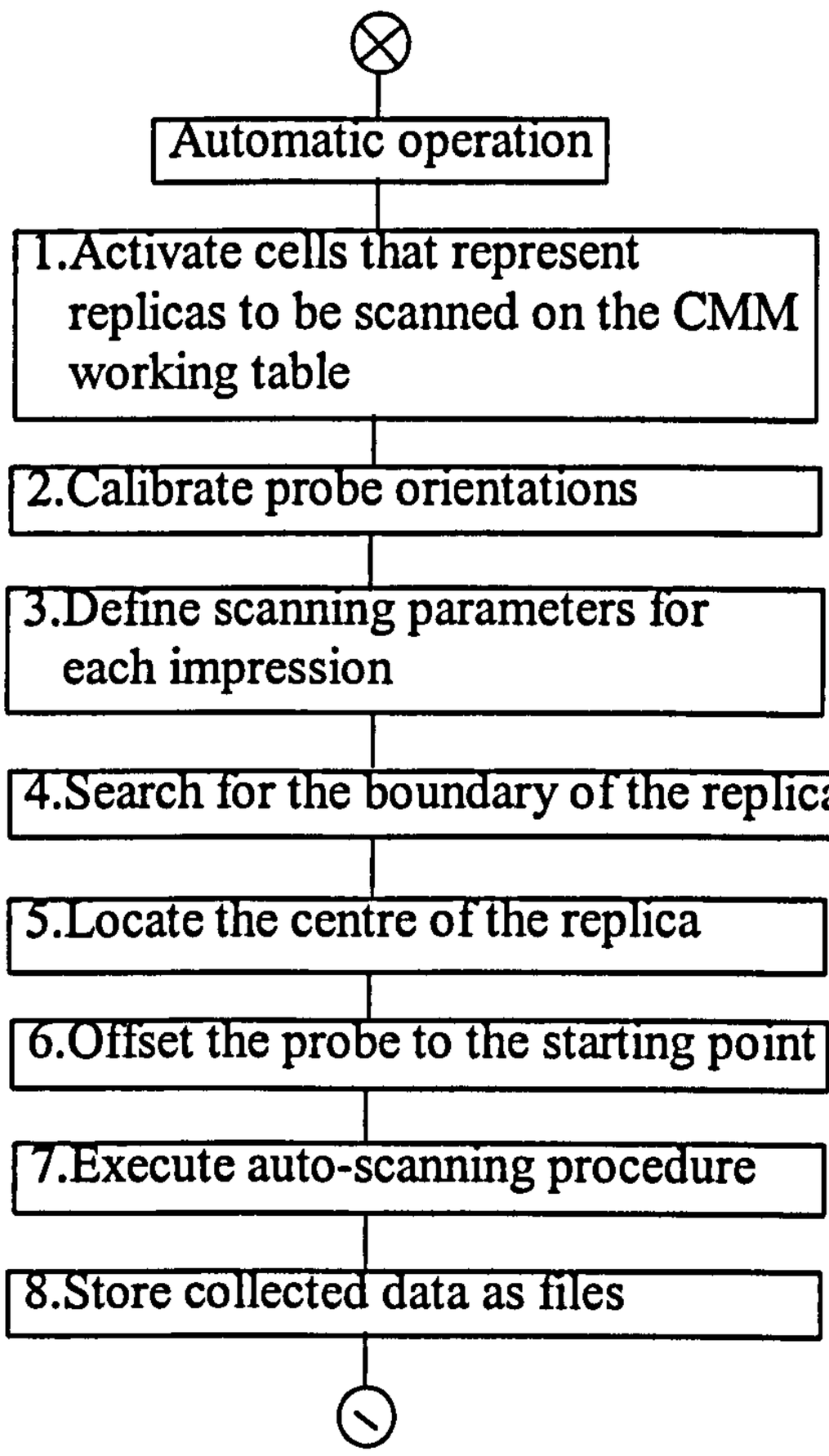

8.2.1.1 Activating cells

Automatic batch scanning is contrlled via menu screens. 36 cells (Fig.8-2), one for each impression are allocated on the working table of the CMM. Each cell contains full information of the scanning parameters to be

applied to the impression, for example the scanning pitch, the scanning speed, the scanning area, the offset in *X* and *Y* direction, and probe orientations; there can also be information on the impression, such as the name of the patient, the tooth specification, information on the treatment and the name of the file. Before parameters can be inputted, software cells corresponding to the impressions placed on the CMM working table need to be activated.

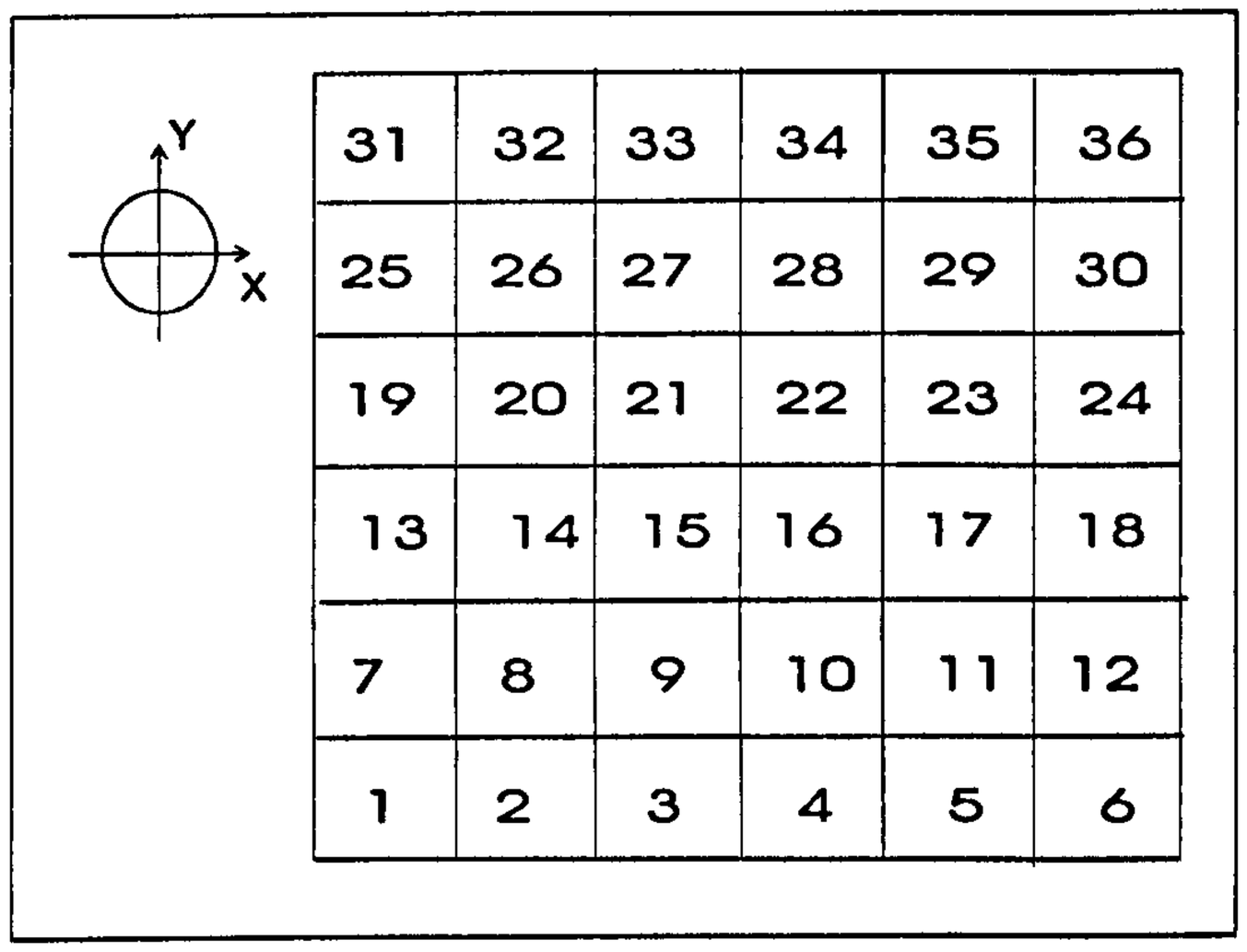

Figure 8-2:The arrangement of impressions on the CMM working table for automatic scanning.

8.2.1.2 Calibration of probe orientation

Each replica may require different probe orientations, this information needs to be inputted into each cell at stage 3. However, the overall probe orientations that are specified by numbers have to be calibrated at stage 2, as part of the preparation for this automatic scanning process.

8.2.1.3 Defining scan parameters for each replica

At this stage the scanning parameters that are related to each replica, which include scanning pitch (sampling side or sampling interval), scanning speed, scanning direction (bi-directional or uni-directional), probe orientations, scanning area defined by lengths in *X1*, *X2*, *X3* in respect to the probe orientations in *X* direction and a length in *Y* direction, as well as the offset lengths in X and Y directions need to be inputted into a data file for each cell.

8.2.1.4 Searching for the boundary of the replica

Impressions to be subjected to a batch scan must be supplied in an identical cubical shape. Their sides can vary, but their heights need to be 5mm±1mm to maintain the stringency (Reisbick and Matyas, 1975; Eames *et al.*, 1979; Lacy *et al.*, 1981), since the scanning area can vary in size and location on the surface of the replica. A sub-datum axis must be defined at the centre of each replica, and the directions of *X*, *Y* and *Z* must be parallel to the CMM machine axes. Before finding the centre, the boundary needs to be searched in four directions by profile scans in +X, -X, +Y and –Y, from these, four points are obtained on each side and denoted as a, b, c and d as shown in Fig.8-3.

.

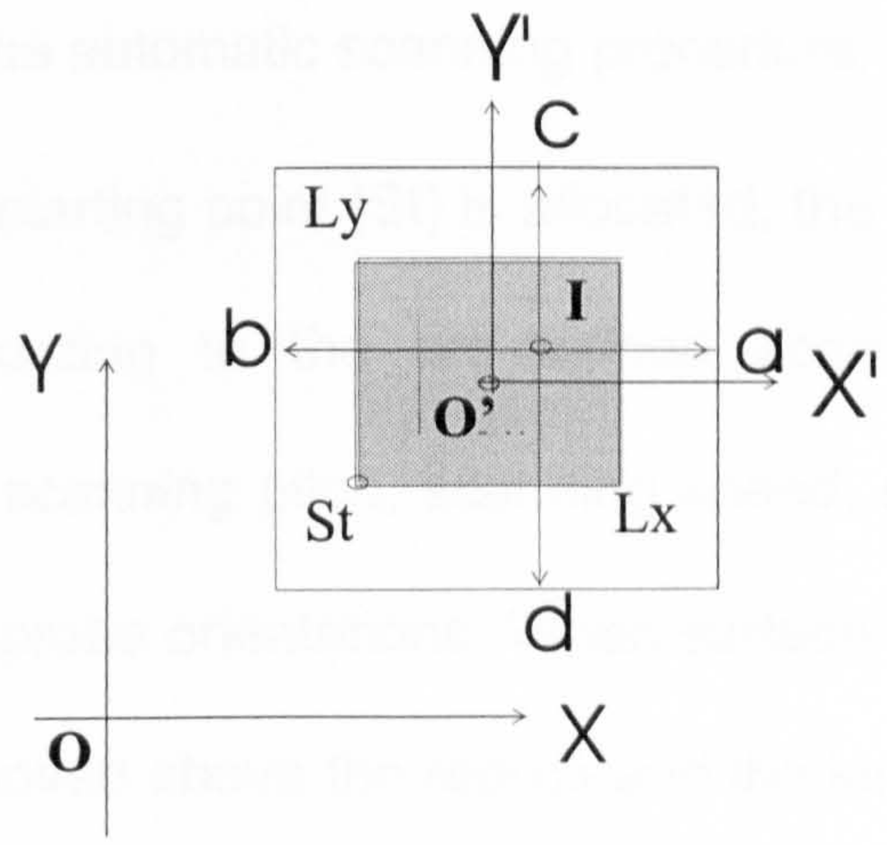

Figure 8-3: Locating the centre of a impression

8.2.1.5 Determining the centre of the replica

From the boundaries of a replica, the centre of the replica is located as half of the lengths O'(x) = ½ (| Ia | + | Ib |) and O'(y) = ½ (| Ic | + | Id |). The centre co-ordinates are used as a sub-datum original (O') of the axis system of this replica. The scanning probe moves to the location of the centre and above the replica from its previous location which could be the finishing position of a previous scan or alternatively above the standard sphere of calibration.

8.2.1.6 Offsetting the probe to the starting point of the scan

From the sub-datum original point (O'), the scanning probe movement offsets in *X* and *Y* directions above the replica (St), which is related to the cell as one of the scanning parameters. Then the laser is turned on and the scanning procedure is commenced.

8.2.1.7 Executing the automatic scanning procedure

Once the scanning starting point (St) is allocated, the laser probe starts its surface scan, according to the pre-defined scanning parameters of scanning direction, scanning pitch, scanning speed, scanning area, laser threshold level and probe orientations. When surface scanning is finished, the laser probe is moved above the replica and the laser beam is switched off. Such a surface scan takes 30 - 50 min., depending on the size of the scan area, for example a surface of an incisor with a size of 4.2mm × 6.5mm takes 20 min. to scan, and the number of digitised points are 3,000.

8.2.1.8 Storing data in files

When the surface scan is finished, co-ordinate data of the scanning result are stored in a data file in binary format. The file name was inputted as one of the scanning parameters in step 3 prior to the scanning operation. File creation takes a few minutes to tens of minutes depending upon the number of points digitised, for example, it takes 8 minutes to store surface co-ordinates of a incisor, with a data file size of 0.8MB.

8.3 Conclusion

The use of this automatic digitisation procedure enabled the successful and efficient completion of several research projects. These projects are listed in the Chapter 9.

9 THE CLINICAL SIGNIFICANCE OF THIS STUDY

9.1 Introduction

The validity of the work described has been confirmed by its successful application in objective clinical research. This Chapter presents further examples of some of clinical investigations which have been enhanced by the application of co-ordinate measurement and analysis as a basis for formal metrology. It must be emphasised that conclusions about the clinical implications of the results are outside the scope of this research and are most appropriately left to those qualified to make them. There is a need for close collaboration with clinical researchers in this type of research. References are made, where appropriate, to the relevant publications that have been produced as a consequence of the research reported in this thesis.

9.2 Successful applications in Dentistry and Bio-engineering

Successfully conducted studies are listed with references below. Some of these reports have already been described in more detail in the previous Chapters.

1. Measurement of primary root caries lesions, to explore the geometrical features of primary root caries by the aid of 3-D co-ordinate measurement (Lynch, *et al.*, 1993(a)).

2. Geometrical assessment of Class I inlay cavity. Geometrical specification in relation to an ideal Class I inlay cavity was defined (Lynch, *et al.*, 1993(b)).
3. Quantification of shoulder dimensions and angles of metal-bonded crown preparations *in vivo*. This was undertaken to provide an objective quality assessment of a specified operation (Seymour *et al.*, 1996).
4. Assessment of three-dimensional structures in clinical dentistry. (Jovanovski *et al.*, 1996).
5. Measurement of tooth morphology using a laser probe fitted to a CMM. A non-contact co-ordinate measurement method and its appliance strategy was described (Zou *et al.*,1996).
6. Use of metrology and clinical methods to measure plaque thickness in an experimentally induced gingivitis. The efficiency of a dental product was evaluated by objective measurement through the aid of co-ordinate metrology. This research was awarded the QED/Maillefer prize for the best Research Poster at the Conference of the British Association of Teaches of Conservative Dentistry (Yeganeh *et al.*, 1996).
7. A three dimensional sequential analysis of the restoration of a root surface lesion. This was undertaken to measure the quality of a particular type of restoration (Lynch *et al.*, 1996).

8. 3-D positioning measurement of orthodontic brackets on a jaw model. This co-ordinate measurement approach provided the on-line co-ordinate change during an orthodontic treatment simulation study (Patel, 1996).
9. Finger joint distortion measurements. This has been undertaken using a non-contact measurement method that provides an alternative measurement of the joint for those who, for medical reasons cannot be X-rayed.
10. Assessment of the geometry of teeth prepared by third and fourth year students to receive metal ceramic crowns. To quantify the quality of the clinical practice of this technique within an undergraduate student group (Seymour, 1998).
11. Three dimensional quantification of plaque on teeth *in vivo*. This achieved a volumetrical measurement of plaque accumulation in a fixed time interval (Yeganeh *et al.*, 1999).
12. Canine gingivitis assessment by computer aided three dimensional co-ordinate metrology (Jovanovski *et al.*, 1999).
13. Three-month assessment of an anti-microbial root sealant. A qualitative measure was achieved by the use of the 3-D co-ordinate measurement method (Baysan *et al.*, 1999).

14. Effect of NAI (Negative Air Ions) on primary root caries. This research quantified the efficacy of a clinical regime using the novel technique of NAI (Burke, 2000).
15. Tooth shape in identical twins studied using optical surface metrology. This novel study provided the quantitative evidence to present the genetic significance of teeth belonging to twins (Kabban, *et al.*, 2001).
16. Measurement of sequential impressions of acetabular cups for a total hip joint replacement using a non-contact measurement system. An on-line 3-D co-ordinate measurement was achieved to assess the wear of the cup during durability simulation tests (Zou *et al.*, 2001).
17. A study of the geometry of preparations for porcelain veneers – a comparison of preparation techniques (Cherukara *et al.*, 2002).

10 CONCLUSIONS

The main objective of this research was to develop a tool to enable the three dimensional free form surfaces found in Dentistry and Bio-Medical Engineering to be measured accurately and efficiently.

The tool that was developed in this research was achieved through the integration of a Co-ordinate Measurement Machine with specially developed software to produce a user friendly package to provide the facility to carry out 'batch' data acquisition, and to allow automated overnight measurement of multiple specimens. The research required considerable investigation into the calibration and use of optical probes in conjunction with the CMM. During the research, special attention was given to data resolution and to measurement fidelity. The conclusion can be made that it was possible to use optical probes as a transducer for data acquisition to achieve the required fidelity over free form surfaces. During the research 'data stitching' was necessary because it was not possible to collect all the surface data using one orientation of the optical probe, this 'data stitching' procedure was successfully achieved.

The research showed that it was possible through well-developed protocols to measure typical 3D free form surfaces with high degrees of fidelity.

The measurement of 3D free form surfaces is of growing interest and importance in Bio-Medical Engineering and research, and is fulfilled by the

equipment, instrumentation and software assembled and developed as a result of this research.

That the current methodology is suitable for typical studies undertaken in dental research is evidenced by comparing it with other, more destructive types of measurement (Lutz *et al.*, 1979; Lutz and Phillips, 1983; Lutz *et al.*, 1984; Mitchum and Gronas, 1982; Taylor *et al.*, 1993) and with those that are non-destructive (Quick *et al.*, 1992). The current methodology is relatively simple to use, but it is still time consuming. A scan of an entire labial surface takes approximately half an hour to acquire the appropriate data for later computational analysis.

11 FUTURE WORK

Despite the increasing applications found, a futher development would provide wider applicability and value.

The directions for possible future research include the following areas:

1. To undertake a detailed review of the opportunities for employing free form surface analysis and surface topography analysis in Bio-Medical applications. Such a review would identify the medical/dental applications which would benefit from formal metrology.

2. The identification of parameters through an experimental and an analytical programme to functionally describe free form surfaces. The areas of Bio-Medical Engineering would be the subject of research both broadly based and in selected areas. Specific work packages could include the areas of tooth form, bones and joints.

3. The identification of parameters, visual displays, filtering methods, data set sizes, communication requirements and calibration routines to provide a basis for creating new International Standards. The stability of parameters related to specified data sets would be determined. Such an area of research would also address design, specification and testing protocols for the identified parameters.

12 REFERENCES

Alcaniz M, Montserrat C, Grau V, Chinesta F, Ramon A and Albalat S (1998); An advanced system for the simulation and planning of orthodontic treatment; Medical Image Analysis; Vol.2, No.1, p61-77.

Allred H (1977); A series of monographs on the assessment of the quality of dental care; The London Hospital Medical College.

Allred H, Smales F C and Morganstein S I(1987); Operational requirements for an advanced dental metrology facility; The London Hospital Medical College.

Aung S C, Ngim R C K, Lee S T (1995); Evaluation of the laser scanner as a surface measuring tool and its accuracy compared with direct facial anthropometrical measurements; British Journal of Plastic Surgery; Vol.48, pp551-8.

Barbour P S M, Stone H M and Fisher J (1999); A hip joint simulator study using simplified loading and motion cycles generating physiological wear paths and rates; Proceedings of Institution of Mechanical Engineers; Part H, Journal of Engineering in Medicine; Vol.213(h6), pp195-200.

Barghi N and Ontiveros J C (1999); A predictable and accurate technique with elastomeric impression materials; American Journal of Dentistry; Vol.12, No.4, pp161-3.

Baribeau R and Rioux M (1991), Influence of speckle on laser range finders; Applied Optics; Vol.30, No.20, pp2873-8.

Baysan A, Lynch E, Jovanovski V, and Zou L (1999), Three month assessment of an antimicrobial root sealant. Journal of Dental Research; Vol.78, p444, Abs. 2712.

Bedford J, Zou L, Jovanovski V and Lynch E (1993); Reproducibility of data collected by a co-ordinate Measuring Machine; Journal of Dental Research; Vol.72, p742, abs. 445.

Beckmann P and Spizzichino A (1963); The scattering of electromagnetic waves from rough surfaces; Pergamon Press, Oxford.

Bernard A and Veron M (1999); Analysis and validation of the 3-D Laser sensor scanning process; Annals of the CIRP; Vol.48, No.1.

Besl P J (1988); Active, optical range imaging sensors; Machine Vision Applications; Vol.1, pp127-52.

Bhat S S and Smith D J (1994); Laser and sound scanner for non-contact 3-D volume measurement and surface texture analysis; Physiological Measurement; Vol.15, pp79-88.

Bigsby R J A, Hardaker C S and Fisher J (1997); Wear of UHMWPE acetabular cups in a physiological hip joint simulator in the anatomical position; Proceedings of Institution of Mechanical Engineers, Part H, Journal of Engineering in Medicine; Vol.211(H3), pp265-69.

Blunt L, Jiang X Q and Stout K J (2000); 3D measurement of the surface topography of ceramic and metallic orthopaedic joint prostheses; Journal of Materials Science; Vol.11, pp235-246.

Bosch J A (Ed.) (1995); Co-ordinate measuring machines and systems; Marcel Dekker, Inc, New York, USA; ISBN 0-8247-9581-4.

Bowsher J (2001); Wear measurement of total replacement hip Joints; Ph.D thesis; Queen Mary, University of London.

Bradley C and Vickers G W (1992); Automated rapid prototyping utilizing laser scanning and free-form machining; Ann CIRP; pp437-40.

Bradley C, Vickers G W and Milroy M (1994); Reverse engineering of quadric surfaces employing three dimensional laser scanning Journal of Engineering Manufacture; Vol.208, pp21-8.

BS6808 Part 2 (1987), Co-ordinate measuring machines, British Standards Institution, London.

BS1134 (1988), Assessment of surface texture, Part 1: Methods and Instrumentation; British Standards Institution, London.

Burke F (2001); The effects of negative air ions (NAI) on root caries lesions *in vitro;* PhD thesis; University of London.

Butler C (1991); An investigation into the performance of probes on co-ordinate measuring machines; Industrial Metrology; Vol.2, No.1, pp59-70.

Caddick C and Wimmer M A (2001); Hip simulator wear testing according to the newly introduced standard ISO 14242; Proceedings of the Institution of Mechanical Engineers, Vol.215 (H), pp429-42.

Chadwick R G (1989); A review: the assessment of the durability of composite resin restorative materials *in vivo*; Clinical Materials; Vol.4; pp241-153.

Chang M and Lin P (1999); On-line free form surface measurement via a fuzzy-logic controlled scanning probe; International Journal of Machine Tools and Manufacture; Vol.39, pp539-52.

Che C and Ni J (2000); A ball-target-based extrinsic calibration technique for high-accuracy 3-D metrology using off-the-shelf laser-stripe sensors, Precision Engineering, Vol.24, pp210-9.

Chee W and Donovan T E (1992); Polyvinyl siloxane impression materials: a review of properties and techniques; Journal of Dentistry; Vol.19, pp39-45.

Cheng W L and Menq C H (1995); Integrated laser/CMM system for the dimensional inspection of objects made of soft materials; International Journal of Advanced Manufacturing Technology; Vol.10; pp36-45.

Cherukara G P, Seymour K G, Samarawickrama D Y D, and Zou L (2000); A study into the variations in the labial reduction of teeth prepared to receive porcelain veneers - a comparison of three clinical techniques, British Dental Journal, Vol.192, No.7, pp401-404.

Clarke T A, Grattan K T V, and Lindsey N E (1990); Laser-based triangulation techniques in optical inspection of industrial structures; Optical Testing and Metrology III, SPIE, pp1332.

Clarke T A (1995); The development of an optical triangulation pipe profiling instrument; Optical 3-D Measurement Techniques III; Weichmann, pp331-340.

Cho M W and Kim K (1995); New inspection planning strategy for sculptured surfaces using co-ordinate measuring machine; International Journal of Production Research; Vol.33, No.2, pp427-44.

Choi W, Kurfess T R and Cagan J (1998); Sampling uncertainty in co-ordinate measurement data analysis; Precision Engineering; Vol. 22, pp153-63.

Chow J G (1997); Reproducing aircraft structural components using laser scanning; International Journal of Advanced Manufacturing Technology; Vol.13, pp723-8.

Corso M, Abanomy A, Di Canzio J, Zurakowski D and Morgano S M (1998)); The effect of temperature changes on the dimensional stability of polyvinyl siloxane and polyether impression materials; Journal of Prosthetic Dentistry; Vol.79, pp626-31.

Christensen G J (1997); A review of impression materials; CRA Status Report; CRA, Provo, Utah 84604, USA.

Dalton G (1998); Reverse engineering using laser metrology; Sensor Review; Vol.18, No.2, pp92-6.

Davis D R and Prebie J S (1986); Accuracy of a hydrophilic irreversible hydrocolloid/ silicone impression materials; Journal of Prosthetic Dentistry; Vol.55, pp304-8.

Delong R and Bramwell M C (1987); Matching an initial surface to a worn surface subject to rotation and translation. *In* The mathematics of surfaces II. Clarendon Press, Oxford. pp137-149.

Delong R, Pintado M R and Douglas W H (1985); Measurement of change in surface contour by computer graphics; Dental Materials; Vol.1, pp27-30.

Delong R, Peterson R and Douglas W H (1989); A laser profiling System for measuring wear of dental materials; Journal of Dental Research; Vol.68, pp907, abs.328.

Delong R and Douglas W H (1991); An artificial oral environment for testing dental materials. IEEE, Transactions on Biomedical Engineering; Vol.38, pp339-345.

Delong R, Pintado M R, Douglas W H, Taylor J and Breuer M (1993); Quantification of clinical changes in the gingival crest height using computer graphics. Journal of Dental Research; Vol.72, pp330, abs. 1811.

Delong R, Pintado M R, Heinzen M, Ko C and Douglas W H (1999); Comparison of contact and optical methods for measuring abrasion wear; Journal of Dental Research; Vol.78, pp161, abs.446.

Dong W P, Mainsah E, Sullivan P J and Stout KJ; 3-D topography – Present and future trends, in Stout K J (Ed.), 3-D Surface Topography – Measurement, Interpretation and Applications, Penton Press, London.

Dong W P, Mainsah E, Stout K J and Sullivan P J (1994); Three –dimensional surface topography – Review of present and future trends, Part II of Three-dimensional surface topography: Measurement, Interpretation and Applications (Ed, Stout K J), Penton Press, London; ISBN 1 85718 0046.

Dorsch R G, Hausler G, Herrmann J M (1994); Laser triangulation: fundamental uncertainty in distance measurement; Applied Optics; Vol.33, No.7, pp1306-14.

Dunne S M (1989); The assessment of size, depth and angular relationships in clinical restorative dentistry; PhD Thesis. University of London.

Eames W B, Sieweke J C, Wallace S W and Rogers L B (1979); Electrometric impression materials: effect of bulk on accuracy. Journal of Prosthetic Dentistry; Vol.41, pp304-7.

Edgeworth R and Wilhelm R G (1999); Adaptive sampling for co-ordinate metrology; Precision Engineering; Vol.23, pp144-54.

Elber G and Zussman E (1998); Cone visibility decomposition of freeform surfaces; Computer Aided Design; Vol.30, pp315-20.

EUR 15314 EN (1994); Performance test procedures for optical co-ordinate measuring probes, Final project report; European Commission; ISSN 1018-5593.

Fan K C (1997), A non-contact automatic measurement for free-form surface profiles, Computer Integrated Manufacturing Systems, Vol.10, No.4, pp277-85.

Fano V, Gennari P U and Ortalli I (1992); Dimensional stability of silicone-based impressions materials; Dental Materials; Vol.8, pp105-9.

Feng H Y, Liu Y X and Xi F (2001); Analysis of digitising errors of a laser scanning system; Precision engineering, Journal of International Societies for Precision Engineering and Nanotechnology; vol.25, pp185-91.

Funtowicz F, Zussman E, and Meltser M (1998); Optimal scanning of freeform surfaces using a laser-stripe; *In:* Israel-Korea Geometric Modelling Conference; Tel Aviv, Israel, February 1998, pp47-50.

Goh K H, Phillips N, and Bell R (1985); The applicability of the laser triangulation probe to non-contacting inspection; International Journal of Productions; Vol.24, pp1331-48.

Gordon G E, Johnson G H and Drennon D G (1990); The effect of tray selection on the accuracy of elastomeric impression materials; Journal of Prosthetic Dentistry; Vol.63, pp12-5.

Hoppe H, DeRose T, Duchamp T, McDonald J, and Stuetzle W (1992); Surface reconstruction from unorganized points; Computer Graphics, Vol.26, No.2.

Humienny, Bialas S, Osanna P H, Tamre M, Weckenmann A, Blunt L and Jakubiec W (2001), Geometrical Product Specifications, Warsaw University of Technology Printing House.

ISO 1036-2 (1994); Co-ordinate metrology: Performance assessment of co-ordinate measuring machines, International Standards Organisation, Geneva, Switzerland, Version E.

Jarvis R A (1983); A perspective on range finding techniques for computer vision; IEEE PAMI; Vol.5, No.2, p122-39.

Ji Z and Lew M C (1989); Design of optical triangulation devices, Optics and Laser Technology; Vol.21, No.5, pp335-8.

John S D and Galip Ulsoy A (1995); An optimisation strategy for maximizing co-ordinate measuring machine productivity, Part 2: Problem formulation, solution and experimental results; Transactions of the ASME; Vol.117, pp610-8.

Johnson G H and Craig R G (1985); Accuracy of four types of rubber impression materials compared with time of pour and a repeat pour of models; Journal of Prosthetic Dentistry; Vol.53, pp484-90.

Johnson G H and Craig R G (1986); Accuracy of addition silicones as a function of technique; Journal of Prosthetic Dentistry; Vol.55, pp197-203.

Johnson N, Lynch E, Zou L and Jovanovski V (1996), A three-dimensional sequential analysis of the restoration of a root surface lesion. Journal of Dental Research; Vol.75, p1165, abs. 285.

Jovanovski V, Zou L, Lynch E and Bedford J (1993); Superposition from 3-D co-ordinate data; Journal of Dental Research; Vol.72, p742, abs.74.

Jovanovski, Zou L, Tay W M, Lynch E and Cox M G (1995); Superposition of co-ordinate data obtained from a sequence of replicas; Journal of Dental Research; Vol.74, p895, abs.588.

Jovanovski V, Tay W M, Zou L, Anderson I J, Cox M G, Forbes A B, Allred H, Morganstein S I and Lynch E (1996); Objective assessment of three-dimensional structures in clinical dentistry using methods of co-ordinate Metrology; Nanobiology; Vol.4, pp55-61.

Jovanovski V, Zou L, Tay W M, Lynch E and Cox M G (1997); Assessment of three-dimensional structures in clinical dentistry; Advanced Mathematical tools in Metrology III 1997; Series on advances in mathematics for applied sciences; Vol.45, pp263-5.

Jovanovski V (1999); Three-dimensional imaging and analysis of the morphology of oral structures from co-ordinate data; PhD Thesis, University of London.

Kabban M, Fearne J, Jovanovski, Zou L and Bryan E (1997); Tooth shape in identical twins studied using optical surface metrology; 16th Congress of the International Association of Paediatric Dentistry, 17-21 September 1997, Buenos Aires, Argentina.

Kabban M, Fearne J, Jovanovski V and Zou L (2001); Tooth size and morphology in twins; International Journal of Paediatric Dentistry; Vol.11, pp333-9.

Kaddick C and Wimmer M A (2001); Hip simulator wear testing according to the newly introduced standard ISO 14242; Proceedings of the Institution of Mechanical Engineers; Vol.215,part H, pp429-42.

Kaiser D A and Nicholles J I (1976); A study of distortion and surface hardness of improved artificial stone casts; Journal of Prosthetic Dentistry; Vol.36, pp373-81.

Kim W S and Raman S (2000); On the selection of flatness measurement points in co-ordinate measuring machine inspection; International Journal of Machine Tool and Manufacture; Vol.40, pp427-43.

Koivunen V (1992); Robust signal restoration and local estimation of image structure; Technical Report; MS-CIS-92-92, University of Pennsylvania, 1992.

Koivunen V and Bajcsy R (1992); Rapid prototyping using three dimensional computer vision, Technical Report; MS-CIS-92-70, University of Pennsylvania, 1992.

Lacy A M, Fukui H, Bellman T and Jendresen M D (1981); Time-dependent accuracy of elastomer impression materials; Part II: Polyether, polysulfides and polyvinylsiloxane; Journal of Prosthetic Dentistry; Vol.45, pp329-33.

Lartigue C, Contri A and Bourdet P (2002); Digitised point quality in relation with point exploitation; Measurement; Vol.32, pp193-203.

Lee K H, Park H, Son S (2001); A framework for laser scan planning of freeform surfaces; International Journal of Advance of Manufacturing Technology, Vol.17, pp171-80.

Lim C P and Menq C H (1994); CMM feature accessibility and path generation; International Journal of Production Research; Vol.32, pp597-618.

Linke B A, Nicholls J I and Faucher R (1985); Distortion analysis of stone casts made from impression materials; Journal of Prosthetic Dentistry; Vol.54, pp794-802.

Lutz F, Imfeld T, Meier C and Firestone A (1979); Composite versus amalgam; comparative measurements of *in vivo* wear resistance: one year report; Quintessence International; Vol.3, pp77-87.

Lynch E, Zou L, Jovanovski V, and Bedford J (1993); Measurements of lesions of primary root caries, Journal of Dental Research; Vol.72, p742, abs.75.

Lynch E, Zou L, Jovanovski V, and Bedford J (1993); Assessment of inlay class I geometry, Journal of Dental Research; Vol.72, p742, abs.74.

Mainsah E, Dong W P, and Stout K J (1995); Holistic calibration of three dimensional surface micro topography instruments; International Journal of Machine Tools and Manufacture; Vol.35, No.2, pp1281-8.

Mainsah E, Dong W P, and Stout K J (1996); Problems associated with the calibration of optical probe based topography instruments, Measurement; Vol.17, No.3, pp173-181.

Mandilos M N (1998); Polyvinyl siloxane impression materials: an update on clinical use, Australian Dental Journal; Vol.43, No.6, pp428-34.

Mendez A J (1985); The influence of impression trays on the accuracy of stone casts poured from irreversible hydrocolloid impressions; Journal of Prosthetic Dentistry; Vol.54, pp383-8.

Millar B J, Dunne S M and Robinson P B (1997); The effect of a surface wetting agent on void formation in impressions; Journal of Prosthetic Dentistry; Vol.77, No.1, pp54-6.

Millar B J, Dunne S M and Robinson P B (1996); An in vivo study of a clinical surfactant used with poly(vinyl siloxane) impression materials; Quintessence International; Vol.27, No.10, pp707-9.

Milroy M J, Weir D J, Bradley C and Vickers G W (1996); Reverse engineering employing a 3-D laser scanner: a case study; International Journal of Advanced Manufacturing Technology; Vol.12, pp111-21.

Mitchem J C and Gronas S G (1982); *In vivo* evaluation of the wear of restorative resin, Journal of the American Dental Association; Vol.27, pp821-8.

Modjarrad A (1988); Non-contact measurement using a laser scanning probe; SPIE, In-Process optical measurements; Vol.1012, p229-39.

Moss J P, Linney A D, Grindrod S R and Moss C A (1989); A laser scanning system for the measurement of facial surface morphology; Journal of Optics and Lasers in Engineering; Vol.10, pp179-90.

Motavalli S and Bidanda B (1991); A part image reconstruction system for reverse engineering of design modifications; Journal of Manufacturing Systems; Vol.10, No.5, pp383-95.

O'Mahony A, Spencer P, Williams K and Corcoran J (2000); Effect of 3 medicaments on the dimensional accuracy and surface detail reproduction of polyvinyl siloxane impressions; Quintessence International; Vol.31,No.3, pp201-6.

Osanna P H, Rezaie K, Durakbasa N M and Heiss C P (1995); Form measurements – A bridge between production metrology and bio-mechanics; International Journal of Machine Tools and Manufacturing; Vol.35, No.2, pp165-8.

Patel S (1996); The effect of forces due to bracket misalignment on orthodontic wire, MSc thesis; University of London.

Raja J, Muralikrishnan B and Fu S Y (2002); Recent advances in separation of roughness, waviness and form; Precision Engineering, Journal of the International Societies for Precision Engineering and Nanotechnology; Vol.26, pp222-235.

Reid c (1995), Performance characteristics of touch trigger probes, Quality today, Buyers Guide 1995; pp152-154.

Reisbick M H and Matyas J (1975); The accuracy of highly filled elastomeric impression materials; Journal of Prosthetic Dentistry; Vol.33, pp67-72.

Revell P, Al-Saffar N and Kobayashi A (1997); Biological action to debris in relation to joint prostheses; Journal of Engineering Medicine; Proc. Inst. Mech. Eng.; Part H 211, pp187-197.

Rioux M (1984); Laser range finder based on synchronized scanners; Journal of Applied Optics; Vol.23, No.21, pp3837-44.

Rioux M, Bechthold G, Taylor D and Duggan M (1987); Design of a large depth of view three dimensional camera for robot vision Optical Engineering; Vol.26, No.12, pp1245-50.

Robinson P B, Dunne S M and Millar B J (1994); An *in vitro* study of a surface wetting agent for addition reaction silicone impressions; Journal of Prosthetic Dentistry; Vol.71, No.4, pp390-3.

Sahoo K C and Menq C H (1991); Localization of 3-D objects having complex sculptured surfaces using tactile sensing and surface description; Journal of Engineering for Industry; Vol.113, pp85-92.

Saito K and Miyoshi T (1991); Non-contact 3-D digitising and machining system fro free-form surfaces. Ann CIRP; 40(1), pp483-6.

Savio E and De Chiffre L (2002); An artefact for traceable freeform measurements on co-ordinate measuring machines; Precision Engineering, Journal of the International Societies for Precision Engineering and Nanotechnology; Vol.26, pp58-68.

Seokbae S, Hyunpung P and Kwan H L (2002); Automated laser scanning system for reverse engineering and inspection; International Journal of Machine Tools and Manufacture; Vol.42, pp889-97.

Seymour KG, Samarawickrama D Y D, Zou L, and Lynch E (1995); Cavo-surface angles of bonded crown preparations *in vivo*; Journal of Dental Research; Vol.75, abs.281.

Seymour K G, Zou L, Samarawickrama D Y D and Lynch E (1996a); Assessment of shoulder dimensions and angles of porcelain bonded to metal crown preparations; Journal of Prosthetic Dentistry, Vol.75, No. 4, pp406-11.

Seymour K G, Zou L, Jovanovski V, Samarawickrama D Y D and Lynch E (1996b); Cavo-surface angles of bonded-crown preparations *in vivo*; Journal of Dental Research, Vol.75, p1165, abs.281.

Seymour K (1998); Variations in the labial 'shoulder' geometry of teeth prepared to receive metal ceramic crowns; PhD Thesis, University of London.

Seymour K G, Samarawickrama D Y D, Zou L, Lynch E, and Jovanovski V (1999a); Labial shoulder geometry and emergence angle of metal ceramic crowns; Journal of Dental Research, Vol.78, p303, abs.1583.

Seymour K G, Samarawickrama D Y D, Zou L and Lynch E (1999b); Assessing the quality of shoulder preparations for metal ceramic crowns; European Journal of Prosthodontics and Restorative Dentistry; Vol.7. No.4, pp 125-9.

Shahrom A W, Vanezis P, Chapman R C, Gonzales A, Blenkinsop C and Rossi M L (1996); Techniques in facial identification: computer aided facial reconstruction using a laser scanner and video superimposition, International Journal of Legal Medicine; Vol.108, pp194-200.

Silvaggi C, Luk F, and North W (1986); Triangulation sensor with 2-D pixel array and centring method; Position and dimension by structured light, Experimental Techniques; p22.

Spitz S N and Spyridi A J and Requicha A G(1999); Accessibility analysis for planning of planning of dimensional inspection with co-ordinate measuring machines; IEEE Transactions on Robotics and Automation; Vol.15, No.4, pp714-27.

Stout K J (1994); Three-dimensional surface topography: measurement, interpretation and applications; Penton press; ISBN 1 85718 004 6.

Stout K J and Blunt L (1995); Application of 3-D topography of bio-engineering; International Journal of Machine Tools Manufacturing; Vol.35, pp219-229.

Summerhays K D, Henke R P, Baldwin J M, Cassou R M and Brown C W (2002); Optimising discrete point sample patterns and measurement data analysis on internal cylindrical surfaces with systematic form deviations; Precision Engineering, Journal of the International Societies for Precision Engineering and Nanotechnology; Vol.26, pp105-121.

Takatsuji T, Osawa S and Kurosawa T (2002); Uncertainty analysis of calibration of geometrical gauges; Precision engineering, Journal of the International Societies for Precision Engineering and Nanotechnology; Vol.26, pp24-29.

Taylor J L, Spencer J L, Breuer M, Delong R, Pintado M R and Douglas W H (1993); Digital technique for measuring changes in gingival contour; Journal of Prosthetic Dentistry; Vol.56, pp4-8.

Tan R (1990), Internal report of optical measurement system, Department of Conservative Dentistry, Barts and The London, Queen Mary University of London; pp 1-3.

Than F M, King T G and Stout K J (1996); The influence of sampling strategy on a circular feature in co-ordinate measurements; Measurement, Vol.19, No.2, pp73-81.

Tjan A H, Whang S B and Sarkissian R (1986); Clinically oriented evaluation of the accuracy of commonly used impression materials; Journal of Prosthetic Dentistry; Vol.56, pp4-8.

Wang Y F and Aggarwal J K (1987); 3D object description from stripe coding and multiple views; Proceedings of the 5th Scandinavian Conference on Image Analysis; Vol.60, No.2, pp669-80.

Weckenmann A, Eitzert H, Garmer M and Weber H (1995); Functionality oriented evaluation and sampling strategy in co-ordinate metrology; Precision Engineering; Vol.17, pp244-52.

Will P W and Pennington K S (1972); Grid coding: a novel technique for image proceessings; Proceedings of the IEEE; Vol.60, No.6, pp669-80.

Williams P T, Jackson D G and Bergman W (1984); An evaluation of the time-dependent dimensional stability of eleven elastomeric impression materials; Journal of Prosthetic Dentistry; Vol.52, p p120-5.

Win P, Van Vliet, Peter H J Schellekens (1998), Development of a fast mechanical probe for co-ordinate measuring machines, Precision Engineering; Vol.22, pp141-152.

Woodward J D, Morris J C and Kahn Z (1985); Accuracy of stone casts produced by perforated trays and no perforated trays; Journal of Prosthetic Dentistry; Vol.53, pp347-50.

Xi F and Shu C (1999); CAD-based path planning for 3-D line laser scanning; Computer-aided Design; Vol.31, pp473-9.

Xong Y L (1990); Computer aided measurement of profile error of complex surfaces and curves: theory and algorithm; Internatioal Journal of Machine Tools and Manufacturing; Vol.30, No.3, pp339-57.

Yang Q and Butler C (1996); A 3-D non-contact trigger probe for co-ordinate measuring machines; Measurement; Vol.17, No.1, pp39-44.

Yau H T and Menq C H (1995); Automated CMM path planning for dimensional inspection of dies and moulds having complex surfaces; International Journal of Machine Tools and Manufacturing; Vol:35, No.6, pp861-76.

Yeganeh S, Lynch E, Jovanovski V and Zou L (1995); Three dimensional quantification of plaque on teeth *in vivo*; Journal of Dental Research; Vol.74, p240, abs.80.

Yeganeh S, Zou L, Jovanovski V, Heath M R and Lynch E (1996a); Reproducibility of digitised sequential replicas; Journal of Dental Research; Vol.75, p1182, abs.419.

Yeganeh S, Zou L, Jovanovski V, Heath M R and Lynch E (1996b); Objective quantification of plaque thickness *in vivo*; Journal of Dental Research; Vol.75, p84, abs.536.

Yeganeh S, Lynch E, Jovanovski V and Zou L (1999); Quantification of root surface plaque using a new 3-D laser scanning method; Journal of Clinical Periodontology; Vol.26, pp692-7.

Yeganeh S, Lynch E, Jovanovski V, Heath M R and Zou L(1999); Clinical and metrology assessment of experimentally induced gingivitis; Journal Dental Research; Vol.75, p895, abs.589.

Yeganeh S (due to be submitted), A study of root caries lesions, PhD Thesis, University of London.

Zou L, Samarawickrama D Y D, Jovanovski V and Shelton J (2001); Measurement of sequential impressions of acetabular cups from a total hip joint replacement using a non-contact measurement system; International Journal of Machine Tools and Manufacture; Vol.41, pp2023-30.

Zou L, Yang Q P, Jovanovski V, Tay WM and Lynch E (1996a), Measurement of tooth morphology using a laser probe fitted on a co-ordinate measuring machine; International Measurement Confederation; Laser Metrology for Precision Measurement and Inspection in Industry, Proceedings IMECO TC No.14, pp11-20.

Zou L, Jovanovski V, Tay WM and Lynch E (1996b); Error distribution on a digitised datum sphere; Journal of Dental Research; Vol.75, pp1165, abs.282.

Zou L, Jovanovski V, Tay W M and Lynch E (1995); The influence of three parameters on laser probe scanning of irregular surfaces; Journal of Dental Research; Vol.73, pp895.

Zou L, Bedford J, Jovanovski V, Lynch E and Burke F (1993); Measurements of lesions of primary root caries; Journal of Dental Research; Vol.73, pp895.

Zussman E, Schuler H and Seliger G (1994); Analysis of the geometrical feature detactability constraints for laser-scanner sensor planning; The International Journal of Advanced Manufacturing Technology; Vol.9, p56-64.

13 APPENDIX I: THE CO-ORDINATE MEASURING MACHINE (CMM)

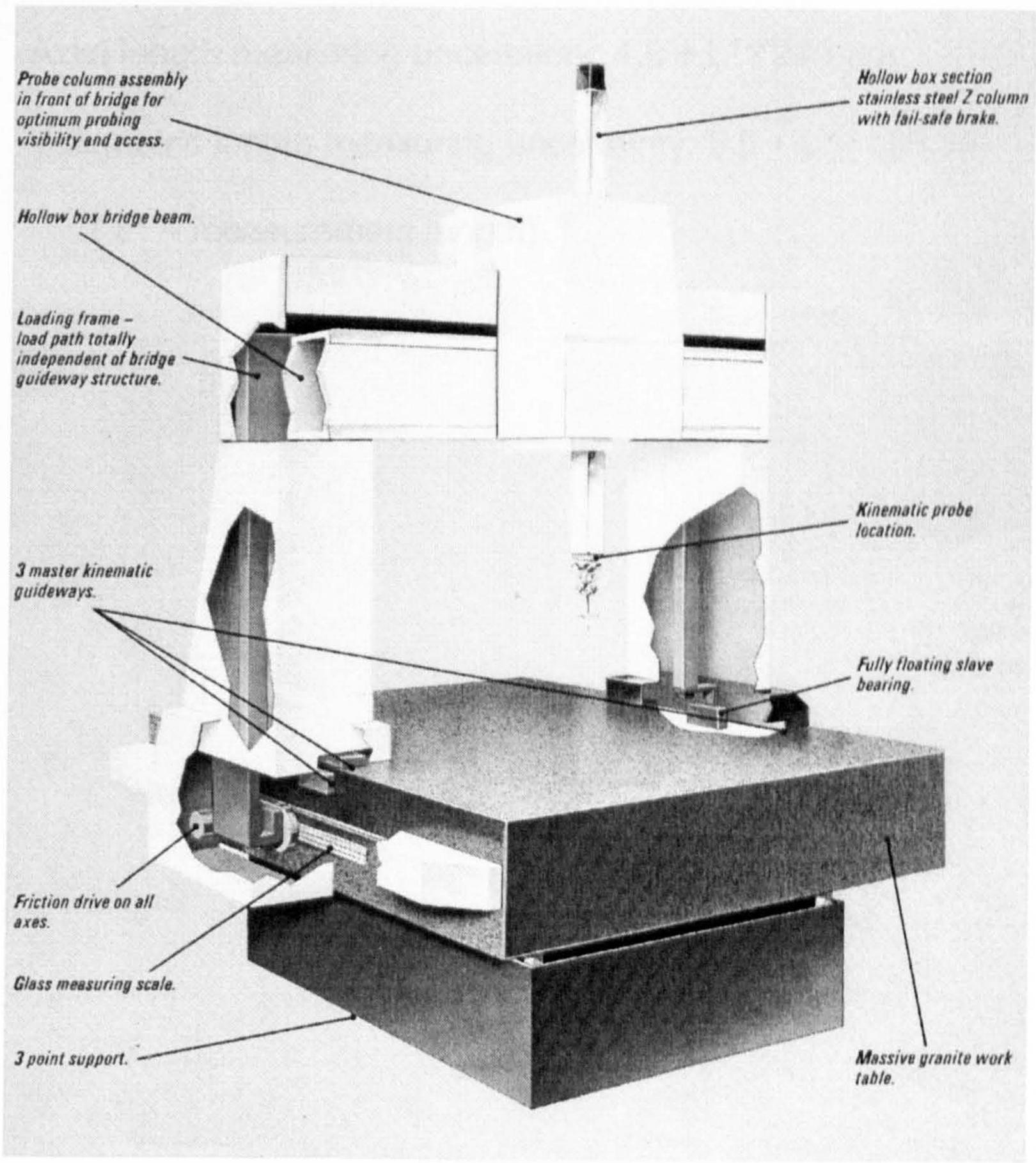

Figure A-2: The Ferranti Merlin II CMM

The Merlin II CMM is typical of those produced by a variety of manufacturers, being a bridge type. The span of the bridge is 500mm. A composite granite worktable of 1100mm × 1300mm × 300mm ensures rigidity and stability. The specifications of the CMM are as follows:

- Resolution: 0.5µm
- Axial length measuring uncertainty: 4.0 + L* / 275 µm
- Volumetric length measuring uncertainty: 5.0 + L* / 150 µm

(L* – measurement length)

14 APPENDIX II: THE OPTICAL PROBE (OP2)

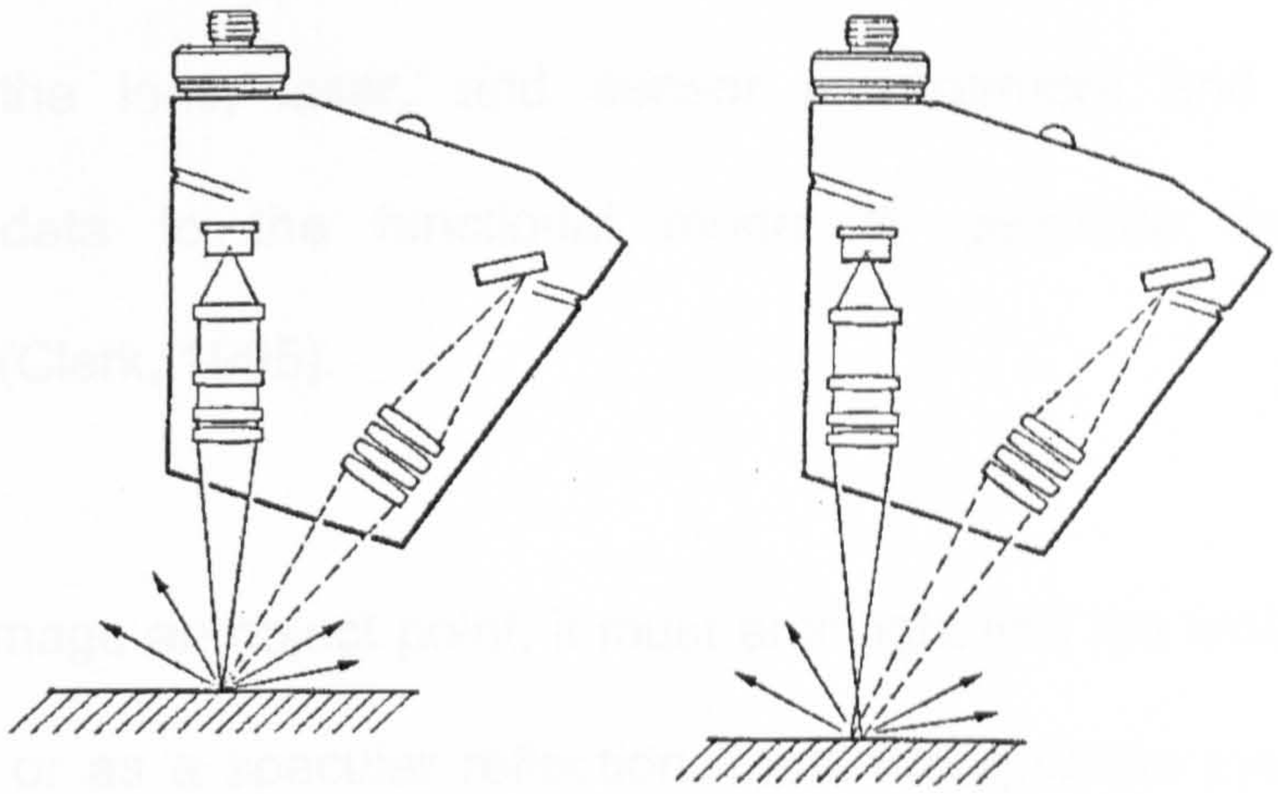

Figure A-2: The OP2 working principles

The triangulation probe emits a beam of laser light in a fixed direction. It images the spot produced by the beam on the measurement object. The optical axis of the imaging system is inclined relative to the beam axis at the so-called triangulation angle (Fig.A-2). Thus the imaged spot moves in the image plane if the object changes its distance relative to the probe. The position of the imaged light spot is measured by a positional sensing device (PSD). The relationship between the relative object position and the signal describing the position of the imaged light spot on the detector has to be determined; usually this is done experimentally. This is the probe calibration. There are two approaches to be adopted for calibration – direct and indirect. Direct calibration uses a look-up table. The relationship between the location of the laser spot image and the measured distance from some pre-defined location on the instrument is

observed at a number of points. This method is used in our measurement system. An indirect method involves constructing the correct functional model for the lens, laser, and sensor arrangement and fitting the calibration data to the functional model to generate the relevant parameters (Clark, 1995).

In order to image an object point, it must emit light into the lens. This may be diffusely or as a specular reflection. Most triangulation systems work with diffused reflections. Thus the sensor can detect a wider range of reflections comparing to the specular reflections from a measurement surface. OP2 (Renishaw, UK) is an optical triangulation based optical laser probe. The wavelength of the laser is 830nm, the power is 5mw (Class II laser), and the size of the laser spot at focus is 25μm in diameter. The sensor detects diffused reflections.

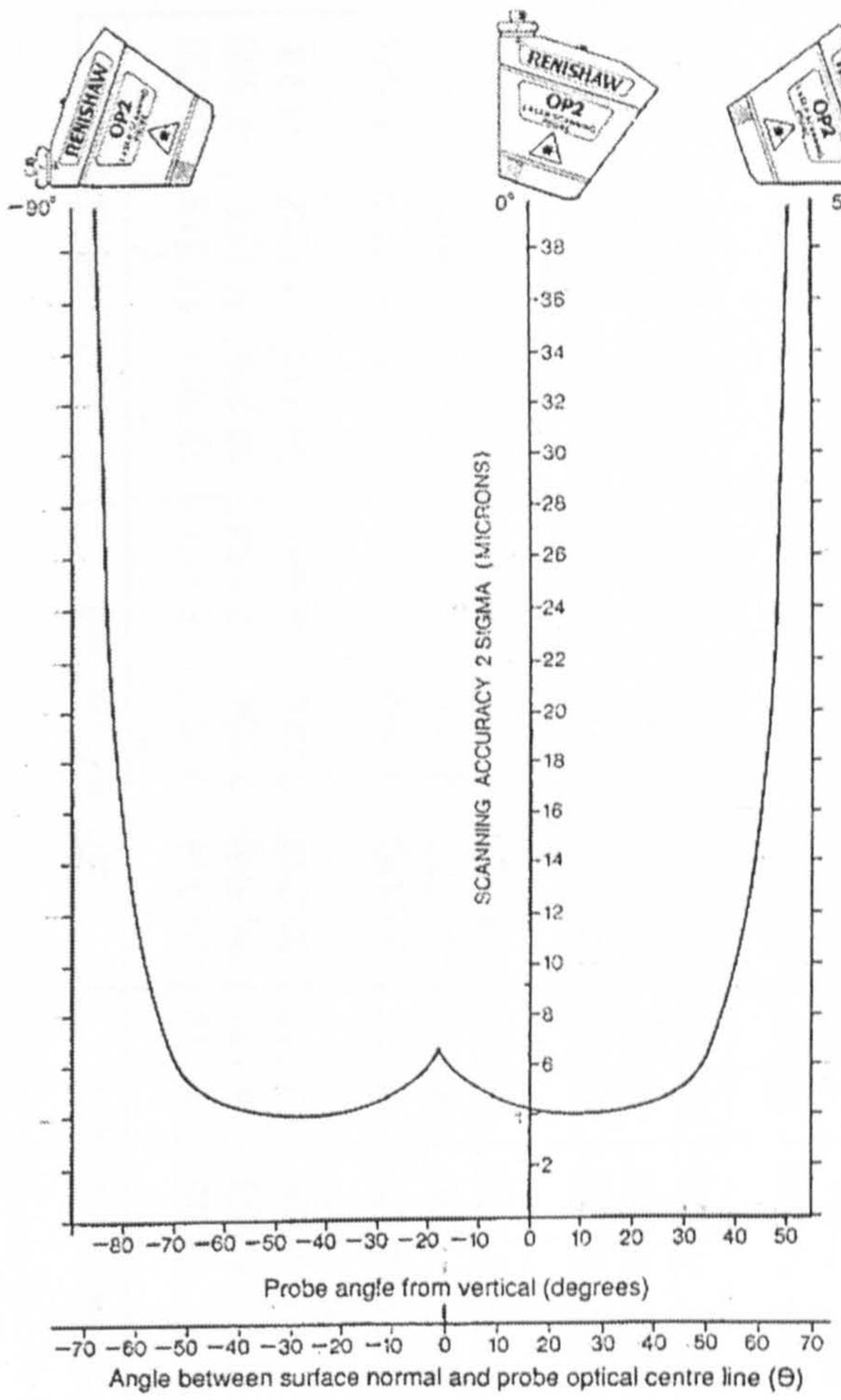

30

FigureA-3: Scan probe orientations as recommended by manufacturer.

Fig. A-3 shows the probe orientation recommendation guidelines given by the manufacturer. It indicates that, at -60° the error is still within 10µm limit. In fact, it is impossible to digitise a single point on a surface by using such a probe angle, when the surface normal is away from the detector of the probe.

15 APPENDIX III: MEASUREMENTS OF POSITIONAL CHANGES FOLLOWING ORTHODONTIC MOVEMENT

Before treatment	centre-upper-left			centre-upper-right			centre-lower-left			centre-lower-right		
	x	y	z	x	y	z	x	y	z	x	y	z
M-horizont-misalign-ur1	-39.07	16.878	-5.382	-39.828	14.05	-4.989	-39.094	16.529	-5.817	-39.983	14.319	-5.635
M-horizont-misalign-ur2	-35.856	7.734	-4.178	-35.566	6.153	-4.121	-36.189	7.704	-4.564	-36.205	6.151	-4.688
M-horizont-misalign-ur3	-38.972	-0.1135	-6.147	-38.729	-1.296	-6.079	-39.252	0.062	-6.644	-38.734	-1.562	-6.78
M-vertical-misalign-1-ur1	-39.331	17.032	-5.13	-39.675	14.428	-5.101	-39.339	16.956	-5.961	-39.608	14.533	-5.904
M-vertical-misalign-1-ur2	-36.051	9.408	-4.831	-36.296	7.389	-4.898	-36.439	9.515	-5.511	-36.488	7.438	-5.421
M-vertical-misalign-1-ur3	-39.125	-0.232	-5.901	-38.377	-1.635	-5.842	-39.209	-0.243	-6.601	-38.668	-1.561	-6.552
M-vertical-misalign-2-ur1	-39.007	16.851	-5.177	-39.323	13.93	-5.457	-38.875	16.518	-6.239	-40.337	14.636	-6.021
M-vertical-misalign-2-ur2	-36.061	9.21	-6.096	-36.309	7.218	-6.105	-36.207	9.046	-6.461	-36.422	7.112	-6.255
M-vertical-misalign-2-ur3	-38.888	0.036	-5.918	-38.517	-1.224	-5.764	-38.752	-0.294	-6.524	-38.501	-1.497	-6.438
M-angle-misalign-1-ur1	-39.202	16.938	-6.367	-39.907	14.332	-5.937	-39.152	16.901	-6.669	-40.046	14.542	-6.318
M-angle-misalign-1-ur2	-35.985	8.542	-4.615	-35.894	7.269	-4.362	-36.474	8.659	-5.374	-36.176	7.225	-4.803
M-angle-misalign-1-ur3	-39.057	-0.019	-5.765	-38.367	-1.492	-5.759	-39.471	0.324	-6.468	-39.099	-1.481	-6.387
M-angle-misalign-2-ur1	-38.679	16.889	-5.707	-39.382	14.393	-5.303	-38.569	16.761	-6.257	-39.536	14.361	-5.885
M-angle-misalign-2-ur2	-35.683	8.909	-4.814	-35.512	7.934	-3.917	-36.118	9.016	-5.146	-35.513	7.974	-4.862
M-angle-misalign-2-ur3	-38.922	0.0995	-6.071	-38.311	-1.324	-5.973	-38.978	0.004	-6.764	-38.588	-1.512	-6.469
M-optimum-align-2-ur1-rpt1	-38.783	17.295	-5.75	-39.476	14.604	-5.557	-38.716	17.13	-6.248	-39.508	14.644	-6.133
M-optimum-align-2-ur2-rpt1	-35.498	8.921	-4.426	-35.596	7.344	-4.499	-35.672	9.002	-4.977	-36.032	7.67	-4.902
M-optimum-align-2-ur3-rpt1	-39.043	0.089	-6.343	-38.4	-1.228	-6.229	-39.128	0.131	-6.913	-38.672	-1.305	-6.953

after treatment	centre-upper-left			centre-upper-right			centre-lower-left			centre-lower-right		
	x	y	z	x	y	z	x	y	z	x	y	z
M-horizont-misalign-ur1	-39.782	17.053	-6.035	-40.536	14.386	-6.038	-39.71	16.988	-6.604	-40.563	14.458	-6.506
M-horizont-misalign-ur2	-40.815	7.382	-6.119	-40.695	5.989	-6.196	-40.944	7.694	-6.8	-40.746	5.792	-7.005
M-horizont-misalign-ur3	-39.419	-1.371	-6.577	-38.903	-1.489	-6.491	-39.409	-0.214	-7.472	-39.063	-1.569	-7.176
M-vertical-misalign-1-ur1	-39.62	16.898	-5.571	-39.961	14.044	-5.564	-39.538	16.553	-6.235	-40.107	14.249	-5.822
M-vertical-misalign-1-ur2	-40.315	8.345	-5.823	-40.479	6.819	-5.81	-40.423	8.385	-6.393	-40.446	6.937	-6.459
M-vertical-misalign-1-ur3	-39.338	-0.579	-6.038	-38.653	-1.878	-5.826	-39.5	-0.373	-6.581	-38.737	-1.881	-6.616
M-vertical-misalign-2-ur1	-39.918	17.247	-6.103	-40.559	14.609	-6.064	-39.952	17.091	-6.651	-40.632	14.672	-6.822
M-vertical-misalign-2-ur2	-40.807	8.376	-6.867	-40.958	6.639	-6.855	-40.788	8.505	-7.275	-41.008	6.908	-7.467
M-vertical-misalign-2-ur3	-39.808	-0.299	-6.008	-39.359	-1.795	-5.828	-39.787	-0.41	-6.933	-39.06	-1.967	-6.799
M-angle-misalign-1-ur1	-39.916	17.325	-6.17	-40.682	14.386	-6.213	-39.881	17.39	-6.853	-40.772	14.489	-6.706
M-angle-misalign-1-ur2	-40.879	7.581	-6.289	-40.938	5.759	-6.071	-41.018	7.793	-6.82	-41.062	6.005	-6.527
M-angle-misalign-1-ur3	-39.442	-0.886	-5.874	-38.823	-2.31	-5.792	-39.546	-0.765	-6.411	-38.941	-2.182	-6.482
M-angle-misalign-2-ur1	-40.035	16.806	-6.694	-40.735	14.306	-6.626	-39.911	16.887	-7.085	-40.754	14.583	-7.089
M-angle-misalign-2-ur2	-40.556	8.041	-7.251	-41	6.365	-6.468	-40.661	7.704	-7.643	-41.126	6.349	-6.927
M-angle-misalign-2-ur3	-39.379	-0.777	-6.896	-38.527	-2.433	-6.981	-39.21	-0.967	-7.561	-38.704	-2.282	-7.363
M-optimum-align-2-ur1	-39.809	17.404	-6.291	-40.519	14.576	-6.205	-39.741	17.359	-6.948	-40.605	14.762	-6.738
M-optimum-align-2-ur2	-40.604	8.394	-6.345	-40.824	6.884	-6.472	-40.599	8.24	-6.843	-41.077	7.25	-6.753
M-optimum-align-2-ur3	-39.585	0.046	-6.616	-39.114	-1.378	-6.319	-39.627	0.073	-7.004	-39.116	-1.719	-7.007

16 APPENDIX IV: GLOSSARY OF TERMS USED IN DENTISTRY RELEVANT TO THIS STUDY (ACCORDING TO BS 4492:1983) :

buccal surface	A surface adjacent to the cheek.
bracket	A metal or plastic precision component welded to a band or attached to a tooth. It receives an archwire or other orthodontic mechanism as part of orthodontic treatment.
caries	A disease process that results in the demineralisation of dental hard tissues by microbial activity.
cast	A reproduction of the surface form of oral or facial tissues obtained from an impression.
cavo-surface angle	The angle formed at any point on the junction of a preparation with the unprepared surface of the tooth.
conservative dentistry	That part of restorative detistry concerned with the restoration of individual teeth. It also includes endodontics, crowning and (in part) fixed bridgework.

Note: The exact definition of this term is different in the UK from that generally accepted elsewhere in Europe, which is given by the FDI/ISO definition, as follows 'That branch of dentistry which is principally concerned with the restoration of diseased or injured tooth structures to the proper form and function while conserving the still healthy parts.'

restorative dentistry	A comprehensive term covering dental care for the dentate, or partially or totally edentulous patient, in order to establish a stable and healthy funtional dentition. It includes aspects of conservative dentistry, periodontics, prosthodontics, and any other branch of dentistry that may be indicated.

Note: The exact definition of this term is different in the UK from that generally accepted elsewhere in Europe, which is given by the FDI/ISO definition, as follows: 'A comprehensive term to cover dental procedures in the dentulous, partially edentulous or

edentulous mouth; these may include operative, endodontic, periodontal, orthodontic and prosthetic procedures'.

restoration	The material result of a series of operative procedures that restore the form, function and appearance of a tooth.
cavity	A tooth lesion caused by actual loss of hard tooth substance, which may arise from caries, trauma, erosion, abrasion, or attrition.
crown	A full or partial replacement of the clinical crown that is attached to the remaining part of the tooth. It is usually made of metal, synthetic resins, or porcelain, or a combination of these materials, and is classified according to the material(s) of construction, method of manufacture, and amount of tooth covered.
crown preparation	A molar or premolar tooth is prepared by cutting a layer to be able to restore with a crown.
cusp	A protrusion of the occlusal surface of the tooth.
porcelain bonded crown	A crown made of cast metal to which porcelian is fused.
denture	A removable prosthesis for natural teeth and their asociated tissures.
fissure	An infolding of the enamel between cusps or ridges.
filling	Any material that is inserted into a preparation or cavity in order to fill it, without necessarily restoring either form or function.
gingiva(e)	The soft investing tissues of the alveolar processes of the jaws and necks of the teeth.
gingival morphology	The form, shape, or profile of gingivae.
impression	A negative imprint from which a positive reproduction, or cast, can be made.

inlay	A restoration, usually made of casting gold alloy or, more rarely, fused porcelain, for a specific preparation, into which it is cemented.
mould	A form in which an object is cast or shaped.
molars	The three most posterior teeth in each quadrant of the jaws in the permanent dentition. They have broad occlusal surfaces with multiple cusps and are adapted to crushing and grinding. In the deciduous dentition there are only two moars in each quadrant.
occlusal	Pertaining to the surfaces of the teeth or tooth substitutes that make contact with those in the opposing jaw.
occlusal surfaces	Those surfaces of molars and premolars which in normal occlusion meet the corresponding surfaces of the opposing teeth.
orthodontics	That branch of dentistry primarily concerned with the extent of normal variations of form and function of bones, soft tissues, and teeth, and the ways in which they affect the occlusion.
onlay	A metal or acrylic covering of the occlusal and/or incisal surfaces.
plaque	Adherent bacterial colonization on the tooth surface, restorations and dental appliances.
premolars	The two teeth in each quadrant of the jaws immediately distal to the canines and mesial to the molars. They have two cusps and are adapted to a grinding action. The premolars are not represented in the deciduous dentition.
preparation	Operations performed upon a tooth to remove diseased, weakened and defective tissue, and to condition and shape sound tissue into a form suitable for the reception and retention of a temporary or permanent restoration.

tissue	A mass of similar cells performing a specialised function.
veneers	Thin tooth-shaped labial laminae of polymeric (and ceramic) materials used in conjunction with filled resin and acid etching to mask discoloured or malformed teeth in the anterior region of the mouth.
veneer preparation	A labial surface prepared by cutting a layer and able to accept a veneer.

17 APPENDIX V: LIST OF PUBLICATIONS

17.1 Papers

1. Cherukara G P, Seymour K G, Samarawickrama D Y D and **Zou L** (2002); A study into the variations in the labial reduction of teeth prepared to receive porcelain veneers - a comparison of three clinical techniques; British Dental Journal; Vol.192, No.7, pp401-404.

2. **Zou L**, Samarawickrama D Y D, Jovanovski V and Shelton J (2001); Measurements of sequential impressions of acetabular cups from a total hip joint replacement using a non-contact measurement system; International Journal of Machine Tools & Manufacture; Vol.41, pp2023-30.

3. Kabban M, Fearne J, Jovanovski V and **Zou L** (2001); Tooth size and morphlogy in twins; International Journal of Paediatric Dentistry; Vol.11, pp333-339.

4. Seymour K, Samarawickrama D Y D, **Zou L** and Lynch E (1999); Assessing the quality of shoulder preparations for metal ceramic crowns; European Journal of Prosthodontics and Restorative Dentistry; Vol.7, No.4, pp125-9.

5. Yeganeh S, Lynch E, Jovanovski V and **Zou L** (1999); Quantification of root surface plaque using a new 3D laser scanning method; Journal of Clinical Periodontology, Vol.26, pp692-7.

6. Seymour K, **Zou L**, Samarawichrama D Y D and Lynch E (1996); Assessment of shoulder dimensions and angles of porcelain bonded to metal crown preparations using a co-ordinate measuring machine; Journal of Prosthetic Dentistry; Vol. 75, pp406-11.

7. Jovanovski V, Tay W M, **Zou L**, Anderson I J, Cox M G, Forbes A B, Allred H, Morganstein S I and Lynch E (1996); Objective assessment of three-dimensional structures in clinical dentistry using methods of co-ordinate metrology; Nanobiology; Vol.4, p55-61.

17.2 Proceedings

1. **Zou L**, Yang Q P, Jovanovski V, Tay W M and Lynch E (1996); Measurement of tooth morphology using a laser probe fitted on a Co-ordinate Measuring Machine; Proceedings of 4th International IMEKO Symposium on Laser Metrology for Precision Measurement and Inspection in Industry; IMEKO TC No.14, pp11-20.

2. Jovanovski V, **Zou L**, Tay W M and Lynch E (1997); Assessment of three dimensional structures in clinical dentistry; The Proceedings of Advanced Mathematical Tools in Metrology III, pp263-265

17.3 Abstracts

1. Seymour K G, Samarawickrama D Y D, **Zou L**, Lynch E and Jovanovski V (1999a); Labial shoulder geometry and emergence angle of metal ceramic crowns; Journal of dental research; Vol.78, p303, abs1583.

2. Baysan A, Lynch E, Jovanovski V, and **Zou L** (1999); Three month assessment of an antimicrobial root sealant; Journal of Dental Research; Vol.78, p444, Ads. 2712.

3. Yeganeh S, Lynch E, Jovanovski V, Heath M R and **Zou L**(1999); Clinical and metrology assessment of experimentally induced gigivitis; Journal Dental Research; Vol.75, p895, abs589.

4. **Zou L**, Jovanovski V, Tay W M and Lynch E (1996); Error distribution on a digitised datum sphere; Journal of Dental Research; Vol.75, p287.

5. Seymour K, **Zou L**, Jovanovski V, Samarawickrama D Y D and lynch E (1996); Cavo-surface angles of bonded crown preparations *in vivo*; Journal of Dental Research; Vol.75, p287.

6. Jovanovski V, **Zou L**, Tay W M, Lynch E and Cox M G(1996); Improved superposition of co-ordinate data obtained from a sequence of replicas; Journal of Dental Research; Vol.75, p287.

7. Johnson N, Lynch E, **Zou L** and Jovanovski V(1996); A three-dimensional sequential analysis of the restoration of a root surface lesion; Journal of Dental Research; Vol.75, p287.

8. Yeganeh S, **Zou L**, Jovanovski V, Heath M R and Lynch E (1996); Assessing the quality of shoulder preparations for metal ceramic crowns; European Journal of Prosthodontal Research Reproducibility of digitised sequential replicas; Journal of Dental Research; Vol.75, p419.

9. **Zou L**, Jovanovski V, Tay W M and Lynch E (1995); The influence of three parameters on laser probe scanning of irregular surfaces; Journal of Dental Research; Vol.74, p895.

10. Yeganeh S, Morris-clapp C, **Zou L**, Jovanovski V and Lynch E (1995); Three Dimensional quantification of plaque on teeth *in vivo*; Journal of Dental Research; Vol.74, p895.

11. Seymour K, Samarawickrama D Y D, **Zou L** and Lynch E (1995); Shoulder dimensions and angles of bonded crown preparation; Journal of Dental Research; Vol.74, p895.

12. Jovanovski V, **Zou L**, Tay W .M, Lynch E and Cox M G (1995); Superposition of co-ordinate data obtained from a sequence of replicas; Journal of Dental Research; Vol.74, p895.

13. **Zou L**, Jovanovski V and Lynch E (1993); Reproducibility of data collected by a Co-ordinate Measuring Machine; Journal of Dental Research; Vol.69, p742.

14. Jovanovski V, **Zou L** and Lynch E (1993); Geometric superimposition of a sequence digitised replicas; Journal of Dental Research; Vol.69, p742.

15. Lynch E, **Zou L**, Jovanovski V and Burke F (1993); Measurements of lesions of primary root caries; Journal of Dental Research; Vol.69, p742.

16. Bedford J, **Zou L**, Jovanovski V and Lynch E (1993); Reproducibility of data collected by a co-ordinate Measuring Machine; Journal of Dental Research; Vol.72, p742, abs 445.

18 ACKNOWLEDGEMENTS

I would like to thank the following persons:

Dr. D Y D Samarawickrama, Principal Supervisor of this study, for his tireless efforts in supervising and guiding this research. He took over this task half way through the study and he made a real difference to the outcome. To him I offer my grateful thanks.

Dr. Julia Shelton, Associate Supervisor, Senior Lecturer at the Interdisciplinary Research Centre, Queen Mary, University of London, for her supervision and consistent encouragement and valuable help.

Dr. Kevin Seymour, Senior Lecturer in the Department of Adult Oral Health, for his valuable suggestions regarding the structure of the Thesis during the writing stage, the scientific suggestions during collaboration over many projects, and his help with correcting the Thesis.

Professor Ken Stout, international expert in dimensional metrology; formerly Dean of Mechanical Engineering at Huddersfield University (1997-2002), formerly Lucas Professor and Dean of Mechanical Engineering at Birmingham University (1989-1997), for his expertise, valuable suggestions, and corrections regarding the final draft of the thesis.

Dr. Christopher Mercer for his meticulous reading and correcting of the text and expert advice on the layout of the thesis. I owe him a great deal.

Dr. Vladimir Jovanovski, former colleague in the Department of Adult Oral Health, for his very efficient software support throughout the development of the co-ordinate measurement system and for his valuable help and advice.

Professor Harry Allred, Head of the Department of Conservative Dentistry until 1994, for founding the Dental Metrology Unit. For his vision and foresight, and for supervising this work at the beginning.

Mr. John Bedford, formerly Senior Engineer at International Metrology Systems (formerly Ferranti), for his consistent help with the hardware and software used in running the CMM.

Mr. Nigel Cross, Senior Research Scientist in Centre of Dimensional Metrology of National Physical Laboratory (NPL), for his profitable support in providing the research model.

All the clinical investigators who provided material for the research: Mr. George Cherukara (who also read the final draft), Mariella Kabban, Mrs. Jaki Heath, Mrs. Sharzad Yeganeh, Dr. Carolyn Morris-Clapp, and Prof. Edward Lynch.

This research could not have been completed without appropriate material support for which I would like to thank all colleagues who taught on postgraduate courses and thereby contributed to the research.

At last but not the least, I would like to thank my parents for laying a good foundation for my life that lead me to greater achievement and emotional support, understanding and help at many difficult times.

I thank my ex-husband and his family members for offering selfless help for looking after my son.

Thanks also to my little darling Haibo, for your patience and perhaps understanding.

IN BRIEF

- The study looked at three different techniques to achieve a depth range of 0.4–0.6 mm consistently for veneer tooth reduction.
- The use of a small round bur to produce dimples as depth guides was found to be superior to two other tooth reduction techniques investigated; viz depth orientation grooves and free hand reduction.
- The results also showed inconsistent preparation depth even when depth gauging techniques, investigated in this study, were used. This was because either some of the depth guides themselves or the subsequent reduction of the tooth surface was inaccurate.
- Therefore, even when such depth gauging techniques are used, the clinician should employ great caution while finishing the tooth preparation. This is because, it is possible to over prepare while finishing the preparation even if the depth guides were accurate.

A study into the variations in the labial reduction of teeth prepared to receive porcelain veneers – a comparison of three clinical techniques

G. P. Cherukara,[1] K. G. Seymour,[2] D. Y. D. Samarawickrama[3] and L. Zou[4]

Objectives: Various techniques have been suggested to enable the operator to produce an even reduction of 0.5 mm of labial tooth enamel during preparation for a porcelain veneer. For example, in addition to the traditional free hand method, longitudinal or horizontal depth orientation grooves and the use of small round burs to produce dimples as depth guides have been suggested. However, there is no published data that compares how effective these techniques are at producing the 'ideal' veneer preparation. In this study three techniques were compared using the technique of co-ordinate metrology.

Method: A single operator using the above three techniques prepared 84 extracted teeth. Impressions of the prepared and unprepared teeth were scanned using a co-ordinate measuring machine (CMM). Measurements of maximum labial reduction along the mid-labial plane were taken and analysed.

Results: The study showed that among the three techniques studied the use of small round burs (D001-012), when used side on at an angle of 45° to the tooth surface to produce dimples as depth guides, resulted in the greatest frequency of tooth reductions closer to the 'ideal' depth chosen for this study, ie within the 0.4 mm – 0.6 mm range.

Conclusion: The study concluded that even after using techniques designed to produce consistent preparations, a single operator still produced preparations with considerable variation from the ideal. The study showed that among the three techniques compared the use of small round burs, when used side on at an angle of 45° to the tooth surface to produce dimples as depth guides, resulted in the greatest frequency of tooth reduction closer to the 'ideal' depth chosen for this study only, ie within the 0.4 mm – 0.6 mm range. It is stressed that this range may not be the ideal in all clinical situations.

It is commonly accepted that, to satisfy the biologic needs of the periodontium, the technical needs of the ceramist and the aesthetic demands of the patient, some form of tooth preparation, confined within the enamel, is mandatory for veneering a tooth.[1,2,3] Such a preparation should also provide a veneer with good cervical and proximal adaptation. Mechanical reduction of enamel prior to acid etching has also been shown to increase the resin retention.[4]

Considering the thickness of enamel on the labial surface of anterior teeth and the minimum thickness of porcelain required for safe technical and clinical handling, a reduction of 0.5 mm of enamel is considered acceptable. However, it is the authors' considered opinion that such a decision to reduce the labial surface of the tooth by 0.5 mm should only be taken after careful individual patient and tooth assessment, thereby allowing for any pre-existing tooth surface loss. Several techniques have been advocated to help in an even reduction of enamel to 0.5 mm in addition to the traditional free hand method. These include the use of longitudinal[5] or horizontal[6] depth orientation grooves, small round burs to produce dimples as depth gauges, specially designed depth gauge burs[7] (LVS-1 or LVS-2; Brasseler Laminate Veneer System Set 4151, Brasseler USA, Savannah, Ga.) and the use of plastic or putty indices. However, there is no published data that compares how effective these techniques are at producing the 'ideal' veneer preparation.

In spite of the advocation of the above techniques, many preparations fall outside the accepted guidelines.[8] One of the reasons for this could be that clinicians do not make use of the various techniques suggested.[8] However, we suspect that even if the suggested techniques and guidelines are followed, variations in tooth preparation result, as suggested by Nattress *et al.*[9] Therefore, the aim of this study was to investigate the variations in reduction of teeth prepared by a single operator to receive porcelain veneers using three commonly used techniques:

- vertical depth orientation grooves
- free hand preparation
- dimples

It is also an attempt to address the issue of how best to achieve the desired depth of reduction of the tooth surface for a veneer restoration. A 3-dimensional co-ordinate measuring machine, with laser scanning probe, was used to provide data.

MATERIALS AND METHODS

Eighty-four extracted human upper central incisor teeth stored in formol saline were used in this study. Teeth were cleaned of extraneous deposits and divided into three groups of 28 teeth

[1]*PhD Student, [2]Senior Lecturer, [3]Senior Lecturer/Honorary Consultant, [4] Dental Metrologist Department of adult oral health, Bart's and the London, Queen Mary's School of Medicine and Dentistry, London E1 2AD.
*Correspondence to: George Cherukara
Email: G.P.Cherukara@qmul.ac.uk

Refereed paper
Received 20.06.01; Accepted 14.11.01

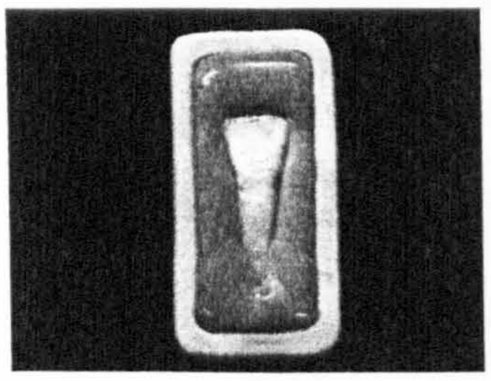

Figure 1 Labial impression of the tooth taken in an acrylic resin rectangular tray, with light-bodied polyvinyl silozane (blue coloured) impression material

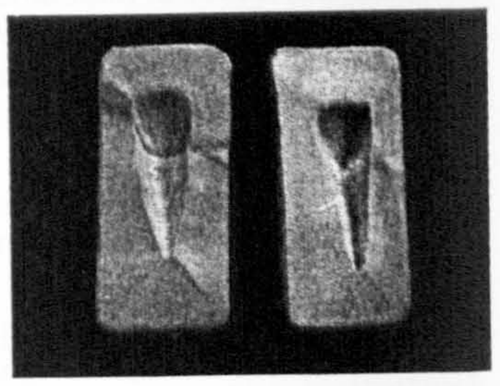

Figure 2 Pre- and post-preparation impressions ready to be scanned using CMM

each. Impressions of the labial surfaces of the crowns and roots of these teeth were taken in rectangular acrylic resin boxes, measuring 35 x 8 x 5 mm, using mid-blue, light-bodied polyvinyl siloxane impression material (Extrude, Kerr, Peterborough, UK), Figure 1. The teeth were mounted in dental plaster to provide better control during tooth preparation. A single operator (GPC) prepared teeth in each group, to receive porcelain veneers, using three different methods, namely: a) depth grooves, b) free hand and c) dimples.

a) In the first method, teeth were prepared by initially placing six vertical depth-orientation grooves on the labial surfaces, following the labial contour along the long axis of the tooth, with a straight fissure bur (R156-012). These depth grooves were eventually joined together with a chamfer finish bur (D198-022).
b) In the free hand technique, the labial surface was reduced using a chamfer finish bur (D198-022), arbitrarily to satisfy naked eye judgement of the preparation depth and quality.
c) With the third batch of teeth a small round bur (D001-012) was used, side on at an angle of 45° to the labial surface of the tooth, to make dimples on that surface. The dimples were made on the teeth in even rows to fill the entire labial surface. Then a chamfer bur (D198-022) was used to prepare the surface, 'joining-up' the dimples.

Once the teeth were prepared, impressions of the prepared teeth were taken as earlier (Fig 2). These impressions, made before and after tooth preparation, were scanned uni-directionally by a co-ordinate measuring machine (Merlin 11, International Metrology Systems, Livingstone, UK) using a non-contact 830 nm wavelength laser triangulation probe (Renishaw OP2, Renishaw, Gloucester, UK). The root surface area in the pre- and post-preparation impressions was used as the common area to superpose and plot the images constructed. The maximum reduction along the mid-labial plane was then calculated and recorded using the pre-loaded software (Direct Computer Control Software Package, International Metrology Systems, UK; and Data Analysis Software Package[10]) by subtraction of these images. This group has used the co-ordinate measuring machine (CMM) previously, in studies relating to tooth preparation quality, with some success.[11, 12, 13]

RESULTS

Data collected from the scans, of the mid-labial region of the three groups of 'pre- and post-preparation' impressions, are given in Tables 1, 2 and 3. An example of a relevant profile is shown in Figure 3.

The greatest depth along the mid labial plane was identified and measured. Preparations that were greater than 0.4 mm and less than 0.6 mm were considered as 'ideal' for the purposes of this study. A simple comparison (Table 4) of the three groups of data revealed that teeth prepared with the free hand and depth orientation groove techniques resulted in greater frequency of deviation of tooth surface reduction from the 'ideal' preparation range of 0.4 – 0.6 mm, as selected for this study. However, the use of dimples to prepare the labial surfaces resulted in greater frequency of preparations closer to this 'ideal'. Although the author was aware of the techniques used while measuring the depth, the metrologist who supervised was not aware of the technique or its significance. The decision regarding the deepest point of preparation was arrived on a consensual basis. Thus an attempt was made to avoid bias towards a technique at the measurement stage.

Analysis of variance (Table 5) also showed that there were statistically significant differences between the groups. However, the Bonferroni test (Table 6) revealed that this significant difference was only between group 1 and group 3.

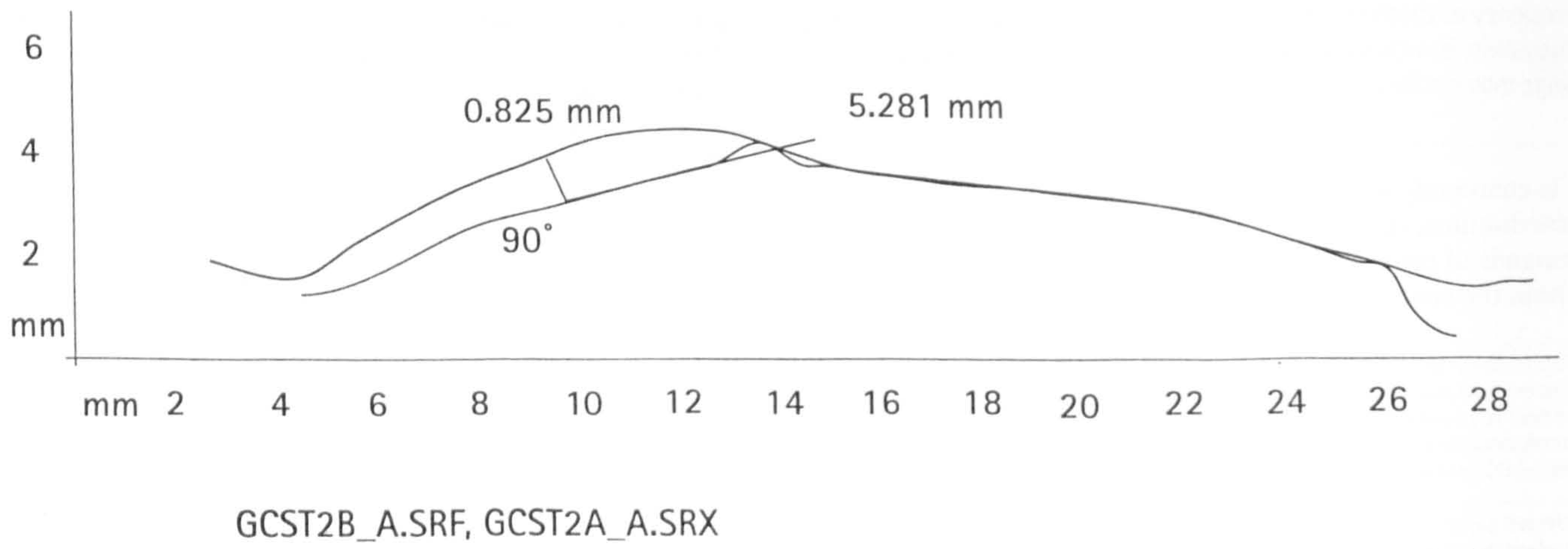

Figure 3 Mid-labial profile and method of measurement of tooth reduction (0.825 mm)

Table 1 Maximum mid-labial reduction of teeth prepared with depth orientation grooves.

Tooth	Mid-labial reduction (mm)
1	0.707
2	0.623
3	0.447
4	0.815
5	0.787
6	0.805
7	0.439
8	0.692
9	0.825
10	0.675
11	0.771
12	0.634
13	0.842
14	0.576
15	0.535
16	0.611
17	0.651
18	0.615
19	0.735
20	0.622
21	0.794
22	1.086
23	0.659
24	0.661
25	0.492
26	0.688
27	0.839
28	0.539
Mean	0.684
Standard Deviation	0.140
Range	0.647
Minimum	0.439
Maximum	1.086

Table 2 Maximum mid-labial reduction of teeth prepared with free hand

Tooth	Mid-labial reduction (mm)
1	0.382
2	0.488
3	0.453
4	0.805
5	0.439
6	0.692
7	0.825
8	0.675
9	0.675
10	0.675
11	1.281
12	0.633
13	0.485
14	0.542
15	0.621
16	0.619
17	0.467
18	0.769
19	0.402
20	0.792
21	0.503
22	0.667
23	0.948
24	0.508
25	0.672
26	0.918
27	0.488
28	0.615
Mean	0.644
Standard Deviation	0.196
Range	0.899
Minimum	0.382
Maximum	1.281

Table 3 Maximum mid-labial reduction of teeth prepared with dimples

Tooth	Mid-labial reduction (mm)
1	0.638
2	0.443
3	0.375
4	0.446
5	0.568
6	0.588
7	0.723
8	*0.413*
9	0.483
10	0.489
11	0.590
12	0.569
13	0.581
14	0.489
15	0.460
16	0.468
17	0.692
18	0.499
19	0.522
20	0.498
21	0.599
22	0.545
23	0.482
24	0.538
25	0.600
26	1.345
27	0.423
28	0.478
Mean	0.555
Standard Deviation	0.175
Range	0.97
Minimum	0.375
Maximum	1.345

DISCUSSION

Upper central incisors with no restorations on the labial aspect of the crown, were chosen for the study as they are the teeth most commonly restored with porcelain veneers,[8, 14] and previous studies on tooth preparation for veneers have also used these teeth.[8, 9] These teeth also have a large, flatter labio-lingual width, as it was thought that the tooth preparation would be affected by teeth with smaller labio-lingual width or greater curvatures of the labial surface ie lower incisors, canines and premolars. The use of non-carious, unrestored teeth prevented the size and sites of disease or restorations from influencing the preparations carried out. Further, these teeth were set in an arch form of dental plaster, as suggested by the work of Seymour.[12] In his study he concluded that having teeth set in an arch form gave the operators a closer representation of the spatial relationships present in the mouth. To reduce inter-operator variability,[9] only a single operator performed the tooth preparations.

As reported in earlier studies[11,12,13] the co-ordinate measuring machine provided data in a very graphic form, with the benefit of reproducibility. A reproducibility of 0.007 mm has been reported after repeated measurements of this type in previous studies.[12]

All previous studies using the CMM[11,12,13] have held the impression material in 8 x 8 mm brass square tubes. The use of rigid acrylic trays of larger dimensions in this study allowed for a larger region of the tooth to be scanned so that an adequate area was available to superpose the pre- and post-preparation images. An impression surface of mid-blue polyvinyl siloxane gave greater accuracy than other materials and colours while using the CMM.[11,13]

The CMM's analytical[12] software allowed measurement of distance in mm to three decimal places (1 µm). Hence data have been quoted at that level. The preloaded software (DCC, International Metrology Systems, UK, and Data Analysis Software Package)[10] identified the mid-labial plane. Scanning of the impressions were done uni-directionally, as bi-directional scanning introduces distortion to the final image giving errors in measurement.[12] Furthermore, the triangulation probe used in this study was of a non-contact type, so the technique was non-destructive. The pre- and post-preparation scans were superposed to analyse the preparation. Superpose is defined as 'to bring into the same position as to coincide' and implies a more mathematically precise overlaying of images than superimpose which is defined as 'to lay above or on top of'.[15,16]

In this study 0.4 mm – 0.6 mm was chosen as the ideal preparation range to meet the practicality of the study. Therefore, preparations falling within this range were considered acceptable during data analysis. However, there is strong support in the literature for

Table 4 Percentage of preparations within the 0.4 – 0.6 mm range.

Technique of preparation	%
Depth groove	21.428
Free hand	35.714
Dimple	82.142

Table 5 Analysis of variance

Source	D.F.	Sum of Squares	Mean Squares	F Ratio	F Prob.
Between Groups	2	0.2453	0.1226	4.1508	0.0192
Within Groups	81	2.3934	0.0295		
Total	83	2.6387			

Table 6 Modified LSD (Bonferroni) est. with significance level 0.05

Mean	Group	Grp 3	Grp 2	Grp 1
0.5551	Grp 3			
0.6442	Grp 2			
0.6845	Grp 1	*		

0.5 mm intra-enamel reduction clinically. This may be refuted by the finding of Ferrari *et al*,[17] who reported that the mean thickness of enamel 2 mm incisal to the cemento-enamel junction of a central incisor was 0.4 mm, hence a preparation 0.5 mm may not be confined entirely to the enamel. Such a finding should lead us to review the present guidelines for tooth preparation for porcelain veneers.

The results of the study showed that despite there being a single operator there was variability in consistency of preparation depth, even within the same group. Neither was consistent labial reduction achieved, despite the various methods used. Free hand tooth preparations showed the greatest variability. However, it was clear that the use of dimples as depth guides produced more preparations within the 0.4 – 0.6 mm range. Hence it appeared to be a more consistent technique. The reason for this consistency may lie in the fact that the shank of the small round bur provides a definite stop when used side on at 45° to the tooth surface while placing the dimples on the tooth surface. Therefore, the placement of dimples improved the accuracy of the depth guides, which helps in the accurate reduction of the tooth surface. This limiting action of the shank of the bur was not noticed with the chamfer finish bur or the straight fissure bur. Hence the inaccuracy and variation, compounded by visual perception of the depth of preparation[18] might have resulted. In addition, the consistency observed with the dimple method might have resulted from the fact that more of these dimples, were placed across the face of the labial surface of the tooth to fill the area. In the case of depth orientation grooves a maximum of only six groves were placed on the labial surface.

It was interesting to note that in each technique there was an out-lying measurement. It was not clear as to why this happened. It may be that whichever technique a clinician used, there is a possibility that things could go grossly wrong. Hence, one cannot blindly depend on any particular technique, rather give attention to detail at every step of tooth preparation. It is intriguing that the highest of these out-liers was in the dimple technique, which was otherwise the preferred technique of the three.

The difference identified between groups two and three in Table 4 was not found to be statistically significant at the 95% confidence interval as demonstrated by the Bonferroni test, possibly because of a type 2 error. This outcome could be used to highlight the need for a judicious sample size selection rather than the selection of an arbitrary number. Similar studies have used a sample size of ten, often for convenience.

It was surprising that although various techniques have been advocated to aid tooth preparation, no attempts to compare them have been made in the literature at the time of this study. The consequences of inappropriate tooth reduction for veneers are:

1. Dentine exposure leading to dentine sensitivity and a susceptible bond to dentine.
2. An over-countered restoration leading to periodontal and aesthetic complications.
3. Technical difficulty in placing the margins of the veneer without adequate tooth preparation.
4. Absence of definite seating landmarks making proper seating of the veneer on the tooth surface for luting difficult.

CONCLUSIONS

It could be concluded from this study that, of the three techniques examined, the use of dimples as depth orientation resulted in achieving the theoretical ideal of 0.5 mm reduction of enamel, although a range of 0.4–0.6 mm was considered acceptable for this study, more often than the other two techniques tested. It can also be concluded that variation in tooth preparation results even when widely advocated guidelines and techniques are followed. The clinician should bear in mind this possibility and the consequences of this variability when preparing teeth to receive porcelain veneers.

Additionally, the fact that an enamel reduction of 0.5 mm may, in any case, expose dentine points us in the direction of a review of the present guidelines for tooth reduction for porcelain veneers.

1 Garber D A. Porcelain laminate veneers - to prepare or not to prepare? *Compend Contin Educ Dent* 1991; **12**: 178-181.

2 Garber D A. Porcelain laminate veneers: ten years later. Part 1. Tooth preparation. *J Esthet Dent* 1993; **5**: 56-62.

3 Garber D A, Goldstein R E, Feinman R A. *Porcelain laminate veneers.*; Quintessence Publishing Co. Chicago, 1988.

4 Jordan R E, Zuzuki M, Gwinnetta J, Hunter J. K. Restorations of fractured and hypoplastic incisors by the acid etch resin technique: *A* three year report. *J Am Dent Assoc* 1977; **95**: 795-803.

5 Miller B J. Porcelain veneers. *Dental Update* 1987; **14**: 381-390.

6 Weinberg L A. Tooth preparation for Porcelain veneers. *New York State Dent J* 1989; **55**: 25-28.

7 Sheets G, Taniguchi. Advantages and limitations in the use of porcelain veneer restorations. *J Prosthet Dent* 1990; **64**: 406-411.

8 Brunion P A, Rihmond S, Wilson N H F. Variation in the depth of preparation for porcelain laminate veneers. *Euro J Prosthodont Rest Dent* 1997; **5**: 89-92.

9 Natttess B R, Youngson C C, Patterson C J W *et al. An in vitro* assessment of tooth preparation for porcelain veneer restorations. *J Dent* 1995; **23**: 165-170.

10 Jovanovski V, Lynch E. *Analysis of the morphology of oral structures from 3-D co-ordinate data.* PhD thesis, University of London, 1998.

11 Seymour K, Samarawickrama D, Zou L, Lynch E. Shoulder dimensions and angles of bonded crown preparations. *J Dent Res* 1995; **74**: 553, Abst 1219.

12 Seymour K G. *Variations in the labial 'shoulder' geometry of teeth prepared to receive metal ceramic crowns.* PhD thesis, University of London, 1998.

13 Lynch E, Zou L, Bedford J, Jovanovski V, Burke F. Measurement of lesions of primary root caries. *J Dent Res* 1993; **72**: 742, Abst 447.

14 Pincus C R. Building mouth personality. *J Calif State Dent Assoc* 1938; **14**: 125-129.

15 Jovanovski V, Zou L, Bedford J, Lynch E. Geometric superimposition of a sequence of digitised replicas. *J Dent Res* 1993; **72**: 742, Abst 446.

16 Little W, Fowler H. W, Coulson J. *The shorter oxford dictionary.* 3rd ed. Oxford: Clarendon press, 1978.

17 Ferrari M, Patroni S, Balleri P. Measurement of enamel thickness in relation to reduction for etched laminate veneers. *Int J Periodont Rest Dent* 1992; **23**: 407-413.

18 Dunne S M. The limitation of visual perception in restorative dentistry. *Dental Update* 1993; **20**: 198-205.

International Journal of Paediatric Dentistry 2001; **11**: 333–339

Tooth size and morphology in twins

M. KABBAN[1], J. FEARNE[1], V. JOVANOVSKI[2] & L. ZOU[2]

[1]*Department of Paediatric Dentistry and* [2]*Department of Adult Oral Health, St Bartholomew's and The Royal London School of Medicine and Dentistry, Turner Street, London, UK*

Summary. *Objective.* To assess concordance of tooth size and occlusal morphology in monozygotic (identical) and dizygotic (non-identical) twins compared to unrelated controls in order to determine how much these dental traits are related to inheritance. *Methods.* Mesiodistal and bucco-lingual dimensions of tooth size in 34 pairs of twins were measured with dial callipers. In addition, the occlusal morphology of nine pairs of teeth was assessed using a co-ordinate measuring machine with a non-contact laser probe. *Results.* The results showed greater concordance in tooth size for both mesiodistal and bucco-lingual dimensions within twin pairs compared to twin and unrelated controls. Furthermore, monozygotic (MZ) twins showed greater concordance than dizygotic (DZ) twins for all permanent teeth with statistically significant variance for the mesiodistal dimension ($P = 0{\cdot}01$) but not bucco-lingual dimension.

Superimposed computer models of the digitized occlusal surfaces showed a high degree of similarity for MZ twins compared to DZ twins. The mean intrapair deviation was 147 μm for MZ, 209 μm for DZ and 258 μm for unrelated controls.

Conclusions. The remarkable similarity in the tooth size and morphology of monozygotic twins suggests a strong inheritability factor to tooth size and shape and that these may be useful as additional tools for zygosity determination along with other dental traits.

Introduction

The use of twins in genetic research is well recognized. Comparisons of physical features within monozygotic (MZ) and dizygotic (DZ) twin pairs can provide valuable insights into the relative contributions of genetic and environmental influences. DZ twins are expected to show about the same intrapair variability as siblings, whereas the differences between MZ twins are usually of similar magnitude to the minor left–right differences often noted in singletons. It has been suggested that 'normal' variation in tooth size is the result of multifactorial inheritance with both genetic and environmental factors being important [1].

The aim of the study was to compare mesio-distal and bucco-lingual tooth dimensions in MZ and DZ twin pairs, to investigate the influence of inheritance for this dental trait. In addition similarities of occlusal shape were investigated.

Correspondence: M. Kabban, South-west London Community NHS Trust, c/o Dental Department, Shotfield Health Centre, Wallington, Surrey SM6 OH7, UK. Tel.: +44 (0)20 8647 0031 ext. 155, Fax: +44 (0)20 8647 2934, E-mail: mariellekabban@yahoo.co.uk

Methods

Ethical approval for the study was obtained from the Hammersmith and Queen Charlotte's and Chelsea Hospitals. Written consent was obtained from the parents of all children prior to examination.

The study group consisted of twins attending the Multiple Births Foundation clinics at Queen Charlotte's Hospital, local twins clubs and twins attending the Royal London Hospital Dental Institute for routine dental care between November 1995 and May 1997. In addition, healthy non-related individuals were matched to each twin pair for age, sex and race.

After obtaining consent, details were recorded of: name, date, hospital, date of birth, sex and zygosity. Race was defined as white Caucasian, Afro-Caribbean,

Asian or mixed race. The order of birth within a twin pair, the birthweight of the twins and any relevant medical history were also noted.

The clinical examination was conducted in a standardized, systematic manner with the child upright in a chair. The following observations were charted: teeth present, clinically visible caries, restorations and any dental anomalies. Upper and lower alginate impressions were taken.

To standardize the dental models as much as possible, all impressions were cast in hard stone on the following day. Impressions from one pair of twins were always cast together. Two different measurement methods were used:

1 Conventional hand measurements of the mesiodistal and bucco-lingual tooth dimension as described by Moorrees *et al.* [2] and used in previous studies.

2 Three-dimensional co-ordinate metrology, using a non-contact laser probe, for occlusal morphology.

Conventional hand measurements

Measurements were carried out under the same uniform external illumination with the dental casts placed on a flat surface. The teeth were always measured in the same order: upper left to upper right and lower left to lower right.

The mesiodistal and buccolingual dimensions were measured using automated dial callipers (Mitutoyo) accurate to 0·05 mm. The callipers had sharpened beaks to facilitate approximal access. The mesiodistal dimension was recorded as the greatest mesiodistal dimension of the tooth crown parallel to the occlusal and labial surface, and the buccolingual dimension as the maximum crown dimension at right angles to the mesiodistal dimension. Each tooth was measured on two separate occasions and the mean of the measurements used to improve accuracy. If a discrepancy of greater than 0·4 mm occurred between the two measurements, the results were discarded and the tooth re-measured twice more. Teeth with caries, or with a restoration involving the mesial or distal surface, or a tooth with a defect on the model were excluded from the study.

The precision of measurement of the operator was tested using double determination. Upper and lower casts from five patients were randomly selected and measured (as above) on two separate occasions, 3 weeks apart to check intra-examiner reproducibility, and by a second examiner to test inter-examiner reproducibility.

Three-dimensional co-ordinate metrology

The occlusal surfaces of nine upper first permanent molars were digitized with a co-ordinate measuring machine (CMM) and compared using a system for co-ordinate data analysis [3,4].

Impressions of the occlusal surfaces were taken from the dental casts using a medium body silicone (Kerr Extrude, SDS Kerr, Orange, CA, USA) in a specially constructed rectangular brass mould. The replicas were trimmed to remove undercuts, the presence of which would occlude regions of interest, and powdered with pyrolytic silica to optimize their reflectivity with respect to the laser positioning detector. Impressions from dental casts could introduce replication error but are sufficiently accurate for the comparisons in this study.

The replicas were digitized by a Merlin Mk II 750 CMM (International Metrology Systems Ltd, Livingstone, UK) fitted with an OP2 triangulation laser probe (Renishaw plc, Wotton-under-Edge, UK). The data set obtained for each replica consisted of approximately 10 000 3-D points spaced at 100 µm intervals in x and y and accurate to 5 µm in z. The occlusal surface was mathematically reconstructed from these points by interpolating them with a bicubic spline surface.

Pairs of occlusal surfaces were superimposed to find their 'best fit' using a least-squares technique. Their similarity was then quantified by evaluating the differences in their z co-ordinates at 10 000 locations and computing the root mean square (RMS) of those differences. Thus, the resulting values represented the standard deviation between superposed surface pairs.

Mirror imaging

To test whether co-twins in MZ twin pairs were each other's mirror image, the teeth on the left side of one twin were compared with those on the right side of the other twin, and vice versa for the teeth on the right side of the first twin and the teeth on the left side of the second twin.

Tooth size in MZ twins was considered to be a mirror image when the difference in tooth dimensions between the left side of one twin and the right side of the other twin ($L_1 - R_2$) were less than the same side difference between them ($L_1 - L_2$) and ($R_1 - R_2$) and vice versa [5].

No mirror-image effect was observed in the 22 pairs of MZ twins, i.e. there was no evidence that one side

of one twin was more concordant with the opposite side of the co-twin. Therefore, for the analysis of individual teeth, left and right teeth were combined and their mean used.

Statistical analysis

Statistical analysis was carried out using the Stata Statistical Software program [6].

To test for the presence of a measurable component of genetic variability, left and right teeth were combined, and comparisons were made of the square of the differences between the two members of MZ twin pairs and the squares of the differences between the two members of DZ twin pairs for both mesiodistal and bucco-lingual dimensions. This is equivalent to a comparison of variances when the expected mean difference between twin pairs is zero.

An *F*-test was used to determine significance.

Results

Examiner reproducibility

Scatterplots were drawn for the mesiodistal and bucco-lingual measurements of all teeth to look for any systematic error. The difference between the first and second measurements plotted against the overall mean of the two measurements showed that, in general, the differences tended to be fairly evenly scattered around a line approximately at 0. Intra-examiner results were less scattered than inter-examiner results.

The mean, standard deviation and range of differences for both intra- and inter-examiner measurements again showed intra-examiner reproducibility to be less variable than inter-examiner reproducibility. The least variation was seen in the intra-examiner results for the bucco-lingual of the lower first and second premolars (SD = 0·02 and 0·03, respectively) and the greatest variation for the bucco-lingual of the lower permanent canine between the two examiners (SD = 0·18).

Demographic details

The final study sample consisted of 34 twin pairs; 22 pairs of MZ twins –12 female and 10 male – and 12 pairs of DZ twins –3 female, 5 male and 4 opposite sexed. The mean age of the group as a whole was 13·1 years, with a mean age of 10·5 for MZ and 15·5 years for DZ. There were 27 white Caucasuan pairs, 2 Asian, 1 Afro-Caribbean and 4 pairs of mixed race.

Hand measurements of tooth size

Measurements of all primary and permanent teeth were analysed. The square of the difference in mesiodistal and bucco-lingual dimensions between one twin and its co-twin and one twin and its matched control were compared (all teeth combined).

A statistically significant result was found in all cases, with twins showing more concordance in tooth dimensions within a twin pair than between a twin and an unrelated matched control (Table 1).

The effect of zygosity was then investigated by comparing the difference in mesiodistal and bucco-lingual dimensions between one twin and its co-twin in MZ pairs and between twins of a DZ pair. The difference was significantly smaller in MZ than DZ for mesiodistal but not the bucco-lingual dimension (Table 2).

Measurements of primary teeth were not analysed, as the comparable number of teeth in each category was considered too small.

A comparison was then made of the variances of dental concordance in MZ and DZ twins for

Table 1. The square of the difference in tooth size between one twin and its co-twin and between one twin and a matched unrelated control.

		Mean	SD	*N*	*P*
Permanent teeth					
Twins	M-D	0·16	0·29	291	
Controls	M-D	0·73	1·43		< 0·001
Twins	B-L	0·35	0·93	294	
Controls	B-L	1·13	2·17		< 0·001
Deciduous teeth					
Twins	M-D	0·08	0·16	127	
Controls	M-D	0·33	0·42		< 0·001
Twins	B-L	0·09	0·16	149	
Controls	B-L	0·28	0·38		< 0·001

M-D = Mesiodistal measurement B-L = Bucco-lingual measurement.
N = Number of teeth comparable.

Table 2. Comparison of dental concordancein monozygotic and dizygotic twins for all permanent teeth.

		Mean	SD	*N* (twin pairs)	*P*
MZ	M-D	0·02	0·06	22	
DZ	M-D	0·10	0·11	12	0·01
MZ	B-L	0·07	0·11	21	
DZ	B-L	0·15	0·14	12	0·23

M-D = Mesiodistal measurement, B-L = Bucco-lingual measurement.

Table 3. Comparison of estimated variances of dental concordance in monozygotic and dizygotic twins for individual teeth (left and right combined).

	Mesiodistal dimension			Bucco-lingual dimension		
	Mean*	*N* (teeth)	*P*†	Mean*	*N* (teeth)	*P*†
Upper I						
MZ	0·02	10		0·30	12	
DZ	0·20	7	< 0·05	0·41	8	NS
Upper M						
MZ	0·14	12		0·05	15	
DZ	0·08	6	NS	0·39	6	< 0·05
Lower I						
MZ	0·03	15		0·16	8	
DZ	0·06	5	NS	0·29	5	NS
Lower M						
MZ	0·10	10		0·02	17	
DZ	0·25	4	NS	0·71	7	< 0·05

I = Permanent central incisor, M = First permanent molar.
NS = Not significant, *Mean of (1st twin − 2nd twin)².
† = *P*-value from *F*-test.

individual teeth. The square of the difference in mesiodistal and bucco-lingual dimensions between one twin and its co-twin in MZ pairs and one twin and its co-twin in DZ pairs were compared for the upper and lower first permanent molars and the upper and lower permanent central incisors. The measurements for other teeth were not compared, as the number of comparable teeth between twins was judged to be too small.

The test of significance used for the ratio of the mean of the squares of the differences was an *F*-test using the assumption that in the population the mean difference in tooth size for pairs of twins is zero.

Only three teeth showed evidence for significantly greater concordance in MZ than in DZ co-twins. These were the upper central incisor for the mesiodistal dimension, and the upper and lower first molar for the bucco-lingual dimension. In all but one tooth (the upper molar for the mesiodistal dimension) there seemed to be greater concordance in MZ than DZ twin pairs, but this did not reach statistical significance (Table 3).

Results obtained with co-ordinate metrology

Figure 1 shows selected cross-sections through pairs of superposed surfaces. The visually evident differences in similarity between the three categories (MZ, DZ and controls) were confirmed by the computed RMS differences, which ranged from 126 μm to 168 μm for MZ twins, 162 μm to 277 μm for DZ twins and 209 μm to 366 μm for controls. Full results are given in Table 4.

Table 4. Difference between pairs of tooth surfaces for upper first permanent molars after least-squares surface fitting.

		Difference (μm)	Mean difference (μm)	SD
MZ twins				
Pair 1	Right side	162		
	Left side	126		
Pair 2	Right side	128		
	Left side	168		
Pair 3	Right side	149		
	Left side	146		
			147	17
DZ twins				
Pair 1	Right side	162		
	Left side	194		
Pair 2	Right side	188		
	Left side	219		
Pair 3	Right side	217		
	Left side	170		
Pair 4	Right side	243		
	Left side	277		
			209	38
Unrelated controls				
Pair 1	Right side	276		
	Left side	336		
Pair 2	Right side	209		
	Left side	211		
			258	61

These results showed a definite trend of increasing inter-surface difference, with the smallest differences seen in the MZ pairs and the largest differences in the controls. An *F*-test was used on the standard

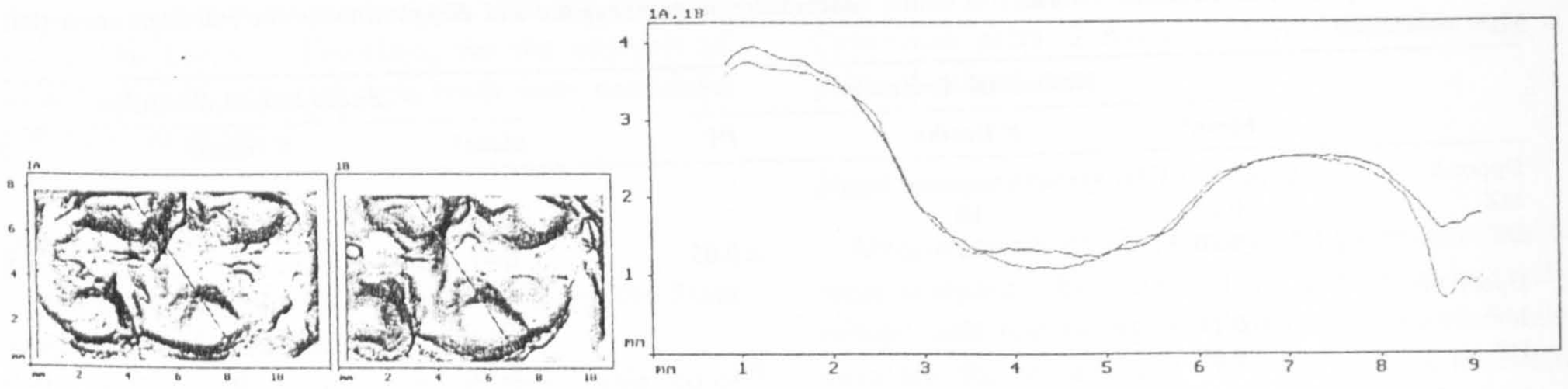

Fig. 1. Cross-sections from each of the three categories.

deviation of the mean differences for each category to determine their significance. A statistically significant result was found only when comparing the standard deviation of the MZ group with that of the control group.

Discussion

The finding of greater dental concordance within twin pairs compared to matched unrelated controls suggests that tooth size is largely inherited.

Between the DZ and MZ twin pairs there was greater concordance in MZ twins compared to DZ twins for mesio-distal dimension ($P = 0{\cdot}01$). However, this was not significant for the bucco-lingual dimension.

This finding might indicate that the two dimensions are under different control mechanisms, with environmental influences on bucco-lingual dimensions exceeding those on mesiodistal dimensions as found by Townsend and Brown [7].

When dental concordance in individual teeth was compared between DZ co-twins and MZ twins, the findings were less marked. Although the MZ co-twins showed closer dental dimensions, this did not always reach significance. One reason for this may be that the final number of comparable teeth was small and that larger numbers are needed for significance. However, one must also consider that studies have suggested that DZ twins may be more alike than siblings as, unless reared apart, they share the same environment pre- and postnatally. Therefore,

the difference in tooth size between DZ co-twins may also be less than expected. This has also been suggested in the work of Sharma *et al.* [8] in their study of dental dimensions of Punjabi twins.

The greater concordance when all teeth are combined compared to individual teeth is difficult to explain. Mirror imaging was eliminated as a cause; however, compensatory developmental interactions as found by Bishara and Jakbosen [9] might be considered.

The lack of mirror-imaging effect found in this study in the teeth of MZ twins is in agreement with Potter and Nance's study of dental dimensions and mirror imaging [10], which found no indication that MZ twinning was associated with an increased degree of mirror imagery.

Although Fearne *et al.* [11] demonstrated a prenatal influence of birthweight on tooth size in the primary dentition, it was difficult to demonstrate this effect on the permanent first molars and incisors in this study. There was a statistically significant effect on the mesiodistal dimension of the lower first permanent molar, but not on any other tooth analysed. Larger numbers would be needed to test this further.

This study suggests that there is a trend for greater concordance in dental dimensions between MZ co-twins compared to DZ co-twins but that the lack of a strong significance means that tooth size measurements on their own cannot be considered sufficient in determining twin zygosity. They may, however, be useful as an additional diagnostic tool in conjunction with other dental traits such as tooth eruption [12] and occlusal morphology [13,14].

The initial findings obtained by 3-D co-ordinate data analysis are promising and confirm greater concordance in MZ twins.

Summary

Greater concordance in tooth size within twins compared to between twins and unrelated controls, and between MZ co-twins compared DZ co-twins suggests that tooth size determination has a strong genetic component, but that environmental factors may also be important. Conventional hand measurements of tooth size are easy to carry out on large numbers and may be a useful adjunct to twin zygosity determination in conjunction with other dental traits, but are not sufficient alone.

Co-ordinate data analysis of digitized replicas yields more accurate results and presents a promising research tool, but requires greater resources and access to specialized equipment.

Résumé. *Objectif.* Evaluer la concordance de la taille des dents et de la morphologie occlusale chez des jumeaux monozygotes (identiques) et dizygotes (non-identiques) comparées à des témoins sans lien familial, afin de déterminer à quel point ces caractéristiques dentaires sont liées à la transmission.
Méthodes. Les dimensions dentaires mésio-distales et vestibulo-linguales ont été mesurées à l'aide compas à cadrans chez 34 paires de jumeaux. De plus, la morphologie occlusale a été évaluée chez neuf paires de dents à l'aide d'un instrument de mesure coordonné avec une sonde laser.
Résultats. Les résultats ont montré une plus grande concordance, à l'intérieur des paires de jumeaux, dans la taille des dents pour les deux dimensions mésio-distale et vestibulo-linguale, comparé au jumeau et aux témoins. De plus, les jumeaux monozygotes (MZ) ont montré une plus grande concordance que les dizygotes (DZ) pour toutes les dents permanentes avec une variance statistiquement significative pour la dimension mésio-distale ($p = 0{,}01$), mais pas pour la dimension vestibulo-linguale.

Des modèles numérisés superposés des surfaces occlusales ont montré un haut niveau de similarité pour les jumeaux MZ par rapport aux jumeaux DZ. La déviation moyenne intra-paire était de 147 µm pour les MZ, 209 µm pour les DZ et 258 µm pour les témoins sans lien.
Conclusions. La remarquable similarité de la taille et de la morphologie chez les jumeaux monozygotes suggère un facteur transmission fort pour la taille et la forme dentaire et que cela pourrait être utile en tant qu'outil supplémentaire de détermination de zygosité parmi d'autres critères.

Zusammenfassung. *Ziele.* Das Ermitteln der Konkordanz der Zahnform und der okklusalen Morphologie bei monozygoten (eieiigen) und dizygoten (zweieiigen) Zwillingen und Vergleich zu nicht-verwandten Kontrollen mit dem Ziel den Einfluß von Erbfaktoren auf diese Zahneigenschaften zu ermitteln.
Methoden. Die mesio-distale und die bucco-linguale Ausdehnung der Zähne wurde gemessen mit dial callipers. Zusätzlich wurde die okklusale Morphologie von neun Zahnpaaren mit einer berührungsfreien Laserapparatur dreidimensional vermessen.
Ergebnisse. Die Resultate zeigten eine größere Konkordanz der Zahngröße sowohl für die mesio-distalen

als auch bucco-lingualen Ausdehnungen bei den ein- und zweieiigen Zwillingen im Vergleich zu den Kontrollen. Außerdem zeigten die monozygoten Zwillingen eine statistisch signifikant höhere Konkordanz im Vergleich zu dizygoten Zwillingen in der mesio-distalen Ausdehnung ($p = 0.01$), nicht aber in der bukko-lingualen.

Die übereinanderprojezierten Computermodelle der Okklusaloberflächen zeigte ein hohes Maß an Übereinstimmung für die monozygoten Zwillinge im Vergleich zu den dizygoten Zwillingen. Die mittlere Abweichung zwischen denZahnpaaren betrug 147 µm bei den monozygoten Zwillingen, 209 µm bei den dizygoten und 258 µm bei den nicht verwandten Kontrollen.

Schlußfolgerungen. Die bemerkenswerte Übereinstimmung hinsichtlich Zahngröße und Zahnform bei den monozygoten Zwillingen weist auf starke Eerbeinflüsse hin. Die genannten Parameter könnten zusammen mit anderen Zahnmedizinischen Befunden nützliche zusätzliche Werkzeuge darstellen für die Untersuchung der Frage, ob Zwillinge eineiig oder zweieiig sind.

Resumen. *Objetivos.* Analizar la concordancia en el tamaño y morfología oclusal de dientes de gemelos monocigotos (idénticos) y dicigotos (no idénticos) comparados con grupos control para determinar el grado de relación de estas características con la herencia.
Métodos. Se midieron las dimensiones mesiodistales y vestíbulolinguales de los dientes de 34 pares de gemelos usando unos calibradores de cuadrantes. Además se analizó la morfología oclusal de nueve pares de dientes usando una máquina de medidas coordinada con una sonda láser sin contacto.
Resultados. Los resultados mostraron una gran concordancia en el tamaño de los dientes tanto mesiodistal como vestíbulolingual entre los pares de gemelos comparados con gemelos y otro grupo control no relacionado. Además, los gemelos monocigotos (MZ) mostraron mayor concordancia que los gemelos dicigotos (DZ) para todos los dientes permanentes con una varianza estadística significativa para la dimensión mesiodistal ($p = 0{,}01$) pero no para la dimensión bucolingual. Los modelos computarizados superpuestos de las superficies oclusales digitalizadas mostraron un alto grado de similitud para los gemelos MZ comparados con los gemelos DZ. La desviación media entre parejas fue de 147 µm para MZ, 209 µm para DZ y 258 µm para los controles no relacionados.
Conclusiones. La similitud notable en el tamaño de los dientes y en su morfología en los gemelos monocigotos sugiere un factor fuerte de herencia en el tamaño y forma de los dientes y que esto podría ser útil como herramienta adicional para la determinación zigótica junto con otras características dentales.

References

1 Bailit HL. Dental variation among populations. An anthropologic view. *Dental Clinics of North America* 1975; **19**: 125–139.
2 Moorrees CFA, Thomsen SO, Jensen E, Yen PK. Mesiodistal crown diameters of deciduous and permanent teeth. *Journal of Dental Research* 1957; **36**: 39–47.
3 Jovanovski V, Zou L, Tay WM, Lynch E, Cox MG. Assessment of three-dimensional structures in clinical dentistry. In: Ciarlini P, Cox MG, Pavese F, and Richter D. *Advanced Mathematical Tools in Metrology III*. Singapore: World Scientific, 1997; 263–265.
4 Jovanovski V, Lynch E. Analysis of the morphology of oral structures from 3-D co-ordinate data. In: *Monographs in Oral Science*, Vol. 17: *Diagnostic Techniques and Validation Criteria for Assessing Oral Health*. Basel: S. Karger AG, 2000; 73–129.
5 Pelsmaekers B, Loos R, Carels C, Derom C, Vlietinck R. The genetic contribution to dental maturation. *Journal of Dental Research* 1997; **76**: 1337–1340.
6 Stata Corporation. *Stata Statistical Software Release 4·0* College Station, Texas: Stata Corporation, 1995.
7 Townsend GC, Brown T. Heritability of permanent tooth size. *American Journal of Physical Anthropology* 1978; **49**: 497–504.
8 Sharma K, Corruccini RS, Henderson AM. Genetic variance in dental dimensions of Punjabi twins. *Journal of Dental Research* 1985; **64**: 1389–1391.
9 Bishara SE, Jakobsen JR. Compensatory developmental interactions in the size of permanent teeth in three contemporary populations. *Angle Orthodontist* 1989; **59**: 107–111.
10 Potter RH, Nance WE. A twin study of dental dimensions. Discordance, asymmetry and mirror image. *American Journal of Physical Anthropology* 1976; **44**: 391–396.
11 Fearne JM, Brook AH. Small primary tooth crown size in low birthweight children. *Early Human Development* 1993; **33**: 81–90.
12 Marenah F. A study of tooth eruption in twins. MSc Thesis, London University, 1993.
13 Lundström A. Tooth morphology as a basis for distinguishing monozygotic and dizygotic twins. *American Journal of Human Genetics* 1963; **15**: 34–43.
14 Townsend GC, Richards LC, Brown R, Burgess VB. Twin zygosity determination on the basis of dental morphology. *Journal of Forensic Odonto-Stomatology* 1988; **6**: 1–15.

J Clin Periodontol 1999; 26: 692–697
Printed in Denmark . All rights reserved

JOURNAL OF Clinical Periodontology
ISSN 0303-6979

Quantification of root surface plaque using a new 3-D laser scanning method

S. Yeganeh, E. Lynch, V. Jovanovski and L. Zou

Department of Conservative Dentistry, St Bartholomew's and The Royal London School of Medicine and Dentistry, Queen Mary and Westfield College, London E1 2AD, UK

Yeganeh S, Lynch E, Jovanovski V, Zou L: Quantification of root surface plaque using a new 3-D laser scanning method. J Clin Periodontol 1999; 26: 692–697.

Abstract. There are no published reports in the literature objectively quantifying thickness of plaque on teeth. The aim of this study was to quantify plaque on a tooth surface and assess if this quantification correlates with a clinical index of plaque from each of 51 patients. Patients were instructed not to perform any oral hygiene on the day of the assessment. The Silness and Löe plaque index was scored and replicas were scanned using a co-ordinate measuring machine (CMM) and laser scanning probe. A replica was obtained from this surface before and after toothbrushing. Plaque adjacent to the gingival margin had a mean thickness of 0.106±0.118 mm (mean±SD) whilst mean plaque thickness 250 μm from the gingival margin was 0.053±0.052 mm (mean±SD). There was a significant correlation between the plaque index and the plaque thickness ($p \leq 0.002$). The finding that plaque is present in the greatest amount adjacent to the gingival margin supports a previously reported hypothesis that primary root carious lesions (PRCL's) may initiate adjacent to the gingival margin. This method quantifies plaque thickness on exposed root surfaces which correlates with the plaque index as well as illustrating how the morphological characteristics of teeth, gingivae and plaque can be studied in vivo from replicas recorded.

Key words: plaque, plaque thickness; 3-D, aetiology of root caries

Accepted for publication 25 January 1999

There have been many methods to measure or quantify plaque in the literature. Epidemiological information on oral health is usually presented using indices, which numerically express the amount and distribution of dental plaque. The simpler indices indicate whether a criterion is present or absent. Green & Vermilion (1960), Quigley & Hein (1962) and Turesky et al. (1970) measured plaque by assessing tooth coverage. The indices used an estimated area of the tooth covered by plaque. Other methods, such as the modified Navy plaque index described by Elliott et al. (1972) identify the presence or absence of plaque, usually visualised by a disclosing dye in up to 9 zones.

Another widely recognised plaque index (PI) is that originally described by Silness & Löe (1964) and later more fully described by Löe (1967). This method relies on estimated measurements of plaque and may be used on a whole mouth or selected teeth basis (Fischman 1986). The American Dental Association (Council on Dental Therapeutics 1985) notes that while 'indices may be well suited to general estimates of cleansing ability, it has been suggested that where plaque/gingival relationships are to be considered, an index should be used to assess plaque on the total tooth surface, which can be accomplished by the Silness & Löe (1964) method and the modified Turesky et al. (1970) method'. This same conclusion was reached at the Symposium on Agents for the control of plaque held at the 1979 annual meeting of the International Association for Dental Research. It was therefore based on the above recommendations that the plaque index described by Silness & Löe be used in this study.

Loesche & Green (1972), Macgregor (1987) and Söder et al. (1993) used computerised techniques to calculate the % of plaque covering a tooth surface. The computerised method relies on 2-dimensional photographs to assessing the disclosed plaque present.

Clinicians perceive that plaque quantity is greatest adjacent to the gingival margin. The aim of this study was to quantify the plaque thickness at various levels adjacent to the gingival margin using a 3-dimensional method and to correlate these measurements to the plaque index described by Silness & Löe (1967).

Material and Methods

Experimental protocol

The study was approved by The City and East London Ethics Committee prior to subject recruitment. A total of 51 pa-

tients (45% female; 55% male) with an average age of 65.5 (ranging from 40 to 85 years) were randomly selected from a subset of patients attending St Bartholomew's and The Royal London School of Medicine and Dentistry. The inclusion criteria for patients were: to be aged over 40 years and have a minimum of 4 teeth. At least 1 tooth was required to have an exposed root surface of 2 mm apical to the cemento-enamel margin. Subjects were not included if they had had periodontal surgery or antibiotics within the last 6 months. The study group had also refrained from mouthwash use. Prior to the 1st examination, all staff were calibrated and trained. The selected subjects received a letter explaining the purpose of the study and were subsequently contacted by phone. If subjects agreed to participate, written informed consent was obtained and medical histories checked. At the 1st visit, a primary impression of the chosen arch was obtained and used to construct study models. An exposed root surface with no clinical evidence of root caries was chosen and noted. For metrological analysis an individual jig, specific to the buccal or labial surface of the chosen exposed root surface, was constructed on the study model. The jig was constructed using light cured special tray material surrounded by a 12 mm×12 mm rectangular brass tube.

At the 2nd visit, the chosen site was dried with air and a replica of the site was made using light-bodied addition silicone impression material (Extrude-Kerr) supported by the jig (Fig. 1). All second examinations were carried out at a morning session so that the periods in which plaque had accumulated were similar. The replica was stored as the site with plaque (coded P1). The chosen root surface was then disclosed with erythrosin and the PI score was recorded. The site was then manually brushed by the examiner with a medium toothbrush (Oral-B) and sterile water with gentle strokes until no disclosed plaque was visible. The site was dried with air and a second replica of the cleaned surface was obtained. The replica was stored as the site without plaque (coded P2). All examinations were performed by a single examiner in a dental chair with good illumination, using a dental mirror, and a 14W-Ash, Williams probe.

Three-dimensional quantification

Data was captured by recording co-ordinates over the surface to be studied using a laser probe. Pilot experiments showed that contact with the replica's surface using a touch probe resulted in unacceptably low accuracy and repeatability. The probe was mounted on a co-ordinate measuring machine (CMM) under on-line computer control (see below).

The probe

The Renishaw OP2 laser probe operates on the principle of optical triangulation. Infra-red light generated by the laser diode is focused onto a replica surface as a 25 μm diameter spot. Scattered light from this spot is imaged through collecting optics onto a position-sensitive device from which an electronic signal related to the surface height is processed in a micro-processor based controller having calibration data unique to each probe. A high degree of accuracy is thus ensured.

The accuracy of the system was assessed by measuring a sphere of known diameter and comparing the measurements to a synthetically generated model (Zou et al. 1996). These and other investigations showed the system's accuracy to be 5–10 μm on the particular materials and type of surface encountered in the study. The repeatability of measuring sequential replicas of the root surface with or without plaque were assessed. 4 sequential replicas of 1 root surface with and without plaque (Fig. 2) were taken from a patient and these replicas scanned. Comparisons between the replicas showed all measurements were repeatable to within 7 μm on the root surface and to within 10 μm on the plaque surface.

The Renishaw OP2 system is made up of 4 main elements: the probe itself containing the laser diode, projection and detection optics including a position-sensing detector (PSD), the front end electronics (FEE) which control and drive the system as well as achieving the 1st-stage amplification and filtering of the signals; the probe controller houses the micro-processor along with analogue and digital signal processing circuits. Some of the control functions include automatic gain adjustments to cater for variations in light intensity and communications with the probe interface which provides power for the laser as well as the communication port to the CMM computer.

The laser itself is a Class IIIb, GaAlAs type with a maximum power output of 5.0 mW, designed to meet the safety requirements of ANSI Z136.1–1980, BS4803 and IEC publication 825. The system has also been fully approved by the Centre for Devices and Radiological Health (CDRH) of the USA Food and Drug Administration (FDA) to meet its regulation 21 CFR 1040.10.

The co-ordinate measuring machine

The co-ordinate measuring machine which forms the heart of the clinical dental metrology unit is a Ferranti Merlin II. It consists of a massive granite work-table which ensures the stability essential for accurate data capture. Into this block a series of stainless steel inserts are positioned to which specimens can conveniently be secured.

The bridge beam corresponds with the x-axis. It is 750 mm long and of rectangular hollow section with solid hardened stainless steel guideways and lead bronze bearings. The lead bronze bearings prevent bearing pick-up. The bridge beam is supported on 2 substantial legs which form the y-axis along the granite work table which travels on similar bearings for a maximum distance of 500 mm. In turn, it supports a square cross-section probe column of hardened stainless steel with a fail-safe brake and a pneumatic counter-balance, which has a vertical transverse of 500 mm in the z-axis.

Each of the three axes (x, y, z) of the CMM has a built-in reference standard consisting of a stainless steel scale etched with 50 lines per mm. An index grating with the same line structure is superposed at a slight angle to produce an interference pattern or Moiré fringe. Photocells in a non-contact reading head convert this pattern into electrical signals which are converted by a processor into a digital display equal to the scales notion. This display instantaneously follows any change in direction, providing accurate information about the probes movement and position. The relationships of the axes to each other allow a point to be located relative to another point in all these planes.

Each pair of replicas from the study were digitised at a pitch of 100 μm, producing a set of (x, y, z) points using the above laser probe attached to the Ferranti Merlin CMM. Apart from the computer software required to run the CMM with its laser probe and to collect and store the co-ordinate data, development of specific software was needed to

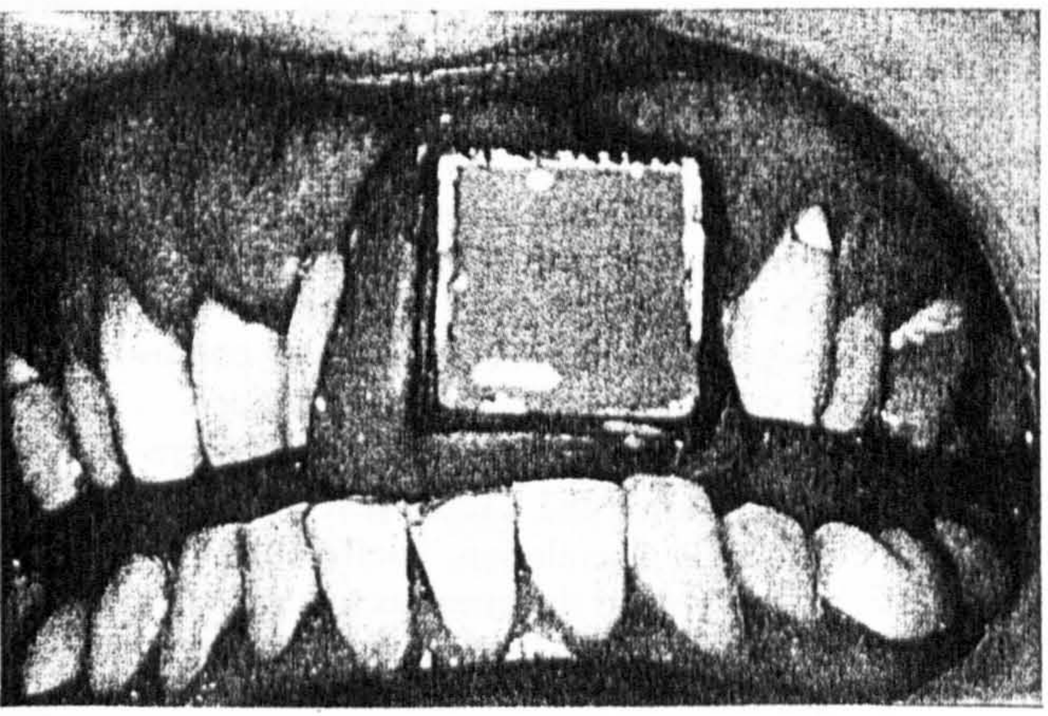

Fig. 1. A replica of the site is taken using light-body-addition silicone-impression material.

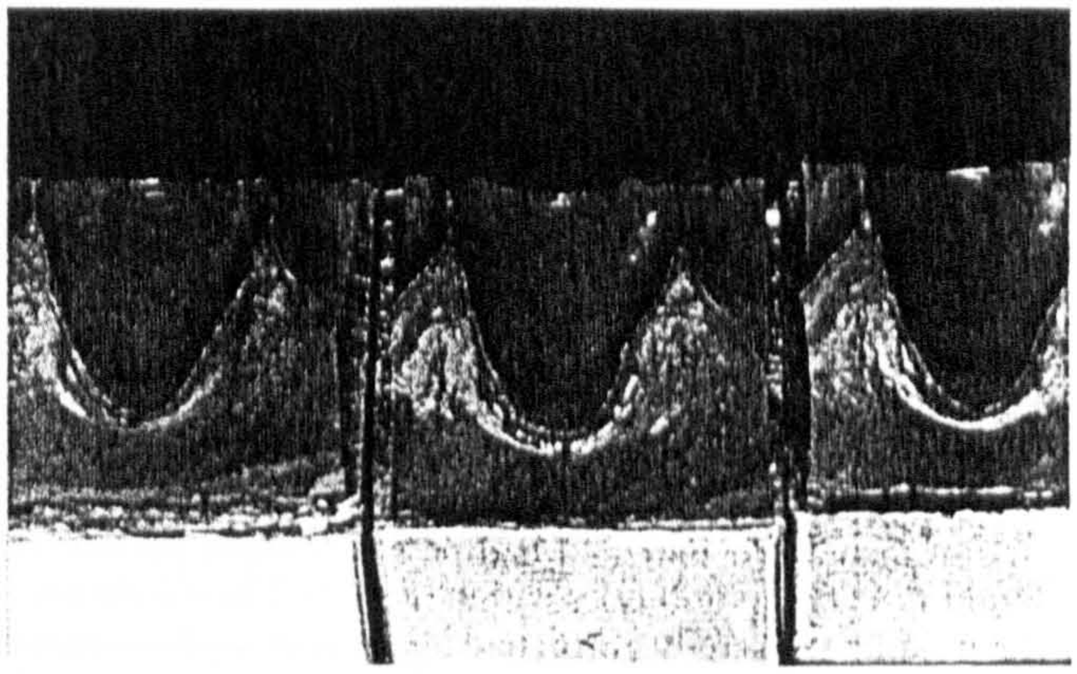

Fig. 2. 4 sequential replicas of plaque on root surface taken to assess repeatability.

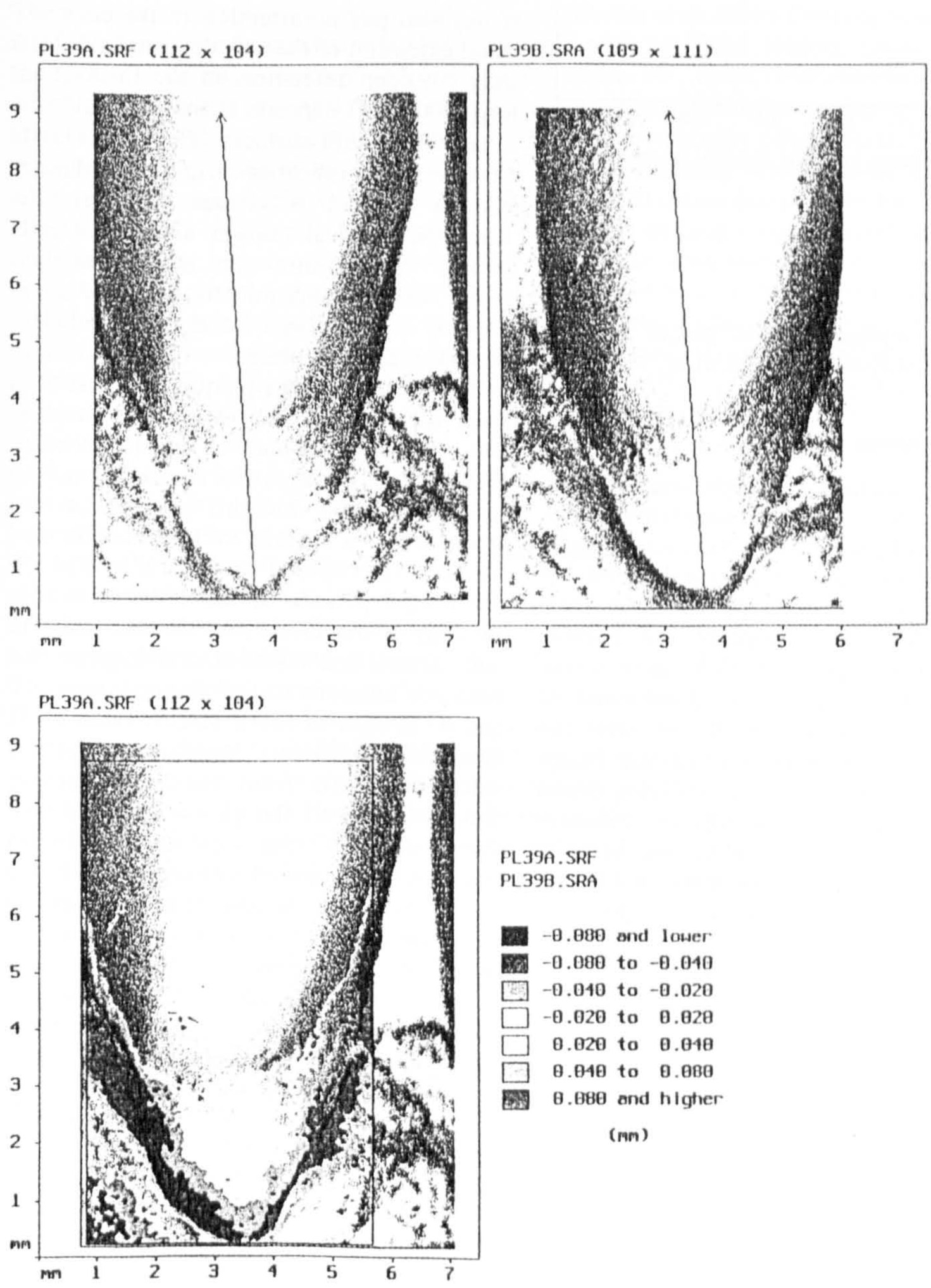

Fig. 3. 2 sequential replicas made immediately before and after removal of plaque. A colour-coded difference map shows the plaque distribution.

enable the data to provide the linear, angular, area and volume measurements required. This was needed to be supplemented with additional software to enable the superposing of data from sequential replicas of the same object to occur. This latter was deemed to be essential if any changes over time were to be accurately measured (Jovanovski et al. 1995).

Data from each replica were then interpolated with a bicubic spline surface (Yeganeh et al. 1995). This representation allows the value of the z-coordinate to be approximated for all values of x and y, and is also suitable for 3-D visualisation. The surfaces of pairs of replicas were then superposed, with the operator selecting different colours to highlight the areas of plaque. The superposed surfaces were compared in pairs by defining a mid-line profile of the 2 replicas (Figs. 3, 4) and measuring the shortest differences at 50 μm intervals starting at the crest of the gingival margin, thereby quantifying the plaque thickness. The surface characteristics of the plaque and root surface were assessed on P1 and P2, respectively. Plaque thickness at the gingival margin was measured and compared with the corresponding PI noted by the same clinical examiner.

Statistical evaluation

The variables of interest in the study were plaque thickness (numerical) and plaque index (ordinal). A non-parametric test of trends (Cuzick's test) was used to assess the relationship between the plaque thickness and the plaque index.

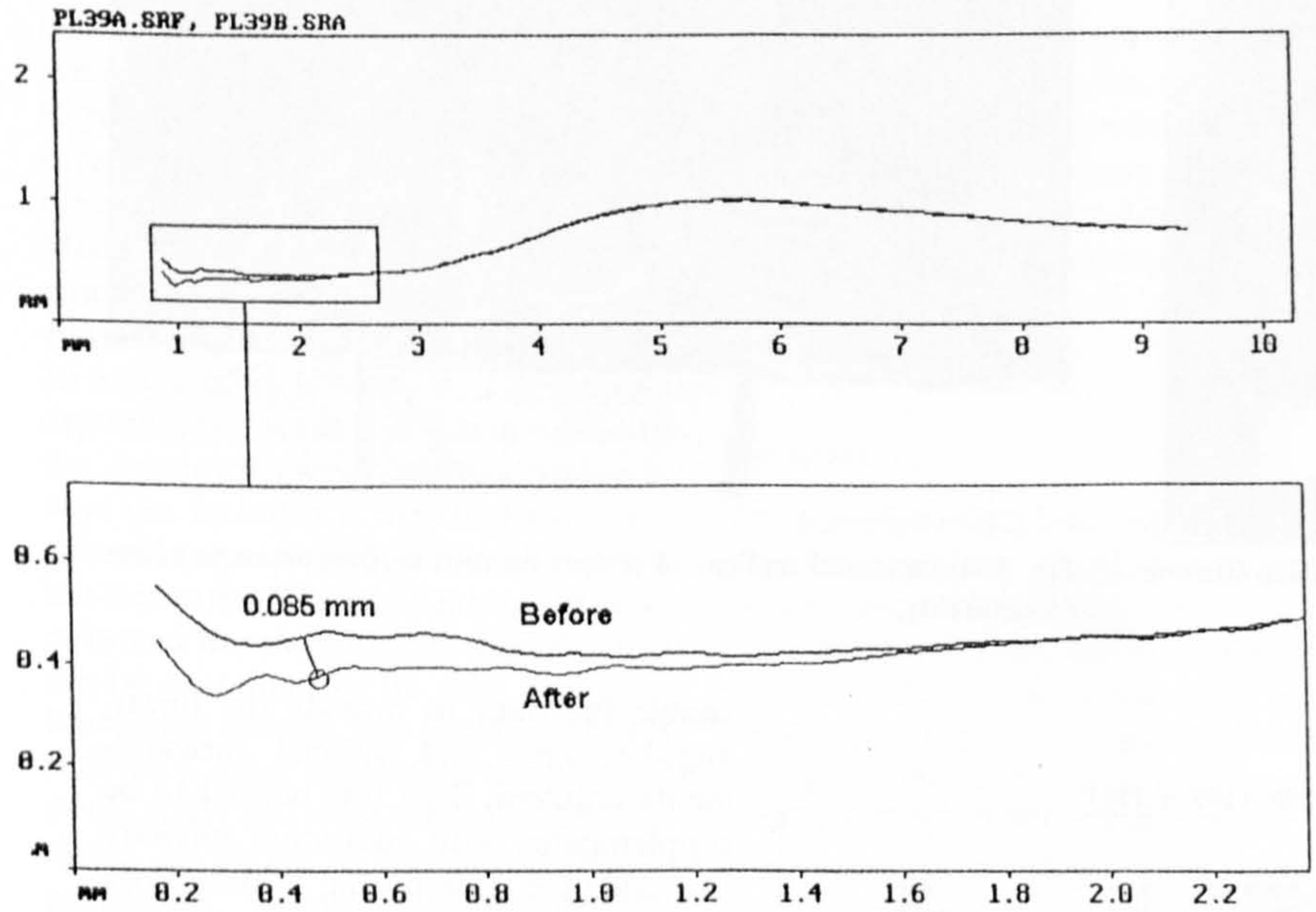

Fig. 4. Superposed surfaces quantifying the plaque thickness near the gingival margin in the bottom profile.

Results

The findings demonstrate the decrease in plaque accumulation as the distance increases away from the gingival margin. This is demonstrated in Table 2. The mean plaque thickness was measured at the gingival margin and ranged from 0.015 mm to 0.029 mm, from 0.043 mm to 0.066 mm, from 0.141 mm to 0.271 mm and from 0.336 mm to 0.560 mm when PI of 0, 1, 2, 3 were respectively recorded by the clinical examiner as demonstrated in Table 1 ($p \leqslant 0.002$ using the Cuzick test of trends), showing a strong linear relationship between the plaque thickness and the plaque index recorded by the same examiner. The mean plaque thickness measured by the system adjacent to the gingival margin increased with higher PI recorded by 1 examiner (Table 1).

The plaque thickness decreased at distances from the gingival margin (Table 2). Plaque accumulation and colonisation were irregular and also varied between individuals. In some subjects, plaque thickness peaked at some distance away from the gingival margin which may be explained by microbial growth out of microscopic cracks on teeth which present as clumps of micro-organisms. This was demonstrated in a study of scanning electromicrographs of these clumps of micro-organisms when replicas of the plaque surface were analysed (Yeganeh et al. 1995).

Discussion

This method complements other methods of clinical quantitative evaluation of plaque. The American Dental Association report (Council of Dental Therapeutics 1985) published in their guidelines for acceptance of chemotherapeutic products that, 'indices may be well suited to general estimates of cleaning ability' but do not offer the precise quantification of plaque. Image analysis methods of quantifying dental plaque area rely heavily on 2-dimensional photographs which can be taken at different angles resulting in different readings by the computer or the operator.

On average, the examination was completed in 20 min, digitisation in 90 min and interpolation and superpositioning in 30 min.

The decrease in plaque accumulation and stagnation away from the gingival margin add to the hypothesis that root carious lesions are initiated and are most active adjacent to the gingival margin (Beighton et al. 1993, Lynch 1994, 1996). The micro-organisms associated with active primary root carious lesions are those of aciduric and acidogenic anaerobes which may colonise better in areas of thicker plaque.

There is a fairly good linear correlation (using the Cuzick test of trends, and not correlation coefficients) between plaque thickness as measured by the system and the plaque index as recorded by the clinical examiner ($p \leqslant 0.002$). The system has the added advantage of storing the data for repeated access for future measurement and assessment. The plaque index scores also pay no attention to the coronal extension of the soft deposits and only consider differences in the thickness of the soft deposits at the gingival area of the tooth surfaces. The plaque thickness quantification using CMM can be assessed at various distances from the gingival margin allowing a greater insight into the mechanism under which the accumulation and adherence of the plaque to the exposed root surface takes place.

The decrease in the plaque thickness from the gingival margin towards the crown of the tooth may be due to several reasons: a stagnation site adjacent to the gingival margin, possibly a smoother root surface more coronally on the areas exposed to the oral cavity for longer periods of time, the morphology of the sound root dentine and soft tissues, less effective oral hygiene methods adjacent to the gingival margin or in case of tooth sensitivity and favourable nutrient, supply to the micro-organisms from the crevicular fluid adjacent to the gingival margin. Newly-exposed root surfaces would also not have matured with higher levels of fluoride, zinc or any other ions as compared with those root surfaces exposed for longer periods.

There are essentially 3 main factors which can affect the accuracy with which the laser probe captures data: the colour and reflectivity of a replica surface; its smoothness or irregularity; and the angle at which the incident beam hits it. Each of these produce variations as they

Table 1. Table of plaque thickness at the gingival margin versus plaque index (PI)

plaque thickness at the gingival margin (mean±SD)	0.015±0.014	0.043±0.023	0.141±0.13	0.336±0.224
plaque index	0	1	2	3

Table 2. Plaque thickness at different distances from the gingival margin (mean±SD)

Distance from gingival margin (mm)	Plaque thickness in mm (mean±SD)
0.000	0.106±0.118
0.250	0.053±0.052
0.500	0.039±0.038
0.750	0.039±0.036
1.000	0.029±0.027
1.500	0.016±0.017
2.000	0.010±0.013
3.000	0.007±0.011
4.000	0.004±0.003

affect the distribution of light within the projected 25 μm spot, which naturally affects its distribution within the image and with it, the centroid of illumination. The worst possible scenario is when light is reflected only from one extreme part of the spot. The colour of the replica from which the probe is capturing data has an affect on the measurement accuracy and repeatability (Seymour et al. 1996). A white material, since it reflects light more effectively than a black or dark coloured material, results in more precise data being captured, whilst a smooth surface rather than an irregular one, such as expanded polystyrene, similarly enhances accuracy. Therefore, the highest levels of accuracy are obtained when the replica material is light coloured rather than dark, when its surface is smooth in texture rather than irregular and if the laser beam hits the surface close to 90° in order to get the best results from the scanning process. In addition, more opaque materials are associated with better results than more translucent materials. The accuracy and the precision of the 3-D data acquisition were also shown by other authors (Mehl et al. 1997) to depend on the angulation of the incident beam, where they found that the precision and accuracy decreased as the inclination increased. A light-body addition silicone (Kerr) impression material which produces a blue coloured, smooth surface was used in this study and the laser beam was used to hit the surface of the replica close to 90°. The method scans impressions; study models were only used to construct occlusal jigs. The occlusal jigs were used as special trays for more localised impressions. We therefore feel that the shrinkage which is normally associated with pouring study models has been avoided by directly scanning the localised replicas.

This novel method has tremendous possibilities as a research tool to quantify 3-dimensional changes. For example, mean changes in gingival contour may be measured to assess the efficacy of a dentifrice or a mouthwash or to quantify tooth surface wear in so-called toothbrush abrasion cavities in longitudinal studies. The morphological characteristics of teeth, gingivae and plaque can be studied in vivo using this method. In extensive clinical trials with large number of teeth, a high accuracy and simplicity of the method are important considerations for the choice of 3-D measurements (Kreulen & Van Amerongen 1991). Mechanical and interferometric sensors, although highly accurate, suffer from long measuring times, require careful handling, and are unable to measure steep inclines and fissures (Hewlett et al. 1992). Other optical systems such as Moiré sensors, phase-shift sensors, etc., suffer from decreased accuracy, although their measuring time is short. In comparison, other reference-free superpositioning systems such as the optical 3-D device described by Mehl et al. (1997), although highly accurate, are able to scan stone models where a linear stability of 9 μm is introduced into the measurement due to dimensional variability within the replica technique (Price et al. 1991). In this study, replication was shown to be precise to within 7 μm on hard tissues and 10 μm on plaque surface.

Conclusion

The results from this study show that the co-ordinate measuring machine (CMM) can combine the benefit of mechanical sensors, with respect to accuracy and the benefit of optical sensors, where short measuring time, contact free and simplicity are achieved. However, the 3-D quantification cannot be performed directly in the mouth, and the replica technique can also contribute towards non-reproducible method error, although this is very small.

This method of quantitative measurement of plaque thickness can be used to determine the plaque distribution on exposed root surfaces; it correlates with the plaque index of Silness & Löe (1967). Plaque thickness is greatest adjacent to the gingival margin.

Zusammenfassung

Bestimmung der Plaquedicke auf Wurzeloberflächen mittels einer neuen 3-D Laser Scanning Methode

In der Literatur finden sich keine Angaben, wie die Dicke bakterieller Plaque auf Zähnen objektiv gemessen werden kann. Das Ziel der vorliegenden Studie war es deshalb, Plaque auf der Zahnoberfläche zu quantifizieren und zu prüfen, wie diese Quantifizierung bei 51 Patienten mit einem klinischen Plaque Index korreliert. Die Patienten wurden gebeten, am Tag der Untersuchung keinerlei Mundhygienemaßnahmen vorzunehmen. Von den Testflächen (kariesfreie freiliegende Wurzeloberflächen) wurden mit einem individuellen Löffel Abformungen genommen, anschließend wurde nach Anfärben der Beläge der Plaque Index nach Silness und Löe erhoben. Nach vollständiger Entfernung der Plaque mit einer Zahnbürste wurde eine 2. Abformung genommen. Die so gewonnenen Replikas wurden mit einer Co-ordinate Meßmaschine (CMM) und einer Laser-Scanning-Sonde eingelesen. Die Plaque, die unmittelbar zum Gingivarand benachbart war, hatte eine mittlere Dicke von 0.106±0.118 mm (Mittelwert±Standardabweichung), während die Plaqueschicht 250 μm koronal des Gingivarandes 0.053±0.052 mm dick war. Es bestand eine signifikante Korrelation zwischen Plaque Index und Plaquedicke ($p \leq 0.002$). Die Beobachtung, daß die größte Menge der Plaque am Gingivarand lokalisiert ist, unterstützt die Hypothese, daß primäre Wurzelkariesläsionen ihren Ausgang vom Gingivarand nehmen. Die vorgestellte Methode mißt die Plaquedicke auf freiliegenden Wurzeloberflächen, die mit dem Plaque Index korreliert; und zeigt, wie morphologische Eingenschaften der Zähne, der Gingiva und der Plaque in vivo von Replikas erfaßt werden können.

Résumé

La plaque sur les surfaces radiculaires: quantification à l'aide d'une méthode nouvelle d'examen 3-D avec balayage par sonde laser

Il n'y a dans la littérature publiée pas de compte rendu où l'épaisseur de la plaque sur les dents est quantifiée objectivement. Le but de cette étude était de quantifier la plaque sur une surface dentaire et d'examiner si cette quantité était corrélée avec un indice clinique de la plaque de chacun des 51 patients. Les patients ont été priés de ne pratiquer aucun soin d'hygiène bucco-dentaire le jour de l'examen. Les scores de l'indice de plaque de Silness et Löe ont été enregistrés et des répliques ont été examinées en utilisant une "Co-ordinate Measuring Machine" (CMM) et un balayage par sonde laser. On préparait une réplique de cette surface avant et après un brossage de la dent. La plaque adjacente au rebord gingival avait une épaisseur moyenne de 0.106±0.118 mm (moyenne±Écart-type), tandis que l'épaisseur de la plaque à 250 μm du rebord gingival était de 0.053±0.052 mm (moyenne±É.T.). Il y avait une corrélation significative entre l'indice de plaque et l'épaisseur de la plaque ($p \leq 0.002$). La plus grande abondance de plaque adjacente au rebord gingival constatée ici conforte l'hypothèse,

émise antérieurement, que les lésions primaires de carie des racines puissent débuter à un niveau adjacent au rebord gingival. Cette méthode quantifie l'épaisseur de la plaque sur les surfaces radiculaires dénudées, épaisseur qui est corrélée avec l'indice de la plaque, et peut en même temps illustrer comment les caractéristiques morphologiques des dents, de la gencive et de la plaque peuvent être étudiées in vivo à partir de l'enregistrement des répliques.

References

Beighton, D., Lynch, E. & Heath, M. R. (1993) A microbiological study of root caries lesions with different treatment needs. *Journal of Dental Research* **72**, 623–629.

Council of Dental Therapeutics (1985) *Guidelines for acceptance of chemotherapeutic products for the control of supragingival dental plaque and gingivitis.* American Dental Association.

Elliott, J. R., Bowers, G. M. Clemmer, B. A. & Rovelstad, G. H. (1972) Evaluation of an oral physiotherapy centre in the reduction of plaque and periodontal disease. *Journal of Periodontology* **43**, 221–224.

Fischman, S. L. (1986) Current status of indices of plaque. *Journal of Clinical Periodontology* **13**, 371–374.

Greene, J. C. & Vermillion, J. R. (1960) Oral hygiene index: A method of classifying oral hygiene status. *Journal of American Dental Association* **16**, 172–179.

Hewlett, E. R. & Orro, M. E. G. T.(1992) Accuracy testing of three-dimensional digitising systems. *Dental Materials* **8**, 49–53.

Jovanovski, V. et al. (1996) Objective assessment of three-dimensional structures in clinical dentistry using methods of co-ordinate metrology. *Nanobiology* **4**, 55–61.

Kreulen, C. M. & Van Amerongen, W. E. (1991) Wear measurements in clinical studies of composite resin restorations in the posterior region: a review. *ASDC Journal of Dentistry in Children* **58**, 109–123.

Löe, H. (1967) The gingival index, the plaque index and the retention systems. *Journal of Periodontology* **38**, 610–616.

Lynch, E. (1994) *Diagnosis and management of primary root caries.* Dissertation. London: University of London, UK.

Lynch, E. (1996) Relationship between clinical criteria and microflora of primary root caries. In: Stookey, G. K, (ed.): *Early detection of dental caries.* Indiana, pp. 175–242.

MacGregor, I. D. (1987) Comparison of the Silness/Löe (1964) index with Gravimetric measurement of dental plaque. *Clinical Preventive Dentistry* **9**, 9–12.

Mehl, A., Gloger, W. Kunzelmann, K. H. & Hickel, R. (1997) A new optical 3-D device for the detection of wear. *Journal of Dental Research* **76**, 1799–1807.

Quigley, G. A. & Hein, J. W. (1962) Comparative cleansing efficacy of manual and power brushing. *Journal of American Dental Association* **65**, 26–29.

Seymour, K., Zou, L., Samarawickrama, D. Y., Lynch, E. (1996) Assessment of shoulder dimensions and angles of porcelain bonded to metal crown preparations. *Journal of Prosthetic Dentistry* **75**, 406–411.

Silness, J. & Löe, H. (1964) Periodontal disease in pregnancy (II). Correlation between oral hygiene and periodontal condition. *Acta Odont Scandinavia* **22**, 121–135.

Söder, P. O., Jin, L. J. & Söder, B. (1993) Computerised Planimetric method for clinical plaque measurement. *Scandinavian Journal of Dental Research* **101**, 21–25.

Turesky, S., Gilmore, N. D. & Glickman, I. (1970) Reduced plaque formation by the chloromethyl analogue of vitamin C. *Journal of Periodontology* **41**, 41–43.

Yeganeh, S. Zou, L. Jovanovski, V. & Lynch, E. (1995) A novel method of three-dimensional quantification of plaque in vivo. *Journal of Dental Research* **75**, 1244.

Zou, L. Yang, Q. P. Jovanovski, V. Tay, W. M. & Lynch, E. (1996) Measurement of tooth morphology using a laser probe fitted on a co-ordinate measuring machine. In: Proceedings of the 4th International IMEKO Symposium on Laser metrology for precision measurement and inspection in industry. Denmark, pp. 11–20.

Address:

Shahrzad Yeganeh
Department of Conservative Dentistry
St Bartholomew's and The Royal London School of Medicine and Dentistry
Queen Mary and Westfield College
London E1 2AD, UK

Fax: 0171 377 7375
e-mail: s.yeganeh@mds.qmw.ac.uk

Eur. J. Prosthodont. Rest. Dent., Vol.7, No. 4, pp 125–129
Printed in Great Britain

Assessing the Quality of Shoulder Preparations for Metal Ceramic Crowns

Kevin G. Seymour, Dayanda Y.D. Samarawickrama, Lifong Zou and Edward Lynch

Abstract – *Previous work by the authors indicates a tendency for academic clinicians to under prepare and over angle shoulder preparations for metal ceramic crowns. This has implications for the final restoration in terms of contour, appearance and strength. This study analysed ninety six preparations, forty eight in vitro and forty eight in vivo, performed by six clinicians. The results show a mean shoulder width of 0.804 ± 0.274mm and a mean shoulder angle of 116 ± 18° for preparations performed in vitro; and 0.892 ± 0.337mm and 121 ± 24° for preparations performed in vivo. Thus, despite recommendations that such crowns should have 1–1.5mm, 90° shoulders, many of the preparations studied here fell short of this, indicating a lack of consistency in preparation geometry and adherence to the perceived 'ideal' preparation for a metal ceramic crown.*

KEY WORDS: Dental crowns; Metal ceramic; tooth preparation

INTRODUCTION

There is a lack of consensus as to what makes the 'ideal' preparation for a tooth to receive a metal ceramic crown. Butel, Campbell and DiFiore[1] listed seven types of marginal configuration that had been suggested, including the knife edge, the flat shoulder, the sloped shoulder, the bevelled shoulder, the chamfer and the deep chamfer with bevel. Despite this variation, it appears that the most commonly advocated labial margin in the UK, USA and Puerto Rico is the flat shoulder[1,2], as this design is said to facilitate the development of desirable appearance[3] and marginal stability during the porcelain firing cycle[4]. Consequently, a shoulder of 1.0–1.5mm has been suggested, combining the amount of reduction necessary for restoration with semi-precious or precious metal alloys (0.3–0.5mm) and porcelain (0.7–1.0mm)[4,5]. Any compromise in this dimension will have unfavourable consequences for contour and appearance[6]. Under preparation of this shoulder has been cited as the reason for many of the problems associated with crowns[7], where it appears that clinicians overestimate the ability of technicians to produce anatomic crown contours while working to the minimum possible thickness of materials, leading to over contoured, unaesthetic crowns[6]. Development of an adequate contour is also closely related to the emergence profile of the crown[8]. It has been suggested that the internal shoulder angle should be in the order of 90°–110°. If it is less than this, there will be unsupported tooth structure labially which is liable to fracture in function. It is also likely that such geometry in the die may not withstand handling during construction. If the angle exceeds 110°, the porcelain will finish at a knife edge, and thus be susceptible to fracture[4,9], again impeding the required emergence profile, and compromising marginal adaptation.

Further to technicians not conforming to the clinicians' prescription[10], clinicians themselves are not conforming to these 'ideal' requirements. We reported previously[11] that academic clinicians, when asked to prepare teeth for metal ceramic crowns, produced shoulders with a width of 0.752 ± 0.174mm (Mean ± S.D. of 24 preparations) and an internal shoulder angle of 108.54 ± 15.06°. Although we may teach an 'ideal' shoulder preparation, it is questionable if we are able to carry this out to the required dimensions.

The above study involved a small, very selected group of clinicians. It was decided therefore to use similar methodology to analyse the preparations of a variety of dentists from a number of backgrounds.

MATERIALS AND METHODS

As part of a wide ranging study looking into the quality of preparations for metal ceramic crowns[12], upper central *incisor teeth* were prepared to receive metal ceramic crowns by three academic clinicians (n=48) and three general dental practitioners (n=48). All academic clinicians were members of the Department of Conservative Dentistry (St. Bartholomew's and the Royal London School of Medicine and Dentistry) with at least six years experience. General dental practitioners were recruited from attendees at Department run Section 63 courses and all had at least six years experience. Each dentist prepared eight teeth *in vitro* in the laboratory, and eight teeth *in vivo* in patients. Teeth used in the laboratory part of the study were extracted central incisors that had been stored in formol saline. All academic clinicians used the burs currently available and used within the Dental School for crown preparation (*Figure 1*) for both *in vitro* and *in vivo* exercises. These were:

- a small diamond fissure bur with 10° taper, ISO number 806 314 168 524 012,
- a wide tapered tungsten carbide fissure bur with 10° taper, ISO number 500 314 168 006, .
- a long tapered diamond bur with a tungsten carbide tip and 5° taper, ISO number 806 500 314 198 020 014,
- a long parallel sided tungsten carbide bur, ISO number 500 314 289 072 012,

- a long tapered tungsten carbide fissure bur with 10° taper, ISO number 500 315 187 072 016.

The general dental practitioners were asked to use their usual burs of preference for crown preparation. Clinicians were asked to prepare teeth for the *in vitro* part of the study hand held. Prepared teeth were replicated in mid-blue light bodied polyvinyl siloxane impression material (Extrude), held in square brass tubes measuring 12 x 12 x 8mm. Each replica was scanned uni-directionally by a co-ordinate measuring machine (Merlin II,) utilising a non-contact 830nm wavelength laser triangulation probe (Renishaw OP2), at 50µm intervals, recording x, y and z surface co-ordinates. These digital data were then manipulated to give images of near photographic quality, which can be analysed for width and angulation. *Figure 2* shows an example of such an image of the labial surface of a tooth prepared to receive a metal ceramic crown. *Figure 3* shows this image manipulated and a profile defined for measurement. *Figure 4* shows the profile and measurement axes which are then set to measure the areas of interest, using the preloaded software (Accudat) for each scan using the measurement references shown in *Figure 5*, where length SW is the shoulder width, and angle SA the shoulder angle.

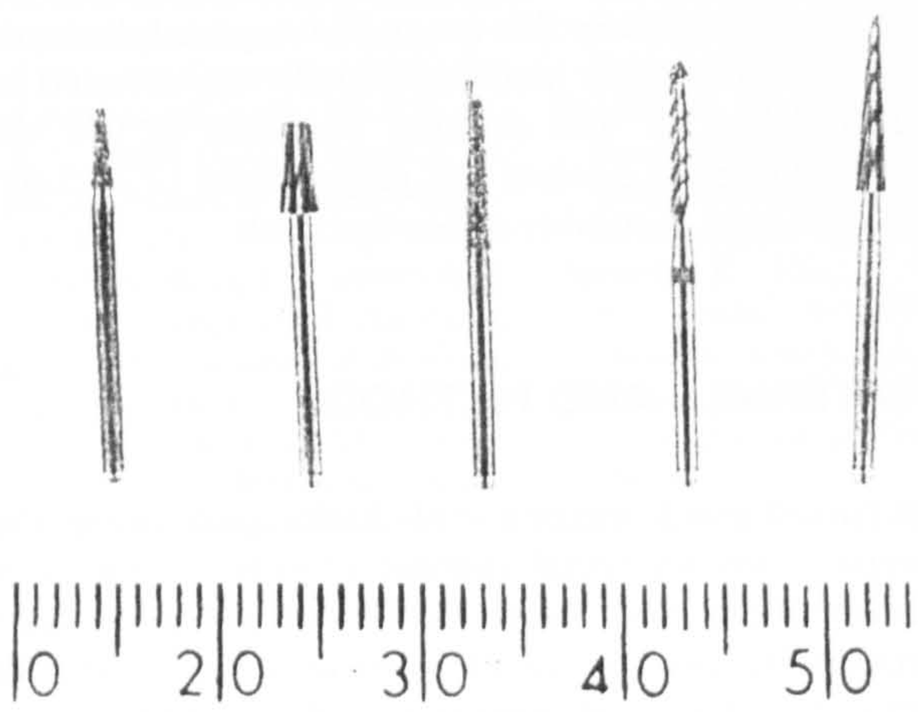

Figure 1. *The Dental School 'crown' burs. Ruler shown is in millimetres.*

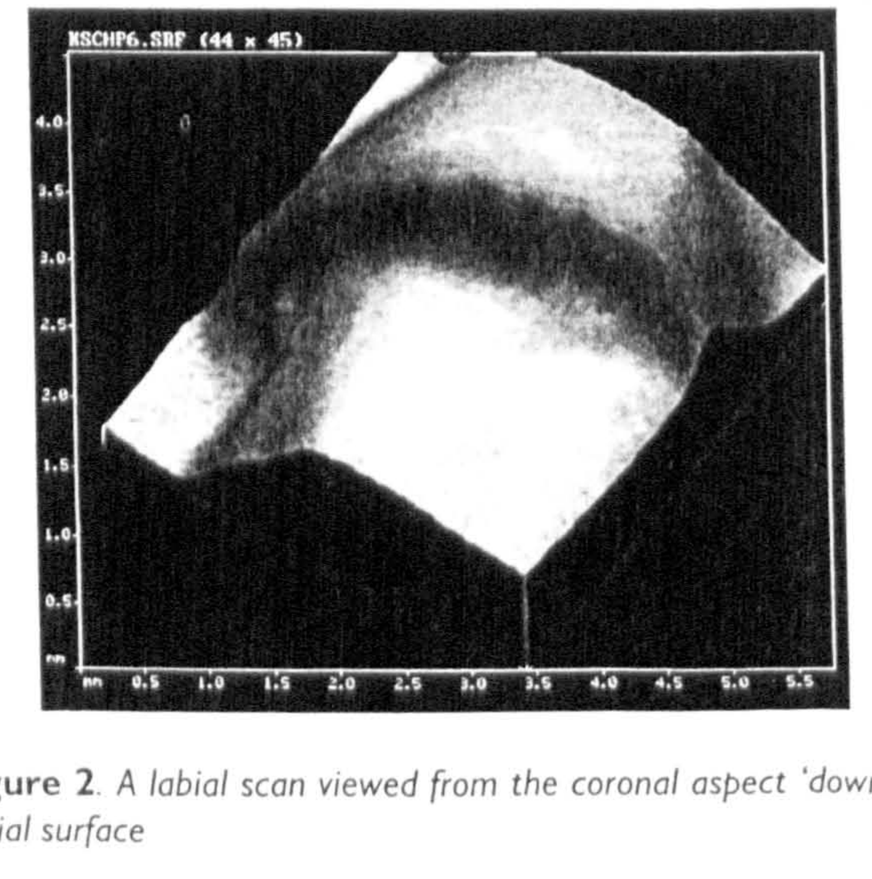

Figure 2. *A labial scan viewed from the coronal aspect 'down' the labial surface*

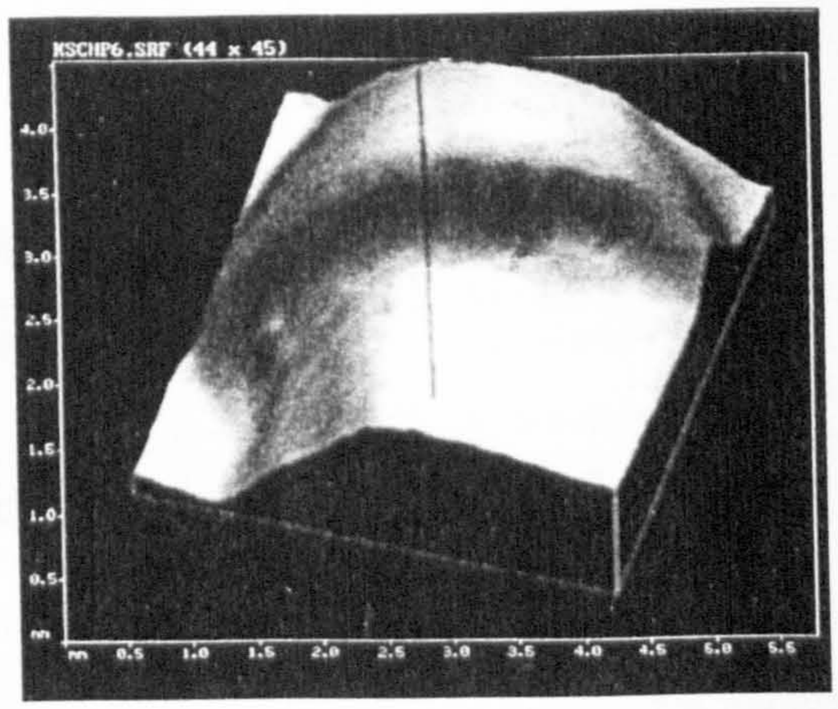

Figure 3. *The labial scan as in Figure 2 with the mid-labial profile defined for measurement*

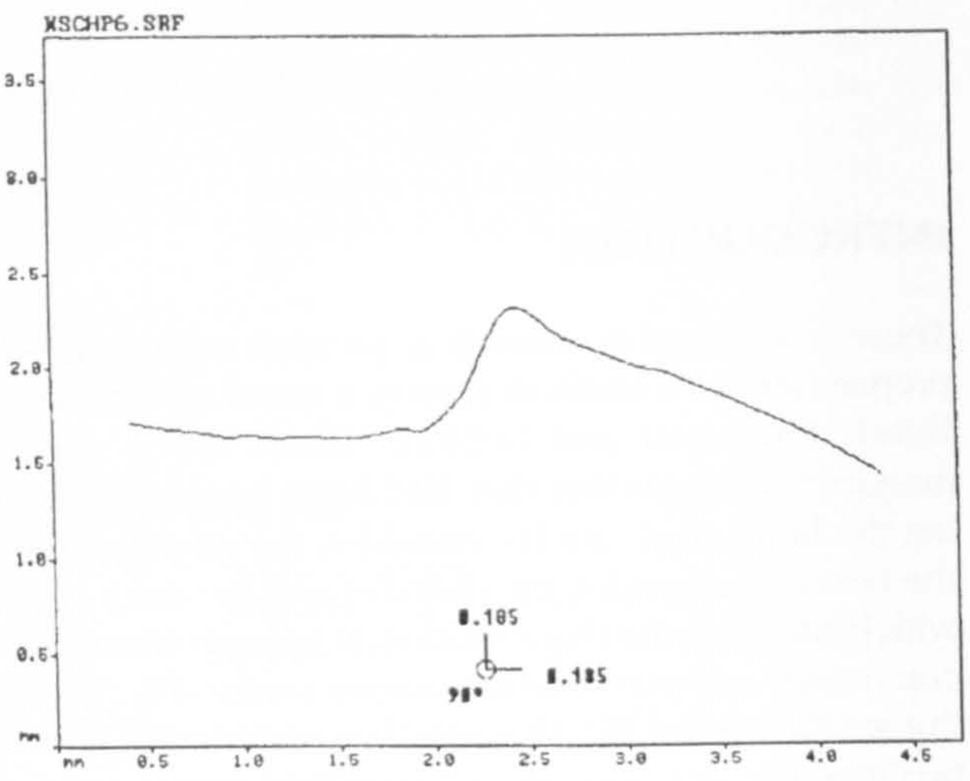

Figure 4. *The mid-labial profile as defined in Figure 3. Scale shown is in millimetres.*

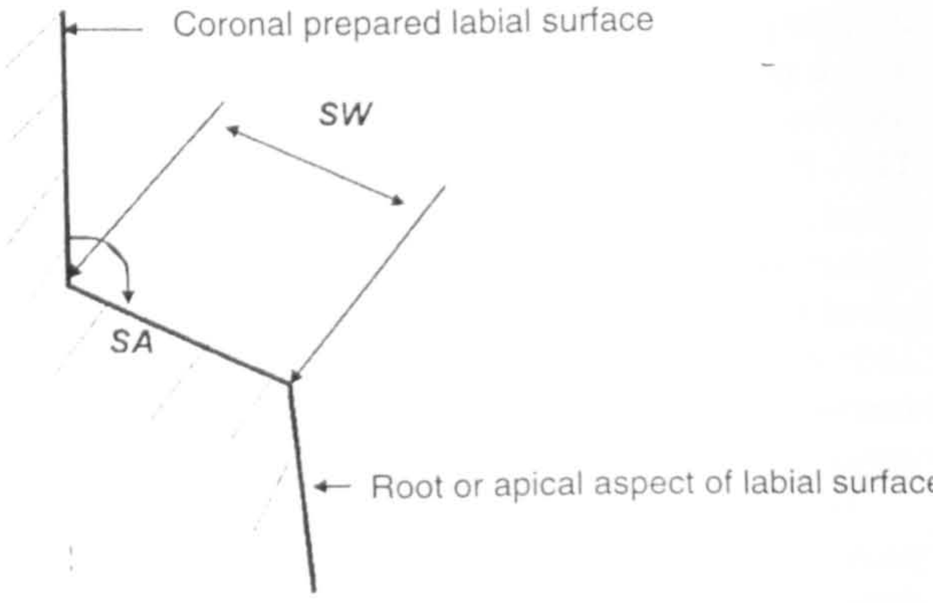

Figure 5. *Diagram of measurement references*

RESULTS

Summary data from the forty-eight *in vitro* preparations are presented in *Table 1* and plotted as frequency distribution functions in *Figures 6* and *7*. Preparations falling within the ideal ranges are shown in light grey shading. It can be seen that of the forty eight preparations, only nine had shoulder widths within the 1–1.5mm range, with one above 1.5mm. Thirty-eight, or 79%, were less than 1mm in width and so could be considered under prepared. With shoulder angle, thirteen were within the 90–110° range, with four less than this. Therefore 65% of preparations were over-angled. Only three preparations had both shoulder width and angle within the ideal ranges, meaning that 94% of preparations were either under prepared, over angled, or both.

Summary data from the *in vivo* preparations are presented in *Table 2* and plotted as frequency distribution functions in *Figures 8* and *9*. Again, of forty-eight preparations, thirteen had shoulder widths within the 1–1.5mm range, with three above 1.5mm. Therefore, thirty-two, or 67%, of shoulder preparations were under prepared. With shoulder angle, nineteen were within the 90–110° range, with one below 90°. Therefore, twenty-eight, or 58%, of preparations were over angled. Only five preparations had both shoulder widths and shoulder angles within the ideal ranges, indicating that 90% of shoulders prepared in patients' mouths were either under prepared, over angled, or both. The example shown in *Figures 2*, *3* and *4* is from the *in vitro* group and shows an under prepared, over angled shoulder.

If both groups of preparations are compared (*in vitro* and *in vivo*), using a simple t test (Excel 97), the only comparison approaching significance is that between shoulder widths, which gives a *P* value of 0.08, indicating a trend for those preparations performed in patients to be wider than those prepared *in vitro*.

Table 1. *In vitro preparations*

	Shoulder Width (mm)	*Shoulder Angle (deg)*
Mean	0.804	116
Standard Deviation	0.274	18
Range	1.406	79
Minimum	0.306	70
Maximum	1.712	149
Count	48	48
Confidence Level (95.0%)	0.079	5

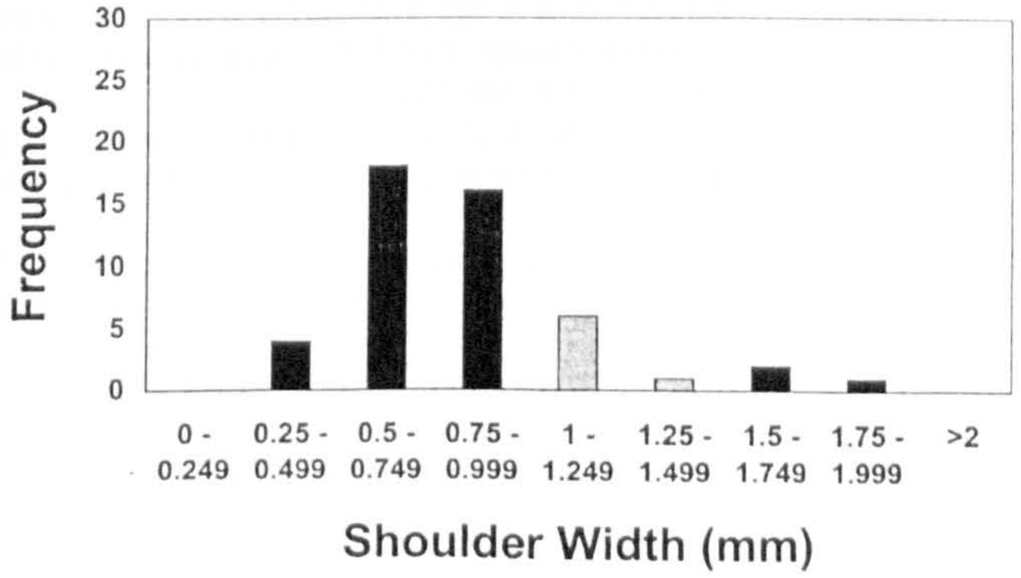

Figure 6. *In vitro shoulder width data. Preparations within the ideal range are shown in light grey shading.*

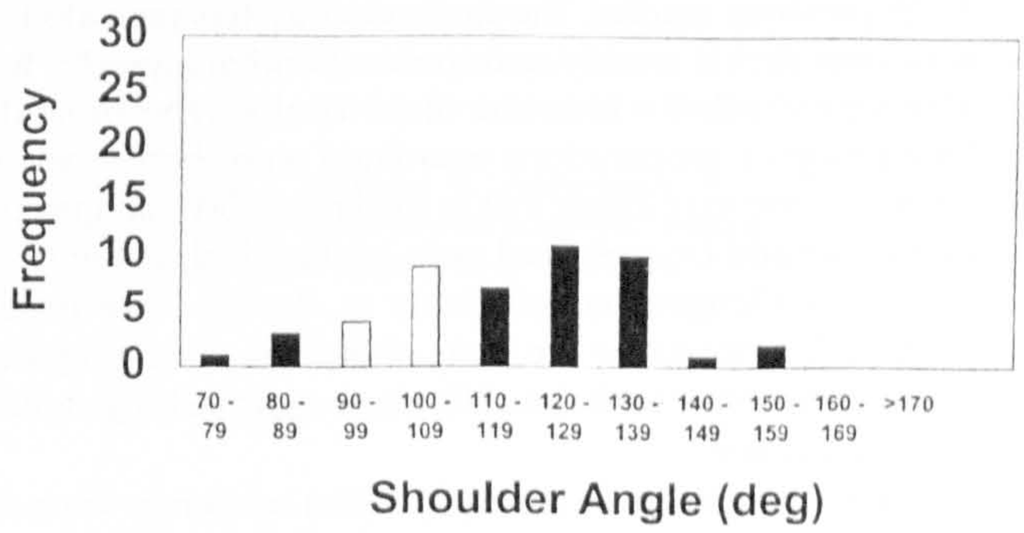

Figure 7. *In vitro shoulder angle data. Preparations within the ideal range are shown in light grey shading.*

Table 2. *In vivo preparations*

	Shoulder Width (mm)	*Shoulder Angle (deg)*
Mean	0.892	121
Standard Deviation	0.337	24
Range	1.568	81
Minimum	0.295	84
Maximum	1.863	165
Count	48	48
Confidence Level (95.0%)	0.098	7

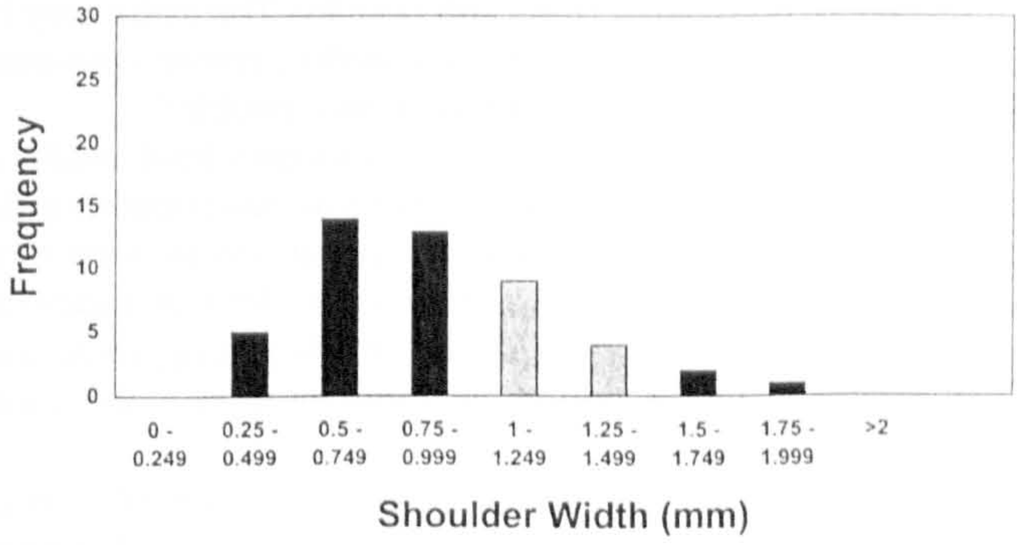

Figure 8. *In vivo shoulder width data. Preparations within the ideal range are shown in light grey shading.*

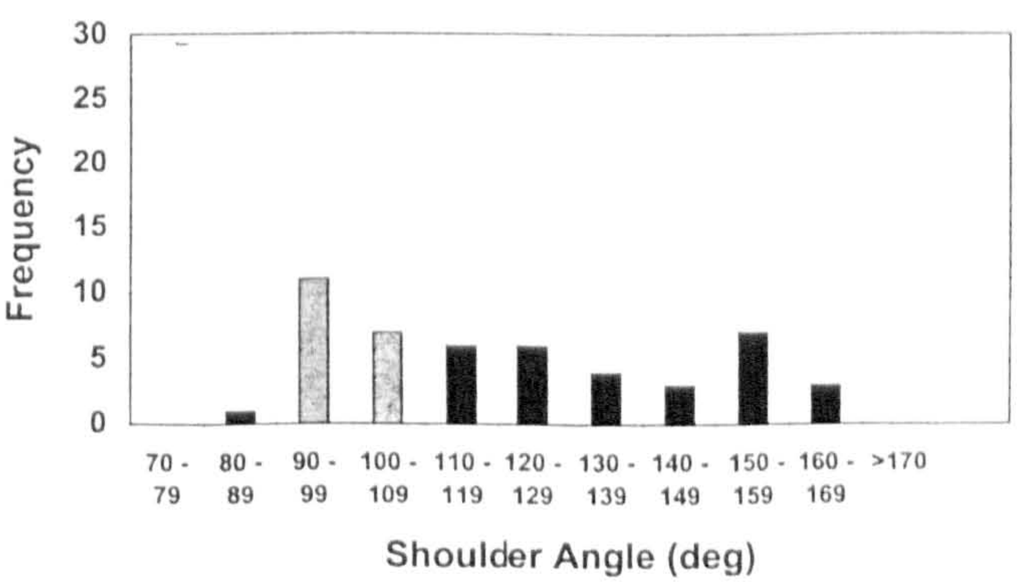

Figure 9. *In vivo shoulder angle data. Preparations within the ideal range are shown in light grey shading.*

DISCUSSION

As in previous studies, the methodology has provided us with data that is readily manipulated and analysed[12]. It is also reproducible within the limits of this type of study. One group of preparations examined were performed *in vitro* and one may argue that in the laboratory such preparations should be prepared near to the ideal as the teeth are not challenged by soft tissue or disease. The results suggest this not to be the case, shoulders were prepared wider in patients, with this difference approaching statistical significance.

All the operators in the study had a tendency to under prepare and over angle the labial shoulders for metal ceramic crowns. The consequences of this under preparation and over angling have already been discussed in the introduction[10,11,13]. It is surprising that more metal ceramic crowns do not fail, given the variations in preparation geometry that have been observed in this study. The literature reveals very few longitudinal or cross-sectional studies of the success of metal ceramic crowns. Those that are documented relate in the most part to bridges rather than to single units. Comparison of these studies is difficult as they vary in design and the materials used. For example, the prosthodontic treatment may have been carried out by a student, general practitioner, specialist, or even by a variety of operators. Authors also vary in their definition of failure, as do operators when considering the replacement of a unit[14]. This is particularly pertinent when considering the aesthetic aspect of crowns[9,15] as the operator may often choose not to replace those with a less than 'ideal' appearance if the patient is satisfied, especially in terms of porcelain opacity. The same may be true for gingival and coronal contour, tissue response, marginal deterioration and emergence profile[15].

Future work should include a longitudinal study of crown performance, beginning with an assessment of the quality of the preparation and relating this to long term prognosis. Those studies that have looked at longevity always begin the time period from the fitting stage and do not take into account the foundation (i.e. the tooth preparation).

The preparations studied here show a notable deviation from the perceived 'ideal' configuration of 1–1.5mm and 90°/100°. One must question the reasons for such deviation. Are operators under preparing and over angling because they are unable to judge small differences in distance and angulation that would improve the preparations?[16] When Dunne[16] investigated the ability of undergraduates and practitioners to adjust the gap in a pair of vernier callipers to 1mm, he found that 70 per cent of readings were below this test size. If carried through to the clinic, these errors of distance estimation would lead to under preparation and the consequences already highlighted. Dunne[16] went on to conclude that the 'dental' millimetre could be described as a distance of 0.7mm!

Another factor is that dentists are 'conservative' by nature, and are constantly aware of the potential for pulpal damage through over-preparation during these procedures. Studies have highlighted just how little protective dentine a preparation of 1.5mm will leave over the pulp[17], so it is perhaps not surprising that crowns are often under prepared, with pulps maintaining vitality following preparation[19].

CONCLUSION

This work has shown that there is a tendency for the academic and general dental practitioners who took part in the study to under prepare and over angle labial shoulder preparations for metal ceramic crowns. This confirms earlier work involving the preparations from one group of clinicians. Such results may lead to an over-contoured crown, a crown with a thin porcelain margin, or a crown with porcelain finishing at an acute angle.

MANUFACTURERS' DETAILS

- Extrude, Kerr, Peterborough, UK
- Merlin II, International Metrology Systems, Livingstone, UK
- Renishaw OP2, Renishaw, Gloucester, UK
- Accudat, International Metrology Systems, UK
- Excel 97, Microsoft Corporation, USA

ADDRESS FOR CORRESPONDENCE

K G Seymour, Department of Conservative Dentistry, St. Bartholomew's and the Royal London School of Medicine and Dentistry, Queen Mary and Westfield College, Whitechapel, London E1 2AD.

REFERENCES

1 Butel, E.M., Campbell, J.C. and DiFiore, P.M. Crown margin design: A dental school study. *J. Prosthet. Dent.* 1991; **65:** 303–305.

2 Hooper, S.M., Huggett, R. and Foster, L.V. Teaching veneer and crown margins in UK dental schools. *Dental Update.* 1993; **20:** 192–196.

3 Sozio, R.B. The marginal aspect of the ceramometal restoration. The collarless ceramometal restoration. *Den. Clin. North Am.* 1977; **21:** 787–801.

4 Shillingburg, H.T., Hobo, S. and Fisher, D.W. Preparation design and margin distortion in porcelain fused to metal restorations. *J. Prosthet. Dent.* 1973; **29:** 276–284.

5 Rosenstiel, S.F., Land, M.F. and Fujimoto, *J. Contemporary fixed prosthodontics.* Second edition. Mosby. 1995.

6 Donovan, T. and Prince, J. An analysis of margin configurations for metal-ceramic crowns. *J. Prosthet. Dent.* 1985; **53:** 153–157.

7 Hunter, A.J. and Hunter, A.R. Gingival crown margin configurations: a review and discussion. Part I. Terminology and widths. *J. Prosthet. Dent.* 1990; **64:** 548–552.

8 Stein, S. and Kuwata, M. A dentist and a dental technologist analyze current ceramo-metal procedures. *Dent. Clin. North Am.* 1977; **21:** 729–749.

9 Pameijer, C.H. and Kikutake, T. Enhancing esthetics in porcelain fused to metal through technique modifications. *Den. Clin. North Am.* 1985; **29:** 753–762.

10 Northeast, S.E., Van Noort, R., Johnson, A., Winstanley, R.B. and White, G.E. Metal-ceramic bridges from commercial laboratories: alloy composition, cost and quality of fit. *Br. Dent. J.* 1992; **172:** 198–204.

11 Seymour, K., Zou, L., Samarawickrama, D. and Lynch, E. Assessment of shoulder dimensions and angles of porcelain bonded to metal crown preparations. *J. Prosthet. Dent.* 1996; **75:** 406–411.

12 Seymour, K.G. *Variations in the labial shoulder geometry of teeth prepared to receive metal ceramic crowns.* PhD thesis. University of London. 1998.
13 Reeves, W.J. Restorative margin placement and periodontal health. *J. Prosthet. Dent.* 1991; **66:** 733–736.
14 Selby, A. Fixed prosthodontic failure. A review and discussion of important aspects. *Aust. Dent. J.* 1994; **39:** 150–156.
15 Marynuik, G.A. In search of treatment longevity – a 30-year perspective. *J. Am. Dent. Assoc.* 1984; **109:** 739–744.
16 Dunne, S.M. The limitation of visual perception in restorative dentistry. *Dental Update.* 1993; **20:** 198–205.
17 Chandler, N.P. The radiographic assessment of pulp size: validity and clinical implications. *New Zealand Dental Journal.* 1989; **85:** 23–26.
18 Jackson, C.R., Skidmore, A.E. and Rice, R.T. Pulpal evaluation of teeth restored with fixed prostheses. *J. Prosthet. Dent.* 1992; **67:** 323–325.
19 Valderhaug, J., Jockstad, A., Ambjornsen, E. and Norheim, P.W. Assessment of the periapical and clinical status of crowned teeth over twenty five years. *J Dent.* 1997; **25:** 97–105.

RESEARCH AND EDUCATION

Assessment of shoulder dimensions and angles of porcelain bonded to metal crown preparations

Kevin Seymour, BDS, MSc,[a] Lifong Zou, BSc,[b] Dayananda Y. D. Samarawickrama, BDS, PhD,[c] and Edward Lynch, MA, BDentSc, PhD[d]

Dental School, London Hospital Medical College, London, United Kingdom

The metal ceramic crown is the most popular extracoronal restoration in the United Kingdom. These restorations may fail because of fracture or esthetics. A potential cause of failure is the quality and width of the facial shoulder preparation. In this study 24 extracted human teeth were prepared to receive metal ceramic crowns by one of three dentists. Preparations were replicated and scanned in the midfacial plane by a coordinate measuring machine with a noncontact probe. The *x*, *y*, and *z* surface coordinates were recorded. The results indicated a mean (±SD) shoulder width value of 0.752 mm (±0.174 mm) and a shoulder angle of 108.54 (±15.06) degrees. From these data it would appear that there are deficiencies in shoulder preparations, particularly in width. These inadequacies may have implications for longevity of the restoration and periodontal health in a clinical situation. (J PROSTHET DENT 1996;75:406-11.)

The metal ceramic crown is currently the most popular extracoronal restoration in the United Kingdom under the General Dental Services, and 1.6 million units were placed in 1993 in England and Wales alone at a cost of £130 million.[1] (Unfortunately, there are no figures available for metal ceramic crowns provided under private contract.) These restorations may fail for a variety of reasons, which have been categorized as (1) material failures, (2) mechanical-human failures, and (3) esthetic failures.[2] Adequate tooth reduction is necessary to minimize potential for failure,[3, 4] and preparations must satisfy specific requirements to ensure space for an esthetic porcelain veneer and sufficient metal for strength. Tooth preparations must be accomplished without compromising the pulp or the supporting structures. Design of the preparation is commonly a combination of the preparation for a full-veneer gold crown lingually and proximally, with additional facial reduction similar to a porcelain jacket crown.[5] There is some controversy about the configuration of the finish line[6]; however, a combination of a shoulder and chamfer margins is commonly recommended.[7]

Controversy also exists about the preparation a facial margin with a flat shoulder and a facial margin prepared with a shoulder and a slight cavosurface bevel. Both shoulder designs blend with a chamfer at the proximal surfaces.[5] It has been claimed that the bevel facilitates a "slip joint" effect that improves marginal adaptation,[8-11] although this claim of "improved" marginal fit has been questioned.[12] The bevel may also be undesirable for esthetic reasons,[7] especially with margins prepared above the gingival crest of anterior teeth.[12-16] Despite disagreement on optimal preparation design, the most commonly advocated facial finish line in the United Kingdom, United States, and Puerto Rico is the flat shoulder.[6, 17] This design facilitates development of desirable esthetics[9] and can improve marginal stability during the porcelain firing cycle[3]; however, the flat shoulder is difficult to prepare.[18]

The ideal shoulder preparation should be from 0.8 to 1.5 mm in width, depending on the casting alloy. Nonprecious alloys can be cast and finished to a thickness of 0.1 mm, which allows 0.7 to 1.4 mm for porcelain. Precious alloys require a thickness of 0.3 to 0,5 mm and 1.2 to 1.5 mm of axial tooth reduction to allow a minimal space of 0.7 mm for porcelain.[4] Obviously, compromises in shoulder width can have unfavorable consequences in contour and esthetics.[19, 20] The internal angle of the shoulder should be 90 to 110 degrees. If the angle is less than 90 degrees, there will be unsupported labial tooth structure that may compromise the die during handling or this unsupported enamel may fracture either during the course of treatment or during function and compromise the marginal adaptation of the crowns. If the shoulder angle exceeds 110 degrees, the porcelain will have a knife edge that may lead to fracture.[3, 4]

Few studies have investigated the adequacy of shoulder preparations. A number of studies have investigated crown failure and the potential reasons for failure.[21, 22] In these

[a]Lecturer, Department of Conservative Dentistry.
[b]Research Assistant, Department of Conservative Dentistry.
[c]Senior Lecturer and Acting Head, Department of Conservative Dentistry.
[d]Senior Lecturer, Department of Conservative Dentistry.

0022-3913/96/$5.00 + 0. **10/1/70668**

studies mechanical failure and esthetics were listed as the most common causes of failure of metal ceramic crowns. In one study the mean life span of the metal ceramic crown was 6.5 years.[22] Improved length of service would be desirable given the cost involved. These particular studies retrospectively examined crown performance beginning at the point of placement of the crown. None investigated the prepared tooth to determine whether shortcomings affected crown performance and longevity. One study evaluated the occlusal reduction for complete crowns on typodont teeth by experienced dentists.[23] Replicates were superimposed and analyzed by reflex microscopy at ×20 magnification. In this study it appeared that even with in vitro conditions the occlusal surfaces of the preparations were flattened. Another study[24] measured the taper of crown preparations with image analysis of stone dies and discovered taper that far exceeded what has been commonly taught in dental schools. Seymour et al.[25] investigated various aspects of metal ceramic crown preparations in vivo and reported insufficient removal of tooth structure at the facial margin. In this study the crowns were found to be overbuilt with a labial overhang.

This last study[25] used a computer-assisted coordinate measuring machine (International Metrology Systems, Livingstone, United Kingdom) to obtain the data. With this apparatus, a polyvinyl siloxane replica of the buccal surface of a lower premolar tooth was scanned by a laser triangulation probe of 0.83 μm wavelength. The surface was scanned at intervals between 20 and 200 μm, and *x*, *y*, and *z* coordinates were recorded. These numeric data were manipulated to provide images of near photographic quality. The data were then further analyzed and profiles were constructed in any given plane. It was from these images that measurements were made with respect to distances and angles. This apparatus has been used with some success in dentistry to give insight into a number of problems related to morphologic features and measurement, and it provided a novel nondestructive method of evaluation with a number of applications for dentistry.[25-31]

The purpose of this study was to use the method of Seymour et al.[25] to examine the shoulder width and angulation of margin preparations for metal ceramic crowns.

MATERIAL AND METHODS

Twenty-four extracted, human, single-rooted, noncarious, unrestored teeth were used in this study. Teeth were cleaned of extraneous deposits and notched with a small diamond stone in the midfacial plane just below the cementoenamel junction. This notch provided a reference mark for superimposition. Teeth were identified, and their maximum faciolingual width was measured with calipers. The teeth were replicated in addition reaction silicone impression material (Extrude, Kerr, Peterborough, United Kingdom) and held in hollow square brass tubes that

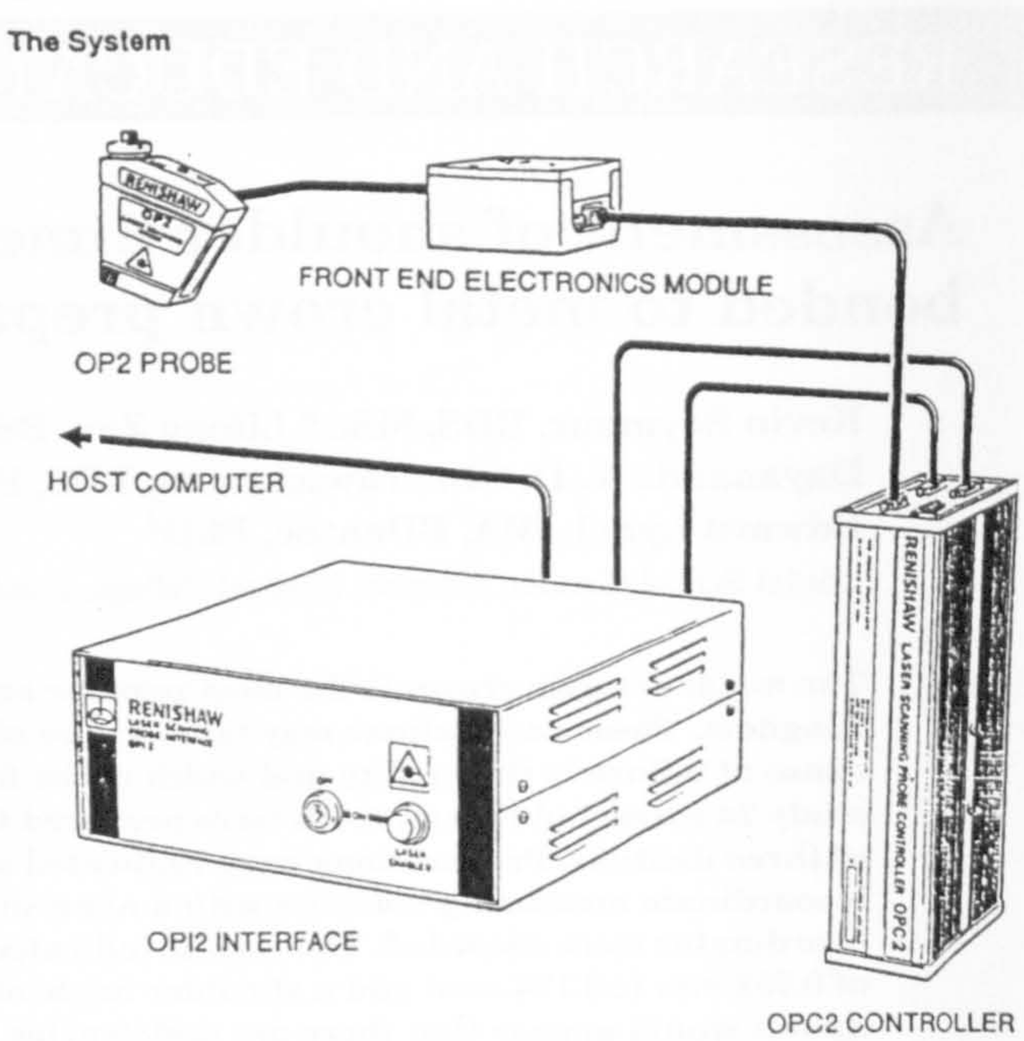

Fig. 1. Diagrammatic overview of system. (Courtesy of Renishaw.)

measured 12 × 12 × 8 mm. Teeth were then distributed to one of three dentists, faculty members with at least 6 years of professional experience, by use of random number tables. The three dentists were asked to prepare the teeth for metal ceramic crowns that would use precious bonding alloy. The prepared teeth were then replicated as previously described, and replicates of before and after preparation were used for data collection. Each replica was scanned in the midfacial plane 10 times by a coordinate measuring machine (CMM) (Merlin II, International Metrology Systems) with a noncontact 0.83 μm λ laser triangulation probe (Renishaw OP2, Renishaw, Gloucester, United Kingdom) by use of the prepared reference points. Images constructed along these planes were then superimposed and plotted. Shoulder width and angle measurements were taken with the preloaded software (Accudat, International Metrology Systems) for each of the 10 scans. Means and SDs were recorded.

A CMM essentially consists of a probe supported on three mutually perpendicular *(x, y, z)* axes (Figs. 1 and 2). Each axis has a built-in reference standard. In the Merlin II this consists of a stainless steel scale etched with 50 lines per millimeter. An index grating with the same line structure is superimposed at a slight angle to produce an integrated interference pattern, or moire fringe. Photo cells in a noncontact reading head convert this pattern into elec-

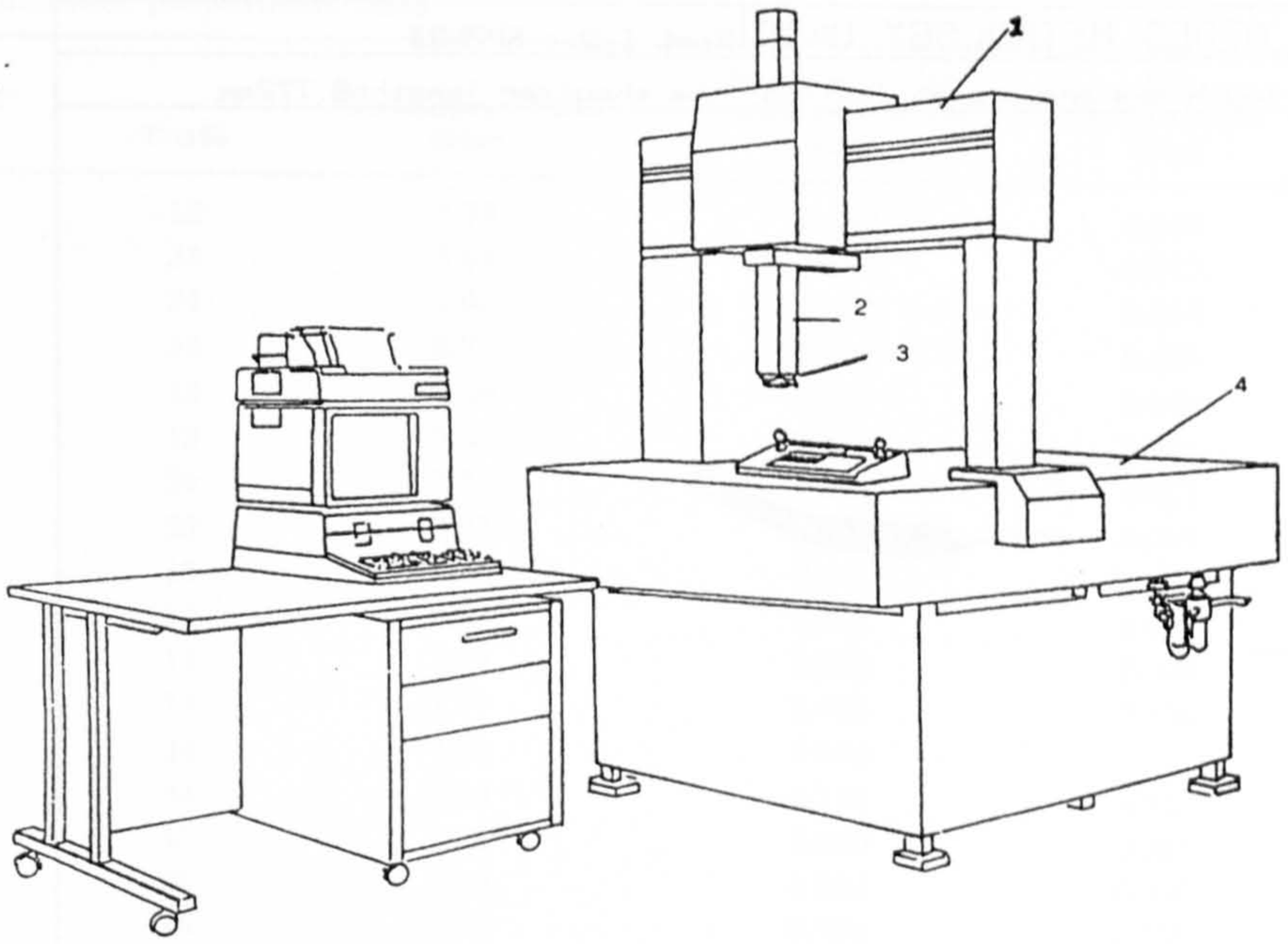

1. Bridge
2. Probe column
3. Kinematic probe mount
4. Work table

Fig. 2. CMM. (Courtesy of International Metrology Systems.)

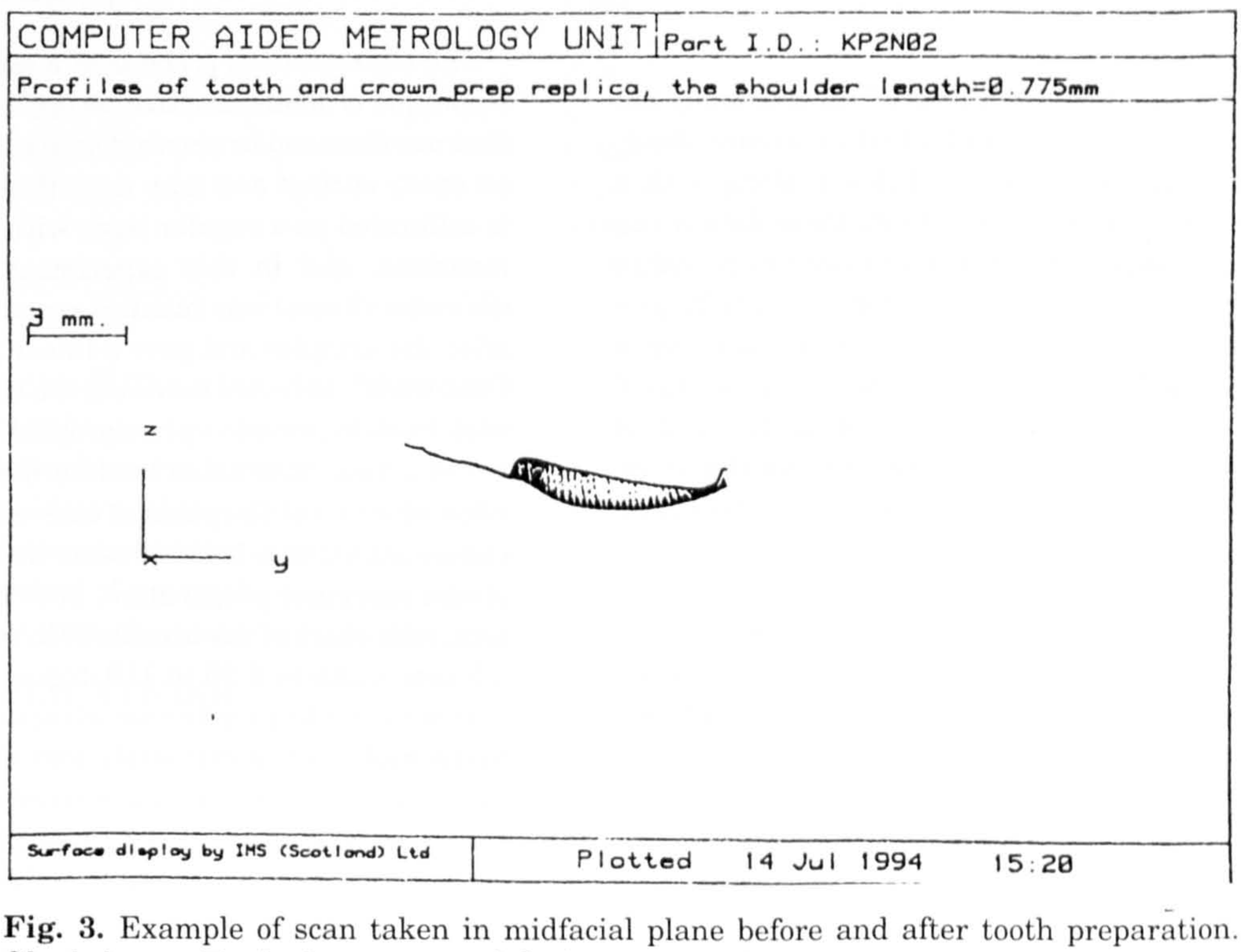

Fig. 3. Example of scan taken in midfacial plane before and after tooth preparation. *Shaded area,* Tooth tissue removed during preparation.

trical signals that are then converted by a processor into a digital display. This digital display instantaneously follows any change in direction and provides accurate information about movement and position of the probes. The relationship of the axes to each other allows a point to be located relative to another point in all three planes with one check. The resulting data can be used to create three-dimensional, near-photographic-quality images that can be manipulated to give various measurements, such as area and volume.

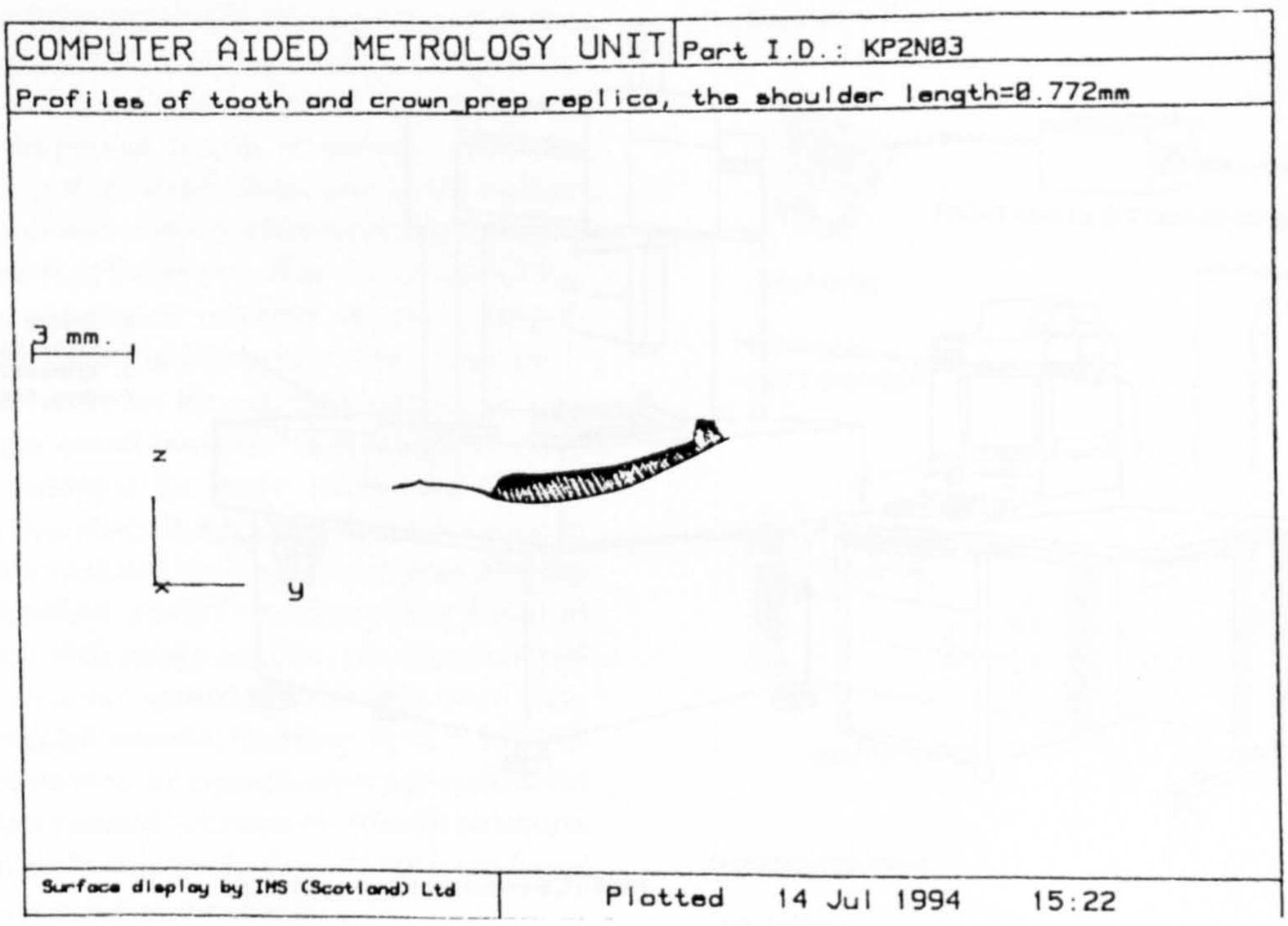

Fig. 4. Example of scan taken in midfacial plane before and after tooth preparation. *Shaded area,* Tooth tissue removed during preparation.

RESULTS

Examples of two sets of profiles used for this study are illustrated in Figs. 3 and 4. Data that relate to each shoulder preparation are presented in Table I, along with a summary of descriptive statistics. From these data it can be seen that of 24 shoulder preparations none were within the recommended range of 1.2 to 1.5 mm in width for precious metal bonding, with a mean throughout the group of 0.752 ± 0.174 mm. Some preparations were only 0.5 to 0.6 mm wide in this plane. For the shoulder angle, 11 of 24 were within the range of 90 to 110 degrees. Of the 13 remaining preparations, 11 were too large and two too small.

DISCUSSION

It was decided to use single-rooted teeth in this study to avoid complications inherent in the preparation of molars in furcation anatomy and the type of margin to be preferred in these areas.[6, 32] Teeth that had large faciolingual widths were also selected because dentists are more likely to reduce shoulder preparations on teeth with small faciolingual widths, such as mandibular anterior teeth. The use of noncarious unrestored teeth permitted the dentists' preparations not to be influenced by the size and position of disease or restorations. The CMM has provided data in a graphic form, which has the benefit of reproducibility. SDs of scans of each sample are reasonably low, with only one greater than 48 μm. A group mean of SDs from 10 scans per sample of ±17 μm is acceptable for studies of this type, particularly when compared with direct measurement of replications, which is less accurate.

The triangulation probe is of a noncontact type, so the technique is nondestructive, as opposed to other machines that use diamond or emerald styli that are dragged across an epoxy surface and may wear the samples.[33] The CMM is calibrated on a regular basis with spheres of known dimensions, and in this experiment a sphere of known diameter (2 mm) was scanned repeatedly both before and after the samples and gave a linear accuracy of ±6.4 μm. Pilot work[25] involved scanning the entire buccal surface of each tooth to provide a photographic-type image; however, use of a superimposable landmark as identified here has allowed scans at the plane of interest for each replicate to reduce scan times. It would seem that in this small in vitro study, marginal preparation, both in width and angulation, falls short of the accepted recommendations of 0.8 to 1.5 mm width and 90 to 110 degree angles.[4]

It is the underpreparation of teeth discussed previously and highlighted in this study that may well contribute to the high rate of failure of metal ceramic restorations that has been observed.[21, 22] An underprepared shoulder has unfavorable implications for the finished crown in either contour or esthetics, where a crown may be overbuilt or the esthetics of the porcelain compromised with a chalky opaque appearance.[20, 34] Overcontoured crowns have consequences for gingival health[35] because many margins are placed subgingivally.[14] Shoulder angle in this study is also of concern because 45% of the prepared shoulders were greater than 110 degrees, and this angle in conjunction with a narrow shoulder will only permit a very thin bulk of unsupported porcelain, which may predispose to frac-

Table I. Shoulder preparation data

Total No.	Tooth	Faciolingual width (mm)	Shoulder width (mean of 10 scans) (mm)	SD (of 10 scans) (mm)	Shoulder angle (mean of 10 scans) (degrees)	Dentist
1	13	7.79	0.687	0.009	101.13	1
2	23	8.33	0.841	0.017	102.38	1
3	34	7.66	0.640	0.015	117.89	2
4	33	6.75	0.736	0.025	101.50	1
5	13	8.56	0.825	0.044	101.00	3
6	13	9.35	1.089	0.014	102.00	1
7	24	7.33	0.561	0.011	129.85	2
8	23	8.27	0.826	0.009	114.52	1
9	13	7.46	0.800		127.00	2
10	14	9.68	1.031	0.004	70.00	2
11	14	8.12	0.688	0.048	121.50	3
12	14	7.37	1.095	0.108	128.25	3
13	34	7.04	0.900		135.00	2
14	24	7.52	0.721	0.028	122.91	1
15	43	7.35	*0.530*	*0.021*	113.50	1
16	25	7.58	0.584	0.015	108.33	2
17	15	7.78	0.761	0.018	86.50	3
18	35	6.61	0.471	0.008	111.00	3
19	15	7.7	0.926	0.014	93.464	3
20	33	6.37	0.759	0.001	99.00	3
21	14	7.93	0.829		96.40	3
22	35	8.05	0.535	0.003	116.14	1
23	15	7.72	0.608	0.019	103.00	2
24	24	7.84	0.604	0.014	102.67	2
Mean			0.752		108.54	
SD			0.174		15.06	
Median			0.748		105.67	
Range			0.624		65.00	
Minimum			0.471		70.00	
Maximum			1.095		135.00	

ture of the restoration.[24] The errors highlighted in this study are similar to those in previous studies of occlusal reduction[23] and taper,[24] where what is taught and commonly accepted is seldom achieved in clinical practice. One aspect of further interest would be to study the reduction of the midlabial portion of the tooth, where esthetic problems occur possibly through similar underpreparation.

CLINICAL IMPLICATIONS

As has been discussed, the clinical implications of this study are that perhaps there is a need to refocus on marginal preparations for metal ceramic crowns because it appears that common causes of failure of these restorations may be due to underpreparation and overangulation of the facial shoulder. Perhaps greater emphasis than at present may have to be placed on this aspect of preparation, not only at the chair side but also during instruction.

CONCLUSIONS

Within the parameters of this in vitro study it appeared that deficiencies occurred in preparations for metal ceramic crowns in shoulder width and angulation. If extrapolated to the clinical situation, these potential inadequacies may have implications for periodontal health and the longevity of the restoration.

We thank our colleagues for allowing scrutiny of their preparations during this study.

REFERENCES

1. General Dental Services analysis of treatments scheduled in year ending March 1993: totals for England and Wales. Eastbourne, United Kingdom: Dental Practice Board, 1993.
2. Bell AM, Kurzeja R, Gamberg MG. Ceramometal crowns and bridges: focus on failures. Dent Clin North Am 1985;29:763-78.
3. Shillingburg HT, Hobo S, Fisher DW. Preparation design and margin distortion in porcelain fused to metal restorations. J PROSTHET DENT 1973;29:276-84.
4. Pameijer CH, Kikutake T. Enhancing esthetics in porcelain fused to metal through technique modifications. Dent Clin North Am 1985;29:753-62.
5. Hobo S, Shillingburg HT. Porcelain fused to metal: tooth preparation and coping design. J PROSTHET DENT 1973;30:28-36.
6. Hooper SM, Huggett R, Foster LV. Teaching veneer and crown margins in UK dental schools. Dental Update 1993;20:192-6.
7. Gardner FM. Margins of complete crowns—literature review. J PROSTHET DENT 1982;48:396-400.

8. Rosner D. Function, placement, and reproduction of bevels for gold castings. J PROSTHET DENT 1963;13:1160-4.
9. Sozio RB. The marginal aspect of the ceramometal restoration: the collarless ceramometal restoration. Dent Clin North Am 1977;21:787-801.
10. Berman LH. The complete-coverage restoration and the gingival sulcus. J PROSTHET DENT 1973;29:301-9.
11. Preston JD. Rational approach to tooth preparation for ceramo-metal restorations. Dent Clin North Am 1977;21:683-98.
12. Hunter AJ, Hunter AR. Gingival margins for crowns: a review and discussion, II: discrepancies and configurations. J PROSTHET DENT 1990; 64:636-42.
13. Silness J. Periodontal conditions in patients treated with dental bridges, II: the influence of full and partial crowns on plaque accumulation, development of gingival pocket formation. J Periodontal Res 1970;5:219-24.
14. Reeves WJ. Restorative margin placement and periodontal health. J PROSTHET DENT 1991;66:733-6.
15. Felton DA, Kanoy BE, Bayne SC, Wirthman GP. Effect of in vivo margin discrepancies on periodontal health. J PROSTHET DENT 1991;65:357-64.
16. British Society for Restorative Dentistry. Guidelines for crown and bridgework. Eur J Prosthodont Rest Dent 1993;1:189-95.
17. Butel EM, Campbell JC, DiFiore PM. Crown margin design: a dental school study. J PROSTHET DENT 1991;65:303-5.
18. Stern N, Grajower R. Tooth preparation for full coverage—basic principles and rationalized clinical procedures. J Oral Rehabil 1975;2:325-31.
19. Stein RS, Kuwata M. A dentist and a dental technologist analyze current ceramo-metal procedures. Dent Clin North Am 1977;21:729-49.
20. Donovan T, Prince J. An analysis of margin configurations for metal ceramic crowns. J PROSTHET DENT 1985;53:153-7.
21. Walton JN, Gardner FM, Agar JR. A survey of crown and fixed partial denture failures: length of service and reasons for replacement. J PROSTHET DENT 1986;56:416-21.
22. Cheung GS. A preliminary investigation into the longevity and causes of failure of single unit extracoronal restorations. J Dent 1991;19:160-3.
23. Freeman JE, Setchell DJ. Occlusal reduction of typodont teeth for full crown preparations by experienced restorative dentists [Abstract]. J Dent Res 1989;68:584.
24. Nolan K, Cassidy M. Computer assisted measurement of full veneer crown taper [Abstract]. J Dent Res 1989;68:584.
25. Seymour K, Zou L, Lynch E. Three-dimensional cavo-surface margin, crown and gingival contour measurements [Abstract]. J Dent Res 1995;74:952.
26. Zou L, Jovanovski V, Bedford J, Lynch E. Generation of photo realistic images from three dimensional data [Abstract]. J Dent Res 1993;72:742.
27. Bedford J, Zou L, Jovanovski V, Lynch E. Reproducibility of data collected by a coordinate measuring machine [Abstract]. J Dent Res 1993;72:742.
28. Jovanovski V, Zou L, Bedford J, Lynch E. Geometric superimposition of a sequence of digitized replicas [Abstract]. J Dent Res 1993;72:742.
29. Lynch E, Zou L, Bedford J, Jovanovski V, Burke F. Measurement of lesions of primary root caries [Abstract]. J Dent Res 1993;72:742.
30. Seymour K, Johnson N, Zou L, Mehmet J, Lynch E. Crestal bone measurement using radiovisiography and a co-ordinate measuring machine [Abstract]. J Dent Res 1995;74:951.
31. Yeganeh S, Morris-Clapp C, Zou L, Lynch E. Quantitative analysis of exposed root surfaces, 'abrasion' cavities and gingivae [Abstract]. J Dent Res 1995;74:951.
32. Wang HL, Burgett FG, Shyr Y. The relationship between restoration and furcation involvement on molar teeth. J Periodontol 1993;64:302-5.
33. Taylor JL, Spencer JL, Breuer MM, DeLong R, Pintada MR, Douglas WH. Digital technique for measuring changes in gingival contour [Abstract]. J Dent Res 1993;72:243.
34. Hunter AJ, Hunter AR. Gingival crown margin configurations: a review and discussion, I: terminology and widths. J PROSTHET DENT 1990;64:548-52.
35. Erpenstein H. The role of the prosthodontist in the treatment of periodontal disease. Int Dent J 1986;36:18-29.

Reprint requests to:
DR. KEVIN SEYMOUR
DEPARTMENT OF CONSERVATIVE DENTISTRY
DENTAL SCHOOL
LONDON HOSPITAL MEDICAL COLLEGE
TURNER STREET
LONDON, E1 2AD
UNITED KINGDOM

New product news

The January and July issues of the Journal carry information regarding new products of interest to prosthodontists. Product information should be sent 1 month prior to ad closing date to: Dr. Glen P. McGivney, Editor, SUNY at Buffalo, School of Dental Medicine, 345 Squire Hall, Buffalo, NY 14214. Product information may be accepted in whole or in part at the discretion of the Editor and is subject to editing. A black-and-white glossy photo may be submitted to accompany product information.

Information and products reported are based on information provided by the manufacturer. No endorsement is intended or implied by the Editorial Council of THE JOURNAL OF PROSTHETIC DENTISTRY, the editor, or the publisher.

Nanobiology, 1996, Vol. 04, pp. 55–61
Reprints available directly from the publisher
Photocopying permitted by license only

Objective Assessment of Three-Dimensional Structures in Clinical Dentistry Using Methods of Coordinate Metrology

V. JOVANOVSKI[a,*], W. M. TAY[a], L. ZOU[a], I. J. ANDERSON[b,c], M. G. COX[b], A. B. FORBES[b], H. ALLRED[a], S. I. MORGANSTEIN[a] and E. LYNCH[a]

[a]*Department of Conservative Dentistry, St. Bartholomew's and the Royal London School of Medicine and Dentistry, Turner St., London E1 2AD;* [b]*Centre for Mechanical and Optical Technology, National Physical Laboratory, Teddington, Middlesex, TW11 0LW;* [c]*Cranfield Royal Military College of Science, Shrivenham, now at School of Computing and Mathematics, University of Huddersfield*

Conservative dentistry is concerned with all aspects of the conservation and restoration of teeth as well as the whole care of the patient. These include the prevention and management of dental caries, the placing of restorations, the construction of crowns and bridges, the treatment of infected pulps, and the replacement of missing teeth. As such, the assessment of three-dimensional structures, including the morphologies and relationships of teeth, the position and contour of the gum, the surface characteristics of fillings, and their adaptation to the teeth in which they are placed is constantly required. Much assessment is subjective, although dentists may enhance this by using plaster casts taken from replicas or impressions of teeth (Allred, 1977; Elderton, 1975). This paper describes an initial phase of work concerned with the application of methods of coordinate metrology and supporting mathematical models and software to quantify various aspects of these structures. Coordinate data representing the surface of a replica is acquired using a suitable measuring instrument having an optical probe. Mathematical analysis of this data then permits detailed information to be deduced concerning the geometry of the surface. In particular, (i) the surface can be displayed graphically and examined from various viewpoints, (ii) lengths, surface areas and volumes can be calculated, and (iii) measurements from replicas obtained at different times can be used to supply accurate information on the changes in the surface due to, for example, decay, plaque formation, restorative work, gum recession, wear, tooth movement or the healing of ulcers. The paper covers problem introduction, data-acquisition methods, mathematical models, computational algorithms and an illustrative example.

Keywords: metrology, morphology, surfaces, dentistry

INTRODUCTION

The examination of structures in the oral cavity in greatest part involves subjective assessments of morphology: When dentists intervene by carrying out some form of treatment, continuing subjective judgements are made of the changes in form brought about. If objective data were available to support the analysis and comparison of form, a much more effective basis could be established for the treatment of patients, and also for the teaching of students.

Dentistry, and particularly Conservative Dentistry, involves the precise replication of teeth and related oral structures in elastic polymeric impression materials.

*Corresponding author

These provide stable negative copies from which a Co-ordinate Measuring Machine fitted with a laser probe, can capture coordinate data. From these data points, a mathematical model of the surface can be produced. Researchers and clinicians, including student clinicians and their teachers, can thus be provided with a means of obtaining objective and accurate measurements and comparisons of morphology.

MATERIALS AND METHODS

The Data Acquisition Hardware

The work of the Dental Metrology Unit at St. Bartholomew's and the Royal London School of Medicine and Dentistry is based on a Ferranti Merlin II Coordinate Measuring Machine (CMM) using an infra-red laser probe ($\lambda = 830$ nm) which is capable of recording the 3D coordinates of points on the surface of an object at a frequency of 50 points per second. The measurements are accurate to within 5 μm (Lynch *et al.*, 1990), but the generality of the overall approach outlined here means that it could exploit other more precise coordinate measuring systems. The CMM is controlled by an IBM PC compatible computer which, in turn, is connected via a local area network to a central file server where data for each replica are stored as soon as they are collected.

The Data Acquisition Software

The data acquisition software, which runs on the CMM controlling computer, allows the unattended processing of a batch of replicas (currently up to 36) which are placed at previously marked positions on the measuring platform of the CMM. The software presents a user-friendly interface to the operator who indicates the occupied positions and enters the acquisition parameters provided by the researcher for each replica. These parameters include the spacing of the captured points and the coordinates of the region of interest, which may consist of a relatively small region of the replicated surface.

The Production of Replicas

The production of replicas is achieved in the current studies by a standard routine which uses square section brass tubing (12 mm × 12 mm) to obtain silicone polymer replicas of, say, a tooth surface and the adjacent gingivae. The surface under investigation is first identified *in vivo*. A routine alginate impression of the whole dental arch in which this surface is to be found is taken and a stone cast or model is obtained from it. The brass tube is placed over the area under investigation and its periphery is modified as necessary using a stone or a file so as to approximate the surface reasonably well. Methacrylate resin is adapted to the outer surface of the tube and onto the neighbouring teeth for stability, whilst permitting its precise removal and repositioning (Figure 1). After being sterilised, the tube assembly is placed in the mouth over the clean, air dried surface to be replicated. A small quantity of impression material is injected, air is blown onto it to ensure that it is spread over the whole surface and the whole tube is filled. After a polymerising time length of four minutes the replica is pushed out of the tube, leaving the tube ready for use in subsequent replication of the same region. The replica is then sprayed with distilled water, dried with an air jet and powdered with pyrolytic silica with a particle size of about 1 µm, to minimise its reflectivity. It is placed on the measuring platform and the data acquisition process is initiated.

The Measurement of Replicas

Each replica is placed, with its "crown" approximately horizontal, in a mount having a flat base and a square horizontal cross-section. The mount is positioned on the measuring platform of the CMM.

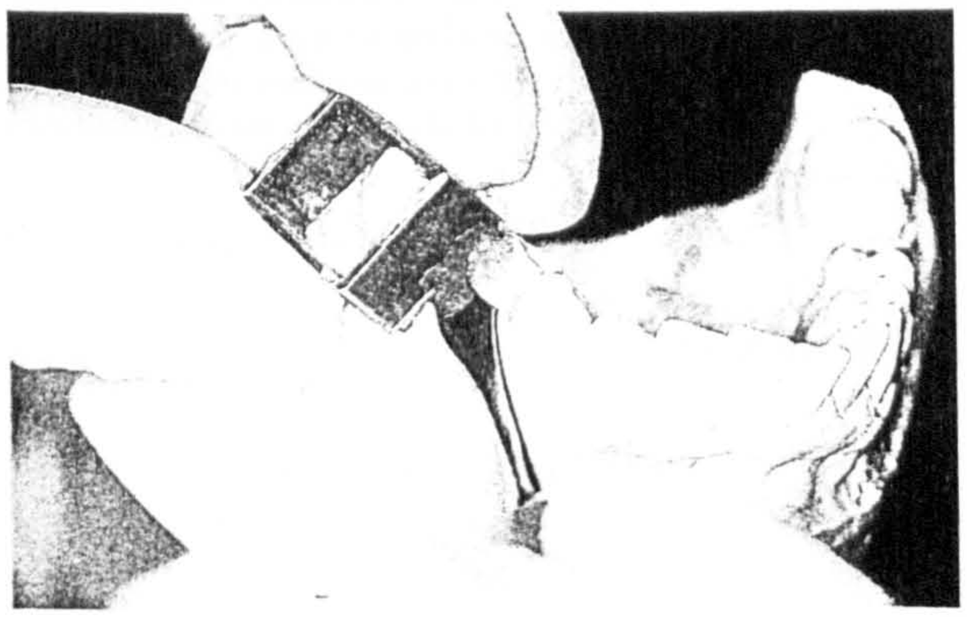

FIGURE 1 A brass tube is placed over the area under investigation, shaped as necessary and methacrylate resin is adapted to the tube and neighbouring teeth for stability. (See Color Plate 1 at the back of this issue.)

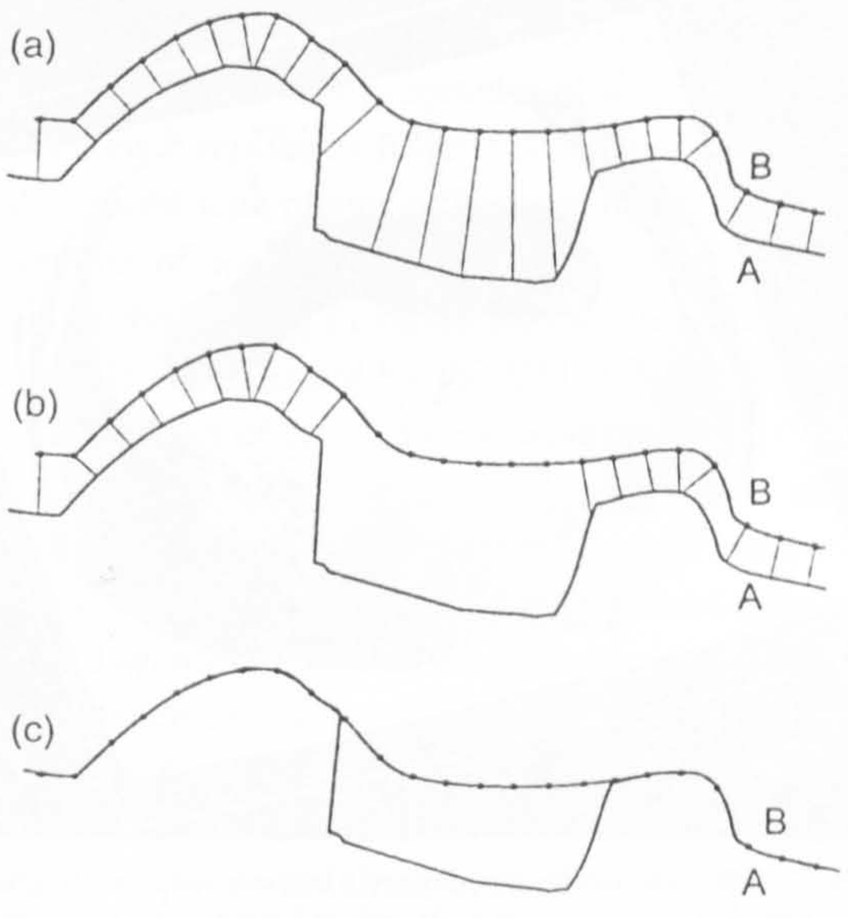

FIGURE 2 Three stages in the superposition of two profiles.

are removed from the two sets, as it is assumed that they lie in a region which has changed (Figure 2(b)). The specified value has to be chosen with care and should be related to the imprecision of the overall process (cf. the first paragraph in this section). We have found that the choice of 50 μm to be generally satisfactory. We now have two sets of representative points A and B from the two profiles.

In two dimensions, the transformation (2) has only one unknown parameter: the matrix $\mathbf{R}$ has the form

$$\mathbf{R} = \begin{bmatrix} \cos\alpha & -\sin\alpha \\ \sin\alpha & \cos\alpha \end{bmatrix}$$

where α is the angle of rotation around the coordinate origin in an anticlockwise direction. This angle can be calculated directly:

$$\tan\alpha = \frac{\sum_{i=1}^{m} \mathbf{a}_i^T \begin{bmatrix} 0 & 1 \\ -1 & 0 \end{bmatrix} \mathbf{b}_i}{\sum_{i=1}^{m} \mathbf{a}_i \mathbf{b}_i}$$

In three dimensions the three rotation angles give rise to a system of nonlinear overdetermined equations in three variables which can be solved by iterative methods such as Gauss-Newton or its variants. Applying (2) to profile A produces a new set of points $A' = f(A)$ (Figure 2(c)). The procedure is repeated on profiles A' and B until suitable convergence criteria are satisfied.

The Software for Visualisation and Measurement

Currently under development is a software package for data visualisation and measurement which runs on IBM-compatible personal computers. This package should allow researchers, clinicians and students to perform their own analyses, relying on the central facility only for the acquisition of data.

To illustrate some of the capabilities of this package we have selected three stages in the treatment of a carious occlusal surface of a human molar tooth. The dimensions of the area of interest are 10 mm × 10 mm and 56 000 points were sampled from each replica.

The first replica taken was that of the untreated surface. Available display views are shaded (Figure 3), wireframe and elevation map. A profile with any plane can be taken, as shown by the dark line.

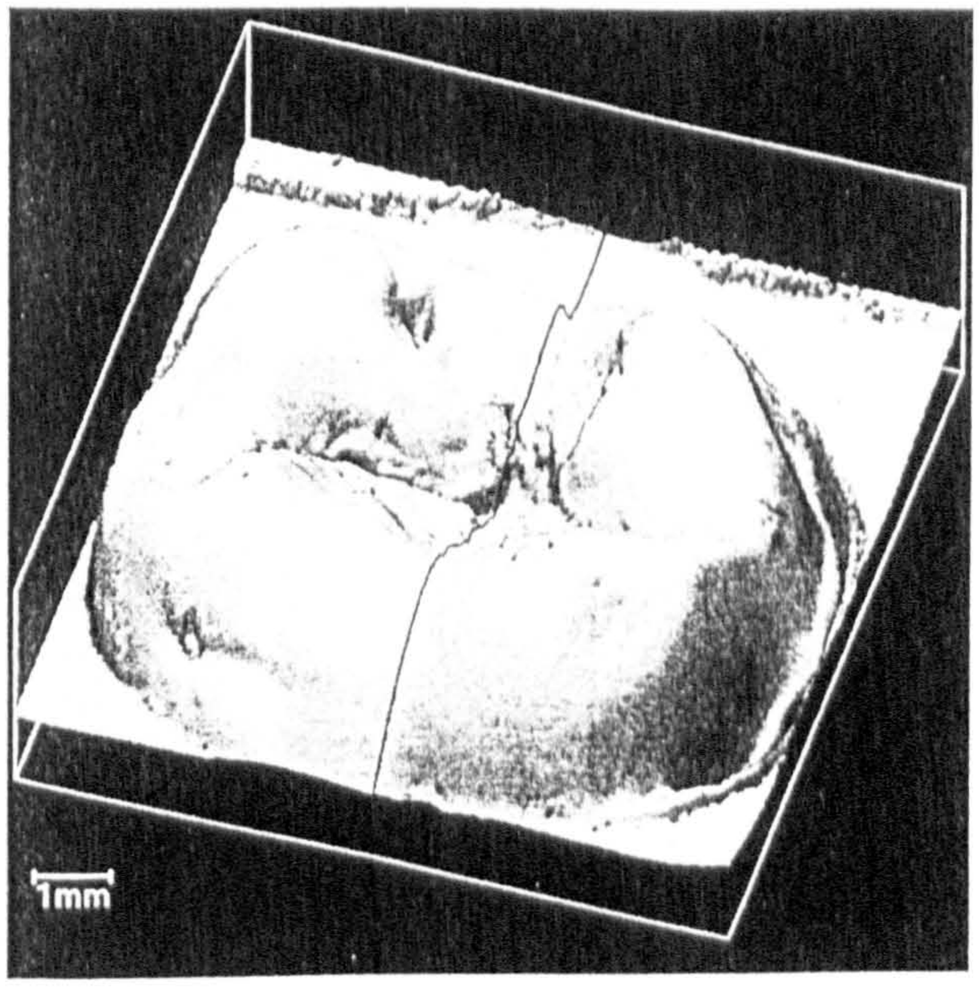

FIGURE 3 The carious occlusal surface of a human molar tooth before treatment. Image reconstructed from coordinate data.

The profile can then be displayed to allow measurement of linear dimensions and angles. The measurements are made with a tool which consists of two segments joined at a common vertex (Figure 4). The endpoints of each segment can be adjusted by the user, giving a constantly updated display of the lengths of the two segments and the angle between them.

A contour map (step = 200 μm) of the first replica can be plotted (Figure 5).

A second replica was made after the cavity was made caries-free, lined, based and prepared for a composite inlay restoration (Figure 6).

The third replica is that of the composite inlay tried into the tooth (Figure 7).

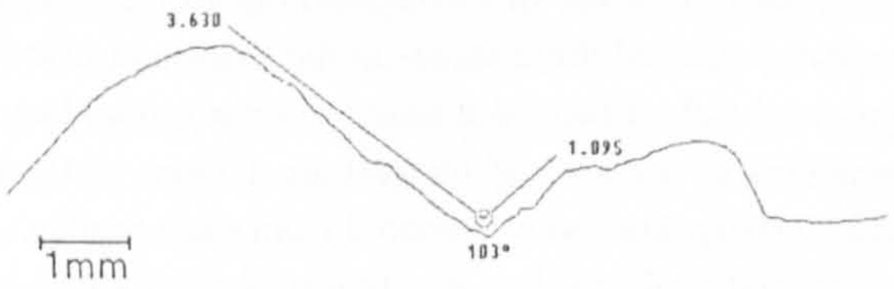

FIGURE 4 Linear and angular measurements of a profile of the

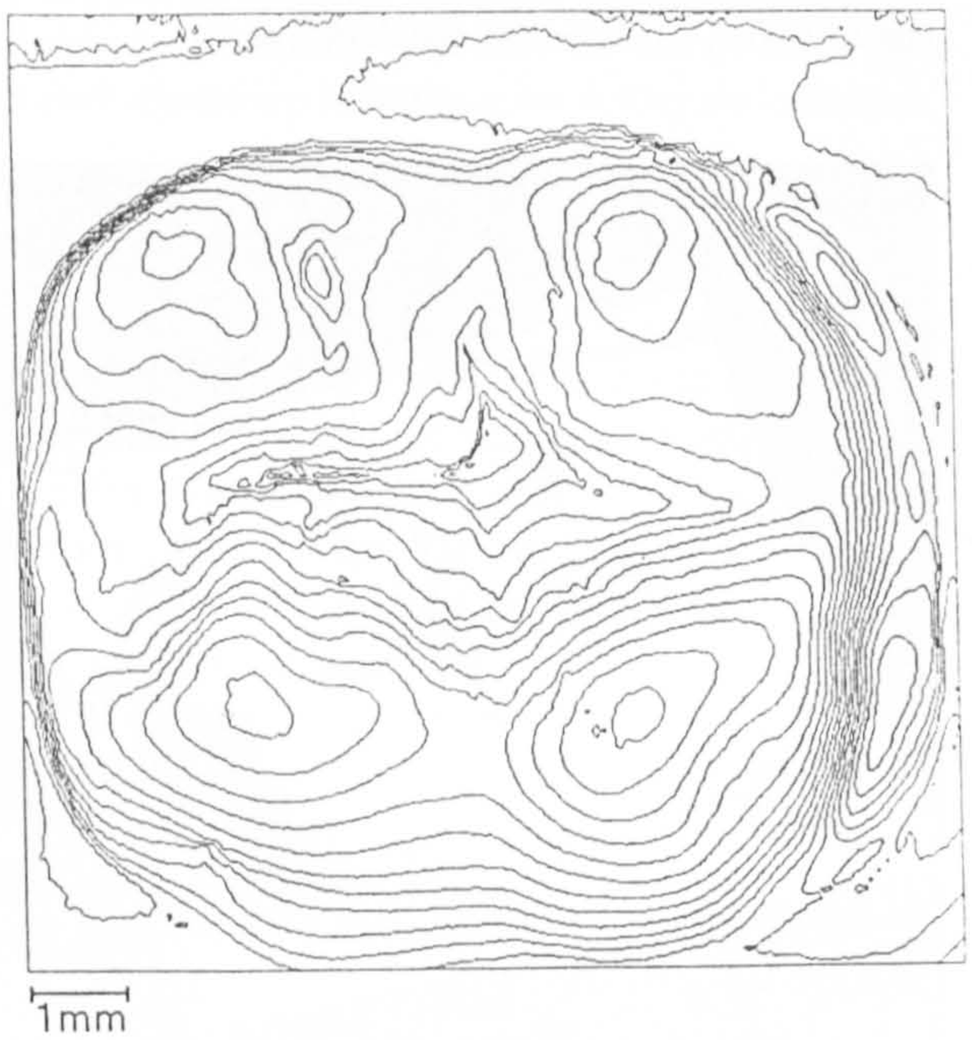

FIGURE 5 A contour map (step = 200 μm) of the carious occlusal surface of a human molar tooth before treatment. Image reconstructed from coordinate data.

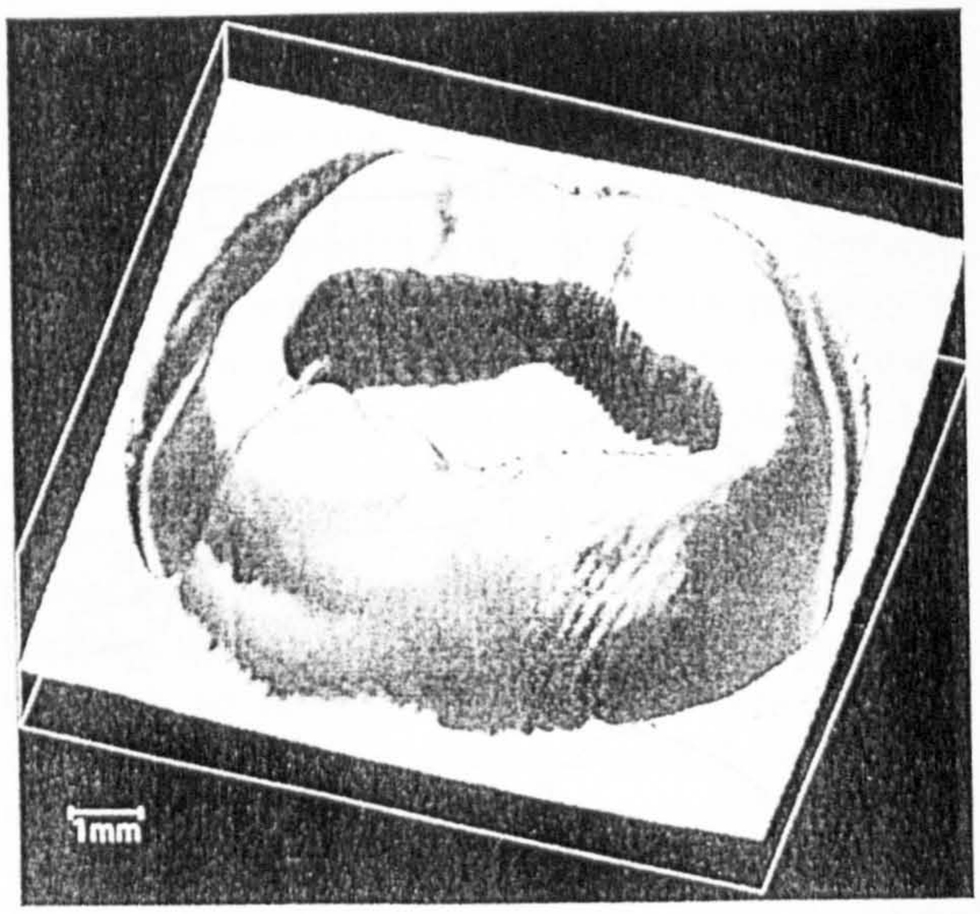

FIGURE 6 The occlusal surface of a human molar tooth which has been made caries-free, lined, based and prepared for a composite inlay restoration. Image reconstructed from coordinate data.

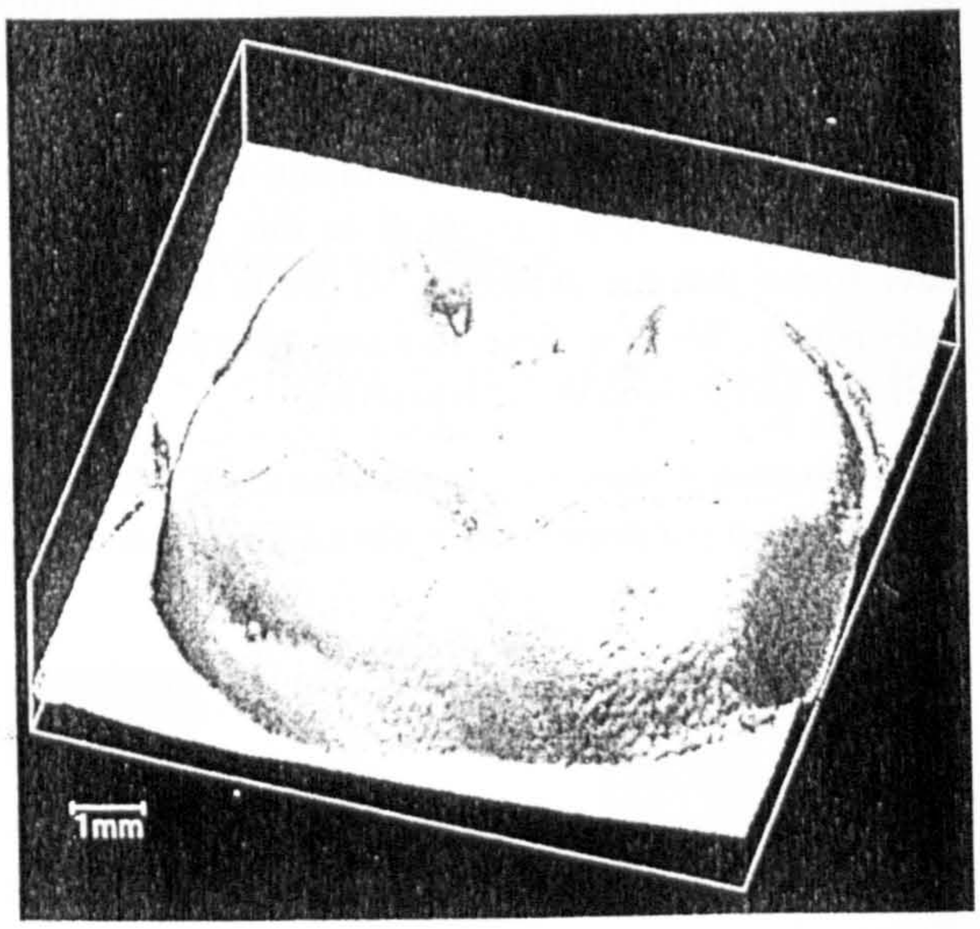

FIGURE 7 The occlusal surface of a human molar tooth after the composite inlay was tried into the prepared cavity. Image reconstructed from coordinate data.

Three corresponding profiles across the molar tooth were superposed. The three profiles were taken (a) before treatment, (b) after inlay preparation and (c) after try-in of the inlay (Figure 8).

The CMM, which operates in terms of a Cartesian coordinate system with x- and y-axes parallel to the measuring platform, is programmed to take measurements on each replica as follows. Consider a set of uniformly spaced scan planes orthogonal to the y-axis. The intersection of any of those planes and the replica is a section of the replica. For each of these sections, a surface profile is measured by the CMM's laser probe in the form of a set of (x, y, z) coordinate points.

Ideally, only the x and z coordinate values would vary along a profile. However, the measurement process is such that the value of y that is nominally constant for a scan plane cannot be perfectly controlled. As a consequence the points in the profile do not lie in a plane curve. In fact they can exhibit significant departure from a plane, and profiles can even intersect. In any case the points obtained in each scan plane are regarded as (generally non-planar) curves in the surface of the replica, defined pointwise as z in terms of x and y. Modelling the surface of a replica requires the construction of a surface from the set of surface curves.

In order to limit the extent of the set of scan planes and the scanning within each such plane, a simple setting-up procedure is used before the bulk of the measurements is taken for a replica.

Starting at the approximate centre of each replica, as determined by the marked positions on the measuring platform, the surface is scanned radially outwards in four directions. The edges of the specimen are clearly identified since there is a significant drop in the value of the measured z coordinate at these points, from which the coordinates of the centre is calculated. Thus, the absolute coordinates of the region of interest can be determined independently of the actual position of the specimens on the measuring platform.

The Mathematical Representation of Surfaces

The data returned by the laser probe consist of discrete (x, y, z) triplets but, in order to compute length, angle, area and volume or to visualise the surface, we need the ability to determine the values of the z-coordinate and the surface normal vector for any values of x and y. The precision, speed and ease with which such computations can be performed is critically dependent on the properties of the mathematical representation of the surface as a function $z = f(x, y)$. Considerable experience with the use of bivariate polynomial splines (Cox, 1993) for a wide range of "difficult" surface fitting problems helped us to conclude that for this purpose bivariate polynomial splines possess the greatest number of desirable properties.

A significant complication in representing the surface in this way, is introduced by the fact that the points recorded by the CMM do not lie on a rectangular grid. This is due to deviations of the probe from an ideally straight line, as indicated above, and the fact that the density of captured points is constant along the length of the surface profile rather than along the x-axis. It was found that the grid could be regularised without introducing unacceptably large errors by performing two successive approximations (Anderson *et al.*, 1993), first along the x-axis and then along y. This procedure is carried out as follows:

First, each scan line is represented by a spatial curve using a suitable least-squares fitting process. This is undertaken by regarding x as a parameter and fitting y as a function of x, and z as a function of x. We expect, of course, much greater variation in the latter function since it corresponds (approximately) to a tooth profile, whereas the former represents the much smaller systematic departure of y from its nominally constant value. The result is a set of spatial curves lying in (or near) the tooth surface, each of which 'almost' lies in the plane orthogonal to the y-axis.

Second, each of these spatial curves is evaluated at a set of uniformly spaced values of the parameter x. (It is not strictly essential that the values of x, at which the spatial curves are evaluated, are uniformly spaced. However, such a choice is simple and convenient for the scan data that we are using). This gives, for each value of x, a set of (y, z) coordinates that represent points approximately on a tooth surface profile of a planar section that is perpendicular to the x-axis. These points will be approximately on surface profiles since we use fitting in order to obtain the spatial curves as functions of x. Each of these profiles is represented as a planar curve using a least-squares fitting process to express z as a function of y. This produces planar curves that approximate tooth surface profiles of planar sections uniformly spaced along and perpendicular to the x-axis.

Third, each of these planar curves is evaluated at a set of uniformly spaced* values of y. The result is an array of z-coordinates that approximate the height of the tooth surface at the vertices of a rectangular mesh defined by the uniformly spaced x and y values.

With the points on a rectangular grid, a spline interpolant of these points to represent the surface can be calculated and used extremely efficiently (Cox, 1993).

The Superposition of Sequential Replicas

Because we are especially concerned with the measurement of changes in morphology it was decided that an early priority should be to attempt to superpose data from a sequence of replicas. It is to be expected that, even in the simple case of replicating and scanning a single surface twice, the coordinates of sampled points on the two surfaces will have very little in common when viewed as two sets of numbers. Some reasons for this are:

- the probable lack of precision when the clinician positions the brass tube assembly;
- possible differences in the orientation of the replicas on the measuring platform;
- the physical properties of the impression material;
- any contamination of the surfaces by blood, saliva, dust or water;
- CMM errors;
- and other variations which are inherent in any clinical procedure.

Superposition of surface data from two nominally identical replicas consists of applying a rigid transformation to one of the sets with the result that pairs of corresponding points have essentially the same coordinates. The term 'corresponding' denotes pairs of points which represent the same point on the surface from which the replicas are taken. In three-dimensional space such a transformation has the form

$$f(\mathbf{x}) = \mathbf{R}\mathbf{x} + \mathbf{t} \qquad (1)$$

where $\mathbf{R}$ is a 3×3 rotation matrix and $\mathbf{t}$ a translation vector. The parameters of this transformation are the angles of rotation around the three coordinate axes and the components of the translation vector.

Let $A = \{\mathbf{a}_1, \mathbf{a}_2, \ldots, \mathbf{a}_m\}$ and $B = \{\mathbf{b}_1, \mathbf{b}_2, \ldots, \mathbf{b}_m\}$ be two sets of coordinate points obtained from a single replica on two different occasions in which points $\mathbf{a}_i$ and $\mathbf{b}_i$ correspond. Taking into account the fact that the data contain measurement errors, the parameters of (1) can be determined from the least-squares solution of the system of equations

$$\mathbf{b}_i = \mathbf{R}\mathbf{a}_i + \mathbf{t} \quad (i = 1, 2, \ldots, m).$$

If $\bar{\mathbf{a}}$ and $\bar{\mathbf{b}}$ are the centroids of sets A and B ($\bar{\mathbf{a}} = \frac{1}{m}\sum_{i=1}^{m} \mathbf{a}_i$ and $\bar{\mathbf{b}} = \frac{1}{m}\sum_{i=1}^{m} \mathbf{b}_i$) it can be shown that the transformation which maps set A into the reference frame of set B has the form

$$f(\mathbf{x}) = \mathbf{R}(\mathbf{x} - \bar{\mathbf{a}}) + \bar{\mathbf{b}} \qquad (2)$$

by which the number of unknown parameters is reduced to three and numerical accuracy is improved by centering the points around the coordinate origin.

The preceding discussion is valid for pairs of surfaces which are nominally identical. As we are dealing with surfaces which have undergone changes, in order to apply such a procedure we require the data acquired from each surface to include a region which remains stable. From such stable regions two sets of representative points are selected, and it is these points that permit the method of superposition to be applied.

This method can be illustrated by its two-dimensional analogue – the superposition of two profiles, A and B, in a plane. It is iterative in nature, being based on a fixed set of points in profile B and a set of points in profile A which is determined adaptively. The two profiles are first brought into approximate alignment using suitable visualisation software. All transformations are applied to profile A, while profile B remains fixed. The set of representative points is selected on profile B at equidistant intervals on the x axis. At each iteration, for each point on profile B, its corresponding point on profile A is determined by the normals through profile B (Figure 2(a)). In order to ensure that only points in stable regions are compared, all pairs of points whose distance is greater than a specified value

*Again, uniformly spaced values are convenient, but not essential.

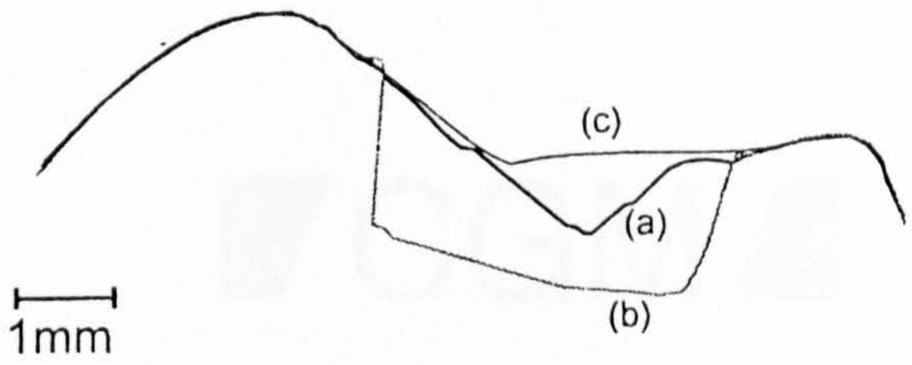

FIGURE 8 Three profiles of a molar tooth. (a) Before treatment. (b) After inlay preparation. (c) After try-in of the inlay.

CONCLUSION

Coordinate metrology is an effective method for obtaining objective data about oral structures. The accuracy is sufficient for this method to be reliable, and with the appropriate mathematical analysis the clinician and researcher can be provided with much valuable visual and quantitative information that would otherwise be unavailable or speculative.

References

Allred, H. (1977) *A Series of Monographs on the Assessment of the Quality of Dental Care*. Experimental Dental Care Project. The London Hospital Medical College, London.

Anderson, I. J., Cox, M. G. and Mason, J. C. (1993) Tensor-product spline interpolation to data on or near a family of lines, *Numerical Algorithms* **5**, 193–204.

Cox, M. G. (1993) Algorithms for spline curves and surfaces, in *Fundamental Developments of Computer-Aided Geometric Modelling* (Piegl, L. Ed) Academic Press, London, pp. 51–76.

Elderton, R. J. (1975) *An in vivo morphological study of cavity and amalgam margins on the occlusal surfaces of human teeth*. Ph.D. Thesis, University of London.

Lynch, E., Tan, R., Tay, W. M., Smales, F. C., Morganstein, S. I. and Allred, H. (1990) Performance of a coordinate measuring machine with a laser probe. *Journal of Dental Research* **69**:344, Abstract No. 1886.

CGM

IMEKO

INTERNATIONAL MEASUREMENT CONFEDERATION
IMEKO

4th International IMEKO symposium on

LASER METROLOGY FOR PRECISION MEASUREMENT AND INSPECTION IN INDUSTRY

PROCEEDINGS

IMEKO TC No. 14

Lyngby, Denmark
October 21-22, 1996

Center for Geometrical Metrology
Technical University of Denmark

CONTENTS

Measurement of form

Measurement of surface

Measurement of displacement

Lasers and interferometry

Applications

Measurement of tooth morphology using a laser probe fitted on a Co-ordinate Measuring Machine

L. Zou, Q.P. Yang[1], V. Jovanovski, W. M. Tay and E Lynch
Dept. of Conservative Dentistry, St. Bartholomew's and the Royal London School of Medicine and Dentistry, Turner Street, London E1 2AD, UK;
[1]Dept. of Manufacturing and Engineering System, Brunel, The University of West London, Uxbridge, Middlesex UB8 3PH, UK.

Summary

Three dimensional measurements of tooth morphology are demanded in various areas of dental research. This can be realised using a Co-ordinate Measuring Machine (CMM) with an optical probe. In order to achieve accurate digitisation of sculptured surfaces like tooth surface, it is necessary to study the measurement errors involving different scanning parameters. This paper discussed the characteristics of the probe error distribution in relation to the measurement of tooth morphology.

Keywords: Co-ordinate Measuring Machine, Laser probe, Morphology

1. Introduction

In recent years, 3D Co-ordinate Measuring Machines (CMMs) have become increasingly important for quality control in modern industries. They can be used for measuring complicated shapes such as sculptured surfaces. Three dimensional measurements of tooth morphology are demanded in various areas of dental research, such as assessing the geometrical shape of crown preparations in terms of shoulder width and preparation angle[1,2,3]; investigating tooth wear and gingival margin changes[4]; and calculating volume changes before and after a treatment regime[5]. The precise replication of the forms of oral structures is essential for representing the oral structure.

The tooth replicas use the most stable dental impression material - a polyvinylsiloxane (Kerr) which has high elastomer characteristics. As the replica can be easily deformed by mechanical contact, a non-contact laser probe (Renishaw OP2, λ=830nm, P(max)=5mw) has been employed despite its surface dependence.

The probe works on the principle of optical triangulation, and is connected to a motorised probe head PH9 (Renishaw). The probe can be rotated in a step of 7.5° in two axes: vertically in the range of -180° to +180° and horizontally in the range of 0° to 105°, with a positioning repeatability (2σ) of 0.5μm. The PH9 probe head is mounted to a CMM (IMS Merlin II), which is of a bridge type, with an axial length measuring accuracy refer to using a mechanical probe: $E(\mu m) = 4.0 + L(mm) / 275$ and volumetric length measuring accuracy $E(\mu m) = 5.0 + L(mm) / 150$, where L is the measured length.

The measuring uncertainty of a CMM is caused by many factors including geometrical errors (e.g. straightness and squareness) of the CMM movement and dynamic errors (e.g. hysteresis and backlashes) [6]. In many cases, however, the errors introduced by the probe are very significant and often exceed the size of the errors from other sources. This is the case especially for optical probes.

Theoretically an accuracy of ±10μm is obtainable, but, in practice, this is compromised not only by inherent inaccuracies in the probe itself but especially by (1) the disturbing intensity distribution of the light spot due to macroscopic and microscopic changes in reflectivity, volume scattering and the geometry of the object surface; (2) ambient light, non-linearity on lateral effect diodes, and delay of the analogue signal [7]. The most significant factor affecting the probe accuracy in dental research is the approaching angle between the surface normal and the incident beam on tooth replicas [8].

The digitised data may not be uniformly spaced due to the variation of the delay in data acquisition. For proper surface visualisation and reconstruction, matched sets of uniformly spaced data points are required. The software creates a regularly spaced grid from the irregularly spaced raw data by interpolation; in effect, interpolating the Z-value for every(X,Y) point at the intersection of each row and column. Then a mirror translation converts the surface points from negative to positive, with the final images as shown in Fig.2.

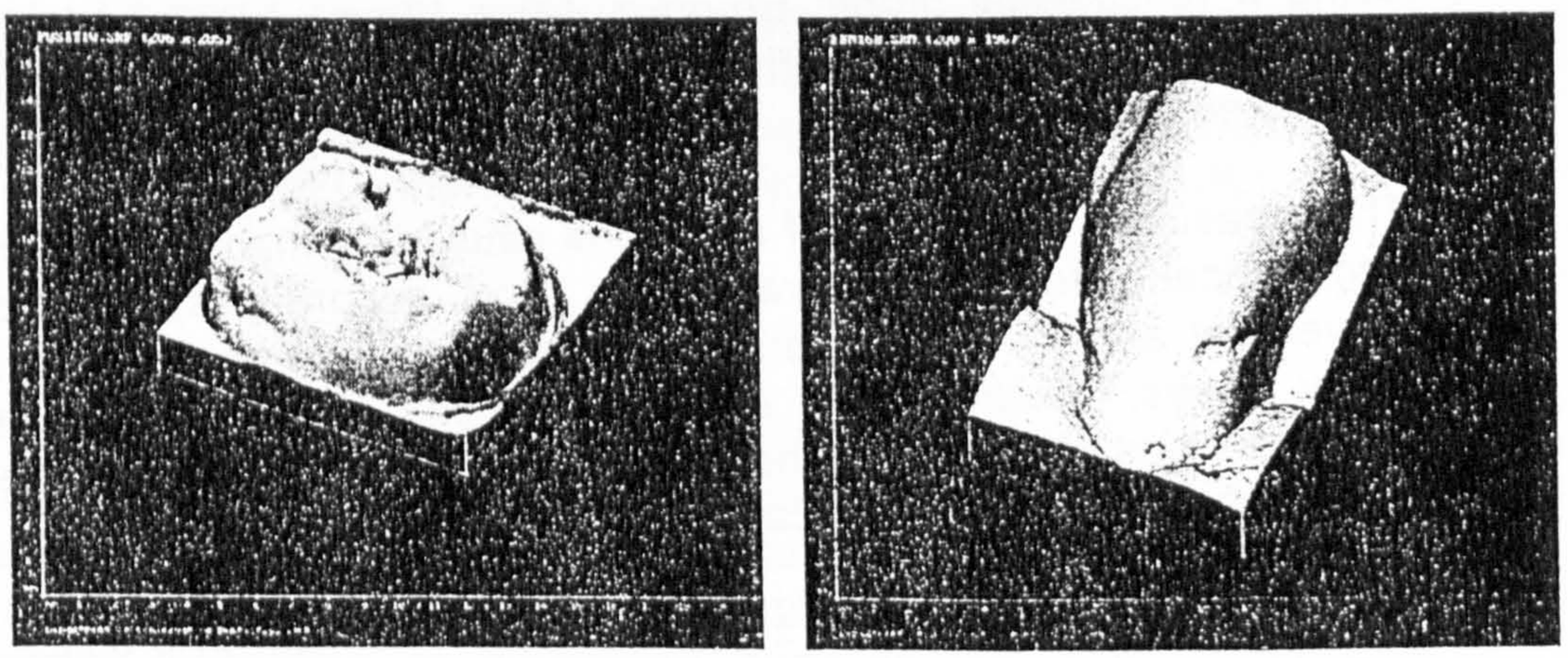

Fig.2 Digitised images of occlusal(left) and buccal(right) tooth surface

3. Digitising parameters

Before carrying out a data digitising procedure, the following four parameters need to be determined: 1) scan pitch, i.e. the interval of the points along a scan line; 2) scan speed, i.e. probe digitising speed in terms of the number of points per second; 3) threshold level which sets the sensitivity of the detector of the probe, and 4) probe orientations, which need to be maintained according to the object geometry.

3.1 scan pitch

Theoretically more measurement points would be more accurate for a surface reconstruction, but the improved accuracy using smaller grid sizes comes unfortunately at the expense of time required for data processing.

In dental research a scan pitch of 50μm has been used for occlusal tooth surfaces, and 70μm for buccal or labial tooth surfaces.

3.2 scan speed

The high scanning speed with a triangulation probe is one of its advantages over mechanically contacting probes. Investigations[7] indicated that delays are produced by processing of the measuring signals, especially with low light levels of the beam spot which require relatively

long integration or averaging time. This introduces uncertainty in the effective reading time of the spot position.

Increasing the scan speed can save time, but the probe has less time for processing. When the scanning speed exceeds the ability of synchronic focus, an error like a missing digit data will occur. A test has been carried out at different speeds, and the results indicated the speed of 10 points per second has the smallest error during the scan[9].

3.3 Threshold level

Investigations[7] have shown that the errors of the triangulation probe are due to different macroscopic and microscopic reflectivities of the measured object. Dark objects have higher thermal losses and require a higher output power and a lower sensitivity of the detector which can be adjusted by changing the threshold level with the CMM software.

To determine a suitable threshold level, a pre-scan with several different threshold levels has to be carried out where the light level is low. The threshold level can not be changed during the entire surface scan, and it has to be set at the lowest level, otherwise a termination of the digitising will occur. A higher threshold level is required with a higher reflectivity of an object and while it gains a smaller error from ambient light background.

3.4 Probe orientation

An optimum probe orientation has been recommended by the manufacturer, which requires the incident beam to be towards the surface normal at a digitising point. The motorised head is limited by a 7.5° step of rotation and the tooth surface's curvatures are changed vary e.g. a tooth lesion may be in a size of 2mm×2mm with a shape of deformed sphere which get surface normal changed from -180 to +180. It is very difficult to meet the recommendation with this case and it is often encountered.

Therefore a digitising error has occurred from the variation of the angle between the incident beam and the surface normal, in order to quantify this error an experiment has been carried out as in the following section.

4. Experiment

4.1 Procedure

The following scanning parameters were used in the experiments: scan pitch = 100μm; measuring speed = 1mm/s; threshold level = 100; with the probe orientations as shown in Fig.3. The probe triangulation plane is in the XOZ plane of the CMM, and the incident laser beam forms an angle of 35° with the beam reflected back to the detector.

The scanning procedures are in two steps:

(1) Datum the top point of the calibration sphere: a square region of 2mm× 2mm at the top part of the sphere is scanned and the top of the sphere (a point T with the highest Z co-ordinate) is defined as the origin of the co-ordinate system.

(2) Starting from the defined point T, four profiles are scanned in the directions: +X, -X, +Y, and -Y. In each of these four directions, the OP2 probe travels until the beam/surface angle exceeds the specified operating range of the OP2 optical probe in its default orientation.

Measurement error is calculated by superposing the digitised profiles with the theoretical sphere generated[10] and then determining the difference between the two.

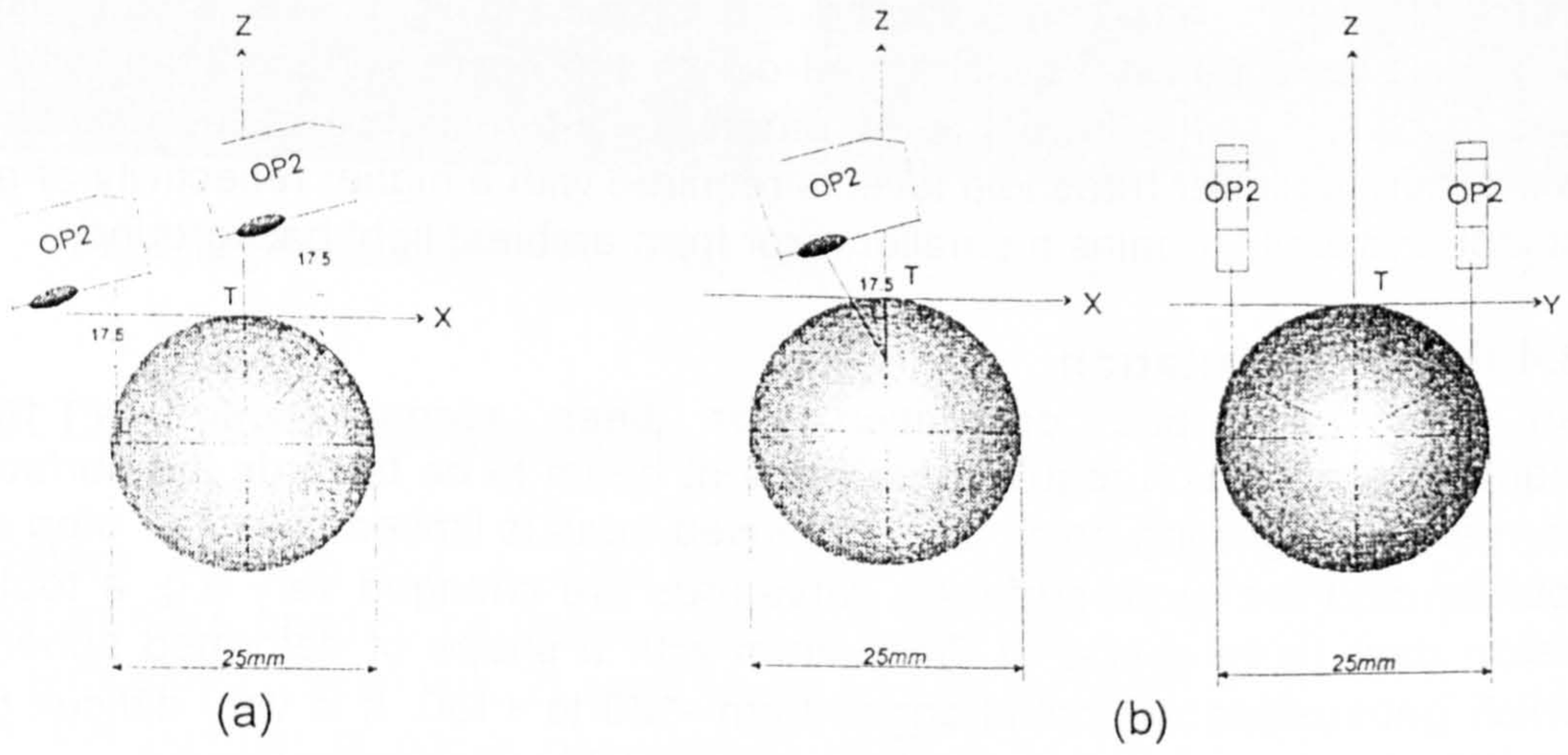

Fig.3 The status of the OP2 probe scanning at the farthest positions along the X axis(a) and Y axis in a front and side views(b)

4.2 Results and discussions

The maximum travel lengths in each of the four directions were: 3.392mm in +X, 10.15mm in -X, 6.492mm in +Y, and 6.412mm in -Y. The angles between the incident beam and the sphere normal at these extreme positions were 15.7° in +X, 54.3° in -X, 31.3° in +Y and 30.9° in -Y.
The errors at the extreme in each directions are 18μm in the +X; 130μm in the -X; 22μm in the +Y; and 16μm in the -Y; which included the variation of the surface texture.

Superposing the digitised profiles in each direction with the theoretical sphere showed a form of the error distribution along the X axis and Y axis (Fig.4).

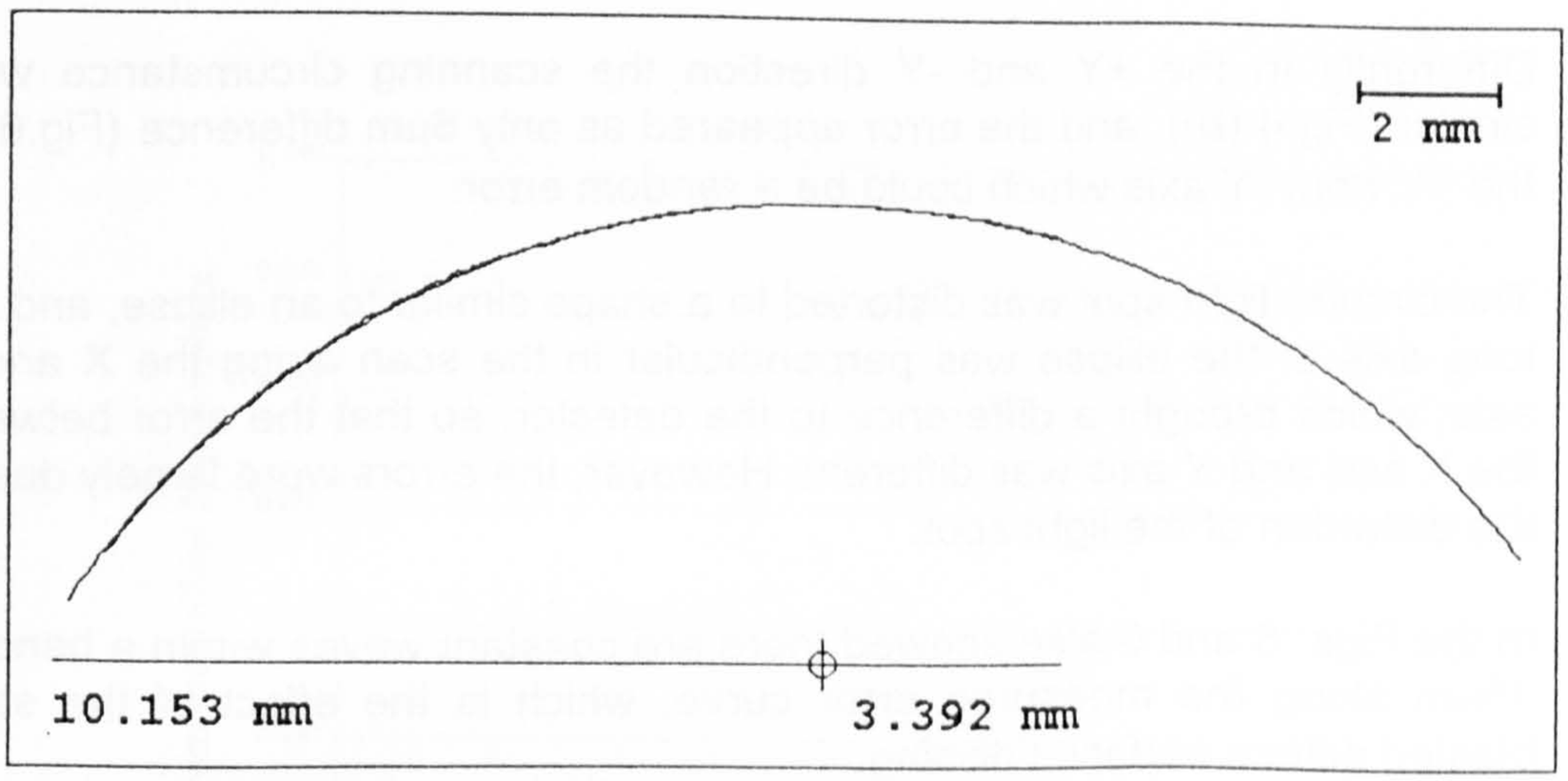

(a)

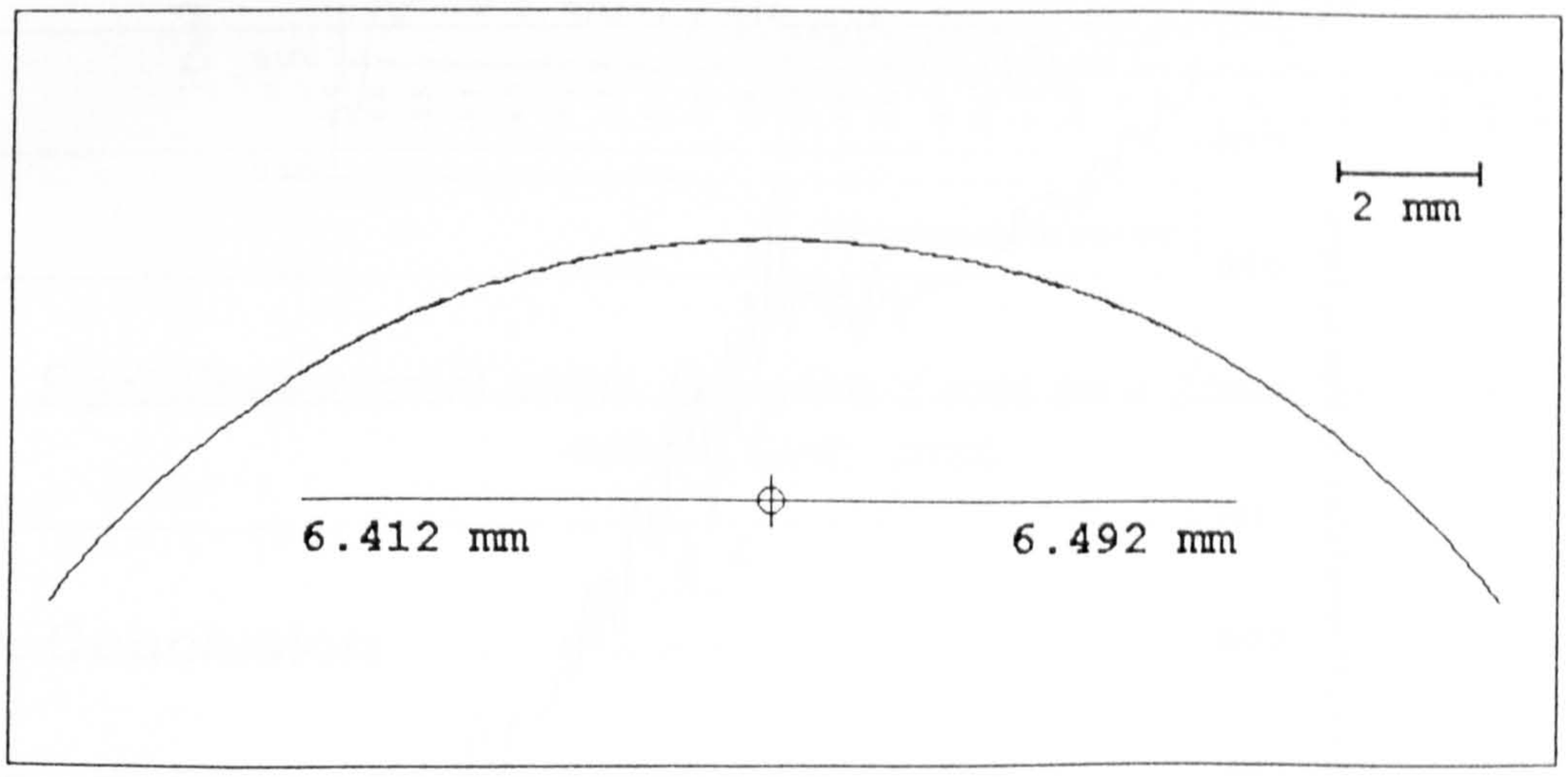

(b)

Fig. 4 The error distribution along the X axis (a) and Y axis (b)

Fig.4 (a) shows that the scanning length in -X is 6.761mm longer than in +X, which is because the probe orientation was arranged as in Fig.3(a), when scanning along the +X, the reflecting beam moves away from the detector of the probe, which causes a termination at the extreme. Opposite along the -X the changing of the surface normal made the beam reflection move towards the probe detector, which obtained a larger scan length, but during this scanning the angle between the incident beam and the surface normal changed from 0° to -54.3°, and this made a larger distortion of the light spot, therefore a larger error appeared as large as 130μm in this case (Fig.5).

Differently in the +Y and -Y direction the scanning circumstance were similar (Fig.4 (b)), and the error appeared as only 6μm difference (Fig.6) in the +Y from -Y axis which could be a random error.

The circular light spot was distorted to a shape similar to an ellipse, and the long axis of the ellipse was perpendicular in the scan along the X and Y axis, which brought a difference to the detector, so that the error between the X axis and Y axis was different. However, the errors were largely due to the distortion of the light spot.

In the Figs. 5 and 6 also showed there are constant waves within a bend of 15μm along the measured error curve, which is the effect of the sand blasted diffuse surface finishing.

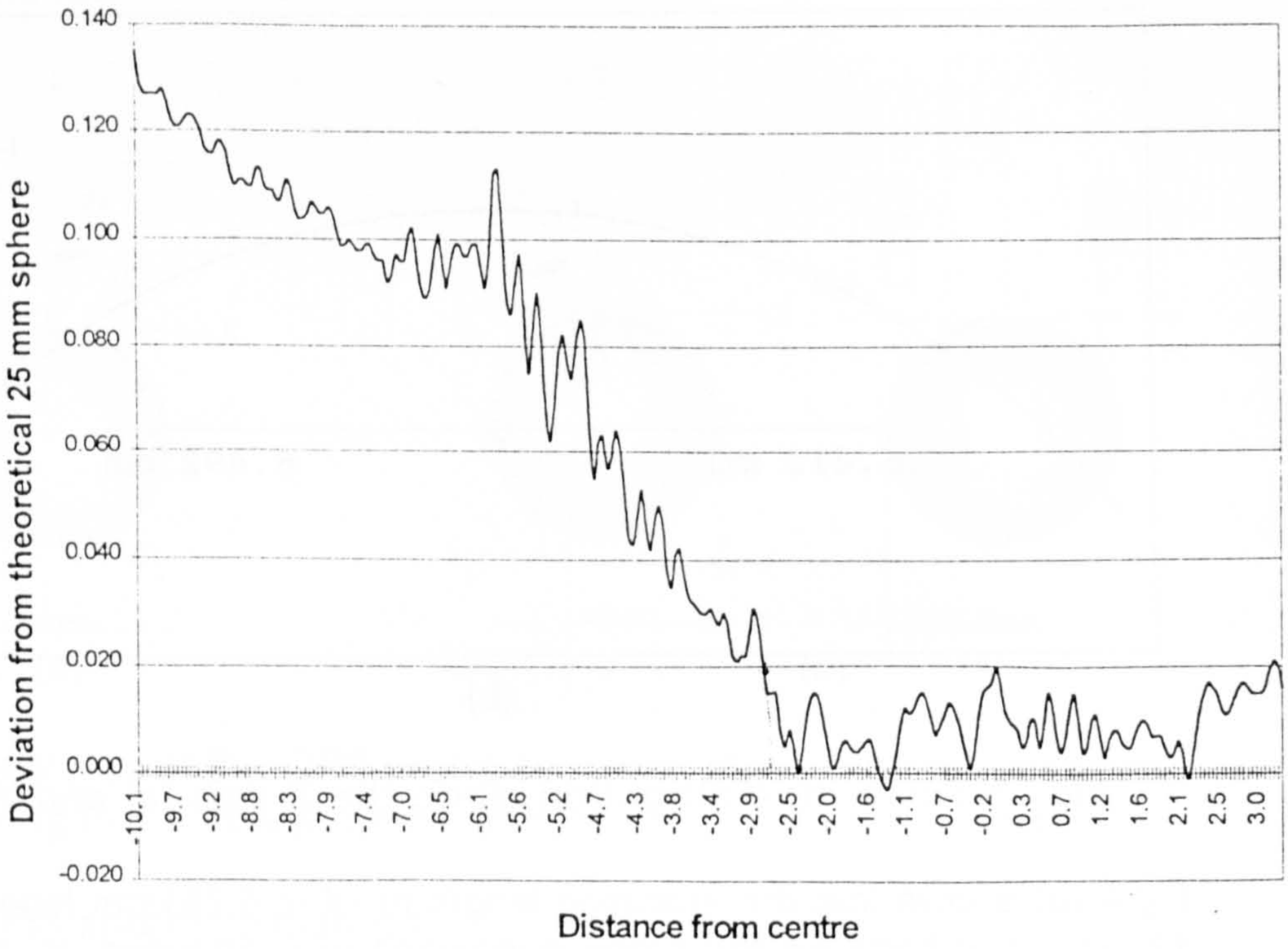

Fig.5 Measurement errors along the X axis on a 25mm diameter sphere (unit : mm)

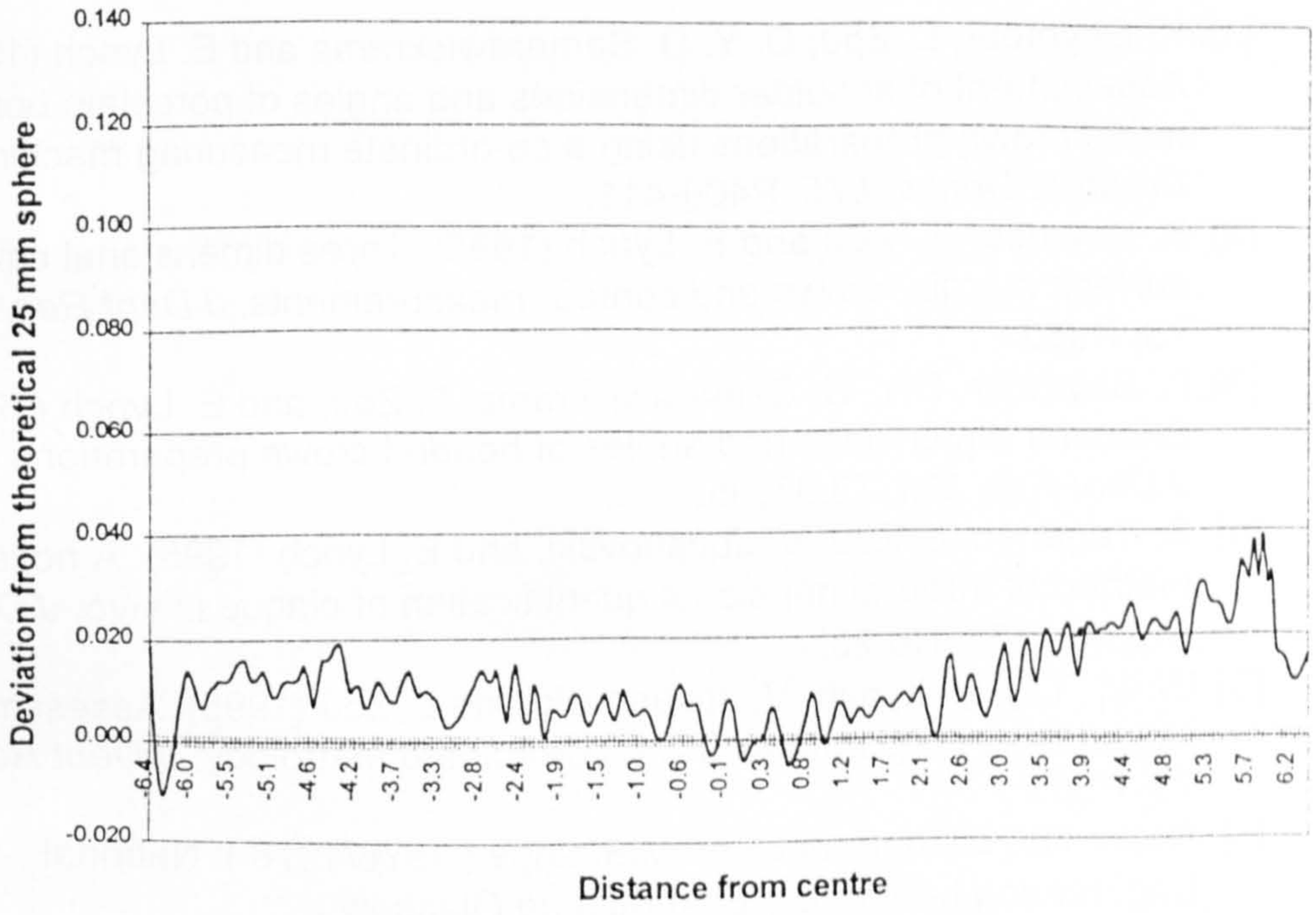

Fig.6 Measurement errors along the Y axis on a 25mm diameter sphere (unit : mm)

6.4

4. Conclusion

This study has produced determinants for the accurate quantification of tooth morphology with the optimal digitising parameters of scan pitch; scan speed; threshold level of laser probe and probe orientation.
The characteristics of the probe error distribution on a standard diffused sphere are discussed which investigate the measurement error effected by changing of the angle between the incident beam and surface normal, and it is in relation to the measurement of tooth morphology.

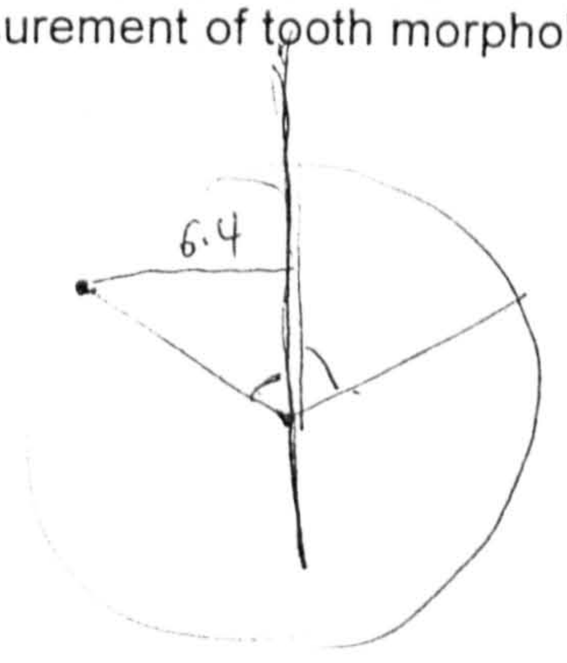

6.4

6.4
25.

References

[1]. K. Seymour, L. Zou, D. Y. D. Samarawickrama and E. Lynch (1996). Assessment of shoulder dimensions and angles of porcelain bonded to metal crown preparations using a co-ordinate measuring machine. *J Prosthet Dent vol.75:* P406-411.

[2]. K. Seymour, L. Zou and E. Lynch (1995). Three dimensional cavo-surface margin, crown and contour measurements. *J Dent Res,* Vol. 73, P952.

[3]. K. Seymour, D.Y. D. Samarawickrama, L. Zou, and E. Lynch (1995). Shoulder dimensions and angles of bonded crown preparations in vivo. *J Dent Res,* Vol. 73, P895.

[4]. S. Yeganeh, L. Zou, V. Jovanovski, and E. Lynch (1995). A novel method of three-dimensional quantification of plaque in vivo. *J Dent Res,* Vol. 73, No.28.

[5]. W. M. Tay, E. Lynch, V. Jovanovski and L. Zou (1995). Assessment of class I inlay preparations using co-ordinate metrology. *J Dent Res,* Vol. 73, P586.

[6]. Nelex 76/78 Conference on Metrology (1976/1978). National Engineering Laboratory East Kilbride Glasgow

[7]. European Commission, Performance Test Procedures for Optical Co-ordinate Measuring Probes Final Project Report, Part 1; Report EUR 155314 EN; 1994.

[8]. C. Butler(1991). An investigation into the performance of probes on coordinate measuring machines. Industrial Metrology 2, Elsever, P59-70.

[9]. L. Zou, V. Jovanovski, W. M. Tay and E. Lynch (1995). The influence of three parameters on laser probe scanning of irregular surfaces. *J Dent Res,* Vol. 73, P895.

[10].V. Jovanovski, L. Zou, W. M. Tay, E. Lynch and M. G. Cox (1995). Superimposition of co-ordinate data obtained from a sequence of replicas. *J Dent Res,* Vol. 73, P895.